ION EXCHANGE FOR THE DESALINATION AND TERTIARY TREATMENT OF WASTEWATER

by

TREVOR BADEN SYDNEY GIDDEY

Submitted
in fulfilment of the requirements
for the degree of
Doctor of Philosophy

University of Cape Town
February 1979

SYNOPSIS

Ion exchange for the desalination and tertiary treatment of waste water has involved the development of both the theory and practice of continuous countercurrent ion exchange (CCIX).

The need for process development arose after a comprehensive review of the principles and properties of ion exchange as these applied to the treatment of saline sewage plant discharge streams. Initial cost studies also indicated that regenerant chemicals constituted the major cost item in an IX plant. On the basis, therefore, of the IX literature review and the cost exercise, the decision was made to use CCIX and to develop a specific process for the treatment of secondary sewage effluent.

A study was made of the kinetic, equilibrium and organic absorption properties of cation and anion resins and how these properties related to the operation of a CCIX unit. Simultaneously, a novel regenerant chemical recovery scheme based on the use of nitric acid and ammonia was formulated and tested.

The various ion exchange reactions involved in the overall desalination and tertiary treatment process were monitored in a CCIX column and from these tests, a steady state theory of the operation of such a column incorporating the previously determined resin exchange properties was proposed and verified.

The next phase of the investigation involved the design, construction and commissioning of an interlinked five column CCIX pilot plant. This was also a new development in that this complexity of CCIX plant had not formerly been operated. Initial test work involved synthetic saline solutions and an hydraulic investigation. This was followed by treatment of secondary sewage effluent during which it was shown that combined desalination and organic removal could be achieved, regenerant chemicals could be recovered and feed water dissolved components concentrated for discharge.

Based on the theory and operation of the CCIX plant, an economic feasibility was conducted. This study showed the very complex economic interrelationships which exist in the CCIX tertiary treatment process and indicated how an optimum design of a larger scale plant can best be approached.

Finally, the work has, in developing a tertiary treatment and desalination process, provided an alternative means of supplementing the ever increasing demand for fresh water in the country.

TABLE OF CONTENTS

LIST OF FIGURES

LIST OF TABLES

NOMENCLATURE

a	area through which mass transfer occurs
c	intercept of operating line $y = mx + c$
C	concentration of ionic species in liquid phase
$\overline{C}$	concentration of ionic species in resin phase
C_L	concentration of electrolyte in liquid phase
C_R	concentration of electrolyte in resin phase
D	diffusivity of ionic species in resin phase
F	volumetric flow rate
$F(t)$	fractional approach to equilibrium
J, J_i	flux in resin phase
k	mass transfer coefficient
K	equilibrium constant
L	equivalent flow rate of liquid $L = FC$
m	slope of operating line
N, N_i	flux in liquid phase
q	concentration of species at liquid-resin interface
$\overline{q}$	mean concentration of species in resin phase
r	ion exchange resin bead radius
R	equivalent flow rate of resin
R'	rate of exchange
Re	Reynolds number
S	stoichiometric ratio $S = R/L$
Sc	Schmidt number
Sh	Sherwood number
t	time
t'	space time within a CCIX column stage
T	absolute temperature
v	liquid volume in a fluidised bed
V	volume of a CCIX column stage
V_L	volumetric flow rate of liquid
V_R	volumetric flow rate of resin
x, x_i	ion fraction, resin phase
y, y_i	ion fraction, liquid phase
z	absolute value of electrochemical valence
Z	film thickness

Greek symbols

α	separation factor	$\alpha_B^A = \frac{y_A x_B}{x_A y_B}$
β	ratio of diffusivities	$\beta = \frac{D_A}{D_B} - 1$
ϵ	settled bed voidage	
ϵ'	fluidised bed voidage	
η	stage efficiency	$\eta = \frac{x_i - x_{i-1}}{x_i - x^*_{i-1}}$
τ	dimensionless time	$\tau = \frac{Dt}{r^2}$
ϕ, ϕ_i	sum of fluxes	$\phi_i = J_i + \psi_i$
ψ	electrostatic potential	

Superscripts

0	at time zero
∞	at time infinity
*	at equilibrium

Subscripts

b	bottom of a CCIX column
L	liquid phase
R	resin phase
t	top of a CCIX column

CHAPTER 1

INTRODUCTION

1.1 BACKGROUND

1.11 Need for reuse of water

Fresh water, like other natural resources, is becoming a scarce commodity in today's world of rapid population growth and industrial expansion. Certain developed areas of the globe which hitherto have had an excess of readily available fresh water, have now to give serious consideration to the provision of sufficient water for both domestic and industrial consumption in the very near future.

One such area is the city of Cape Town, South Africa, and its surrounding districts. In the past, the Cape Peninsula has relied upon natural precipitation and runoff into the dams at its three major catchment areas, Wemmershoek, Steenbras and Table Mountain. Recently, a further storage facility at Voëlvlei has been included in the water supply system. Together, these present sources provide an assured 168 000 megalitres of fresh water annually [1]. It has, however, been estimated that the population growth over the last forty years to the turn of the century in the Cape Peninsula will be from 1 million to 3 million [2]. It has also been estimated that the water demand during this same forty year period will increase from 85 000 to 450 000 megalitres annually - a shortfall on present assured supply by the year 2000 of 282 000 megalitres per year. Present plans for extra water catchment to supply Cape Town's needs will, it is envisaged, provide a further 200 000 megalitres per year; thereafter, alternative sources for supplementing the city's fresh water will have to be provided.

1.12 Sources of recoverable water

Cape Town has at its disposal the following potential water resources, each requiring different degrees of treatment for potable use:

(i) sea water
(ii) natural precipitation (rainfall)
(iii) surface water and runoff
(iv) underground water
(v) reclaimed sewage plant discharge.

Cost considerations usually make sea water the least attractive source compared with the others listed. Natural precipitation has been fully accounted for in section 1.11, and the local topography and the absence of large rivers make surface water an unreliable source. This leaves either reclamation of presently used water or underground resources as the remaining means of supplementing the water supply.

Henzen [1] has carried out a comprehensive investigation into the feasibility of using the vast underground water source below the Cape Peninsula. Henzen studied the geological structure of the subterranean sand beds of the peninsula with a view to replenishing the water drawn from underground sources with secondary sewage effluent and thereby possibly preventing sea water encroachment into the ground water system. It was hoped that the sand beds would simultaneously provide a filtering and tertiary treatment action to the sewage water being introduced. The abstracted water, however, has a high dissolved solids content, on average 1 200 mg/ℓ, and would require desalination to bring it within the limits of a grade A water (Table 1.1) specified by the state Health Authorities as the quality necessary for human consumption.

TABLE 1.1

Quality of a grade A water

South African Bureau of Standards (1971)

Arsenic	50 µg/ℓ
Cadmium	50
Chrome (hexavalent)	50
Copper	1 000
Cyanide	10
Lead	50
Zinc	5 000
Chloride	250 mg/ℓ
Sulphate	250
Iron	0,3
Calcium	N.S.
Magnesium	100
Hardness ($CaCO_3$)	20-200
NO_3 as N	10
TDIS	500
pH	6-9

The other potentially recoverable source of water is sewage plant discharge. This water passes, at present, only once through the 'system' before being discharged into the sea, for only a fraction is recycled as cooling water to a local power station. Heunis [3] shows that 50% of present fresh water used, ends up in the sewer system.

Secondary sewage effluent in the Cape Peninsula is discharged from four sewage works. The largest of these at the present time, Athlone, treats a mixed domestic-industrial waste. Prentice [4] has investigated the degree of mineralisation of fresh water during its passage through the 'system'. Prentice concludes that the major increase in salinity which occurs - the dissolved solids content of fresh water and two sewage works discharge streams is compared in Table 1.2 - results from the following sources: (a) infiltration of sea water into old sewers lying below sea level, (b) industrial discharge of high salinity streams into the sewerage system.

TABLE 1.2

Comparison of composition of domestic sewage effluent and tap water

	Tap Water	Milnerton Sewage	Athlone Sewage
Na	50	300	120
K	-	22	20
Ca	15	55	45
Mg	10	55	20
NH_4-N	0	18	18
Cl	75	480	200
SO_4	<10	155	120
PO_4	-	24	10
NO_3-N	<1	53	44

1.2 WATER RECOVERY SYSTEMS

Water upgrading and recovery systems can presently be divided into two major categories: (a) those that provide a desalination function and (b) those that provide a tertiary treatment function. There are, at the moment, very few systems which simultaneously perform both operations - if both are required, the one usually follows the other.

1.21 Desalination systems

Desalination of water for potable purposes varies between two extremes - (a) the situation where the only available water source is extremely saline, e.g. the sea with a total dissolved solids (TDS) content of 35 gm/ℓ, and (b) where water is abstracted from boreholes with a TDS between 1 gm/ℓ and 10 gm/ℓ. The developed technology available for treating the extremes is chosen on the basis of cost. In general, plants for upgrading sea water are based on phase change processes such as evaporation or freezing, whilst those used for borehole water are membrane processes, reverse osmosis or electrodialysis, and ion exchange. All of the process types outlined have been tested and are in use in various commercial plants around the world. The experience gained in operating such plants is reported in one volume of the JAWWA [5] by authors such as Krebs et al. on distillation, Moore on reverse osmosis, Halpern et al. on electrodialysis and Fraser et al. on freezing processes. Probstein [6] reviews the operation of these various desalination techniques.

For upgrading the low salinity borehole waters (TDS less than 5 000 mg/ℓ), Quinn et al. [7] and Bresler and Miller [8] show that usually only ion exchange and reverse osmosis are economically competitive. The authors provide figures for capital and operating costs of both ion exchange (IX) and reverse osmosis (RO) plants capable of treating the water under review. They conclude that RO becomes more attractive as the salinity level increases and that under certain conditions, a combination of IX and RO is better. Ion exchange suffers from the disadvantage of requiring a chemical input proportional to the salinity level of the water to be treated, and consequently, at high TDS levels, it no longer remains a competitive desalting technique. At low TDS levels the water pretreatment charges and power costs of RO mitigate against its use when compared with IX.

1.22 Tertiary treatment systems

The tertiary treatment of water includes both the unit operations of a conventional sewage plant and those associated with drinking water pre-treatment - flocculation, filtration, chlorination.

The South African national organisation for water research, the NIWR, has developed a tertiary treatment process which has upgraded secondary sewage water to the level of potable water. This physico-chemical (PC) reclamation plant has been used for augmenting Windhoek, SWA, water supply since 1969. The unit processes in the PC plant consist of lime treatment, flocculation, ammonia stripping, recarbonation, sand filtration, activated carbon treatment and chlorination.

Cillie et al. [9] and van Vuuren et al. [10] describe the operation of the PC plant, and the effectiveness of each treatment step in reducing the organic and toxic salt levels within the plant. The disadvantage of this type of treatment, although very effective in lessening the organic and bacteriological content of the water, is the TDS increase it imposes on the treated water, and its inability to remove salts present in the water which do not precipitate in the lime treatment step.

If the TDS increase in fresh water is of the order of 200 mg/ℓ after one pass through a domestic 'system', as Henzen and Funke [11] point out, then a PC plant treating water for recycle would not fulfill the total treatment function, but conversely, neither would desalination alone, for organic material has also to be removed. A combination of both systems is necessary.

1.23 Combined organic and salt removal

A certain degree of organic chemical removal does occur when RO and IX desalination plants are operated. In fact, operators of IX units producing low conductivity water for high pressure boilers embark on elaborate water pretreatment procedures in order to prevent the IX resins from removing the organics from the water and thereby becoming 'fouled' - where, over a period of time, the resins show a capacity loss due to irreversible organic uptake.

It is only very recently that thought has been given to the possible use of IX and RO as a combined desalination and tertiary treatment operation. This has only come about through the supposed development of RO membranes and IX resins with the ability to desorb organics which they have removed from the 'raw' water. Pollio and Kunin [12] proposed the use of a modified form of the weak electrolyte resin system, the Desal process, as an economical tertiary treatment. The modification included a flocculation step which performed most of the organic removal, with the resins providing a polishing step.

1.3 OBJECTIVES OF THIS STUDY

In order to obtain a system which would fulfil the requirements of organic removal and desalination, the following aims were formulated:

(i) to develop a new or evaluate an existing ion exchange process to provide a simultaneous desalination and tertiary treatment of saline secondary sewage effluent;

(ii) to test the process in laboratory and pilot plant scale equipment for technical feasibility;

(iii) to develop and test design criteria in order that a large scale plant may be designed and costed.

1.31 Process development

The ion exchange literature must be reviewed and any feasible IX processes capable of meeting objective (i) are to be tested. On the basis of the results obtained and a cost study to be undertaken, conclusions are to be drawn on the IX process which will best achieve the desired objective of a 'complete' tertiary treatment, bearing in mind the cost parameters most likely to affect the overall viability of the process. Consideration is to be given to resin type and properties, column configurations and other IX process considerations in deciding upon a suitable scheme.

1.32 Process testing

Based on the results of the initial test work and cost studies, the chosen IX process is to be further developed in both laboratory and pilot scale. Cognisance is to be taken of the long term effects of the operation

on resin properties and of the problems associated in operating, on a continuous basis, the plant and equipment ultimately chosen. Testing is to be directed towards providing the results required for evaluation of both the process economics and the design criteria developed to predict plant performance.

1.33 Process design

The third objective of the programme is to develop criteria which may be used for the design and costing of a large pilot scale or full-scale IX facility based on the developed process. The criteria are to be tested in the operation of the process during laboratory and pilot scale work and are to be, if possible, of a general nature so that they can perhaps be applied to similar IX operations.

CHAPTER 2

PRINCIPLES AND PROPERTIES OF ION EXCHANGE

2.1 RESIN MANUFACTURE AND STRUCTURE

2.11 Background

Ion exchange as a unit operation has made enormous strides since the exchange properties of soils were scientifically documented by Thompson and Way in the middle of the nineteenth century. Kunin [13] shows graphically that the number of papers published in the field of ion exchange has increased exponentially from the beginning of this century.

The principle of ion exchange is accepted to be the reversible interchange of cations or anions between a solution phase and a solid phase according to the following reactions:

$$R^- - A^+ + B^+Y \rightleftharpoons R^- - B^+ + A^+Y \quad \text{(Cation exchange)} \qquad (2.1)$$

$$R - X^- + A^+Y^- \rightleftharpoons R - Y^- + A^+X^- \quad \text{(Anion exchange)} \qquad (2.2)$$

The solid (resin) phase is designated R in the above reactions, and the ions which take part in the exchange (A^+,B^+ for cation exchange X^-,Y^- for anion exchange) are called the counter-ions. The ions in solution with the same charge as that of the ion exchanger (Y for cation reaction, A for anion reaction) are termed the co-ions.

The exchange of ions discovered by Thompson and Way occurred between ammonium ions in solution and calcium ions present in the alumino-silicate fraction of the soil. These clay minerals or zeolites were the forerunners to the modern day synthetic ion exchange resins. Today still, the natural zeolite clinoptilolite is widely used [14,15] for removing ammonia from water. The properties of the zeolites and their crystal structure which gives rise to their ability to exchange ions, is well explained by Grimshaw and Harland [16].

2.12 Manufacture and structure

Most ion exchange resins in use at present are manufactured synthetically. This involves either polymerisation of a monomer containing ion exchange

groups, or introduction of ion exchange groups into the polymer matrix. The reaction techniques are sufficiently sophisticated so that a range of ion exchange resins capable of meeting most requirements, can be tailor made.

2.121 Polymerisation and resin structure: Most commercially produced ion exchange resins are porous polymer spheres of varying diameter. For certain applications, granular resins are also manufactured. The structure of the resins is generally characterised by the pore-size distribution of the spherical beads, and the degree of 'crosslinking' between polymer chains within the bead.

Formation of a polystyrene resin (Figure 2.1) via a typical reaction route, that of 'pearl' polymerisation, would involve the addition of monomer to an agitated aqueous solution at the temperature required for polymerisation to proceed (usually 85° to 100°C). The monomer solution, a mixture of

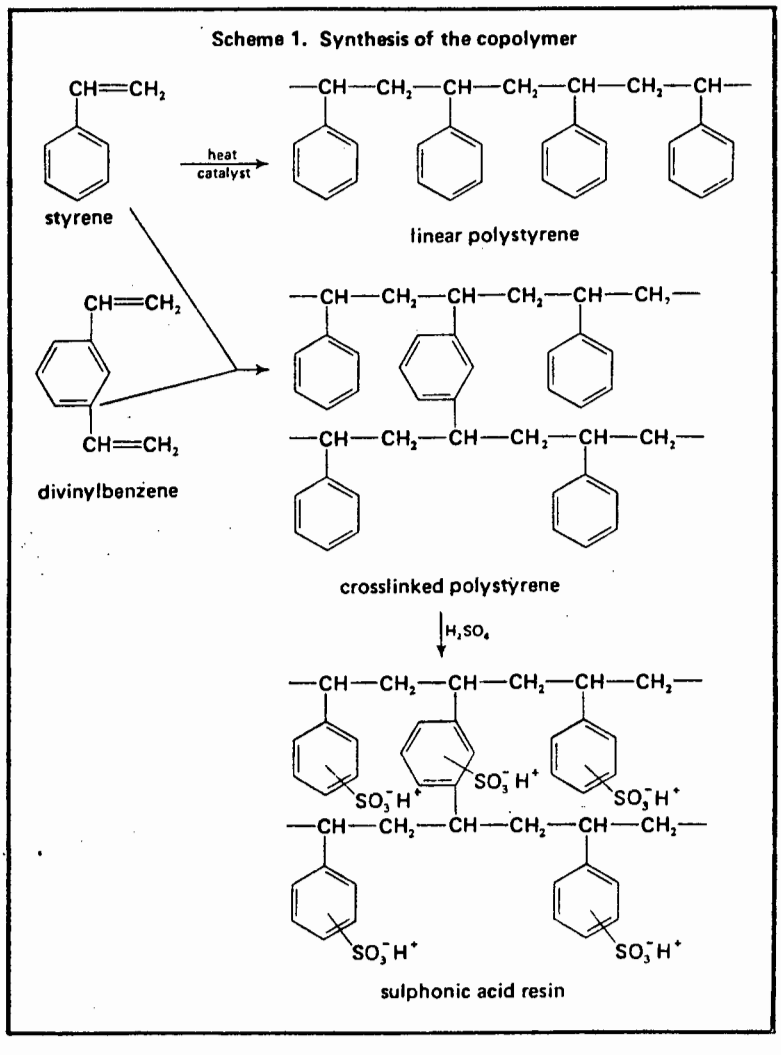

FIGURE 2.1

Preparation of a styrene based strong acid resin

styrene and divinylbenzene, would on addition form small droplets which remain suspended in the reaction mixture. By varying the degree of solution agitation and the type of suspension stabiliser (gelatin, sodium methacrylate etc.), the size of the suspended droplets and ultimately the bead size can be varied within wide limits. The purpose of the divinylbenzene (DVB) is to cause the interlinking of polystyrene (polymer) chains. By changing the percentage of DVB present in the polymer, different degrees of cross-linking are attained.

Dorfner [17] cites the following resin properties as being affected by the DVB content of the bead:

(i) solubility
(ii) mechanical stability - exchangers with a low DVB content are soft and mechanically unstable, while highly cross-linked products are brittle and hard
(iii) exchange capacity - volumetric capacity decreases as cross-linking decreases due to increased resin swelling
(iv) swelling and moisture content - vary inversely with percentage DVB
(v) volume change - less at high DVB content
(vi) chemical and oxidation resistance - improves with DVB content.

The pore-size distribution of the resin is controlled both by the degree of cross-linking, and by the method of manufacture. Most commercial resins conform to one of three size distribution types, viz. gel, macroporous or isoporous. Figure 2.2 depicts the pore-size distribution within each resin type. Smallest pore-size distribution occurs in the isoporous resins, where manufacture is specifically aimed at obtaining regular spacing of polymer cross-links. Gel resins show a greater size distribution than do isoporous resins, but a more uniform structure than macroporous resins. Martinola et al. [18] have carried out an extensive investigation of the pore-size distribution of macroporous resins, and show that pore diameters can vary within the range 100-70 000 Å, depending upon the resin tested.

Resins produced by pearl polymerisation generally have a gel-type structure. In order to produce a macroporous (macroreticular) resin, the solution in which polymerisation occurs is changed, usually by the addition of a diluent such as toluene, which is a good solvent for monomer, but not for polymer. As polymerisation proceeds, the solvent is squeezed out of

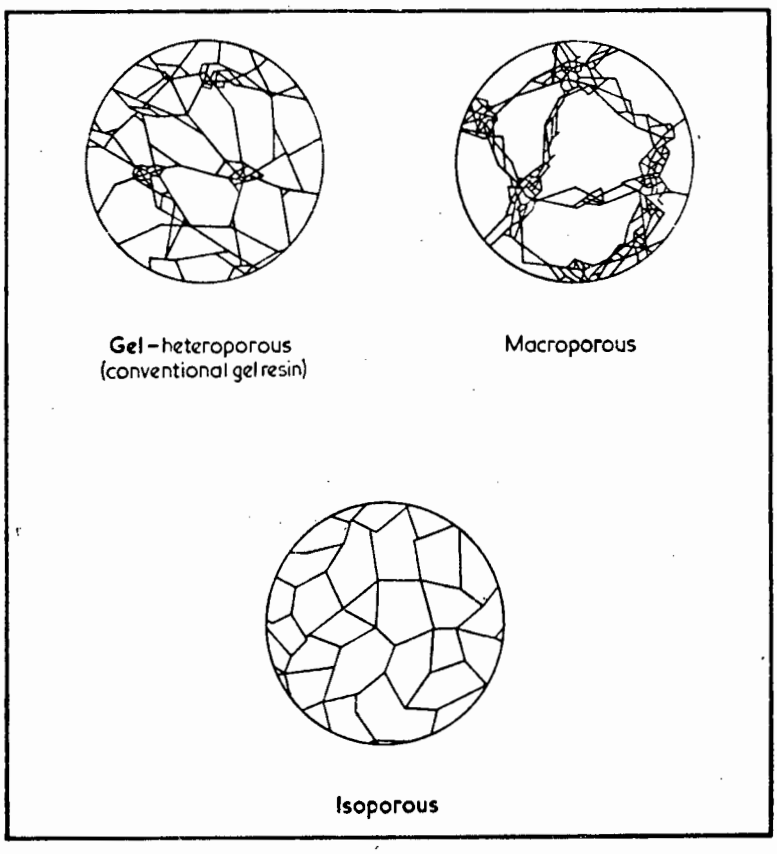

FIGURE 2.2

Schematic diagram of resin pore structure

the growing polymers, and uneven distribution of solvent within the forming beads results. If the excess solvent is removed on completion of reaction, areas of high and low degrees of cross-linking result. This produces the macroporous structure, which combines the favourable characteristics of both high and low degrees of cross-linking, viz. high chemical and mechanical stability, low swelling and volume change and greater resistance to osmotic shock.

Kunin [19] lists the following factors as being favourably affected by increasing the size of resin pores: (i) the rate of ion exchange, (ii) the capacity for ions of high molecular weight.

2.122 Functionality: The chemical groups within an ion exchange resin bead that are involved in the exchange reaction are either cationic or anionic. Most resins contain only one charge type, although amphoteric resins containing both positive and negative groups are synthesised for special applications [20]. The functional group type imparts the exchange properties

to the resin and much research effort is directed towards improving the exchange specificity of the groups attached to the polymeric backbone; resins with metal chelating groups [21] used for metals separation in mineral processing are an example.

2.1221 Cation resins. Cation resins are broadly divided into two types, referred to generally as either strong acid or weak acid. The difference between the two is dependent upon the pK value of the group attached to the resin matrix.

Strong acid resins are produced (Figure 2.1) when the polymer is sulphonated, and a sulphonic acid group ($-C-SO_3^- H^+$) formed. Most weak acid resins contain a carboxylic acid group ($-C-COO^- H^+$) instead of the sulphonic acid molecule. These two cation resins exhibit exchange properties analogous to the reactions that sulphuric and carboxylic acids undergo in solution. At high solution pH, both groups are completely dissociated and both will exchange cations for their hydrogen ions. In the presence of a base (NaOH), the reaction will be irreversible, and proceeds to completion, the products being Na-form resin and water. When the resins are placed in a low pH solution, i.e. a pH less than the pK of the carboxyl group, only the sulphonic acid will dissociate. Consequently, only the sulphonic acid has the ability to exchange at low pH conditions, as its pK value is low.

'Regeneration' after an exchange reaction (i.e. the reconversion of, for example, a sodium loaded resin to its original hydrogen form) is achieved more easily with a weak acid resin The pH of the external solution needs only to be maintained below the resin pK for a sufficient period so that the reaction may go to completion for regeneration to be achieved. In contrast, the strong acid resin regeneration reaction will only reach an equilibrium and will not proceed to completion. Regenerant acid solution has therefore to be successively renewed in order to achieve complete resin conversion. Further, any acid which when placed in solution can produce a pH lower than the pK of the resin will regenerate a weak acid resin. Only a strong acid (HCl, H_2SO_4, NHO_3) will regenerate a sulphonic acid group.

Because the dissociation of the carboxylic group of a weak resin will occur only at relatively high pH values (generally pH >3), reaction between

hydrogen form resin and sodium chloride is unlikely to occur to any great extent, for the reaction product would be Na-form resin and HCl-solution. Production of HCl reduces solution pH and causes reversal of the reaction. Weak acid resins, in contrast to strong resins, cannot be used to 'split' neutral salts such as NaCl. They are only able, dependent upon the actual resin structure, to 'split' salts which in solution have basicities significantly higher than resin pK values, typically bicarbonate and carbonate salts.

Both strong and weak resins will exchange one metal cation for another, e.g. $R - Na + K \rightleftharpoons R - K + Na$ irrespective of the co-ion (anion) present in the solution, since the degree of dissociation of Na-sulphonate and Na-carboxylate (the forms of the loaded resins) is similar. If metal cation exchange is required at pH values less than 7, hydrogen ions will start competing for resin sites, with the weak resin showing perhaps a greater affinity for H^+-ions than for either of the two metal ions.

2.1222 Anion resins. Unlike cation resins, anion resins cannot readily be divided into strong base and weak base. Anion resins acquire their properties from the attachement of a nitrogen atom to the resin matrix, to form groups with the following amine structures:

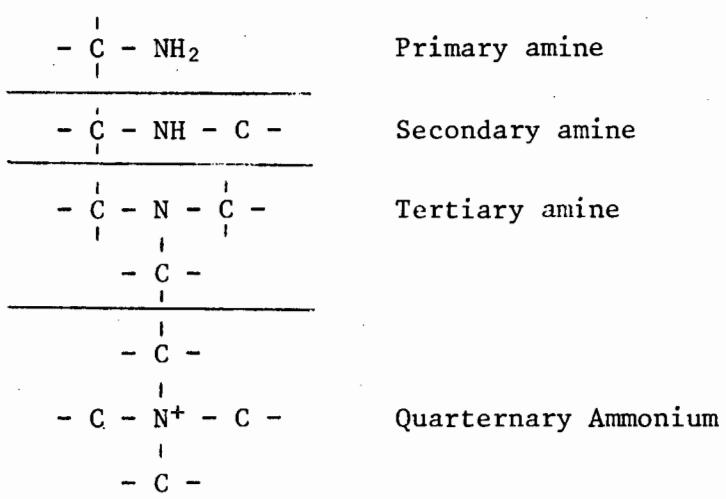

The quaternary ammonium group, due to its high degree of dissociation behaves analogously to a strong acid resin. It is capable of 'splitting' neutral salts in an exchange of an hydroxyl ion for some other anion, and it is also able to exchange under high solution pH conditions. Like all strong resins,

the quaternary ammonium requires an excess of strong base (e.g. NaOH, KOH) for regeneration to the hydroxyl form.

The primary secondary and tertiary amine resins constitute the weak base group. The exchange mechanism of this class is different from the cation and strong-base resins in that a hydrogen co-ion has to participate in the exchange. This group of resins is therefore only capable of taking part in ion exchange reactions when the solution pH is low enough to provide the necessary hydrogen ions. The reaction occurs in two steps:

(i) protonation of the amine group, e.g.

$$R - NH_2 + H^+ \rightarrow R - NH_3^+ \qquad (2.3)$$

(ii) Association between the protonated amine and the counter-ion, e.g.

$$R - NH_3^+ + Cl^- \rightarrow R - NH_3^+ Cl^- \qquad (2.4)$$

The affinity of the amine groups for hydrogen ions varies from primary to tertiary and also with the organic structure to which the N-atom is bonded. Consequently, a wide pH range exists at which weak base resins exchange under optimum conditions. Gustafson et al. [22] have analysed the structure and properties of a range of anion resins and show how the exchange properties vary with resin structure.

Conversion of weak base resins to the free base (unprotonated) form is accomplished with any solution which is able to raise the pH to a level higher than the pK of the amine group. Provided sufficient base solution is present to maintain a high pH throughout the period of the reaction, the regeneration will proceed to completion.

2.2 RESIN EQUILIBRIA

When a particular form of either strong or weak cation or anion resin is placed into an electrolyte solution containing a given concentration of counter-ions, a number of mass transfer processes commence. The extent to which the swelling, solute sorption and ion exchange proceed depends on the structure and functionality of the resin, and the properties of the solution in which it is placed. Together, the resin and solution govern the equilibrium point at which the respective mass transfer operations stop.

2.21 Solvent and solute sorption

2.211 Solvent sorption: If a resin containing ionogenic groups - the functional groups (cf. section 2.122) which take part in the exchange reacton - is placed into a solvent, diffusion of the solvent into the spherical bead occurs. In order to accommodate the sorbed solvent, the resin swells. Sorption and subsequent swelling proceed until an equilibrium is attained, at which point the forces involved in the mass transfer are balanced.

Two opposing forces interact in the sorption process. Firstly, the ionogenic groups attempt to surround themselves with as many polar solvent molecules as possible in an attempt to reduce the functional group concentration within the bead; secondly, in opposition to the sorption, are the forces holding the resin matrix together, i.e. the cross-linking of the polymer chains. Consequently, equilibrium is attained when the elastic forces of the resin matrix are counterbalanced by the dissolution forces of the ionogenic groups.

Helfferich [23] lists, and Lal and Douglas [24] have measured some of the following factors as being important in determining the degree of solvent sorption and swelling which is likely to occur:

(i) the nature of the solvent - polar solvents are better swelling agents because they interact more strongly with the ions in the resin;

(ii) concentration of the solution - resins swell more when solution concentrations are low. Any increase in concentration reduces the osmotic pressure difference between the interior of the resin and the solution, thereby reducing the 'driving force' for solvent uptake;

(iii) degree of cross-linking - highly cross-linked resins will swell less due to the rigidity of the cross-linked matrix;

(iv) functional group and counter-ion - the affinity of both for solvent dictates the effect they have on the degree of sorption and swelling.

Points (ii) and (iv) are important when the life of an ion exchange resin is considered. In general, when a resin is regenerated a concentrated solution is used whilst the loading operation is performed in dilute solutions.

The changes in counter-ion and solution concentration cause the resin to swell and shrink, placing a strain upon the cross-link bonds. Resin bead disintegration from this 'osmotic shock' can occur. Highly cross-linked (e.g. macroporous resins) which undergo less volume change (cf. Figures 2.3 and 2.4) can be used to reduce this effect.

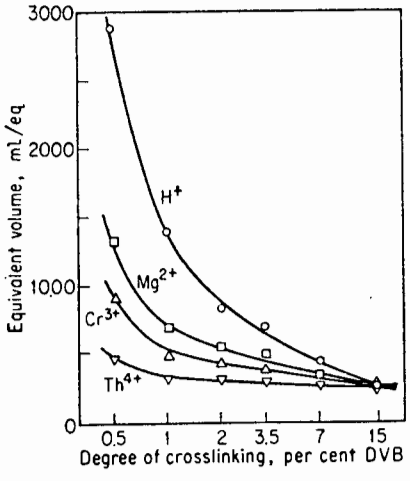

FIGURE 2.3

Effect of counter-ion type on the swelling of resins

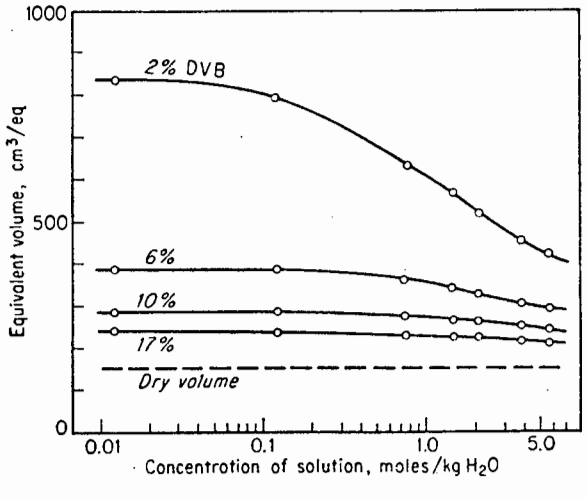

FIGURE 2.4

Effect of solution concentration on the swelling of cross-linked resins

2.212 Solute sorption: When A-form resin and a dilute solution of a strong electrolyte AY are contacted together, Y co-ions start diffusing into the resin matrix under a concentration difference driving force. Such diffusion will lead to charge separation, with an accumulation of positive charge in the solution and negative charge in the exchanger, and will tend to reverse the diffusion direction of Y co-ions. The potential which causes the reversal, the "Donnan potential", counteracts the tendency of Y co-ions to migrate into the bead. An equilibrium is thus established at which the electric field and the concentration difference are balanced. The Donnan potential causes a repulsion of co-ions from the resin and thus prevents electrolyte sorption, since an excess of A ions cannot be sorbed because of electroneutrality requirements. A measure of the degree of electrolyte sorption can be made by comparing the concentrations of Y ions inside and outside the ion exchange resin bead.

In discussing Donnan exclusion and electrolyte sorption, Helfferich [23] and Diamond and Whitney [25] make the following points:

(i) the Donnan potential is greater when the concentration difference between resin and solution is large. At high resin capacities (highly cross-linked resins are not swollen and have a higher unit volume capacity) the concentration difference between resin and solution is high. Consequently, the efficiency of electrolyte exclusion increases with decreasing solution concentration and increasing resin capacity and cross-linking (cf. Figure 2.5).

(ii) the higher the charge of the co-ion, the more efficient will be the exclusion (cf. Figure 2.6).

(iii) the degree of exclusion is also dependent upon interactions between the mobile ions and the resin groups. A weak acid resin in contact with solution with a pH < pK_{acid} will contain undissociated carboxyl groups. The Donnan potential is then reduced and simultaneously the efficiency of co-ion exclusion. Analogously, a weak base resin in the free base (unloaded) form is able to sorb basic electrolytes such as NaOH, NH_4OH.

(iv) weak (undissociated) electrolytes are little affected by Donnan exclusion, and are thus easily sorbed by resins. Naturally, a change in pH causing dissociation of the electrolyte will strip the resin of the electrolyte.

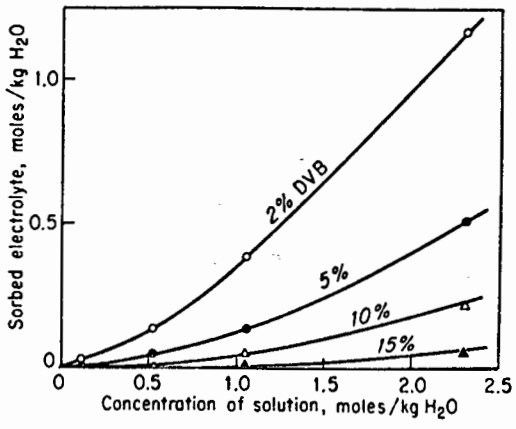

FIGURE 2.5

Effect of concentration on electrolyte sorption in cross-linked resins

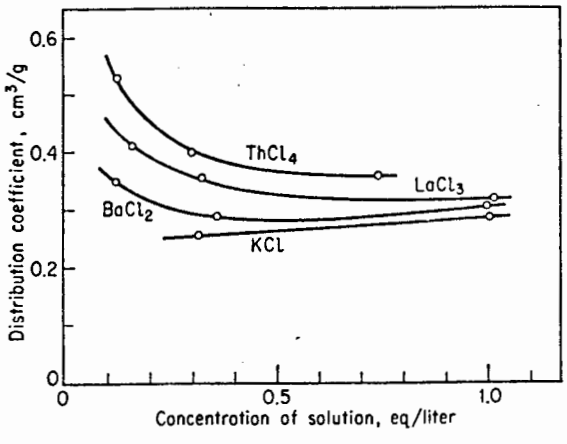

FIGURE 2.6

Effect of co-ion charge on electrolyte sorption in an anion resin

In the case of a macroreticular resin with its large pore size distribution (cf. section 2.121), areas in which electrolyte sorption are both high and low occur. This is due to the low concentration of ionogenic groups in the large pore volume which has a low level of cross-linking. Consequently, the resin exhibits the properties of both low and high DVB content (cf. Figure 2.5) when electrolyte sorption is considered.

2.22 Ion exchange

The following reaction, between a cation exchange resin in A form and solution containing a strong electrolyte BY, will occur when the two are mixed together:

$$R - A + BY \rightleftharpoons R - B + AY \qquad (2.5)$$

The reaction will proceed to some equilibrium point, at which the solution and the resin will contain both competing counter-ions A and B. The reaction (2.5) is, in general, reversible (unless AY is an insoluble salt, in which case the reaction proceeds to completion) and the same equilibrium will be attained irrespective of the direction from which it is approached.

At equilibrium, the concentration ratio of the counter-ions A and B in the resin phase will be different from that in the solution phase, with the ion exchanger selecting one ion in preference to another. In order to place this preference on a quantitative basis, various authors have defined parameters such as the 'law of mass action' (Cosgrave and Strickland [26]), 'equilibrium quotient' (Bucher et al. [27]), 'separation factor', 'selectivity coefficient', incorporating mass or molar concentrations and with or without activity coefficients, to describe the equilibria between resins and solutions. This work will adopt the nomenclature used by Helfferich [23] for expressing resin equilibria, and no attempt will be made to qualify the parameters chosen by thermodynamical treatment as Boari et al. [28] and others have done.

For equation (2.5), an equilibrium constant K, equal to the ratio of the forward and backward reaction velocity constants [29], may be defined such that

$$K_B^A = \frac{(\overline{C}_A)^{Z_A} \cdot (C_B)^{Z_B}}{(\overline{C}_B)^{Z_B} \cdot (C_A)^{Z_A}} \qquad (2.6)$$

where $\overline{C}_A$, $\overline{C}_B$ - concentration of A and B in the resin phase

C_A, C_B - concentration of A and B in the solution phase

Z_A, Z_B - absolute value of the electrochemical valence of A and B

Depending upon the concentration units in which C_A, C_B are expressed, K_B^A may be defined, for an ion exchange equilibrium, as the molal or molar selectivity coefficient.

Alternatively, it may be more convenient to depict the equilibrium relationship graphically in terms of an ion exchange isotherm (equilibrium curve). It is then easier to redefine the concentration units in terms of dimensionless equivalent ionic fractions x (the resin phase) and y (the

solution phase), where

$$x_A = \frac{Z_A \bar{C}_A}{Z_A \bar{C}_A + Z_B \bar{C}_B} \qquad x_B = \frac{Z_B \bar{C}_B}{Z_A \bar{C}_A + Z_B \bar{C}_B} \tag{2.7}$$

and

$$y_A = \frac{Z_A C_A}{Z_A C_A + Z_B C_B} \qquad y_B = \frac{Z_B C_B}{Z_A C_A + Z_B C_B} \tag{2.8}$$

and

$$x_A + x_B = 1, \quad y_A + y_B = 1 \tag{2.9}$$

On the basis of these concentration units, the equilibrium of equation (2.5) may be defined in terms of a separation factor α_B^A by the following

$$\alpha_B^A = \frac{x_A y_B}{x_B y_A} \tag{2.10}$$

Graphically, α_B^A represents the ratio of the shaded areas in Figure 2.7 when x_A is plotted against y_A.

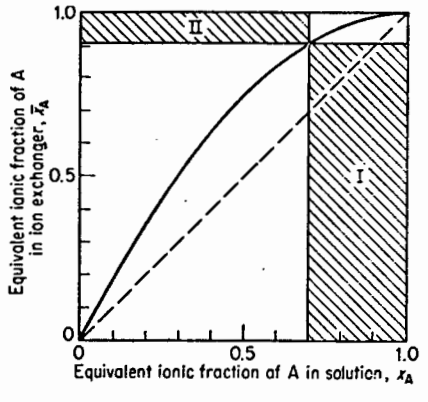

FIGURE 2.7

Ion exchange equilibrium curve

The shape of the curve in Figure 2.7 indicates the selectivity the resin has for species A over species B, for the curve has a negative slope throughout the whole range, i.e. it lies above the diagonal (dotted line) when plotted as $x_A = f(y_A)$. Further, a measure of the degree of preference is the ratio of the shaded areas or the size of the separation factor. An α_B^A value of unity indicates no preference whilst values of α_B^A greater than one are a measure of the preference for A over B. Values of $\alpha_B^A < 1$ indicate a preference for B over A. Factors which affect α are solution concentration, resin type and properties, temperature and ions involved in the exchange. These effects are discussed below.

2.221 Parameters which affect selectivity

2.2211 Counter ion valence and solution concentration:

As a rule, the ion exchanger prefers counter-ions of high valence, and the preference increases with decreasing solution concentration and increasing resin capacity. The effect may be explained in terms of the Donnan potential (cf. section 2.213). The forces attracting counter-ions into the resin bead are proportional to the ionic charge of the counter-ion. Hence, the ion with higher charge is preferred. As explained in section 2.212, the absolute value of the Donnan potential increases with decreasing solution concentration and increasing resin capacity. The result of this effect can readily be seen from the data of Rao and David [30], presented in Figure 2.8, for the exchange of copper and sodium ions at different solution concentrations. At the two highest solution concentration curves, in Figure 2.8, a selectivity reversal occurs. At 3,ON and 4,ON, the resin shows a preference for sodium ions, exhibited by the positive curve shape at these concentrations.

In the case of exchange of univalent ions, any change in Donnan potential with solution concentration would have an equivalent effect on both counter-ions, and no change in resin selectivity would be expected on these grounds. The results in Chapter 4 for the exchange of ammonium for sodium on a strong acid resin bear this out.

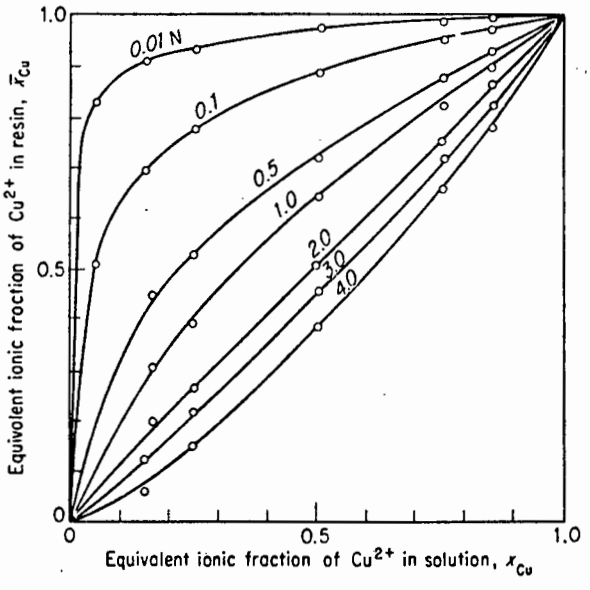

FIGURE 2.8

Effect of concentration on the Na-Cu cation equilibrium

2.2212 Effect of counter-ion type and resin structure on selectivity: Reichenberg [31] presents a detailed treatise on the effect of resin structure and counter-ion type on selectivity based on his experimentation with sodium and potassium ions and various resins, and the results of others in the field. The conclusions reached are that the resin prefers

(i) counter-ions with the smallest hydrated ionic radius, i.e. ions which cause the least amount of resin swelling;

(ii) counter-ions with organic groups which resemble most the exchange matrix;

(iii) counter-ions which have the least association with co-ions in solution.

These factors are explained in terms of the electrostatic attractions between resin ions and counter-ions, interactions of the solvent molecules with one another, complex formation which may occur, and resin swelling and cross-linking which may help or hinder counter-ion uptake. As a result of the above factors, the following selectivity sequence for cation and anion resins is considered to apply:

Ba > Pb > Sr > Ca > Ni > Cd > Cu > Co > Zn > Mg Divalent cations

Tl > Ag > Cs > Rb > K > NH_4 > Na > Li > H Monovalent cations

Citrate > SO_4 > Oxalate > I > NO_3 > CrO_4 > Br > Cl > F Anions

Naturally, the sequence could change with different resin and solution combinations.

2.2213 Effect of temperature and pressure: External pressure on the ion exchange system would have an effect analogous to an increase in cross-linking. However, the overall effect is small, for normal swelling pressures within a bead can be as high as several hundred atmospheres; a slight change in external pressure relative to the swelling pressure would be negligible.

Slight temperature variations around an ambient level of 18°C have little effect on resin selectivity. Semmens and Gregory [32] tested the equilibria of anions resins with organic acids under different temperature conditions, and their results are reported in Figure 2.9. The change in the degree of ionisation of water and therefore pH is utilised in processes where regeneration of resins is accomplished at temperatures of 90°C and more. Special weak resins are employed in the two thermal regeneration processes in commercial use today, the Sirotherm [33] process and Rohm and Haas's new resin [34] XD-2.

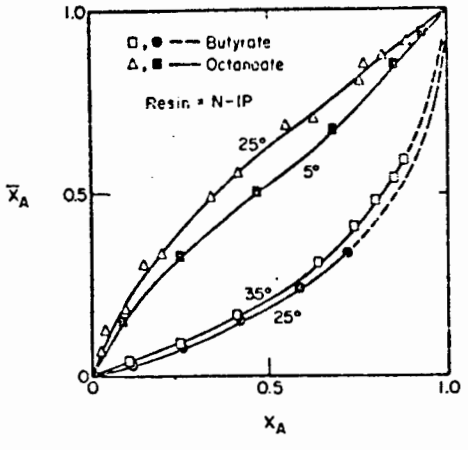

FIGURE 2.9

Effect of temperature on resin equilibria

2.3 RESIN KINETICS

When A-form resin and a strong electrolyte solution BY are contacted a reaction, equation (2.5), commences and continues until equilibrium is attained. The speed with which the exchange (2.5) occurs is finite, and depends upon the resin and solution properties. Boyd et al. [35] first outlined the steps involved in the exchange of two counter-ions. They considered a resin-solution mixture to consist of two phases as depicted in Figure 2.10, with the solution phase made up of two parts - (i) the bulk solution and (ii) a thin film surrounding the bead. The following steps were considered as part of the exchange:

(a) Diffusion of B through the bulk solution and film to the resin bead surface.
(b) Diffusion of B within the resin bead.
(c) Chemical exchange between R-A and B at the exchange sites within the resin particle.
(d) Diffusion of the displaced A out of the resin particle.
(e) Diffusion of A through the solution film and away from the resin.

In the above sequence, steps (a) and (e) and (b) and (d) occur simultaneously in order that electroneutrality is preserved.

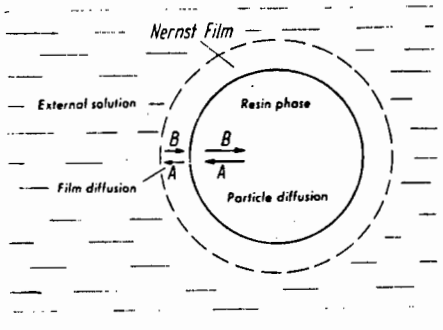

FIGURE 2.10

Schematic diagram of ion exchange resin bead

The overall rate of an ion exchange reaction is controlled by the slowest of the steps outlined above. In general, this is considered to be either diffusion of counter-ions through the liquid film, or diffusion of ions within the resin bead itself. Only in cases where chemical reaction between the functional group and the exchanging species (e.g. formation of chemical complexes with chelating resin groups) occurs, is step (c) above considered to be rate controlling.

Helfferich [23] depicts schematically (Figure 2.11) the concentration profiles that are likely to occur when ideal 'film' diffusion and 'particle' diffusion control applies to the ion exchange bead.

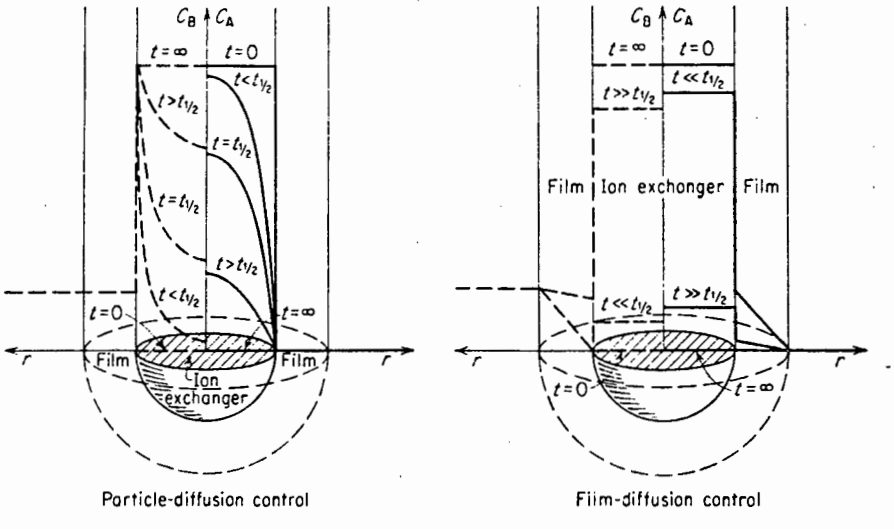

FIGURE 2.11

Concentration profiles during ion exchange

The concept of a diffusion 'film' surrounding a resin bead is an idealization developed by Nernst, and resistance to mass transfer in the liquid phase is assumed to lie entirely within the Nernst film. When film diffusion is controlling exchange, a concentration gradient exists across the film and provides the 'driving force' for exchange to proceed. Particle diffusion is assumed so much faster than film diffusion, that concentration gradients which may exist within the bead are instantaneously levelled out - cf. Figure 2.11.

For particle (pore) diffusion control, no gradient across the Nernst film is assumed to exist. Figure 2.11 shows the radial profiles of the two exchanging species within the bead. Interruption of the exchange by removal of the resin beads from solution is an easy method of distinguishing which mass transfer step is rate controlling. On re-immersion, an instantaneous increase in the rate of pore diffusion controlled exchange will occur, for the internal concentration gradients have had an opportunity to level out during the interruption. Typical results of the test are shown in Figure 2.12.

A detailed outline of the theories and mechanisms of the two types of exchange is presented below. In general, particle diffusion is now described in terms of the Nernst-Plank theory and film diffusion by either a 'driving force' gradient across the film or in terms of Nernst-Plank theory. Both exchange types have also been described mathematically by various empirical rate expressions.

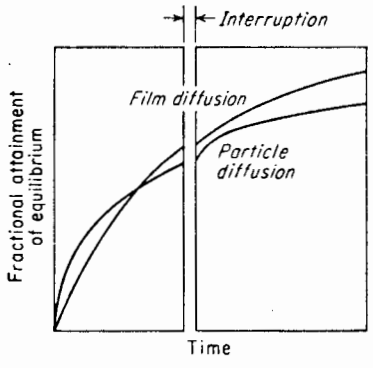

FIGURE 2.12

Results from an interruption test

2.31 Particle diffusion

In the course of this investigation, when dealing with the loading and regeneration of resins performing a desalination function, an attempt will be made to maximise the rate of exchange. The eventual rate limiting step, when the flow past the resin beads is high or the solution concentration is high, is likely to be pore diffusion controlled.

2.311 Factors affecting particle diffusion: Pore diffusion is the phenomenon whereby counter-ions move within the solution contained in the resin pores. The rate of movement of the ions within the pores is generally an order of magnitude lower than in a solution of infinite volume. This is due to the 'tortuosity' of the pores. Increasing the degree of cross-linking of a resin decreases the ability of the bead to swell and contributes to a smaller pore size-distribution (cf. section 2.2). Under these conditions, the counter-ion diffusivities (a measure of their mobility) are decreased. Logically, the rate of exchange is dependent upon the speed with which the counter-ions are able to diffuse. It can therefore be concluded that the rate of exchange is directly dependent upon the counter-ion diffusivities, which in turn are dependent upon the resin pore structure.

The only other resin property to have a bearing on pore diffusion rate is the bead diameter. (The external solution properties have no effect on pore diffusion.) Increasing bead diameter increases the diffusion path length. Consequently, the rate is inversely proportional to the bead diameter.

2.312 Particle diffusion rate models: First attempts at formulating expressions for the rate of pore diffusion controlled ion exchange, were by way of empirical diffusion equations of which Vermeulen's [36] quadratic driving force expression is perhaps the best known. Glueckauf [37] compares four empirical expressions for resin separation factors (section 2.22) varying between >3 and <100. Included in the comparison are the linear and quadratic driving force expressions

$$N_A = \frac{kD}{r^2}\left[q_A - \bar{q}_A\right] \qquad \text{Linear Driving Force} \qquad (2.11)$$

and

$$N_A = \frac{kD}{r^2}\left[\frac{q_A^2 - \bar{q}_A^2}{2\bar{q}_A}\right] \qquad \text{Quadratic Driving Force} \qquad (2.12)$$

where N_A - flux of species A

k - constant

D - diffusivity

r - bead radius

q_A - concentration of A at the bead surface

$\bar{q}_A$ - mean concentration of A within the bead.

The conclusion drawn by Glueckauf is that each rate expression is applicable for a given separation factor (α_B^A) range.

Further attempts at deriving a more generalised expression for diffusion in the resin sphere were based on Fick's Law. In this case, the flux of A within the resin bead when A and B counter-ions are exchanging according to equation (2.5) is:

$$J_A = - D \frac{d\overline{C}_A}{dZ} \tag{2.13}$$

where J_A - flux of A
D - diffusivity of A in the bead
$\overline{C}_A$ - concentration of A at some point in the bead
Z - length parameter

Incorporating material balance considerations with the flux equation (2.13) and converting for spherical geometry the following rate expression (often referred to as Fick's second law of diffusion) describing diffusion in the bead is derived

$$\frac{\partial \overline{C}_A}{\partial t} = D\left(\frac{\partial^2 \overline{C}_A}{\partial r^2} + \frac{2}{r}\frac{\partial \overline{C}_A}{\partial r}\right) \tag{2.14}$$

where r - distance from centre of the bead.

Analytic solutions for equation (2.14) under various initial and boundary conditions are presented by Crank [38] and the analogous heat transfer expression has also been solved by Carslaw and Jaeger [39]. The solutions are usually in terms of a 'fractional approach to equilibrium' parameter defined as

$$F(t) = \frac{\overline{C}_A^0 - \overline{C}_A(t)}{\overline{C}_A^0 - \overline{C}_A^\infty} \tag{2.15}$$

where $\overline{C}_A^0$ - concentration of A in the resin at time t = 0
$\overline{C}_A^\infty$ - concentration of A in the resin at equilibrium (t = ∞)
$\overline{C}_A(t)$ - concentration of A in the resin at time t.

The solutions of equation (2.14) further show that F(t) is only dependent upon the dimensionless time parameter τ

where $$\tau = \frac{Dt}{r_0} \tag{2.16}$$

and D - diffusivity
t - time
r_0 - radius of the resin bead

2.3121 Homogeneous sphere model: It was Schlogl and Helfferich [40] who first raised doubts about the ability of Fick's second law (equation 2.14) to adequately describe the rate of ion exchange when two different counter-ions A and B are participating. Schlogl felt that the exchange flux for each of the counter-ions was not the same, for the ions in solution each have different mobilities. These varying mobilities are coupled together when exchange occurs, and produce an electric potential gradient. The flux of each of the ions in solution is then given by the Nernst-Planck equations, and therefore, for the exchange in equation (2.5), the overall flux for each counter-ion is equal to the sum of the fluxes due to Fickian diffusion and the electrochemical gradient. I.e. for i = ion A or B,

$$\phi_i = (J_i)_{\text{diffusion}} + (J_i)_{\text{electrochemical gradient}} \tag{2.17}$$

where $$(J_i)_{\text{diff}} = - D_i \frac{d\bar{C}_i}{dr} \text{ and } (J_i)_{\text{elec grad}} = - \frac{Z_i D_i \bar{C}_i F}{RT} \frac{d\psi}{dr} \tag{2.18}$$

and ϕ_i - overall coupled flux of counter-ion i
Z_i - valence of species i
ψ - electric potential
F,R - constants
T - absolute temperature

Preservation of electroneutrality throughout the bead dictates that the fluxes of A and B should be equal but opposite so that

$$Z_A\phi_A + Z_B\phi_B = 0 \tag{2.19}$$

On the basis of a fixed resin exchange capacity, the total counter-ion concentration in the bead is fixed and given by

$$Z_A\overline{C}_A + Z_B\overline{C}_B = \overline{C} \tag{2.20}$$

where $\overline{C}$ is resin exchange capacity.

Conditions (2.19) and (2.20) allow equation (2.18) to be rearranged so that the electric potential gradient is eliminated. The overall flux for counter-ion A then becomes

$$\phi_A = -\left[\frac{D_A D_B (Z_A^2 \overline{C}_A + Z_B^2 \overline{C}_B)}{D_A Z_A^2 \overline{C}_A + D_B Z_B^2 \overline{C}_B}\right] \frac{d\overline{C}_A}{dr} \tag{2.21}$$

Helfferich et al. [41] have solved equation (2.21) for the exchange of univalent ions by a finite difference numerical technique based on the following assumptions:

(i) that the resin is an homogeneous phase

(ii) that the solution volume is infinite, and that the concentration of of A in solution is zero

(iii) that equilibrium exists at the bead solution interface, and that the magnitude of the separation factor $\alpha = 1$.

Their solution has been computed for diffusivity ratios of A and B varying such that $0{,}1 < D_A/D_B < 10$. Plesset et al. [42] have solved the same flux equation (2.21) but for the exchange of univalent ions for divalent ions. Kataoka and Yoshida [43] have extended the work of the above authors to include the situation where resin swelling occurs simultaneously with exchange. Their predictions show better agreement with experimental results when appreciable (>10%) change in resin diameter occurs during conversion.

Turner et al. [44] have solved equation (2.21) for the case of finite solution volume, equal equivalents of resin and solution together, and a separation factor $\alpha > 1$. Turner's aim was to check the applicability of the diffusivity term in equation (2.21) for the exchange of univalent ions on a gel resin. Under these conditions equation (2.21) can be rearranged as follows:

Define equivalent ion fractions x_A and x_B such that

$$x_A = \frac{Z_A \bar{C}_A}{\bar{C}} \quad \text{and} \quad x_B = \frac{Z_B \bar{C}_B}{\bar{C}} \tag{2.22}$$

then, from equation (2.20)

$$x_A + x_B = 1 \tag{2.23}$$

and for univalent ions

$$Z_A = Z_B = 1 \tag{2.24}$$

Substituting into (2.21), the flux for A becomes

$$\phi_A = - \frac{D_A}{1 + \beta x_A} \frac{d\bar{C}_A}{dr} \tag{2.25}$$

where $$\beta = \frac{D_A}{D_B} - 1 \tag{2.26}$$

Turner then defined an interdiffusion coefficient D such that

$$D = \frac{D_A}{1 + \left[\frac{D_A}{D_B} - 1\right] x_A} = \frac{D_A}{1 + \beta x_A} \tag{2.27}$$

and showed, by comparison of a numerical solution of equation (2.25) using an implicit scheme with experimental data, that the interdiffusion coefficient varied with composition of the resin according to equation (2.27).

2.3122 Bi-disperse pore model: Weatherley and Turner [45] repeated Turner's [44] earlier work, but with a macroporous resin instead of the previous gel resin. The results showed that the 'homogeneous sphere' kinetic model described by equation (2.25) was no longer adequate in predicting exchange rates.

Following the work of Ruckenstein et al. [46], Weatherley predicted that a macroporous resin could be considered to consist (cf. Figure 2.13) of two types of pores. This bi-disperse pore size distribution could mean

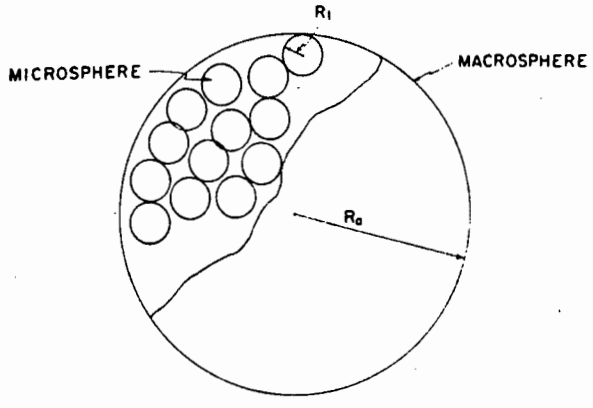

FIGURE 2.13
Schematic diagram of an ion exchange bead

that counter-ion diffusivities would be different at various points within the resin bead. Further, the macropores, due to their large size, would not necessarily exclude bulk solution electrolyte via Donnan exclusion (cf. section 2.212) as efficiently as a gel resin might.

Based on the assumption of two counter-ion diffusivities and macrosphere and microsphere bead radii, the following equations analogous to the 'homogeneous sphere' model in equation (2.25) can be written to describe the mass transfer in a macroporous resin

$$\frac{\partial C_i}{\partial t} = \frac{D_i}{r_i^2} \cdot \frac{\partial}{\partial r_i} \left(r_i^2 \frac{\partial C_i}{\partial r_i}\right) \quad \text{micropore diffusion} \tag{2.28}$$

$$\frac{\partial C_a}{\partial t} = \frac{D_a}{r_a^2} \cdot \frac{\partial}{\partial r_a} \left(\frac{\partial C_a}{\partial r_a}\right) - \frac{B(1-\varepsilon_a)}{\varepsilon_a R_i} \cdot D_i \left(\frac{\partial C_i}{\partial r_i}\right)_{r_i=R_i} \quad \text{macropore diffusion} \tag{2.29}$$

Weatherley's solution to equations (2.28) and (2.29) is presented in Figure 2.14, where suitable choice of the macro and micropore diffusivity ratio provides a good comparison of experimental and predicted results. Weatherley further mentions that the change in counter-ion interdiffusion coefficient (2.27) with composition, is not nearly as concentration dependent as it is in the case of gel resins. Use of an average interdiffusion value for complete conversion of the resin from one form to another does

not introduce a significant error.

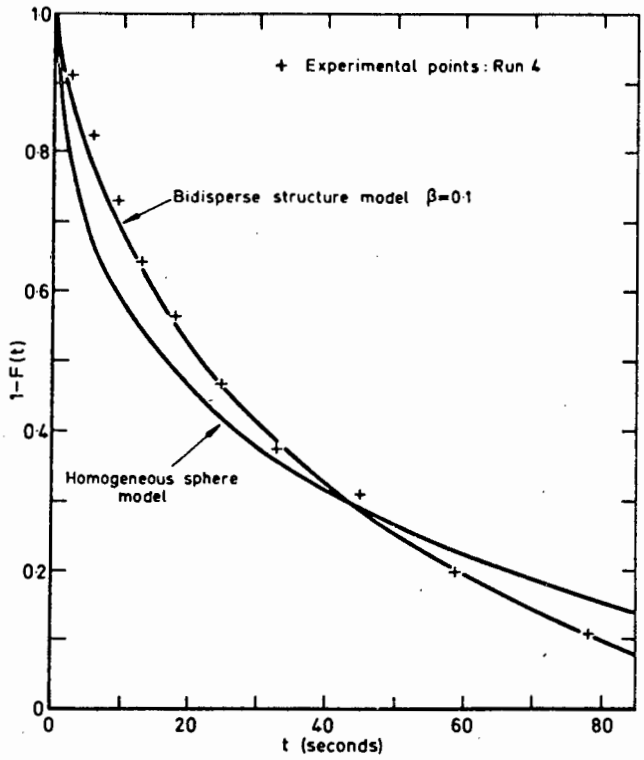

FIGURE 2.14

Comparison of pore diffusion rate models

2.32 Film diffusion

2.321 Factors affecting film diffusion: When the rate controlling step of an ion exchange reaction is film diffusion, it is usually the solution properties which dictate the control. Two major solution properties are generally responsible. Firstly, the 'film thickness'; it is a function of the flow of solution around the resin bead, and the degree of shear which exists between the solid and liquid. As the film thickness decreases, due to increasing shear forces, so the rate of mass transfer through the film increases. Ultimately, diffusion through the film is no longer rate controlling. Correlations of the flow properties and mass transfer in the film have been derived by various authors, and are outlined in section 2.4322.

Secondly, the solution concentration has a direct effect on the rate of exchange. Since the assumption upon which film diffusion is based, that of equilibrium at the bead-solution interface, is determined by the composition of the bead at any point in time, the gradient across the film (i.e. the difference in concentration between the bulk solution and the equilibrium at the bead surface, cf. Figure 2.11) is directly proportional to the concentration of the bulk solution. As bulk solution concentration increases, so does the concentration gradient. Helfferich [23] states that at concentrations higher than 0,1N, film diffusion control is no longer rate controlling for the high concentration gradient makes film diffusion faster than particle diffusion.

Two properties of the resin bead, the bead diameter and the resin capacity (the number of exchange sites per unit volume) have an effect on film diffusion rate. Logically, as the bead radius increases, so the area per unit volume of resin through which transfer can take place decreases, and so does the rate. Solution of equation (2.31) (section 2.322) illustrates this dependence.

2.322 Rate theories: Initial attempts at a quantitative explanation of film diffusion controlled mass transfer between two phases were made on the basis of the two film theory, i.e. resistance to transfer was assumed to exist either in the Nernst film or in an analogous film in the 'other' phase. Considering the film diffusion controlled case in Figure 2.11, and the following assumptions

(i) that the bulk solution is perfectly mixed
(ii) that equilibrium exists at the resin surface

the following rate expression for a linear concentration gradient across the film was postulated:

$$R = k_L a(C_A - C_A^*) \qquad (2.30)$$

where R - rate of exchange

k_L - mass transfer coefficient

a - area through which exchange can occur cm^2/cm^3

C_A - concentration of A in the bulk solution

C_A^* - concentration of A at the resin surface in equilibrium within the resin

Various authors, Marchello and Davis [47], Rao et al. [30], Kuo et al. [48] have evaluated batch kinetic tests controlled by film diffusion using equation (2.30). The comparison of computed data from the integration of (2.30) and experimental data has shown good agreement. However, equation (2.30) has no mechanistic basis other than that diffusion across a hypothetical film is controlled by a linear concentration gradient.

The other approach adopted in deriving a quantitative description of film diffusion has been made on the basis of Fick's first law and modifications thereof. Glaski et al. [49], and Smith and Dranoff [50] have undertaken a comparison of the following rate expressions (based on the monovalent exchange of equation (2.5)),

(i) based on Fick's law, where the flux across the film is given by

$$N_A = - D \frac{dC_A}{dZ} \tag{2.31}$$

where N_A - flux of species A
D - diffusivity
Z - film thickness

(ii) when incorporating the electrostatic potential gradients which occur when ions diffuse with Fick's law, as suggested by Schlogl and Helfferich [40], the flux for component A becomes

$$N_A = - D_A \frac{dC_A}{dZ} - \frac{C_A F}{RT} \frac{d\psi}{dZ} \quad \text{ionic diffusion model} \tag{2.32}$$

where $\frac{C_A F}{RT} \frac{d\psi}{dZ}$ - ionic flux of exchanging counter-ions.

Equations (2.31) and (2.32), with the appropriate boundary conditions and material balance consideration, have been solved by Glaski [49] and compared with experimental results. The comparison has shown that the ionic diffusion model, the ordinary diffusion model and a mass action model are all adequate for a description of film diffusion.

2.33 Electrolyte sorption

The rate of electrolyte (AY or BY) sorption or desorption can be calculated from the Nernst Planck equation (2.18), but with the equation applying to a counter-ion and the co-ion Y. Based on electroneutrality throughout the bead, the flux coupling produces an equation

$$Z_A J_A + Z_Y J_Y = 0 \qquad (2.33)$$

where J_A, J_Y - flux of A and Y
Z_A, Z_Y - valence of the ions (negative for Y).

Substituting (2.33) into (2.18) and rearranging allows the potential gradient term to be eliminated and an equation analogous to (2.21) is derived. In general, the concentration of Y in the bead will be significantly less than A or B since the latter are present as both sorbed electrolyte and exchangeable ions. On the assumption of low co-ion concentration, the diffusivity term of (2.21) can be rearranged as follows:

Assume $$\overline{C}_Y << \overline{C}_A \qquad (2.34)$$

then $$\left[\frac{D_A D_Y (Z_A^2 C_A + Z_Y^2 C_Y)}{Z_A^2 D_A C_A + Z_Y^2 D_Y C_Y}\right] \qquad (2.35)$$

becomes $$\frac{D_A D_Y (Z_A^2 C_A)}{Z_A^2 D_A C_A} = D_Y \qquad (2.36)$$

and the flux equation for electrolyte sorption reduces to

$$J_A = - D_Y \frac{d\overline{C}_A}{dr} \qquad (2.37)$$

which is equivalent to Fick's second law of diffusion (cf. equation 2.13).

Equation (2.37) shows that the rate of electrolyte sorption is dependent on the diffusivity of the co-ion within the bead, and can be predicted for a gel resin by the solutions of equation (2.14) given by Crank [38] with suitable choice of the diffusivity (D_Y), bead radius (r) terms, and the equilibrium conditions.

2.4 CHARACTERISTICS OF ION EXCHANGE COLUMNS

2.41 Background

Most ion exchange operations are conducted in columns, with solution passing sequentially through layers of ion exchange resin beads. Until fairly recently, most columns were of the fixed bed type consisting of a cylindrical section, domed ends and internal distributors. Solution flow was routed either downwards through a packed bed of resin, or upwards through a fluidised bed. Recent column developments have included the use of 'moving' resin beds. In columns of this type, resin is moved from one column to another or from one section of column to another section in order to perform the load and regeneration (the reversal of the loading step) exchanges. A description of each of the column types is given below.

2.42 Fixed bed columns

A fixed bed column is one in which all the resin operations (e.g. loading, regeneration, washing) are conducted in one vessel. By variation of the direction of solution flow through the column, different load and regeneration properties of the resin bed can be attained. Each of these different flow configurations, outlined below, have found favour with ion exchange column operators for achieving specific improvements to exchange efficiencies.

2.421 Co-current load and regeneration: The normal operation of a fixed bed ion exchange column would consist of the following three sequential steps:

(i) resin loading - feed solution is passed downflow through the packed resin bed and exchange takes place;

(ii) backwash - a liquid stream, usually feed, is routed upwards through the bed of resin causing bed expansion and resin fluidisation. The purpose of the backwash is to classify the bed, and remove any particulate matter which may have become trapped within the bed;

(iii) resin regeneration - a regenerant stream followed by a rinse stream is passed in an analogous manner to the feed through the packed bed in downflow.

The form of operation outlined, is termed co-current packed bed, for both feed and regenerant pass downflow through the resin.

An alternative flow system, co-current fluidised bed, results when both feed and regenerant solution flow in the same direction but upwards through a fluidised resin bed.

The disadvantage of both of the co-current flow systems is that their regeneration efficiency is not high. This is due to the concentration of ions for which the resin has the greatest affinity being highest in the resin beads closest to the point at which feed contacts the resin. In order for the regenerant to remove these ions from the resin, it has to 'push' them through the whole length of the resin bed, with the resin throughout the bed preferring the counter-ion that is being stripped.

The other disadvantage of this type of packed bed is the high pressure drop across the bed which can result when particulate matter is trapped in the bead interstices. This is likely when the feed solution has not been filtered before the ion exchange step.

2.422 Counter-current load and regeneration: This mode of operation is typified by the Lewatit fluidised bed process [51], (cf. Figure 2.15), in which feed and regenerant solution flow in opposite directions though the resin. Normally, feed solution flow would be upwards in order to alleviate the pressure drop problems outlined above.

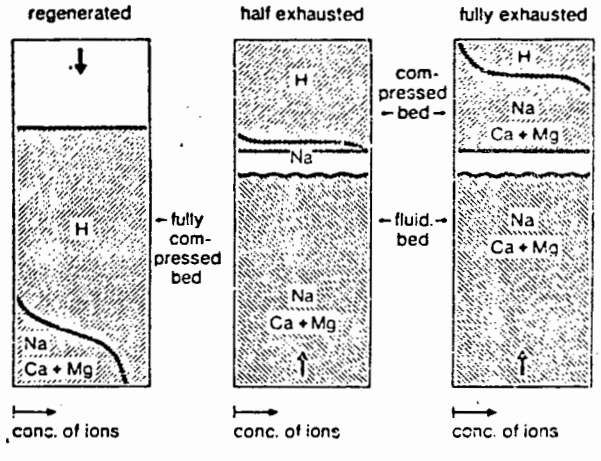

FIGURE 2.15

Loading in a countercurrent fixed bed

The advantage of this type of operation is the greater regeneration efficiency which can be achieved. Figure 2.15 shows a bed in varying degrees of exhaustion. The divalent ions calcium and magnesium predominate at the bottom of the bed, allowing for easier removal by the hydrogen counter-ion during countercurrent regenerant flow.

2.423 Design of fixed bed columns: To date, the design of fixed bed columns has been undertaken on the basis of data supplied by the resin manufacturers and rule of thumb considerations evolved during the operation of columns. Using the load and regeneration steps of a cation column removing the sodium fraction from a saline solution in a two bed desalination operation as an example, the following reactions occur:

$$R - H + NaCl \rightarrow R - Na + HCl \qquad \text{Resin Load} \qquad (2.38)$$

$$R - Na + H^{+} \rightarrow R - H + Na^{+} \qquad \text{Resin Regeneration} \qquad (2.39)$$

Suitable design of the cation column would be based on the following:

2.4231 Bed capacity: The allowable level of sodium ions in the treated water dictates the capacity of the resin bed. During the load step (equation 2.38) the product water from the column contains initially only hydrogen cations. As the resin becomes exhausted, the sodium content of the product water slowly increases giving rise to the breakthrough curve of Figure 2.16. The volume of feed which has passed through the bed up to the point at which the sodium content of the product water exceeds the allowable level, is the breakthrough capacity of the bed. The affinity of the resin for the loading ion (sodium) and the flow characteristics of the column determine the steepness of the breakthrough curve in Figure 2.16. The volume of resin in the bed (section b, Figure 2.16) over which the load ion concentration fraction varies from zero to one is called the exchange zone. When sodium ions appear in the column effluent and the load exchange is stopped, the exchange zone volume of partially loaded resin remains. The necessity of this 'dead volume' of resin in fixed bed columns results in greater resin inventories for a particular ion exchange operation.

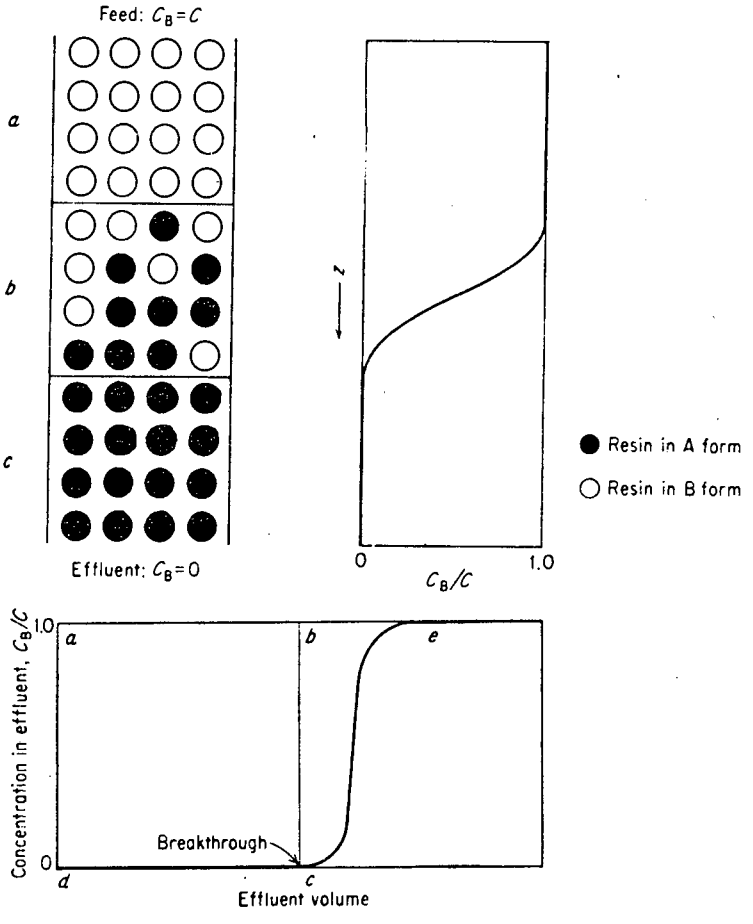

FIGURE 2.16

Fixed bed column breakthrough curve

2.4232 Flow rate and pressure drop: In packed bed operation, pressure drop is dependent both on flow rate and the nature of the water to be treated. In general, the resin manufacturer will recommend a certain linear velocity through the resin. This value would have been determined by experimentation, and would usually be sufficiently high so that film diffusion (section 2.32) would no longer be the rate controlling mechanism. On the basis of a required volumetric flow rate, the cross-section of the packed bed column would be determined.

In the case of a fluidised bed column, the linear velocity would be determined by the fluidisation characteristics of the resin. In general, a 100% expansion of the packed resin bed would be deemed sufficient and the linear velocity necessary to achieve this value would be used as the basis for determining column diameter.

2.4233 Regeneration: On termination of the load cycle, the length of which is determined by the concentration and volumetric flow rate of the feed water and the breakthrough capacity of the bed, feed flow is stopped and the regenerant introduced. In the case of equation (2.39), the regenerant would be a strong acid. The volume of regenerant required to achieve complete conversion of the resin is dependent upon the relative affinities of the ions being exchanged. For strong acid resins, an excess of 200%-300% above stoichiometric requirements of equation (2.39) may be necessary. The concentration of sodium ions in the stream leaving the bed during regeneration is shown in Figure 2.17.

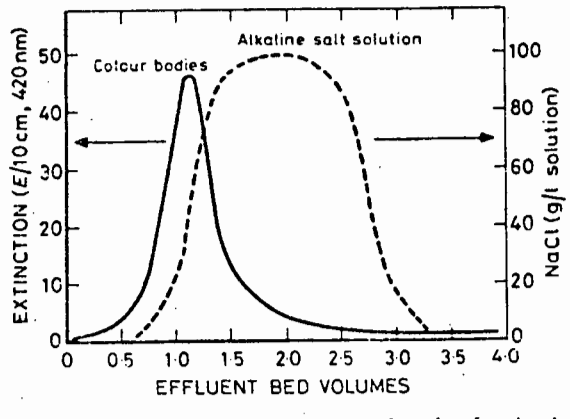

Course of regeneration in the decolourisation of remelted sugar using the fluidised bed process

FIGURE 2.17

Regeneration exchange effluent concentration volume curve

Following the introduction of a sufficient excess of regenerant, that fraction of acid still remaining within the bed has to be washed out. The volume of wash water necessary to achieve the required degree of washing varies, being dependent upon the resin properties. Gel resins would require slightly less wash, for Donnan exclusion would prevent acid entering the resin pore structure whilst weak acid or base resins would require correspondinly greater wash for Donnan exclusion of these resins in the presence of an acid or base is virtually absent.

2.43 Moving bed columns

The development of moving bed columns is a recent phenomenon aimed at improving the efficiency of the batch contact system embodied in fixed beds, and to produce load and regenerant product streams with constant compositions in contrast to the effluent history curves presented in Figures 2.16 and 2.17. Gilwood [52] points out that these two factors result in significant savings of both capital and chemicals.

Moving bed columns are divided into two basic types, those in which resin is in the form of packed beds, and those where the resin is a series of fluidized beds. The flow in the packed bed type can be either co-current or countercurrent, i.e. solution and resin flows are either in the same or in opposite directions. Fluidized beds are based on countercurrent flow systems, hence the general term continuous countercurrent ion exchange (CCIX).

Moving bed ion exchange has found application in virtually every field in which fixed beds used previously to dominate. Haines et al. [53] outline a zinc recovery process from pickle liquors, Naden et al. [54] remove copper from leach tailings, Newman [55] removes chromates from cooling tower blow-down, Higgins [56] desalinates well water and Doshi et al. [57] remove copper from a rayon spinning wash stream, all using moving bed ion exchange processes.

2.431 Packed beds: The patent literature abounds with packed moving bed columns, but only a few types have been tested commercially. Of these, the Higgins or Chem-seps contactor and the Asahi system are perhaps the best known.

Bingham and Chopra [58] give an exact description of the Chem-seps process. The essential features are a closed loop column in which resin is periodically 'pushed' around from one section to another. The conventional load, regeneration and wash steps are each conducted on the pulsed quantities of resin. The AVCO system, a development by Gold et al. [59] operates in a manner similar to the Higgins contactor.

The Asahi process has two separate columns for load and regeneration, and moves resin between them. Blesing [60] states that the Asahi process has fewer valves in resin lines when compared with Chem-seps, and is therefore superior, for less resin attrition is likely to occur.

2.432 Fluidised beds: The fluidised moving bed systems which have been developed to a point of commercial use are based on the Cloete-Streat [61] contact system. A parallel development by Rosenbaum et al. [62] for the U.S. Bureau of Mines and the South African National Institute for Metallurgy has resulted in almost identical continuous countercurrent fluidised moving bed ion exchange contactors being placed in use for the recovery of uranium from leach liquors.

The advantage of this system over the packed bed type is that it can accommodate particulate matter in the feed, e.g. a slime pulp in the case of uranium recovery.

2.4321 Operation of a fluidised bed column: Figure 2.18 outlines schematically the details of the N.I.M. version of the Cloete-Streat contactor. Although operation is termed continuous, solution and resin flows do not occur simultaneously, but periodically. For the first time period in the cyclic operation, solution enters the bottom of the column and flows upwards, fluidising the resin in each 'stage' (the stages are created by resin separator plates within the column and do not necessarily correspond to mass transfer equilibrium stages) of the multistage column. At the end of the solution flow period (the length of the period is determined by the desired operating conditions), the resin within each 'stage' is allowed to settle. On completion of resin settling, solution flow through the column is allowed to reverse, and a packed bed of resin moves downwards from one 'stage' to the next. When one 'stage-volume' of resin has been transferred down, the bottom 'stage-volume' leaves the column, and the upward solution flow through the column is resumed.

In the manner outlined above, solution and resin contact each other under countercurrent but periodic flow conditions. Horn et al. [63,64] have modelled the periodic operation of a continuous flow reactor and a distillation column. They conclude that, under certain operating conditions, higher operating efficiencies can be achieved with periodic processes. They further show that in the operation of a periodic process a pseudo steady state is achieved; in that although the solution composition leaving the top of the column will vary with time during the solution flow period, the limits of the composition change and the rate of the composition change are the same for each successive period, allowing an average composition over a flow period to be established.

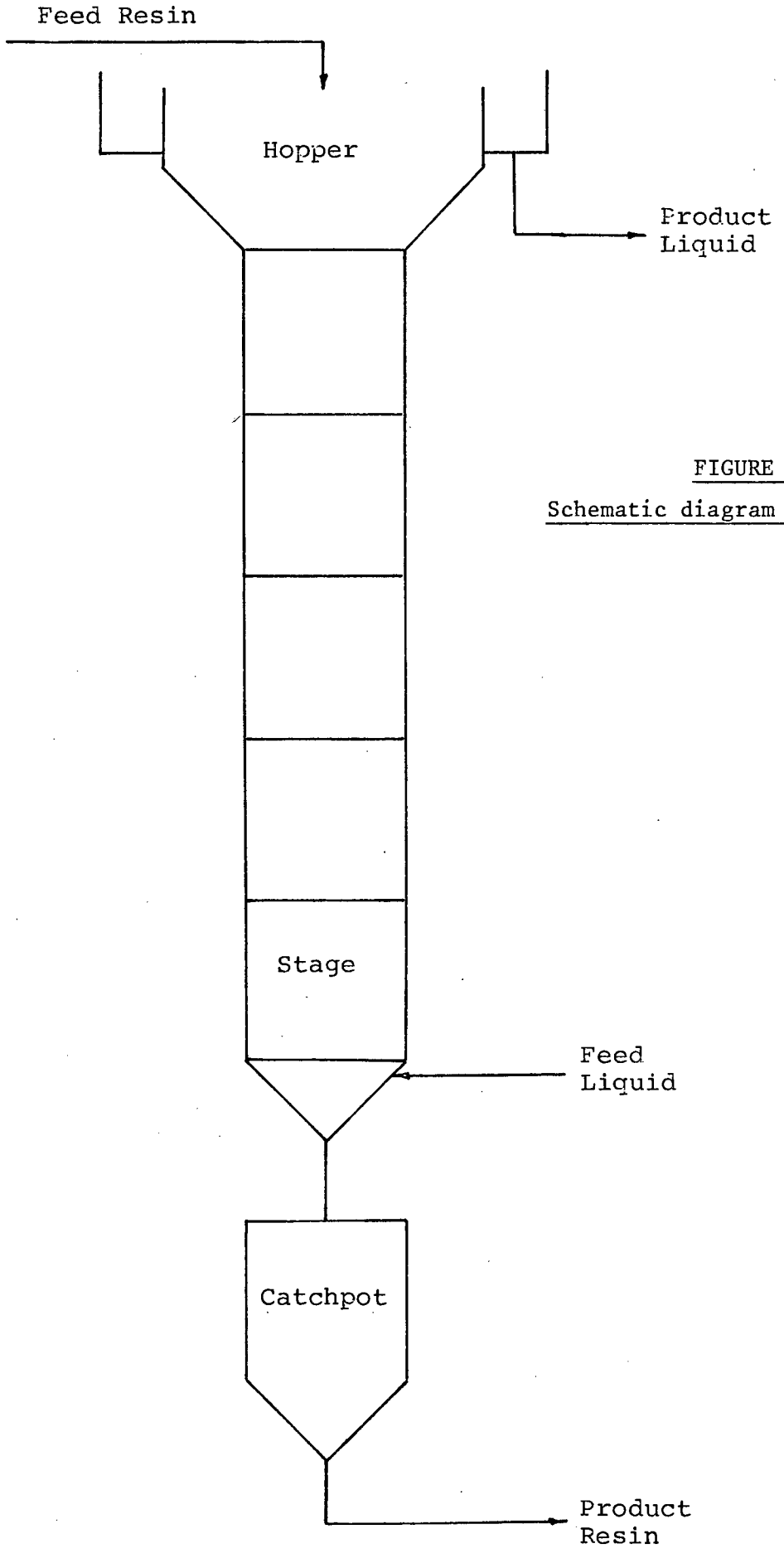

FIGURE 2.18

Schematic diagram of a CCIX column

2.4322 Existing models of the fluidised bed column: Present models of the fluidised bed column outlined in Figure 2.1 are based on film diffusion control of the exchange reaction, and in a manner analogous to the design of two phase absorption systems, these models rely on a mass transfer coefficient derived from the linear driving force relationship outlined in section 2.322, equation (2.30).

Extensive investigation by various researchers has been directed towards determining accurate values for the mass transfer coefficient of equation (2.30) under various solution flow conditions through both packed and fluidised beds. In most cases, the results have enlarged on the work of Rowe et al. [65,66] who investigated heat and mass transfer from a flowing fluid to a single sphere and an array of spheres. Rowe's results were published in the form of an empirical correlation containing the Sherwood Schmidt and Reynolds numbers in the following form:

$$Sh = A + B.Sc^{m}Re^{n} \qquad (2.40)$$

Snowdon and Turner [67,68,69] investigated the effect of Reynolds number and bed voidage for uni-univalent and uni-divalent ion exchange reactions. They show that Sherwood number is inversely proportional to the fluidised bed voidage, and that the mass transfer coefficient is dependent on the solution composition. Koloini [70] tested resins with different size distributions and found results analogous to those of Snowdon.

Dodds et al. [71] and Slater [72] have used the above correlations in their attempts to predict the performance of a multistage fluidised bed column. These authors model the CCIX column on the basis of the time dependent variation of resin and solution compositions. Dodds's very complex model relies on a successive calculation of the mass transfer within each 'stage' of the column in order to predict the composition of the resin and liquid streams leaving a 'stage'. In this manner, a sequential calculation is performed up the column with the composition distribution through each 'stage' being updated on each successive cycle, until a pseudo-steady state is attained. Dodds assumes perfect mixing of both phases within each 'stage' and a given concentration distribution of resin beads within each 'stage' in calculations for his model.

Slater adopts a simpler approach, and writes the mass transfer function for each 'stage' at pseudo steady state. He then proceeds to solve the differential equations simultaneously in order to predict the composition changes which occur with time during each cycle in each stage of the column. Slater assumes, as does Dodds, that perfect mixing of each phase occurs within each stage of the column. Slater does, however, add that this is probably not the case and that plug flow of liquid and mixing of resin is more likely. Snowdon and Turner [67] based their assumption of plug flow of liquid through a bed of resin, on the evidence of previous tracer experiments.

Streat and Gupta [73] advocate the use of the Nernst-Planck equations as an alternative mass transfer function for prediction of the performance of a multistage fluidised bed column.

2.4323 Proposed model of the fluidised bed column: Considering the multistage fluidised bed ion exchange column to be a continuous contact device which can be operated at steady state, with the mass transfer rate being controlled by either film or pore diffusion depending on the column operating conditions, allows the view to be taken that the system can be modelled on the same basis as such other stagewise contact devices, distillation and absorbtion columns. This approach would simplify the design of CCIX columns and dispense with the elaborate calculation procedures adopted by Slater and Dodds. Further, if some method of estimating the 'stage efficiency' of the CCIX column can be derived a graphical design procedure of the McCabe-Thiele type can be adopted and used to describe fully the ion exchange system.

On the basis of the foregoing, the following nomenclature is outlined for the CCIX column presented schematically in Figure 2.19:

F_L, F_R - volumetric flow rates of liquid and resin
C_L, C_R - concentrations of ionic species in liquid and resin
y_A, x_A - ion fraction of counter-ion A in liquid and resin
t , b - subscripts denoting top and bottom of the column.

For conversion of resin and liquid streams within the column according to equation (2.5), the following mass balance over the column can be written for counter-ions A and B, based on the assumption that any volume changes that may occur within the column are negligible, that operation is at steady state and

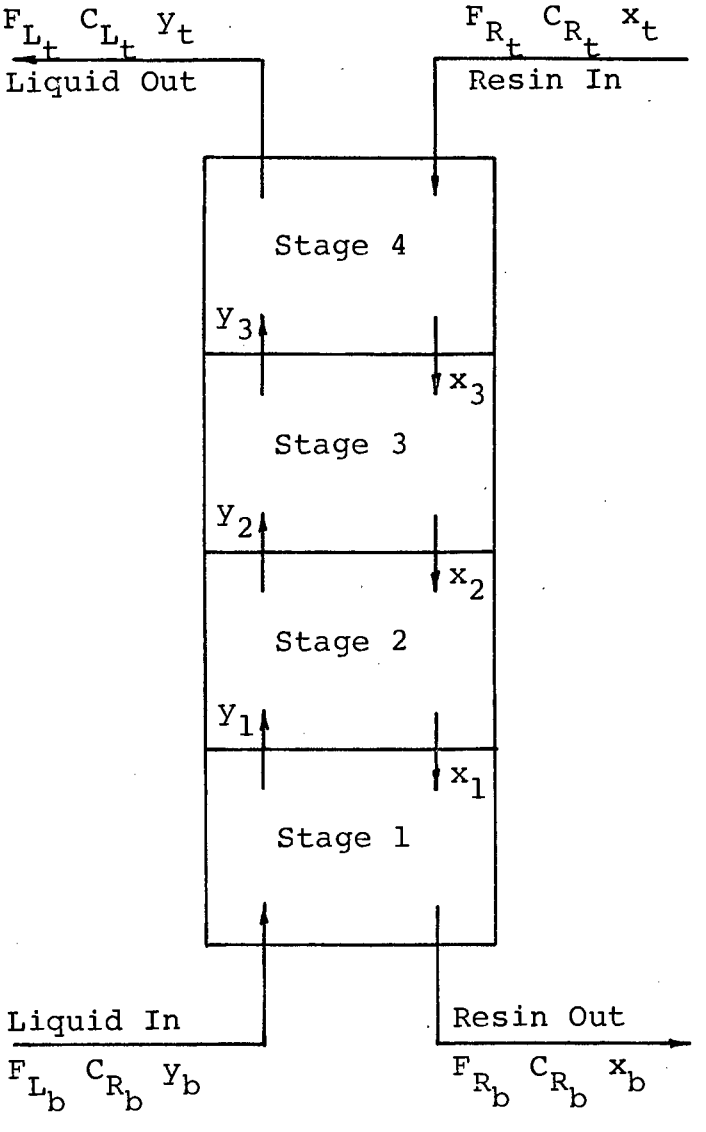

Note: The volume between each resin separator is called a stage and these are numbered from the bottom up. The stream compositions crossing the resin separators are then numbered as shown.

FIGURE 2.19

Schematic diagram of flows in a CCIX column

that for each equivalent of A moving from solid to liquid phase, an equivalent of B moves in the opposite direction, thereby maintaining electroneutrality.

Then, $$F_L C_L (y_{A_t} - y_{A_b}) = F_R C_R (x_{A_t} - x_{A_b}) \quad (2.41)$$

and $$F_L C_L (y_{B_t} - y_{B_b}) = F_R C_R (x_{B_t} - x_{B_b}) \quad (2.42)$$

If we now define the equivalent resin and liquid flow rate variables R and L such that

$$L = F_L C_L \text{ and } R = F_R C_R \quad (2.43)$$

we can write an equation for ion fraction of A in terms of the other streams such that

$$y_{A_t} - y_{A_b} = R/L \; (x_{A_t} - x_{A_b}) \quad (2.44)$$

Assuming that the equivalent flow rates of resin and liquid do not change through the column, a mass balance analogous to (2.44) can be written such that x_A and y_A at any point 'n' in the column are related by

$$y_{A_n} - y_{A_b} = R/L \; (x_{A_n} - x_{A_b})$$

or $$y_{A_n} = S\, x_{A_n} - [S\, x_{A_b} - y_{A_b}] \quad (2.45)$$

where S = R/L is the stoichiometric ratio of resin equivalents to liquid equivalents moving through the column.

Equation (2.45) is the operating line equation, defining the exchange occurring in a steady state CCIX column. It may be plotted on an x,y diagram with the equilibrium relationship expressed in terms of the separation factor equation (2.10). A typical situation is presented in Figure 2.20.

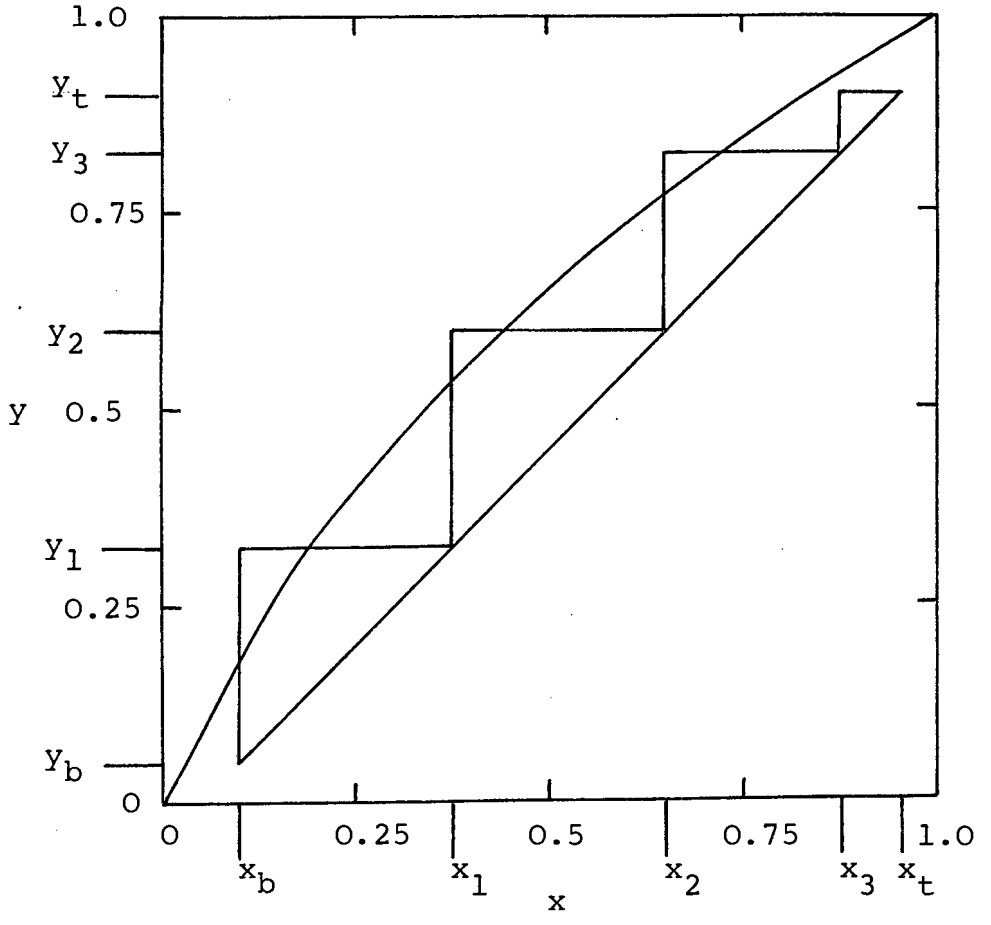

FIGURE 2.20

x-y diagram for a CCIX column

For any physical stage 'n' within the column, the change in resin composition over the 'stage' is defined by

$$x_n - x_{n-1} \tag{2.46}$$

i.e. the difference between the resin compositions at the top and bottom of the physical stage as predicted by the mass balance. (Because a countercurrent contact occurs within each physical 'stage' of the column, more than one equilibrium stage may exist within the volume of the physical stage; hence the appearance of a composition change over a physical stage extending beyond a resin liquid equilibrium point.) The maximum change in resin composition that can occur over the stage is for the bottom resin, x_{n-1}, to be in equilibrium with the bottom liquid, y_{n-1}. The degree to which the actual composition change approaches the theoretical maximum can then be used as a measure

of the exchange that has occurred. A 'stage efficiency' can then be defined for any physical stage n of Figure 2.19 by

$$\eta_n = \frac{x_n - x_{n-1}}{x_n - f(y_{n-1})} \qquad (2.47)$$

where $f(y_{n-1})$ expresses the equilibrium relationship, equation (2.10), and η_n is a fractional measure of the exchange which can occur in stage n.

The degree of resin conversion which does occur in a stage is dependent upon the conditions under which the CCIX column is operated. In order to relate this conversion to the theory of the Nernst-Planck equations it is necessary to define a time variable which measures the time that an element of liquid and resin are in contact within a column stage. The following parameters are thus defined for the ion exchange column:

Let V - gross volume of any stage of the column

v_n - volume available for solution flow in stage n

then $v_n = \varepsilon'_n V$

where ε'_n - void fraction of stage n when resin is fluidised.

On the basis of these parameters, the required 'contact time' or 'space time' parameter, t'_n, can be defined such that

$$t'_n = \frac{v_n}{F_L} = \frac{\varepsilon'_n V}{F_L} \qquad (2.48)$$

where t'_n is the time required for the passage of one void volume of solution through stage n of the column. If the resin size distribution within each stage is the same, then the space time, t', is the same throughout any section of the column.

Assuming that solution flow through the column occurs under 'plug-flow' conditions, that there is no mixing between different size fractions of resin in a stage, and that the transfer of resin from one stage to the next occurs by plug-flow, then under steady state conditions and following the approach of Levenspiel [74], the space time required for the conversion of resin x_n to x_{n-1} can be determined from integration of the mass transfer rate equation

according to the following:

$$t' = \overline{C} \int_{x_{n-1}}^{x_n} \frac{dx}{-\phi} \tag{2.49}$$

where $\overline{C}$ - capacity of the resin

ϕ - rate expression (Nernst-Planck equation (2.21))

On the basis of the equality of the space time, t', of a plug flow reactor at steady state with the conversion time, t, of a batch system (cf. Levenspiel [74]) when the conditions of mixing between resin and liquid are identical so that either the same film diffusion controlled driving force exists or mass transfer is pore diffusion controlled, the fractional approach to equilibrium parameter F(t) of equation (2.15) can be redefined in terms of the space time t', so that

$$F(t) = F(t') = \frac{\overline{C}_A^{\,0} - \overline{C}_A(t')}{\overline{C}_A^{\,0} - \overline{C}_A^{\,\infty}} \tag{2.50}$$

For a resin of fixed capacity $\overline{C}$ so that $x_A = \overline{C}_A/\overline{C}$, F(t') can be written as

$$F(t') = \frac{x_A^{\,0} - x_A(t')}{x_A^{\,0} - x_A^{\,\infty}} \tag{2.51}$$

where

$x_A^{\,0}$ = resin composition at the start of a time period

$x_A(t')$ = resin composition at the end of a time period

$x_A^{\,\infty}$ = resin in equilibrium with liquid at time $t' = \infty$

Then, comparing equation (2.51) with a column stage which has a space time t', the following equivalences are derived:

$$x_A^{\,0} \equiv x_n, \quad x_A(t') \equiv x_{n-1}, \text{ and } x_A^{\,\infty} \equiv f(y_{n-1})$$

and

$$F(t') \equiv \eta_n = \frac{x_n - x_{n-1}}{x_n - f(y_{n-1})} \tag{2.52}$$

Equation (2.52) shows how the solution of the Nernst-Planck equations (2.18 or 2.21) (or the measurement of the exchange kinetics) in terms of a fractional approach to equilibrium can be used to predict, through the stage efficiency defined by equation (2.47), the performance of a continuous countercurrent fluidised bed column. Where the reaction is pore diffusion controlled, a direct comparison of the fractional approach to equilibrium for a batch or CCIX column exchange can be made, for it is then not necessary to include assumptions about hydrodynamics in the analysis. In the case of film diffusion control of the rate, an assumption of 'film thickness' is necessary and then, in order to relate batch F(t) and CCIX η values, some correlation between column hydrodynamics and 'film thickness' is necessary, hence the present approach of modelling the CCIX on the basis of a mass transfer coefficient (section 2.4322) which is correlated with flow conditions via equation (2.40).

Based on the theory outlined above, it is only necessary to know the contact time within a stage of the CCIX column and the solution of equation (2.21) under the same hydrodynamic conditions for the exchange in question in order to determine a 'stage' efficiency; bearing in mind that, as explained in section 2.3121, η may vary with resin composition, x, even though space time t' remains constant.

Having established the applicability of a stage efficiency, an operating line (2.45) and an equilibrium curve (2.10) to the operation of a CCIX column, it allows a theory analogous to the McCabe-Thiele stepwise procedure, as outlined in Smith [75] or van Winkle [76], to be used to predict the performance of a CCIX column.

CHAPTER 3

FACTORS INFLUENCING THE DEVELOPMENT OF AN ION EXCHANGE TERTIARY TREATMENT PROCESS

3.1 BACKGROUND

A number of ion exchange (IX) systems have been developed for desalination, and found able simultaneously to remove organic material. The reason for the development of these various systems results from the fact, as will be demonstrated in section 3.2, that the over-riding cost in ion exchange desalination is that of regenerant chemicals. The system types when desalination is for potable water (as opposed to high purity boiler feed water) production contain either a strong and weak resin combination, or two weak resins. In order to evaluate the relative merits of these systems, their practicality for the particular wastewater (Table 3.1 gives the composition of such a water) being treated has to be considered, and most of all, their relative costs. For practical reasons, the Desal process was considered the best of the available weak resin systems and a strong acid-weak base combination with possible schemes for the recovery of regenerant chemicals in the form of usable products as the best alternative. The operation of the two systems is briefly outlined in section 3.11 below. A cost comparison of the two schemes was made (cf. section 3.2) in order to elucidate the high cost areas of the IX process and to determine what cost advantage the weak resin system has over the strong-weak combination. The data available at the time and on which the comparison was based, was for operation in fixed bed columns.

TABLE 3.1

Composition of Milnerton secondary sewage effluent

Component	Composition (mg/ℓ)
Na	360
K	22
Ca	64
Mg	65
Cl	570
SO_4	185
NO_3 as N	12
NH_4 as N	1
HCO_3	170
PO_4	7
COD	96
TDIS	1400

The choice of a weak resin system such as Desal, is generally based on its lower operating costs, for these resins usually have the disadvantage of low operating capacities. If regenerant chemicals can be recovered or reused, and in section 3.3 a number of proposals for achieving either recovery or reuse of chemicals is outlined, then the cost advantage of weak resins falls away.

Associated with the efficiency of operation of an ion exchange plant is the choice of equipment in which to conduct the desalination. In section 3.4, the various column types are discussed together with the effect each has on the cost and ease of plant operation, and the choice of a 'best' column is made.

3.11 Operation of an ion exchange process

A conventional ion exchange process for water desalination consists of a cation resin and an anion resin in series. Both the resins can be strong electrolyte resins, but at least one needs to be strong in order to split neutral salts or else two weak resins have to be coupled in a special process such as Desal. For the production of extremely high purity water, the series configuration of the two resins can be followed by a mixed bed column - both cation and anion resins together in one vessel.

3.111 Strong acid-weak base system: In general, the conventional IX desalination plant producing potable water from a saline source could consist of a strong cation resin column followed by a weak anion column. The reactions that occur in this system are:

$R - H + NaCl \rightarrow R - Na + HCl$	Cation Load	(3.1)
$R' - N + HCl \rightarrow R' - NHCl$	Anion Load	(3.2)
$R - Na + H^+ \rightarrow R - H + Na^+$	Cation Regen.	(3.3)
$R' - NHCl + NH_3 \rightarrow R' - N + NH_4Cl$	Anion Regen.	(3.4)

The cation resin performs the neutral salt splitting function and the anion resin 'picks-up' the acid molecule. Like all weak resins, the anion resin supposedly requires only a stoichiometric equivalent of regenerant. The cation resin, however, requires two to three times the stoichiometric equivalent for adequate regeneration, with the operating capacity being dependent upon the the regenerant excess. Figure 3.1 indicates this dependence.

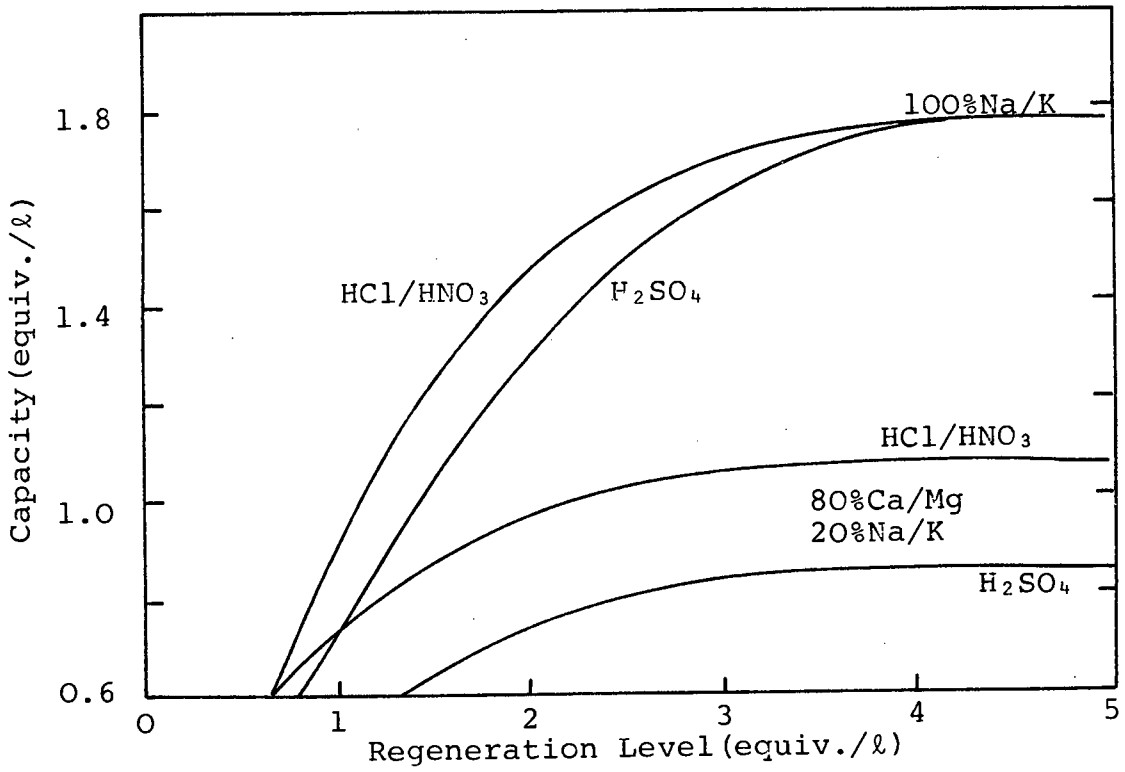

FIGURE 3.1

Resin capacity as a function of regeneration level for Zerolit 225

In contrast to the Desal process (section 3.112) the anion resin operating capacity when being loaded as in equation (3.2) is approximately twice that of the same resin when being loaded in the bicarbonate cycle (3.5). Consequently anion resin requirements are halved in this IX configuration as compared with the weak electrolyte Desal process.

3.112 A weak electrolyte configuration: The Desal process is a three column IX system based on weak resins and claimed to operate at low cost. The resins used are a weak base anion (Amberlite IRA-68) and a weak acid cation (Amberlite IRC-84). The flow configuration is outlined in Figure 3.2, and the reactions which occur in each column are as follows:

$$R' - NH_2CO_3 + NaCl \rightarrow R' - NHCl + NaHCO_3 \quad (3.5)$$

$$R - H + NaHCO_3 \rightarrow R - Na + H_2CO_3 \quad (3.6)$$

$$R' - N + H_2CO_3 \rightarrow R' - NH_2CO_3 \quad (3.7)$$

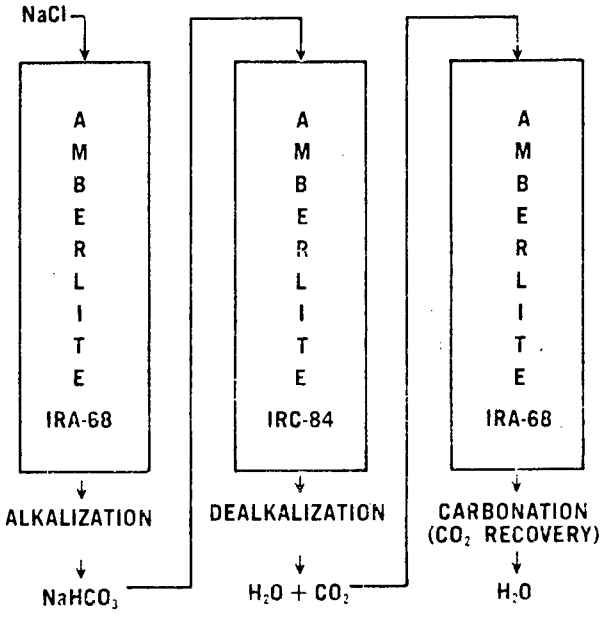

Figure 1. Flow sheet deionization process

FIGURE 3.2

Flow configuration of the Desal process

$$R' - NHCl + NH_3 \rightarrow R' - N + NH_4Cl \qquad \text{Anion Regen.} \qquad (3.8)$$

$$R - Na + H^+ \rightarrow R - H + Na^+ \qquad \text{Cation Regen.} \qquad (3.9)$$

The principles upon which the Desal process are based are (i) the supposed ability of the weak resins to be regenerated with a stoichiometric quantity of regenerant and (ii) the method of splitting the neutral NaCl salt using the bicarbonate ion, a task which normally cannot be accomplished by weak resins (cf. Chapter 2.122).

Initial tests on the Desal process were geared towards determing the operating capacity of the resins (i.e. the number of equivalents of an ion that could be loaded onto a given volume of resin before the level of that ion in the effluent stream was higher than the acceptable limit) and the stoichiometric excess (regeneration level) of regenerant required to regenerate the resins (i.e. the ratio of the equivalents of regenerant to equivalents of loaded ion required to regenerate the resin to the point where a given operating capacity is attained.)

Results of tests on the anion resins of the Desal process are presented in Tables 3.2 and 3.3. (Details of the experimental procedure are outlined in Appendix B.) Contrary to expectations, the operating capacity of the weak anion resin does show some variation with regeneration level. This indicates that the resin possesses some strong base character (cf. Chapter 2.122). The change in operating capacity with flow, Table 3.3, is due to the change in kinetics (cf. Chapter 2.3).

TABLE 3.2

Effect of regeneration level on the operating capacity of Amberlite IRA-68

Regen. Level	Op. Cap. (meq/mℓ)
2,61	0,61
2,12	0,61
1,79	0,59
1,42	0,51

TABLE 3.3

Effect of flow rate on the operating capacity of Amberlite IRA-68

Flow (BV/hr)	Op.Cap. (meq/mℓ)
8,2	0,63
11,8	0,62
16,2*	0,61
20,0	0,61

* Manufacturer's recommended flow

Operating capacity data on the cation resin was obtained simultaneously with the above, and the information obtained on the resin properties was used in the cost evaluation of section 3.2.

3.2 COSTS INVOLVED IN DESALINATION BY ION EXCHANGE

In order to determine what the critical cost areas are when operating an ion exchange plant, the following cost study was undertaken.

3.21 Parameters used in the evaluation

3.211 Water composition and flow: The calculations are based on a 365 days/year continuous daily flow of 55 million litres and the two water compositions given in Table 3.4; in order that the effect on desalination costs of an increased TDS could be included. The plant is designed to produce a product water containing 50 mg/ℓ of NaCl.

TABLE 3.4

Compositions used in cost study

Component	Water A	Water B
Na	240	360
K	27	27
Ca	50	50
Mg	23	23
Cl	270	405
SO_4	120	120
HCO_3	332	332

3.212 Equipment: The major equipment cost is that of the ion exchange columns. Cost figures for the columns were based on the steel and fabrication charges. Erection of the columns and the costs of ancilliaries such as pipes, pumps and controls were determined from the formulae presented by Zastrozny [77].

In the evaluation, columns were sized on the basis of (i) a maximum solution flow of 16BV/hr (the resin manufacturer's recommendation), (ii) a length to diameter ratio of 1,0, (iii) sufficient freeboard for 100% bed expansion during backwash, (iv) a maximum diameter of 4 metres. Because of these size restrictions, an increase in feed water flow means extra column trains have to be incorporated in the design. Economies of scale are therefore limited, and consequently only one flow rate, 55 million litres per day, was costed. Higher flows would merely show a proportionate increase in capital charges.

3.213 Resin: The cost of resin was ascertained locally from resin manufacturers' agents. On the basis of manufacturers' claims, resin life was assumed to be five years, proportioned on the basis of a 20% annual replacement requirement.

3.214 Running costs:

3.2141 Labour: The total annual cost of labour was assumed constant irrespective of plant size and throughput. The labour charge was based on four operators and a shift supervisor.

3.2142 Regenerant chemicals: Two acids, sulphuric and nitric (both of which are manufactured in the Cape Peninsula) were considered for cation regeneration, and ammonia solution (also locally manufactured) for the anion columns. Carbon dioxide was costed on the basis of a 50% yield from the combustion of coal. Prices for these chemicals were determined on the basis of the delivered costs at the assumed site of the plant.

3.215 Capital: The cost of money was placed at 8,5% p.a. and the payback period of the capital sum was assumed to be 20 years. The price of real estate and civil works was not included in the estimation of capital costs.

3.22 Discussion of cost figures

The complete design and costing of the IX plant was programmed on a computer following the method of Downing [78]. This enabled rapid calculation of different feed flows and compositions, and column configurations. For this study only two column configurations are compared - the anion-cation-anion train of the Desal process, and the strong cation, weak anion train of the conventional process.

Using the flow rate and composition of the water, the resin volumes required to perform the desalination were calculated on the basis of the operating capacity data. From the resin volume and the column dimension constraints, the number of columns was evaluated. On the basis of the resin capacity and the degree of desalination, the regenerant chemical quantities were determined. All items were then costed from the available data and the following cost information was calculated.

3.221 Comparison of water costs:

3.2211 Effect of column configuration: A direct comparison of the effect of the Desal process train versus the conventional weak base strong acid train is made in the columns 2 and 3 of Table 3.5. In terms of cost per unit volume of water, the configurational difference represents a 9% saving for the conventional system, this despite the fact that regenerant chemical requirements are marginally higher for this system.

The increase in the annual value of chemicals required for regeneration is a result of the greater stoichiometric requirement of the strong acid resin over that of the weak acid resin. This increase in acid requirements is, to a measure, offset by the decreased chemical requirement of the weak base resin when operating on the acid cycle (cf. equations (3.2, 3.5 and 3.8) as opposed to the bicarbonate exchange.

The net decrease in product water cost for the conventional system is due to the 120% increase in capacity of the weak base resin operating in the free base form. Weak anion resins are expensive, and besides halving the volume requirements on doubling the capacity, the second weak anion column of the Desal process has been eliminated, further decreasing the expenditure on anion resin and capital costs. Together, these two factors lower annual outlay for anion resin replacement by a third, and thus offset any increase in regenerant costs, thereby producing a system which desalinates water at a lower cost.

3.2212 Effect of regenerant acid type: The water treatment costs using the two locally manufactured acids, nitric and sulphuric, are compared in columns 1 and 2 of Table 3.5 in the Desal configuration. Although sulphuric acid is significantly cheaper than nitric acid (approximately R2 000 per tonne equivalent), a 20% greater stoichiometric excess of sulphuric acid is required to achieve a given resin operating capacity (cf. Figure 3.1). Furthermore, should the resin be loaded with calcium or magnesium ions, the sulphuric acid has to be introduced at a concentration of less than 5% to prevent precipitation occurring in the packed bed columns. This necessitates the use of product water for acid dilution. Consequently, the water recovery with sulphuric acid regeneration is 81% as opposed to the 90% when using nitric acid. On the basis of a 90% water recovery, the treatment cost figure of column 1, Table 3.5,

TABLE 3.5

Annual cost of desalination

	1		2		3		4		5	
Composition	Water A		Water A		Water A		Water B		Water B	
Configuration	Desal		Desal		Conventional		Desal		Conventional	
Regenerant System	H_2SO_4/NH_3		HNO_3/NH_3		HNO_3/NH_3		HNO_3/NH_3		HNO_3/NH_3	
Costs of Items	Rand	%	Rand	%	Rand	%	Rand	%	Rand	%
Capital	227 000	11,7	227 000	9,5	123 000	5,5	227 000	6,9	123 000	3,7
Labour	26 000	1,3	26 000	1,0	26 000	1,2	26 000	0,8	26 000	0,8
Anion Resin	125 000	6,4	125 000	5,3	40 000	1,8	125 000	3,8	40 000	1,2
Cation Resin	43 000	2,2	43 000	1,8	24 000	1,1	43 000	1,3	24 000	0,7
Ammonia	828 000	42,8	828 000	34,8	550 000	24,7	1 242 000	37,3	850 000	25,7
Acid	677 000	34,9	1 115 000	46,9	1 461 000	65,7	1 673 000	50,2	2 250 000	67,9
Carbon Dioxide	15 000	0,7	15 000	0,6	-	-	22 000	0,7	-	-
Total	1 941 000		2 379 000		2 224 000		3 336 000		3 313 000	
R/1000 ℓ	0,119		0,132		0,123		0,185		0,183	

Note: These figures are based on costs prevailing in December 1974.

would be reduced by 11% to 10,7c per 1 000 litres. This would increase the marginal cost difference by sulphuric versus nitric acid from 11% to 23% (13,2c against 11,9c and 10,7c per 1 000 litres).

3.2213 Effect of water composition: For the same total flow, the water composition affects the regenerant requirements (cf. columns 4 and 5, Table 3.5). Since the same excess of regenerant is required to strip the resin irrespective of feed water salinity, the salinity increase means only that the resin is stripped proportionately more frequently, thereby increasing the annual chemical costs. However, the resin is being cycled faster with a higher salinity water so that the effective resin utilisation is greater and the cost of resin per unit volume of water consequently less. The latter saving is negligible compared to the increase in regenerant consumption and so is effectively hidden in the overal cost; which has increased by 50% for Water A over Water B (cf. Table 3.5) for the same flow conditions and column configuration.

3.222 Comparison of individual component costs: For each column configuration and water composition presented in Table 3.5, the contribution of the items capital, chemicals, resin and labour towards the total cost is computed. Analysis of these contributions shows that the cost of chemicals constitute the overriding proportion of the total. The lowest percentage, 78%, is recorded for the Desal process with sulphuric acid and ammonia as regenerants.

3.2221 Regenerant chemicals: The major significance of the cost of acid and alkali is reflected in the percentage of total costs these components contribute when feed water salinity level increases. For Water A with a TDS of 730 mg/ℓ the nitric acid and ammonia together constitute respectively 82% and 90% of desalination costs, for Water B with a 985 mg/ℓ TDS level the contributions are 88% and 94% respectively for the same chemicals and column configurations. The conclusion is drawn that, under local economic conditions, it does not matter what configuration of columns or resins is used for the desalination, chemical costs alone will ultimately determine process feasibility.

3.2222 Capital: Amortization of capital, after chemicals, is the next largest running cost in the study presented in Table 3.5, contributing as it does between 4% and 12% of total costs. The lower figure, as expected, is for the high salinity water.

Although relatively insignificant in comparison with chemicals, should a low cost regeneration technique be developed, consideration would have to be given towards reducing capital outlay. Alternative technology will be considered (cf. section 3.4) to circumvent this problem.

Included in the capital costs is the original monetary outlay for resin purchase. In section 3.2213 it was pointed out that resin utilisation efficiency was increased through faster resin cycling. An inherent fault of fixed bed systems is the quantity of resin which remains 'idle' except for the short period during which it is being loaded. This 'idle' resin requires initial capital expenditure which is then not efficiently utilised.

3.2223 Resin: The replacement costs of resin, at 20% per annum, are very small. This figure is, however, based on information determined for resins treating 'pure' saline water, i.e. water without organics and particulate material. In the case of ion exchange as a 'complex' tertiary treatment, this 20% may well have to be revised in the light of experimentation. Further, should a major portion of, especially the anion resin, capacity be permanently 'lost' due to irreversible resin fouling, the 5% contribution of the anion resin to running costs in the case of the Desal system on Water A, may in fact be underestimating the true value.

3.223 Conclusions: On the basis of the costs determined in the evaluation, it would appear that the Desal process holds no cost advantage over a conventional strong acid weak base system. In fact, the extra operating complexity involved in the Desal process mitigates against consideration of this system for further investigation.

3.3 OUTLINE OF METHODS FOR THE RECOVERY OF REGENERATION CHEMICALS

3.31 Background

The cost study of section 3.2 has shown clearly that, in order to reduce the running costs of an ion exchange desalination plant, consideration must be given either to reducing or to recovering the cost of the chemicals used for regenerating loaded resins.

This topic has been of primary concern to many investigators in the field of ion exchange, and the methods proposed to overcome the problem are many and varied. A direct result of chemical costs has been the development of processes such as the Desal [79], Ducol [80], Sul-bi-Sul [81] and Sirotherm [33]. The Desal process is based on resins which require only a small excess of regenerants for stripping, the Ducol process on the use of lime and cheap acid for resin regeneration. The Sul-bi-Sul is based on a sulphate-bisulphate conversion under different concentration conditions and Sirotherm uses hot water to strip the loaded resins. In this manner, each attempts to reduce the regeneration costs, for it is this factor alone which precludes the use of ion exchange for waters with a salinity level of over 3 000 mg/ℓ - as alternative technology (reverse osmosis) becomes more economical.

An alternative approach to the above is either to recover the chemicals used in the regeneration so that they may again be used or to recover the chemicals in a form in which they have a certain residual value.

3.32 Methods for the recovery of chemicals for reuse

A patent by Kunin [82] typifies this approach. Saline solution used for stripping an anion resin which has decolourized a sugar solution is recovered by treating it with an oxidizing agent such as hydrogen peroxide or sodium hypochlorite.

3.321 Organic acids and bases as regenerants: In a series of patents, [83] members of the Aerojet-General Corp. U.S.A. have proposed the use of organic acids and alkalis as regenerant chemicals. This restricts the resins to being of weak electrolyte type.

The recovery of regenerants occurs when the spent regenerant streams from the anion and cation columns are mixed together. The organic acid and

base used then combines to form the salt of an organic macromolecule. This compound is removed from the mixture by solvent extraction and recovered from the solvent by distillation. On heating, the organic salt splits into two components with different volatilities allowing the distillation process to recover each in a pure form so that it may be re-used. The process has certain obvious limitations; it is complex, relies on weak resins and replaces the cost of regenerant chemicals with an energy cost.

3.322 Use of a strong acid and ammonia:

3.3221 Hydrochloric acid: In a method outlined by Busch and Lynn [84], and Vermeer et al. [85] ammonia solution is used for stripping the weak base resin and hydrochloric acid the strong cation resin. The resin system therefore, is of the conventional type and the acid and base used is also standard technology. The recovery of chemicals is based on the predominant anion in the feed water being chloride. Then, using magnesium hydroxide in the following reactions, the regenerants are recycled.

$R - Na + HCl \rightarrow R - H + NaCl$	Cation Regen.	(3.10)
$R' - NHCl + NH_3 \rightarrow R' - N + NH_4Cl$	Anion Regen.	(3.11)
$2NH_4Cl + Mg(OH)_2 \rightarrow MgCl_2 + 2NH_3 + 2H_2O$	Ammonia Recovery	(3.12)
$MgCl_2 + H_2O \rightarrow MgO + 2HCl$	Acid Recovery	(3.13)
$MgO + H_2O \rightarrow Mg(OH)_2$		(3.14)

The disadvantages of the scheme outlined, are that, as before, a complex energy intensive process is needed to recover the chemicals and that with feed water containing low chloride levels, the recovery is no longer effective.

3.3222 Sulphuric acid: When the feed water anion is predominantly sulphate and a market for gypsum ($CaSO_4$) exists within close proximity of the desalination process, the following scheme may advantageously be used in preference to the above. The chemical recovery reactions (3.12),(3.13),(3.14) are then replaced by:

$$(NH_4)_2 SO_4 + Ca(OH)_2 \rightarrow CaSO_4 \downarrow + NH_3 \qquad (3.15)$$

With sulphuric acid being used as the cation regenerant, the two spent regenerant streams can be mixed and dosed with lime and the following regenerant

scheme employed:

$$2R - Na + H_2SO_4 \rightarrow 2R - H + Na_2SO_4 \quad (3.16)$$

$$(R'-NH)_2SO_4 + 2NaOH \rightarrow 2R' - N + Na_2SO_4 + H_2O \quad (3.17)$$

$$Na_2SO_4 + Ca(OH)_2 \rightarrow CaSO_4 \downarrow + 2NaOH \quad (3.18)$$

In this method, the chemical inputs are lime and sulphuric acid which are then recovered in the form of gypsum. A disadvantage is the loss of chemical which occurs when the feed water contains chloride ion and also the low demand, in most instances, for $CaSO_4$.

3.33 Methods for the recovery of chemicals for alternative use

The recovery of gypsum when using lime and sulphuric acid, as outlined above, is an example of the recovery of regenerant chemicals for alternative purposes.

In the Cape Peninsula where, as outlined in Chapter 1, an ion exchange desalination process is required, one of the major industries is a chemical plant producing ammonium nitrate for use as fertiliser by reacting manufactured ammonia and nitric acid together. The use of ammonia and nitric acid as regenerant chemicals in this investigation is therefore given major consideration, as is the recovery of usable products from the spent regenerant streams.

Using ammonia and nitric acid as regenerant chemicals, and assuming the water composition to be that given in Table 3.4 where NaCl is the predominant species, then the following resin regeneration reactions apply:

$$R - Na + HNO_3 \rightarrow R - H + NaNO_3 \quad \text{Cation Regen.} \quad (3.19)$$

$$R' - NHCl + NH_3 \rightarrow R' - N + NH_4Cl \quad \text{Anion Regen.} \quad (3.20)$$

3.331 Recovery of NH_4NO_3 from mixed spent regenerants:

3.3311 Double decomposition: The initial regenerant recovery proposed was based on mixing the spent streams containing $NaNO_3$ and NH_4Cl and attempting to obtain, by a double decomposition scheme analogous to that used by Freeth and Cocksedge [86], NH_4NO_3 and NaCl.

However, the required double decomposition had been extensively investigated by Rengade [87], who reported that the equilibrium relationships were unfavourable. At best, an 82% NH_4NO_3 with 18% NaCl could be obtained. As it was anticipated that the recovered NH_4NO_3 would be used as a fertiliser, the high NaCl content was unacceptable.

3.3312 Extraction with liquid ammonia: This alternative relied on the extremely high solubility of NH_4NO_3 in liquid ammonia, and the very low solubility of NaCl in the same solvent as reported by Hunt and Boncyk [88]. However, the method required the extraction to be performed at high pressure and extremely low water content which would mean that high evaporative costs would negate any potential cost savings.

3.332 Separate recovery of ammonia and nitrate ions: The methods considered in this section rely on ammonia recovery via the lime dosing scheme outlined in equation (3.15), and propose methods for the recovery of the nitrate ion from $NaNO_3$.

3.3321 Production of potassium nitrate: The South African fertiliser industry imports a million tonnes of KCl annually for incorporation into mixed fertilisers. The chloride ion is, however, an undesirable contaminant.

A double decomposition reaction between $NaNO_3$ and KCl, viz.,

$$KCl + NaNO_3 \rightarrow KNO_3 + NaCl \qquad (3.21)$$

is proposed. Moldovan [89] outlines the technology for pure salts, with a flow diagram presented in Figure 3.3. Initial test work on this scheme using the water composition of Table 3.4 yielded a 95% pure KNO_3 product. The major disadvantage is the energy required for the evaporative step of reaction (3.21).

3.3322 Production of NH_4NO_3 and $NaHCO_4$: Mellor [90] outlines a method whereby $NaHCO_3$ and NH_4NO_3 can be produced from $NaNO_3$ according to the following

$$NaNO_3 + NH_3 + CO_2 + H_2O \rightarrow NH_4NO_3 + NaHCO_3 \qquad (3.22)$$

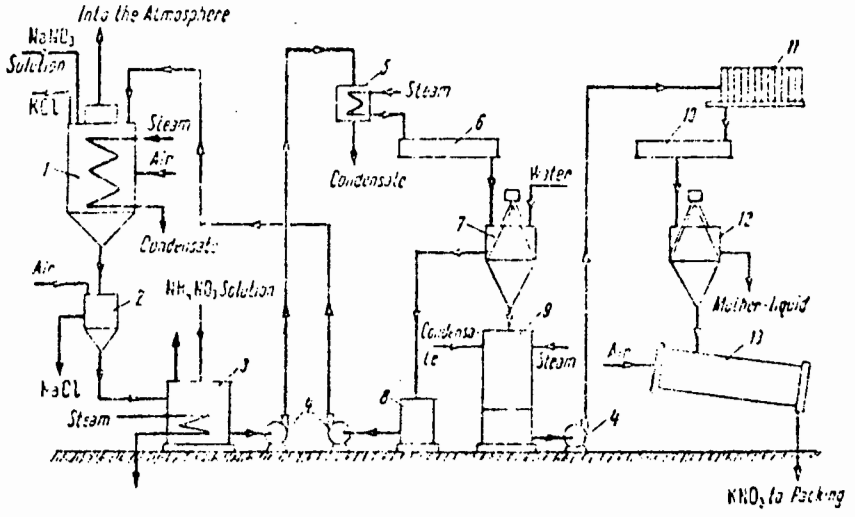

Flow Diagram of Potassium Nitrate Production by Double Decomposition Reaction:

1 — Reactor; *2* — Filter; *3* — Tank for potassium nitrate solutions; *4* — Centrifugal pumps; *5* — Pressure vessel; *6, 10* — Crystalizers; *7, 12* — Centrifuge; *8* — Collector for primary mother-liquor; *9* — Steaming unit; *11* — Plate-and-frame filter; *13* — Drying drum.

FIGURE 3.3

Flow diagram of potassium nitrate production by double decomposition reaction

Process steps require initial evaporation to raise the $NaNO_3$ concentration to acceptable levels, followed by cooling. Any magnesium or calcium ions present would cause wastage of CO_2 and contamination of the product $NaHCO_3$.

3.333 Recovery of ammonium nitrate by an ion exchange route: All of the regenerant recovery methods outlined suffer from one or other disadvantage. An alternative to the above, and the method ultimately chosen for detailed further investigation is one based on the ability of a cation resin to exchange metal cations for an ammonium ion. Using feed water NaCl as an example the following load and regeneration scheme is proposed:

$$R - H + NaCl \rightarrow R - Na + HCl \qquad \text{Cation Load} \qquad (3.23)$$

$$R' - N + HCl \rightarrow R' - NHCl \qquad \text{Anion Load} \qquad (3.24)$$

The first step in the regeneration sequence is the use of ammonia to strip the anion resin and produce ammonium chloride:

$$R' - NHCl + NH_3 \rightarrow R' - N + NH_4Cl \qquad (3.25)$$

The next step is to take the spent anion regenerant NH_4Cl and pass this through the metal-loaded cation resin. The following exchange then takes place:

$$R - Na + NH_4Cl \rightarrow R - NH_4 + NaCl \qquad (3.26)$$

The ammonium-loaded cation resin is now regenerated with the strong nitric acid to produce NH_4NO_3 and conversion of the resin to hydrogen form

$$R - NH_4 + HNO_3 \rightarrow R - H + NH_4NO_3 \qquad (3.27)$$

Should the feed water salts not be NaCl, the reaction sequence is exactly the same and works as follows:

$$R' - NHA + NH_3 \rightarrow R' - N + NH_4A \qquad (3.28)$$

where A - Cl, SO_4, NO_3, PO_4, etc.

$$R - M + NH_4A \rightarrow R - NH_4 + MA \qquad (3.29)$$

where M - Na, K, Ca, Mg, etc.

The resin conversion of equation (3.29) is most favourable when the exchanging ions are ammonium and sodium, and least favourable when they are calcium and ammonium. However, the aim would be to have the spent anion regenerant stream as concentrated as possible in order that the waste brine stream (the product stream of reactions (3.26) or (3.29)) carries with it the minimum quantity of water. As outlined in Chapter 2.22 the equilibrium between a monovalent and divalent ion changes with concentration and if the concentration is sufficiently high the resin preference can reverse (cf. Figure 2.8).

In order to gain most benefit from the recovery system outlined, the concentration of the recovered ammonium nitrate (AN) stream needs to be as high as possible - (i) to maximise the water recovery of the overall process and (ii) to reduce to a minimum any subsequent evaporation costs. The concentration of the nitric acid used for the resin stripping and the type

of column operation determine the AN concentration. Consideration has therefore to be given to the resin type which will best 'stand up to' high acid concentrations and to the column type which will most easily allow the production of concentrated solutions.

3.3331 Test of ammonium nitrate recovery in fixed bed columns:

The ion exchange regenerant recovery system was tested by sequentially loading a cation and anion resin train with feed water having the composition of Table 3.1. (Experimental details are outlined in Appendix B.) On completion of loading the sodium content of the cation bed was calculated by mass balance. Concentrated ammonia solution was introduced into the anion column and the spent regenerant allowed to pass through the cation resin. The composition of the solution leaving the cation column was monitored, and the breakthrough curves are presented in Figure 3.4.

The breakthrough curves for sodium and ammonium in Figure 3.4 show that an exchange does occur, but that the separation is not sharp - a function of the separation factor of the two ions. The 'cumulative elution of sodium' curve indicates that only 75% of the loaded sodium has been stripped before ammonium ions appear in the effluent. On this basis, if a pure AN is required an excess of ammonium ions will have to be used to strip sodium. Alternatively, complete recovery of ammonium ions in the AN will mean a sodium contamination to the extent of 25% by mass of the cations.

Figure 3.5 gives an indication of the concentration of ammonium and sodium ions that are stripped off the resin with nitric acid. Two points are indicated in the figure; (i) that the ratio of ammonium to sodium ions in the liquid stream is high, due to the almost complete resin conversion achieved by the use of an excess of spent anion regenerant in the previous reaction and (ii) that although a 3N nitric acid stream was used for regeneration, the average concentration of AN in the 'peak' sample is only 1,4N. This dilution is a consequence of the wash that is required between ion exchange reactions, and which leaves the resin pores containing water. This pore solution is forced to diffuse out of the beads when the Donnan potential changes under the high acid concentration, thereby diluting the desired product.

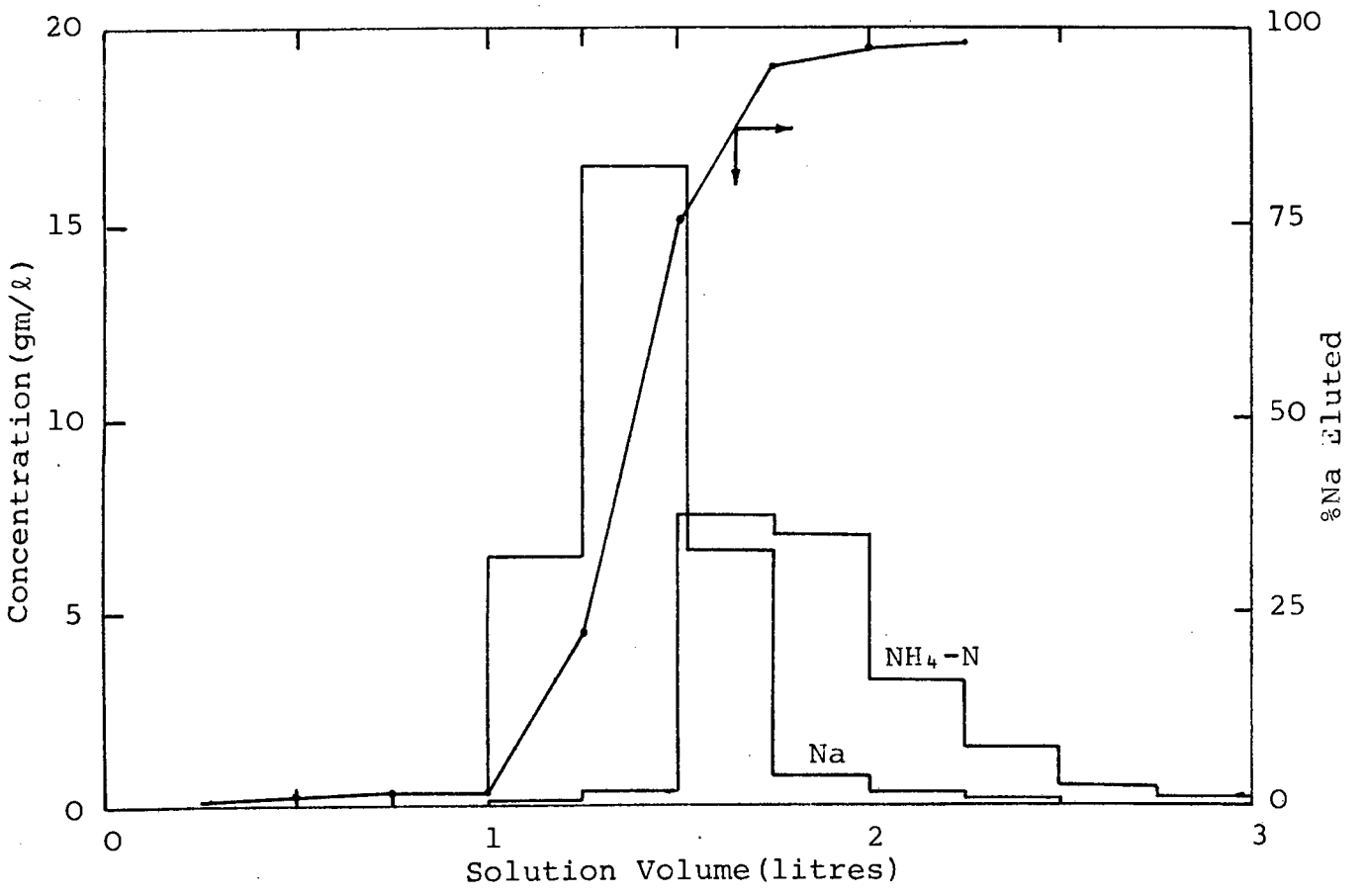

FIGURE 3.4

Breakthrough curves: ammonium-sodium exchange in a fixed bed column

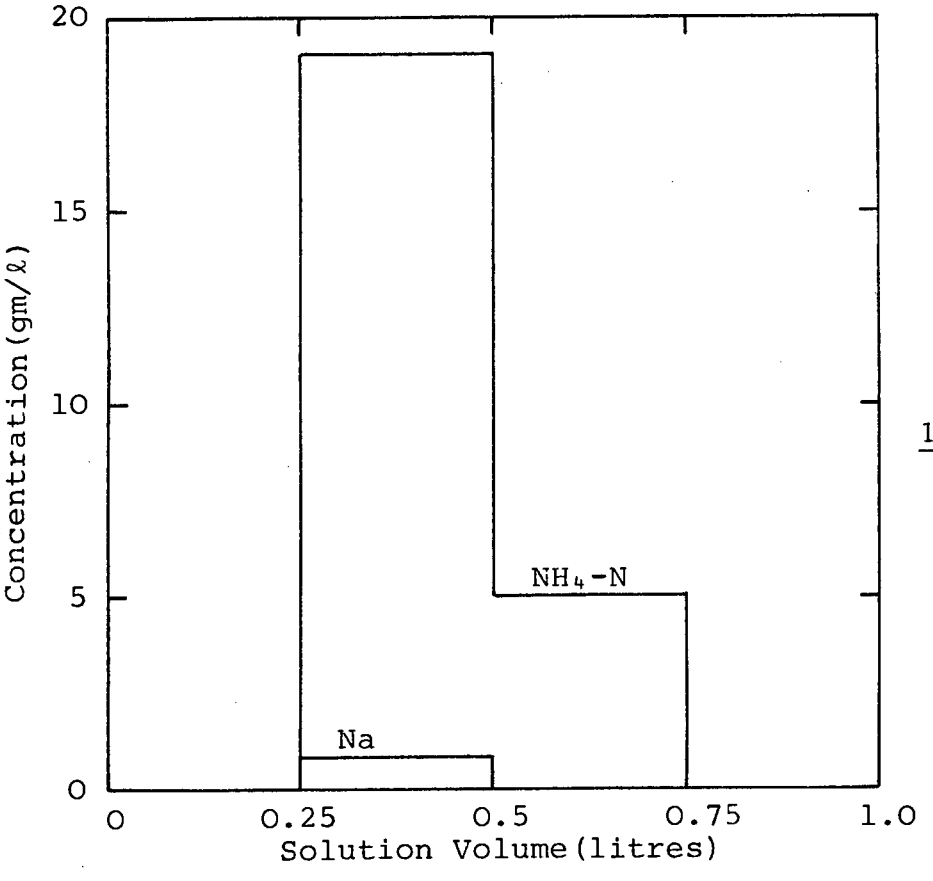

FIGURE 3.5

Breakthrough curves: Regeneration of ammonium loaded resin with nitric acid

These shortcomings of the regenerant recovery scheme are due to the method of operation of a fixed bed. The exchange reaction has been shown to work and thought needs only to be given to improving the efficiency of the operation to make the process viable.

3.4 CHOICE OF ION EXCHANGE COLUMN TYPE

In Chapter 2, the two major ion exchange column types were outlined. The conventional fixed bed column has been proven in many applications, whilst the moving bed system is a relatively new development. The latter type has the advantage of providing a nearly-continuous process, favoured by chemical engineers. However, a 'carousel' system of fixed beds, where a regenerated column is added at the end of a train of columns in series as a loaded one is removed from the beginning of the train, developed for use in the uranium industry [91], simulates a moving bed system in a series of fixed bed columns. A process, similar to the carousel system, but one which stores and moves liquid streams of different compositions and concentrations, has been proposed by Vajna [92]. However, the piping and flow control in the Vajna and carousel systems, where both the resin loading and regeneration reactions need to be conducted in the same fashion, becomes unwieldy. In order to choose a column type, consideration must be given to the cost of the system, and its suitability and ease of operation when treating the water under consideration.

3.41 Influence of water type on column choice

The development work for this project is based on the treatment of humus tank effluent (HTE) as feed to the plant, where HTE is the overflow stream from the secondary settlers of the biological trickling filters. As such, the water is likely to contain a certain quantity of particulate matter. Although the initial treatment step may well be filtration, the possibility exists that the ion exchange resin will have to deal with a stream containing finely suspended solid material.

Further, should the regenerant recovery scheme of section 3.333 be contemplated, it is extremely likely that, in the event of the feed water containing quantities of calcium and sulphate, the concentration of the reaction (3.29) would exceed the solubility product of $CaSO_4$ with the

consequent formation of a precipitate in the resin bed. Alternatively, if an excess of ammonia is used in the anion regeneration step, equation (3.28), the pH of the spent regenerant entering into reaction (3.29) will be high causing further precipitation of hardness ions in the resin bed.

Consideration of the possibility of particulate material fouling a packed bed unit precludes the use of column types such as the conventional downflow column and CCIX units such as Asahi and Chem-Seps (cf. Chapter 2.4) in favour of columns which operate with fluidised beds.

3.42 Influence of cost on column choice

Column type can affect the initial capital cost of the plant and the subsequent running costs.

3.421 Capital: Koto [93] has conducted an economic appraisal of the Desal process in a conventional fixed bed and a moving bed process. Koto concludes that the moving bed costs are of the order of 30% less in initial capital outlay due only to the reduced resin inventory. As outlined in the comparison of fixed and moving bed (CCIX) columns in Chapter 2, CCIX utilises the total resin inventory at every instant of time in contrast to fixed bed, where only the 'adsorption zone' is reacting. This means that initial resin inventory for a fixed bed system has to be that much higher.

Since both CCIX and fixed bed systems are conducted in columns and the peripheral equipment such as pumps, piping, controls, would be similar for each, there is no capital cost incentive influencing the choice of one system as opposed to the other.

3.422 Running costs:

3.4221 Resin replacement: The lower resin inventory of a CCIX system means that annual resin replacement costs may be lower. The cost study of section 3.2 showed how resin costs for Water A over Water B were reduced due to the higher utilisation efficiency of the resin. Resin life was, however, set at five years. With the higher frequency of load and regeneration that the resin would have to undergo in CCIX, the necessity for swifter resin replacement may arise. Further, in CCIX, resin is moved around. This could cause resin breakup and loss through attrition when, with the preference of a

fluidised bed over a packed bed for reasons such as precipitate formation outlined in section 3.41, fine resin is washed out of the column. This means that if resin breakage occurs in a fluidised bed system, more frequent 'topping up' of the resin inventory is required.

3.4222 Regeneration and recovery of chemicals: Takeuchi [94] has compared the costs of the Desal process and a strong acid weak base process in CCIX equipment. Takeuchi concludes that the benefit enjoyed by weak resins over strong resins in fixed bed equipment with regard to regenerant chemical requirements no longer applies in CCIX equipment. In his results, Takeuchi shows that the efficiency of CCIX-type contact means that excess strong acid resin regenerant requirements are no longer an overriding consideration and that by suitable CCIX column design the same stoichiometric excess of regenerant as is normally used for weak cation resins will perform the stripping of a strong cation resin in a stage-wise countercurrent process.

One of the considerations in any regenerant recovery system is the concentration of the spent regenerant stream. In this respect, fixed beds are at a disadvantage in that, for regeneration of the resin, they require the necessary acid or base to be introduced to the column and then 'pushed through' by a water wash stream. This produces the break-through curve characteristic of the results presented in Figure 3.5. CCIX equipment, by the nature of its operation, produces a product or spent regenerant stream of constant composition, with the composition being dependent upon the conditions of operation. This makes the recovery of a high concentration stream that much easier, and also eliminates the need to dispose of dilute spent regenerant which would be required in a fixed bed system.

Further, the inherent higher efficiency of CCIX over fixed bed (cf. Takeuchi's results), means that the wash step that must follow a regeneration is also more efficient. The quantity of desalinated product water which is normally used for resin washing is thus reduced with consequent benefit to the overall process in terms of water recovery (i.e. fraction of influent water that is recovered as product)

3.43 Conclusions and column choice

On the basis of the foregoing discussion of the merits of fixed and CCIX columns the choice of a column type is made. The likelihood of particulate matter occurring within a column indicates the need for a fluidised bed over a packed bed resulting in a choice of system being reduced to either fixed or moving fluidised bed. On the basis of the cost and concentration advantages of the moving bed (CCIX) system, this must be favoured above fixed bed. The final choice has therefore to be between a fluidised bed carousel (simulates CCIX) system or fluidised bed CCIX itself. After consideration of the complexity of the two fluidised bed systems (carousel and CCIX), and the ease of operation of each, the CCIX process was chosen.

CHAPTER 4

DETERMINATION AND DISCUSSION OF RESIN AND COLUMN PROPERTIES

4.1 INTRODUCTION

Having made the choice, in the previous chapter, of a strong acid weak base resin configuration and a fluidised moving bed column, there remains the task of developing and testing an ion exchange system based on this equipment and resin type and the proposed regenerant chemical recovery scheme. Further, the CCIX column design criterion based on the steady state stagewise calculation procedure outlined in section 2.4323 must also be investigated. A design technique such as this, will facilitate calculation of the feasibility of the IX process for the treatment of various different waters, each with specific salinity levels. In order to achieve the two aims of process development and design testing, various properties of the cation and anion resins must be determined and considered in conjunction with the properties of the CCIX column.

The water compositions of Table 1.2 show the salinity of sewage plant discharge streams in certain areas of Cape Town. However, besides the salt content of the water, there remains a residual of non degraded organic material which would be contacted with the resins in an IX desalination. A series of resin 'life' tests now become necessary in order to ascertain how the combination of the salt and organic content of the water affect the capacity of the resin and to determine whether, should some fouling of the resins occur, the fouling is reversible. Further, a range of commercial resins are available each with very similar chemical properties but with possibly different resistances to organic fouling; therefore, some form of resin comparison must be undertaken. During the comparison, outlined in section 4.2, certain other physical properties of the resins which become relevant when operation in a CCIX column is considered will be determined. These are factors which affect the resin fluidisation properties under different solution concentration and flow conditions and include the degree of resin swelling or density change which occurs with change from one counter-ion to another, and the voidage of a packed bed of resin.

In any two phase mass transfer process (with ion exchange a typical example) the two properties of the 'system' with the most effect are (i) the amount of material which is transferred between phases, and (ii) the speed with which this material is transferred. For any calculation on a two phase system, it is necessary to evaluate the appropriate equilibrium and kinetic properties. In the case of ion exchange, both equilibria and kinetics are dependent on the resin and solution which is being contacted and need to be separately determined for each resin-solution system that is considered. Sections 4.3 and 4.4 present equilibrium and kinetic results.

The CCIX column that is to be used in the development of an ion exchange tertiary treatment process has, to date, only been modelled as an unsteady state contact device. The investigation of the CCIX column undertaken in section 4.5 will show that it can be considered to operate at a pseudo steady state condition. Further, when the column is at steady state, it then becomes possible to perform a stagewise calculation and to show how the degree of exchange can then be related, through the resin-solution kinetic and equilibrium properties, to a batch exchange. In this manner the design procedure for a CCIX column outlined in section 2.4323 will be used to predict the performance of the column.

4.2 PROPERTIES OF THE ION EXCHANGE RESINS

In South Africa at the present time, it is possible to purchase the resins of most of the major resin manufacturers. Because, however, the Permutit and Rohm Haas companies are, in contrast to the other manufacturers, directly represented in this country, it was decided to restrict the test work on resins to their Zerolit and Amberlite range.

The pore structure of resins was discussed in section 2.121, when the three size distributions gel, macroreticular and isoporous were mentioned. Of the three, the macroreticular structure was chosen for detailed testing for it has, according to the manufacturers, a greater ability to withstand the effects of (i) an oxidising regenerant such as nitric acid, and (ii) being continuously cycled between solutions of high and low concentration. The relevant resins from the two manufacturers are (a) strong cation - Amberlite IR-200 and Zerolit 625, and (b) weak base anion - Amberlite IRA-93 and

Zerolit MPH. For testing in the pilot plant work (cf. Chapter 5), the Zerolit resins were chosen on the basis of availibility.

4.21 Physical properties

In the operation of a full-scale ion exchange plant, the resins will be continuously cycled between load and regeneration columns. The rate at which they are cycled is dependent upon the 'capacity' of the resin and the volume of resin present within a column, for a given feedwater flow rate. The resin volume is set by the CCIX column size and the fluidisation properties of the particular resin. Should either the resin capacity or its fluidisation properties change with time, allowance would have to be made and plant operating conditions changed. Naturally, other resin properties such as kinetics and equilibria would also have an effect on plant operation.

4.211 Volume and density: Resin volume is used as a basis for most resin properties. The method of volume measurement is outlined in Appendix A and is based on either a free settled volume (FSV) or a tapped volume. The former measure is used in this work. Because the resin can swell or shrink during an exchange, the volume measurement must be associated with a given resin-form.

Besides the counter-ion within the resin matrix affecting the resin volume, it also affects the resin density. Typically, a heavy metal counter-ion will cause a greater weight increase than a volume increase during an exchange, and so raise the resin density. Table 4.1 gives the mass of 30 mℓ (FSV) of Zerolit 625 in H, Na and NH_4 counter-ion forms. The data show how both swelling and counter-ion type together affect resin density.

TABLE 4.1

Variation of Zerolit 625 bulk density with counter-ion type

Resin Form	H^+	Na^+	NH_4^+
Mass of 30 mℓ(FSV)	24,184	25,580	25,343
Bulk Density gm/mℓ	0,806	0,853	0,845

The bulk density figures of Table 4.1 include a resin voidage in the volume measurement. On the basis of a voidage value of 0,32 (section 4.214), the actual resin density varies from 1,19 to 1,25 gm/mℓ.

4.212 Capacity: The total capacity of an ion exchange resin is determined by the number of exchange groups present in the resin matrix, whilst the operating capacity is a measure of the total capacity when under the influence of the resin equilibrium properties. When resin capacity is determined in a fixed bed column, as most of the resin properties in this investigation are determined, the number of ions loaded onto the resin up to some point on the breakthrough curve (cf. Figure 2.16) is used as a measure of the operating capacity. If the capacity is expressed on a volumetric basis, the degree of resin swelling, caused by a change in the loaded ion, will mean a capacity change. Similarly, a slight variation in resin manufacture will also result in a capacity change.

Table 4.2 gives the total capacity on a volumetric basis for the two anion and cation resins under test, when loaded with different ions. (The experimental details are outlined in Appendix A). The small variation in capacity is due to the low degree of swelling which occurs in macroreticular resins due to the structure of the resin matrix.

TABLE 4.2

Variation of resin capacities with counter-ion type

Resin	Zerolit 625		Amberlite IR-200		Zerolit MPH		Amberlite IRA-93	
Form	Na	H	Na	H	Cl	OH	Cl	OH
Capacity (meq/mℓ)	1,480	1,491	1,475	1,481	1,203	1,211	1,189	1,195

4.213 Fluidisation: In the operation of a fluidised bed CCIX column, the cost is affected by the column diameter and the volume of resin in the column. If the solution flow through a given diameter column could be increased, a lowering of treatment costs would result. The degree to which the solution flow may be increased depends on the resin fluidisation properties, for, at high flow rates, resin may be carried out of the column.

Resin fluidisation is dependent on the relative density of the resin beads and the solution with which the resin is in contact, as well as the particle size distribution of the resin. Because resin density changes with counter-ion type (cf. Table 4.1) and solution density changes with concentration, it is necessary to determine the fluidisation properties for these various density differences.

The method of determination requires that a given volume of resin be placed in a column of known cross-section and that the required solution be passed upwards through the resin bed. At each solution flow rate, the height of the fluidised resin bed is measured. (The experimental details are outlined in Appendix A).

The results are expressed in terms of a percentage bed expansion (% BE) and a superficial linear velocity (LV). The % BE is defined as the increase in FSV bed height at the given flow rate expressed as a % of the FSV bed height and is calculated as follows:

$$\% \text{ BE} = \frac{\text{Fluid Bed Ht} - \text{FSV Bed Ht}}{\text{FSV Bed Ht}} \times 100 \qquad (4.1)$$

Of the two types of resin (cation and anion) the biggest density change occurs during the conversion of anion resin from free base (FB) to the chloride form in the anion load reaction (cf. equation 3.24). In Figure 4.1, the fluidisation properties of the two anion resins, Zerolit MPH and Amberlite IRA-93, are compared. The curves were measured under the same temperature conditions for both the free base and the chloride-loaded forms of the resins using tap water and 1N NH_4Cl solution as the fluidising media. The reason for testing the particular combinations outlined is based on a consideration of the resin and liquid streams which may occur together when the anion load and regeneration reactions expressed in equations 3.24 and 3.25 take place in a CCIX column. In practice, when operating a CCIX column (cf. Chapter 5) consideration need only be given to the condition which causes maximum fluidisation, for this dictates the column control settings which result in stable operation.

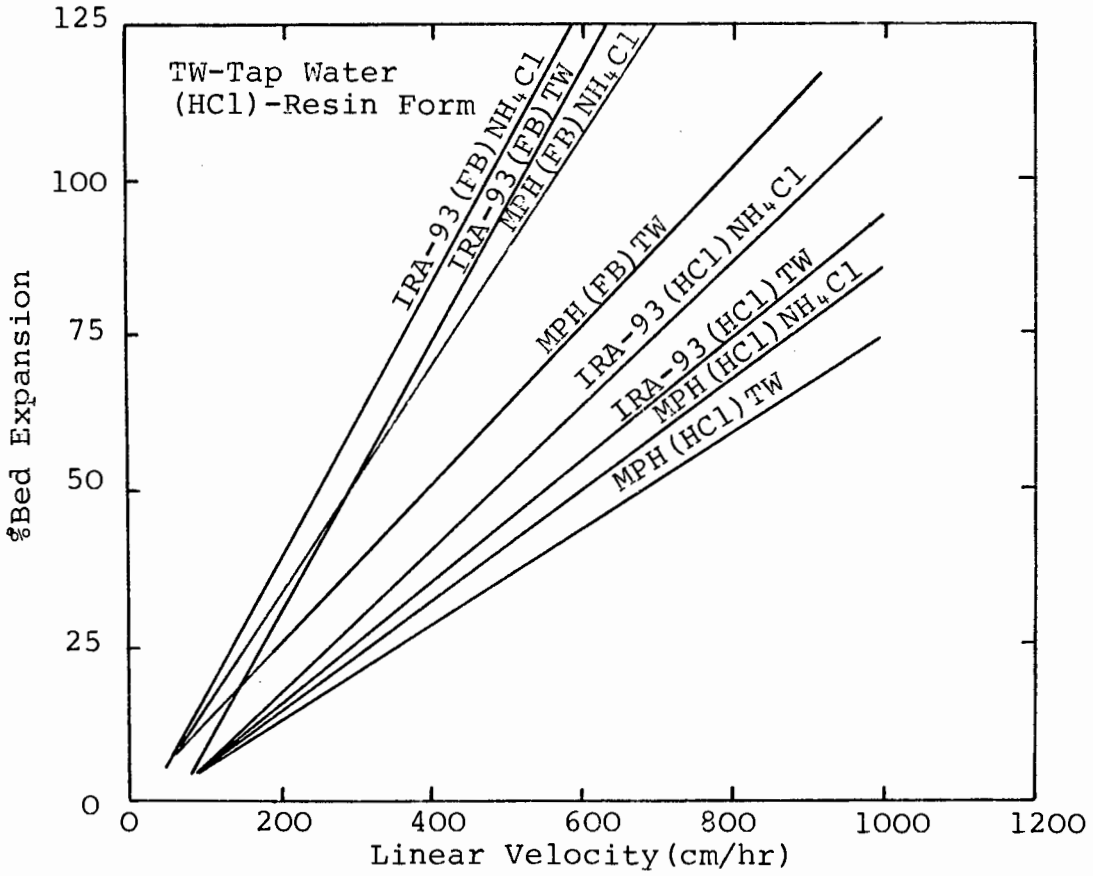

FIGURE 4.1

Fluidisation properties of Zerolit MPH and Amberlite IRA-93 resins

From the curves in Figure 4.1, the resin choice on the basis of fluidisation properties would be Zerolit MPH. The curves for both FB (free base) and Cl-type resin show clearly that, for a given % BE, Zerolit MPH needs a higher flow to achieve the level of fluidisation. As mentioned previously, this has a cost advantage in terms of solution throughput in a CCIX column. Further, the FB and Cl-forms of IRA-93 show a greater BE divergence at a given linear velocity than does the MPH. The divergence means that, at the conditions set for the anion load reaction (equation 3.24) in a CCIX column, a greater inventory of IRA-93 resin would be required to ensure that each stage of the column would remain full during resin fluidisation (cf. Chapter 5).

The reason for the difference in the fluidisation properties of the two anion resins can be explained in terms of the pore size distribution and the crosslinking (cf. Chapter 2.12). The MPH resin has a higher level of cross-linking and smaller pores, so that, although it has an advantage on the basis of fluidisation, it may be at a disadvantage when resin fouling is evaluated (section 4.22).

The two samples of the Amberlite and Zerolit cation resins tested showed identical fluidisation properties. Variation occurred when the resin counter-ion was changed from H to NH_4 to Na. In Figure 4.2, the effect of these changes on the fluidisation properties of Zerolit 625 is shown. The curves indicate that because the density change is small (cf. Table 4.1), the change in % BE, with counter-ion type at a given linear velocity, is also small. Similarly, when solutions of different concentration are passed in upflow through a given resin type, the level of fluidisation shows only a marginal variation because typically, the density change of a nitric acid solution in the concentration range of interest 0 to 3,0N is only 10%.

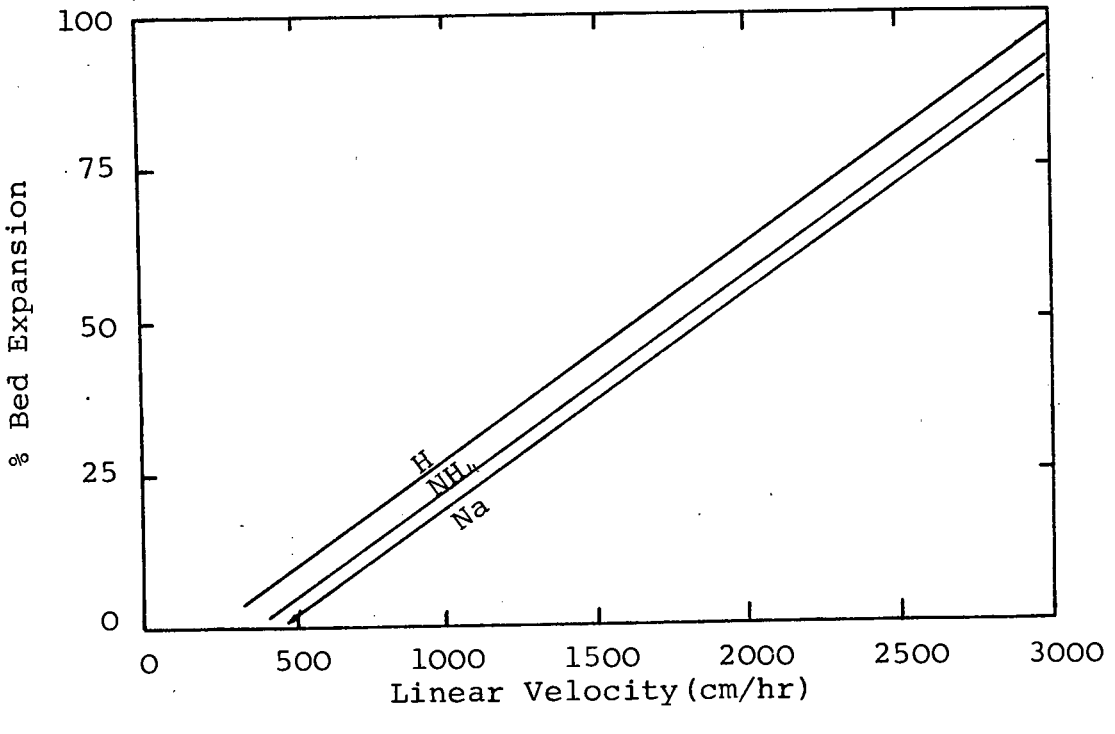

FIGURE 4.2

Fluidisation of Zerolit 625 in NH_4, Na and H form

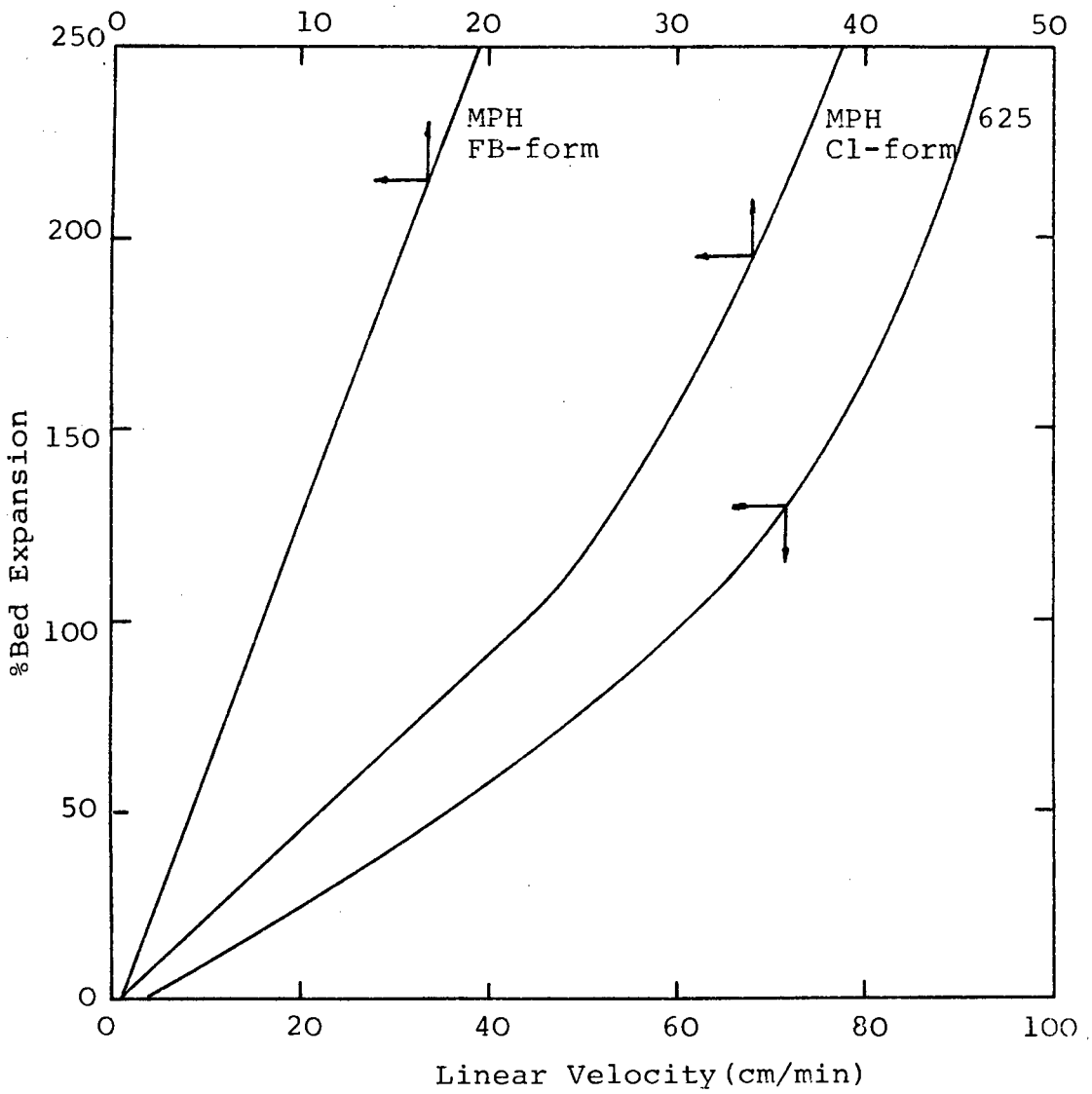

FIGURE 4.3

Fluidisation curves for Zerolit 625 and MPH resins

Figure 4.3 compares the fluidisation properties of the Zerolit anion and cation resins in the bed expansion range 0 to 250%, using low salinity tap water as the fluidising medium for each curve. The density difference of the resins is clearly indicated by the results presented. As an approximation, to achieve a desired bed expansion the flow through the cation resin needs to be twice the flow through the loaded anion resin and four times the flow through the FB anion resin.

4.214 Voidage: The voidage of a free settled volume (FSV) of resin is dependent on the resin form and the bead size distribution of the resin sample on which the test is conducted. The voidage is determined (cf. Appendix A) by measuring the volume of solution that is present within the resin bed interstices of a sample of FSV resin. The solution volume, when expressed as a fraction of the FSV volume, is a measure of the voidage.

As a bed of resin is fluidised, so the voidage of the expanded resin increases. By knowing the voidage of a settled resin bed and the degree of resin fluidisation, the voidage for any level of bed expansion can be computed from the following expression:

$$\varepsilon' = 1 - \frac{1-\varepsilon}{1+BE} \qquad (4.2)$$

where ε' - fluidised bed voidage

ε - settled bed voidage

BE - fractional bed expansion = %BE/100

Figure 4.4 presents a curve of equation (4.2) based on a measured settled bed voidage of 0,32 determined for the bead size distribution of the Zerolit cation resin and 0,31 for the Zerolit anion resin in free base form.

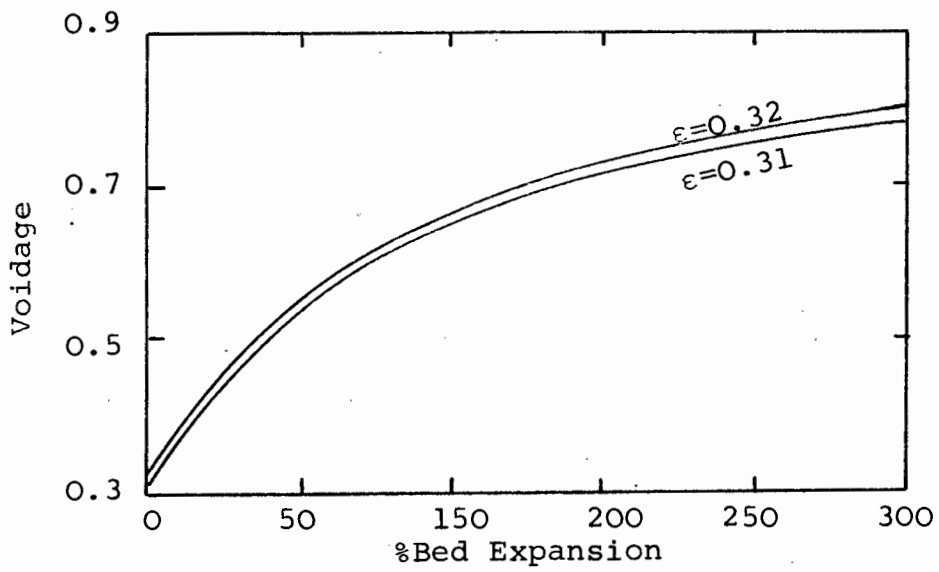

FIGURE 4.4

Fluidised bed voidage curves

4.22 Resin fouling and life tests

One of the problems associated with the use of ion exchange resins in a desalination function on treated sewage water is the possibility of permanent fouling of the resin, with a consequent loss of ion exchange capacity and the need for more frequent resin replacement in an ion exchange plant. A measure of the rate and degree of resin fouling on a range of resins is therefore necessary to determine which resin, on the basis of organic fouling, is best. Such a series of tests is outlined below.

4.221 Background: When ion exchange was first used for desalination, the ability of the anion resins simultaneously to remove organic material from the water in fact hindered their performance, because the resins tended to become fouled. However, this fouling led to the development of new resins which, although still becoming loaded with organics, did not lose capacity. Nowadays, these new resins are being considered in the role of organic scavengers during the upgrading of water.

To date, the mechanism by which anion resins 'take up' organics is still being debated but it would appear to be an adsorption-ion exchange combination, depending upon the particular organic species present in the water. In the case of sewage effluents, the variety of organic compounds present is so great, (Painter [95] lists some which have been positively identified) that the resin loading mechanism on this water is even less likely to have been quantified, especially since organic resins without functional groups (e.g. the XAD range of resinous adsorbents from Rohm and Haas [96]) have proved, in certain instances, to be as efficient as the ion exchange resins for removing organics.

From the work conducted on the organic uptake of resins by such authors as Kim et al. [97], Junk et al.[98], Oehme et al. [99] and Hinrichs et al. [100], the following parameters have been shown to have an effect:

(i) the relative size of the resin pores and the organic molecules;

(ii) the resin matrix type, e.g. styrene-divinylbenzene, phenol-formaldehyde;

(iii) the pKa of both the organic molecule and the resin functional group and the pH at which adsorption occurs.

(iv) the period of time for which resin and organic molecule are in contact.

In general, any resin is fouled by one of two mechanisms by a solvated molecule, either (i) the fouling molecule is held so strongly by the functional group that normal regeneration techniques do not remove it, more likely in the case of strong electrolyte resins, or (ii) the molecule is large and becomes trapped within the resin matrix and blocks the functional group, so preventing other ions from exchanging at the blocked resin site. A phenomenon which may occur, and which is often erroneously interpreted as resin fouling, is a capacity loss due to degradation of the functional groups within the resin by, typically, strong oxidising agents.

Besides the 'capacity loss' effect organic fouling does have on an anion resin, it may also affect the desalination operation by increasing the normal wash water volume required to wash resin after regeneration. The purpose of the wash water is to remove the regenerant solution from the resin bed. In the case of an anion resin, this may be a NaOH or ammonia solution. When organic molecules from a wastewater are trapped in the resin matrix they have the ability, because they are usually organic acids (e.g. humic and fulvic acids), to exchange their carboxylic acid hydrogen ions for the cation present in the regenerant solution, e.g. sodium or ammonium. During the subsequent wash, these exchanged cation sites slowly hydrolyse and release their sodium or ammonium cation. As this hydrolysis step is slow and pH dependent, large volumes of wash water are required to effect satisfactory washing. A determination of an increase in resin wash water requirements is thus also indicative of the level of organic fouling.

Having established the parameters which control the organic loading of a resin, it now becomes possible to formulate a technique to rejuvenate an organically fouled resin. To achieve resin rejuvenation, it is necessary to provide a solution environment external to the resin bead which is more favourable for the organic molecule than is the resin environment. Blesing [101] outlines how ethanol/acid and ethanol/brine/caustic regenerants were used to achieve resin capacity recovery. These regeneration techniques either convert hydrophobic organics to hydrophilic form and then allow them to diffuse out of the resin matrix by providing long contact times, or they supply a solution phase for which the organic molecule has a higher preference. In this manner, a certain degree of, and sometimes all, lost capacity may be recovered.

Fouling of cation resins by organic molecules is not documented in the literature, probably because it very rarely occurs; primarily due to the fact that the organics are generally acids or contain acid groups within their structure and are consequently repelled by the Donnan effect (cf. Chapter 2) in cation resins.

Capacity loss on cation, and anion, resins can and does occur from exchange with inorganic ions that are then so strongly held by the resin that normal regeneration techniques do not remove them. In the case of cation resins, these ions can take the form of heavy metal complexes (especially cyanide complexes), or polyvalent metals, e.g. Mn^{4+}; for anion resins anionic complexes of amphoteric metals are usually the problem, e.g. silicates, aluminates.

4.222 Organic loading of anion resins: In order to provide a complete tertiary treatment for sewage plant discharge using ion exchange, it is necessary to determine the degree of organic removal which the weak base resins under consideration for use in the IX process are able to achieve. Test work of this nature has been conducted by Tilsworth [102] on lake and well water, Anderson et al. [103] on surface waters and Brown et al. [104] on contaminated river water. In each case, the authors tested a number of anion resins and concluded, separately, that each particular water could be upgraded by an anion resin with minimal capacity loss.

For the purposes of the organic loading investigation, the five weak base anion resins, two gel type and three macroreticular listed in Table 4.3, were chosen for testing. The objective was to compare the resins' ability to remove organics from the water (measured in terms of the reduction of the chemical oxygen demand (COD) of the water [105]) and to withstand the effects of organic fouling. Details of the experimental procedure are outlined in Appendix B.

TABLE 4.3

Weak base resins chosen for initial organic removal tests

Resin	Matrix type	Matrix structure
Zerolit MPH	Styrene-DVB	macroreticular
Amberlite IRA-68	Acrylic-DVB	gel
Amberlite IRA-93	Styrene-DVB	macroreticular
Dowex MWA1	Styrene-DVB	macroreticular
IMACTI A27	Epoxy Amine	gel

Secondary purified sewage effluent (humus tank effluent (HTE)), with the composition given in Table 4.4 was used in the tests. The water was pretreated by passage through a sand filter and cation exchange column prior to use on the anion resins. The testwork was conducted in down-flow mode in fixed bed columns, and the degree of resin fouling was monitored by both the column operating capacity to a 10% chloride breakthrough and the resin wash water requirements (cf. Appendix B).

TABLE 4.4

Composition of secondary sewage effluent used for anion resin COD removal comparison

Component	Composition (mg/ℓ)
Na	380
Ca	60
Mg	60
NH_4 as N	1
Cl	575
SO_4	163
NO_3 as N	10
COD	40

Initially, twenty load regeneration and wash cycles were conducted on the five anion resins and a comparison of the level of fouling of each resin made. The operating capacity was determined during each load cycle and plotted against the cycle number. Figure 4.5 shows typical curves for two of the resins. From these plots, the degree of capacity change was evaluated by a least squares straight line fit of the data from cycle 5 to cycle 20. Cycle 5 was chosen to make allowance for the capacity loss which tends to occur with a new resin when initially contacted with organics. The slope of the fitted straight line is then an indication of the change in capacity over the fifteen cycles. Table 4.5 lists, for the five resins, the operating capacity change which occurred over the fifteen test cycles. Because the load cycles were continued to a 10% chloride breakthrough, and because the resins each have different capacities, the total mass of organic material loaded onto each of the resins during the test cycles is not the same; the relative organic loadings are given in Table 4.5.

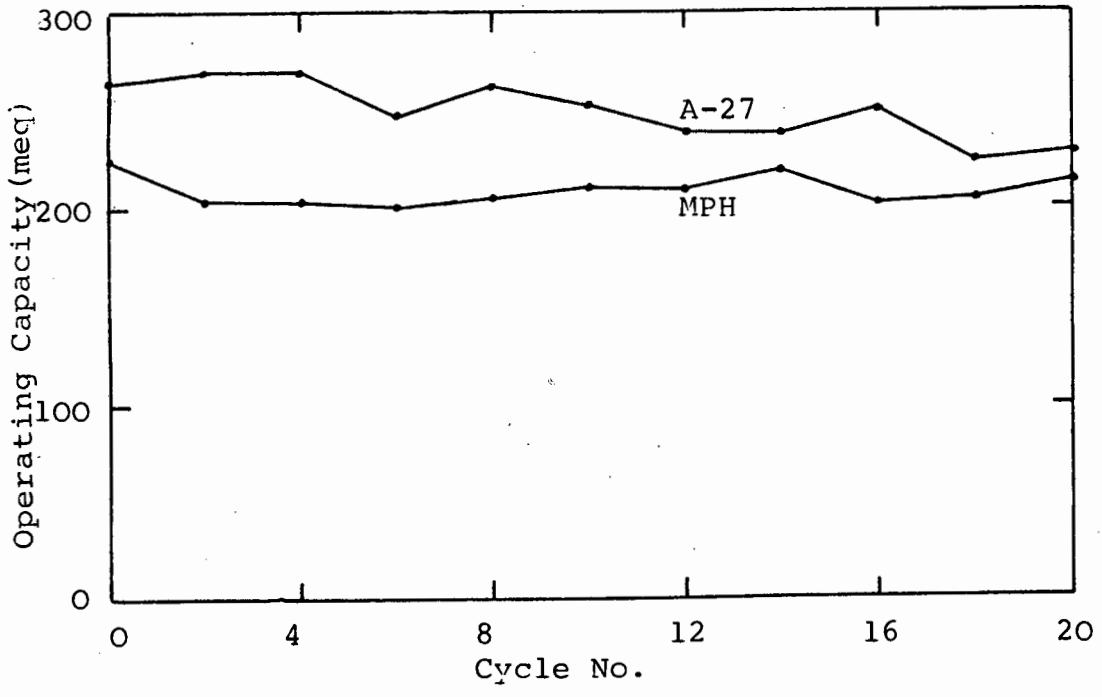

FIGURE 4.5

COD removal by anion resins:

Capacity variation with cycle no, Zerolit MPH Imacti A27

TABLE 4.5

Operating capacity change on anion resins during organic loading tests over 15 cycles

Resin	% Capacity Change	Relative Loading
MPH	+ 1,4	1,0
IRA-93	+ 2,2	1,0
IRA-68	+ 3,3	1,4
MWA1	- 0,5	1,2
A-27	- 8,0	1,3

Two of the tested resins Dowex MWA1 and Imacti A27 show a net capacity loss over the test cycles while the other three resins show, what is at first sight, a rather surprising result - a capacity gain. However, Brown et al. [104] recorded exactly the same behaviour when they monitored the weak base capacity of anion resins. During the manufacture of a weak anion resin, a certain number of strong base functional groups are always simultaneously

formed. In a series of tests such as these, the strong base groups degrade to form weak base groups and so cause an apparent capacity increase - hence the results of Table 4.5.

In Figure 4.6, the wash water requirements of the Zerolit and Imacti resins are compared at various points in the twenty cycle test programme.

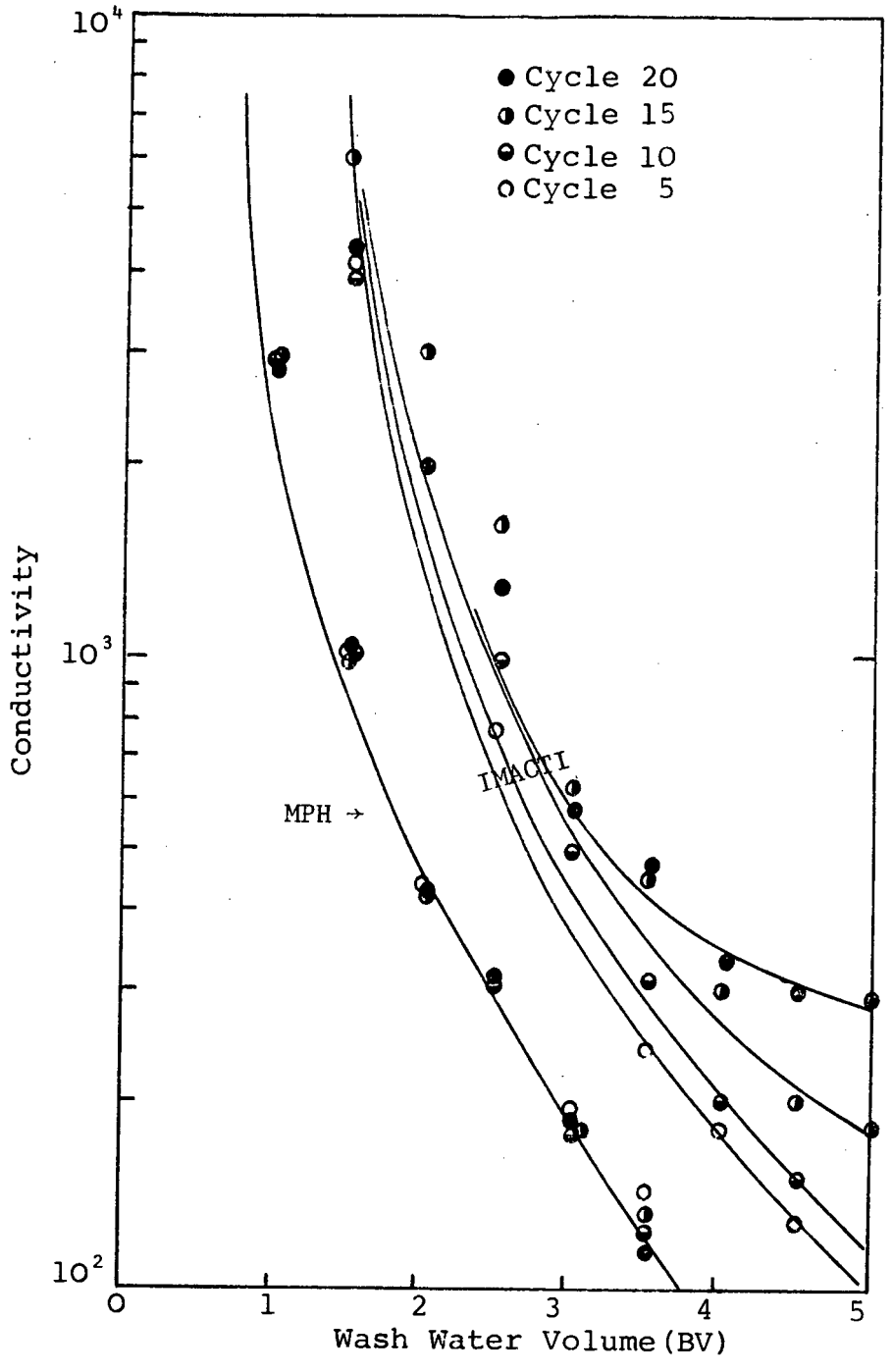

FIGURE 4.6

Wash water requirements of Imacti A27 and Zerolit MPH resins

Like the capacity determination results, these tests show clearly that the MPH resin does not appear to have fouled whilst the A27 has fouled. This is measured by observing the conductivity reduction which is achieved by a given volume of wash water. Because of the Zerolit resin's slightly lower volumetric capacity, a given conductivity reduction could be achieved on the 'new' Zerolit resin with less wash water than was required for the 'new' Imacti resin. After the 20 cycles, however, the 'new' resin conductivity reduction could still be achieved with the same wash volume on the Zerolit resin but not on the Imacti resin. The increase in wash water required to achieve the conductivity reduction previously attained on the 'new' Imacti resin is the result of organic fouling.

Despite the capacity decrease which occurred on two of the resins, all five resins were able, over the test period, to effect a reduction in the level of organics present in the feed water. In terms of the COD reduction, there was not much to choose between the resins. In Table 4.6 the average reductions for each of the five resins are compared over the twenty load cycles. The different resin capacities account for the variation in the volume to 10% chloride breakthrough shown in Table 4.6.

TABLE 4.6

COD reduction on anion resins

Average over 20 load cycles with feed COD=40 mg/ℓ

Loaded Volume (BV)	% Chemical Oxygen Demand Reduction based on 40 mg/ℓ				
	MPH	IRA-93	IRA-68	MWA1	A27
5	65	58	63	65	65
15	65	68	65	65	65
25	65	68	60	70	63
35	65	65	63	70	63
45	65	60	60	68	63
55	55	58	65	65	63
65			58		58
75			55		

The only two resins to record a marked visual change during the organic loading tests were the gel types - IRA-68 and A27. The former changed in colour from white to dark brown while the latter changed from cream coloured to black. The macroreticular resins showed a slight darkening over the test period.

For comparison of organic removal capabilities only, an HTE water from an overloaded sewage treatment plant was passed through volumes of MPH and IRA-93 resin equal to those used in the life tests (cf. section 4.223). The organic level of this HTE water from the Athlone Works was then reduced in a laboratory aeration tank, and the anion resin loading repeated. As before, the anion feed was pretreated in a cation column and the degree of COD removal by the anion resin used was monitored. A summary of these results is presented in Table 4.7.

TABLE 4.7

Average organic removal by resins from the high COD Athlone plant discharge

Stream after specified treatment	Treatment System			
	With further biological treatment		Without further treatment	
	COD (mg/ℓ)	% Reduction of step based on HTE	COD (mg/ℓ)	% Reduction of step based on HTE
HTE	130	-	130	-
aeration	95	27	-	-
filtration	75	15	100	23
cation column	65	8	70	23
anion column	12	41	35	27

As each of the six loading tests on the two water types of Table 4.7 were conducted to the same 10% breakthrough criterion of the life tests, the COD levels are directly comparable. The two interesting points which emerge are (i) the reaction products of the biological treatment of sewage water to low residual COD values are readily adsorbed by ion exchange resins hence the 12 mg/ℓ COD level of the treated water, and (ii) that insufficient biological treatment leaves certain organic components in the water which

are now more readily exchanged on a cation resin and consequently, a change in the fraction of total organics adsorbed by each resin occurs. Clearly the chemical composition of the water affects the ultimate degree of COD removal which an ion exchange system is able to achieve. Without determining the exact organic constituents of the water and investigating the affinity of the resins for each of these constituents, no valid explanation for the differences in COD removal shown in Table 4.7 can be proposed.

4.223 Life tests: In an ion exchange plant, the ability of the resins continuously to perform their exchange function will have an influence on plant costs. When an HTE water is being considered as a feed solution, then the life of the resins assume even more importance, and published resin life data are less readily available. There exists, then, a need to determine an approximate resin life under conditions which will most closely simulate eventual operating conditions.

Equal volumes of the two Zerolit and Amberlite macroreticular resins MPH, 625, IRA-93 and 200, were placed into respective small diameter columns, with the object of putting them through a large number of load, regeneration and wash cycles. (Detailed experimental procedure is outlined in Appendix B. The four macroreticular resins were chosen for further testing after consideration of (i) the required regenerant stream concentration which (cf. section 2.211) would cause gel resin beads to fracture as a result of bead expansion and contraction, (ii) that the anion resins were able to effect a satisfactory COD reduction without capacity loss over 20 cycles, and (iii) the dominant share of the local market that the Amberlite and Zerolit manufacturers hold. The average composition of the feed solution, passed upwards through the resin beds so that resin fluidisation occurred, during the test period is given in Table 4.8. The anion resin feed was "de-cationised" in a separate large cation column. The regenerant chemicals were respectively 3,ON solutions of nitric acid and ammonia, and the wash water was low salinity tap water. The flow cycling was continuous and automatically controlled. At various intervals, controlled load cycles were conducted and resin samples withdrawn and investigated before being replaced. In this manner, the effects of (i) the combined salt-COD load on the resins, (ii) the high regeneration chemical concentration, and (iii) the fluidised bed operation on the resin could be assessed at various points in the life of the resins.

TABLE 4.8

Average feed water composition used in resin life tests

Component	Composition (mg/ℓ)	
	Cation Feed	Anion Feed
Na	300	<25
Ca	55	0
Mg	55	0
NH_4 as N	15	0
K	22	0
SO_4	155	155
Cl	480	480
NO_3 as N	12	12
PO_4	24	24
COD	60	50
pH	7,4	<2,0

4.2231: Capacity: The capacity of the resins was determined by the breakthrough method outlined in Appendix B. For the cation resins, a 10% sodium breakthrough point was used and for the anion resins a 10% chloride breakthrough. Typical breakthrough curves for the four resins, obtained during the controlled test at cycle 900, are presented in Figures 4.7 and 4.8.

In Figure 4.7, the small difference in the capacity of the two cation resins is indicated by the relative 'closeness' of the two curves. For the average feedwater sodium content of 300 mg/ℓ, the breakthrough capacities would be determined from the load solution volumes as the two curves pass through the 30 mg/ℓ point. Because the other cations are present in the feed at a considerably lower level than sodium, and the resin has a higher affinity for these ions than for sodium, they could, if the feed flow were not stopped, show similar breakthrough curves but at greater solution volumes. For further comparison, the COD values of the solution leaving the cation columns are included in Figure 4.7. These COD curves show that very little (approximately 10%) COD reduction occurs on the cation resins.

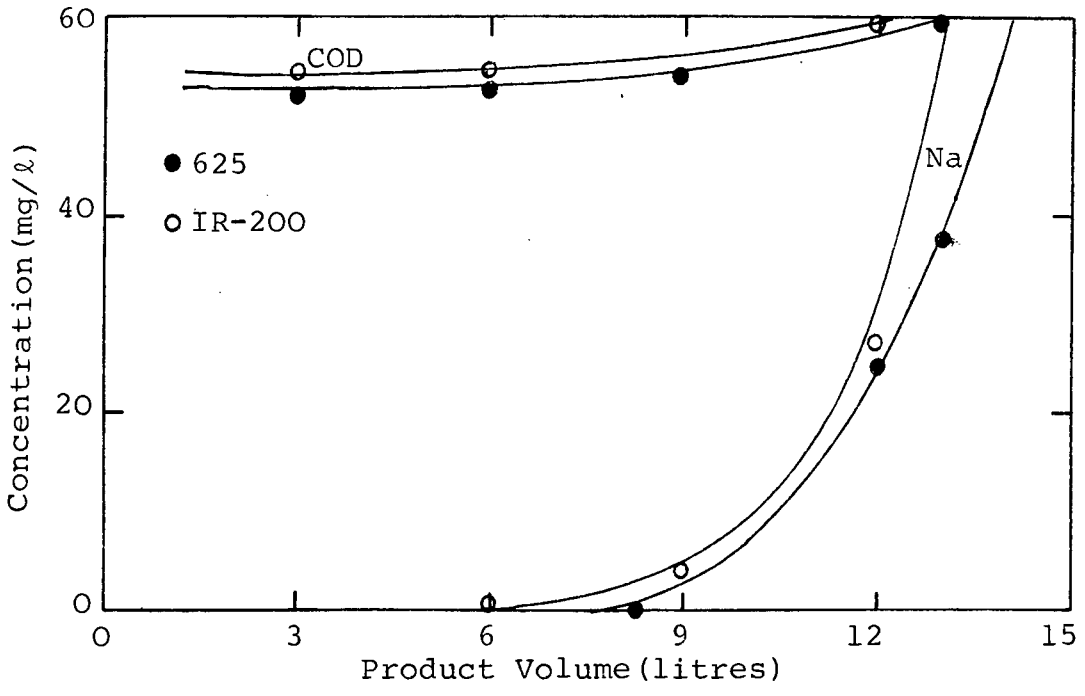

FIGURE 4.7

Resin life tests

Breakthrough capacities of cation resins: Cycle 900

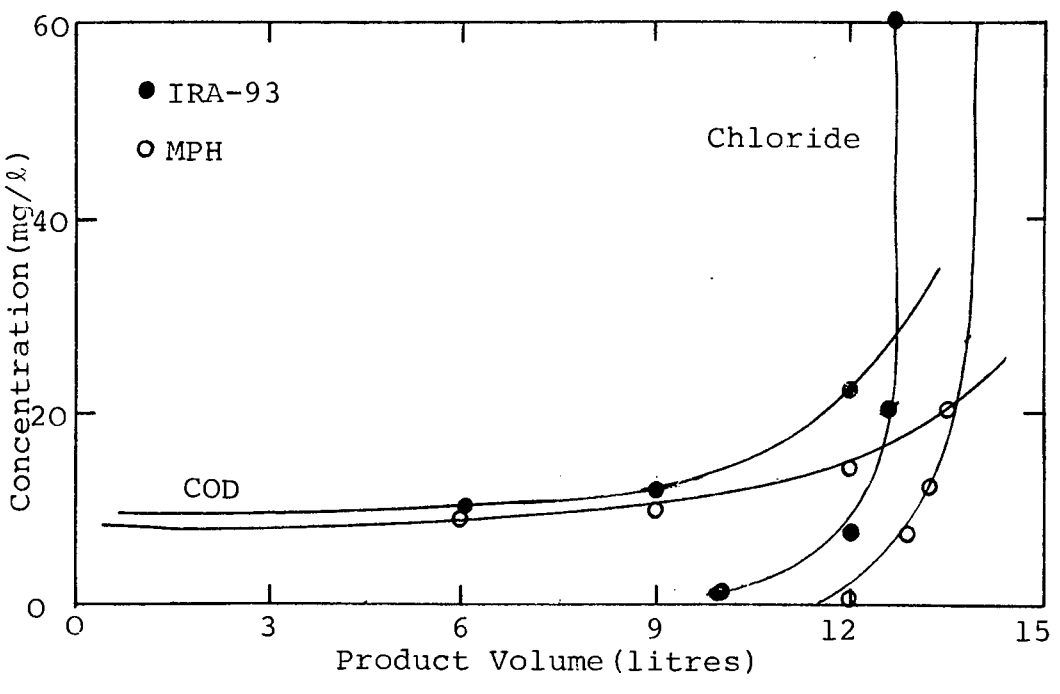

FIGURE 4.8

Resin life tests

Breakthrough capacities of anion resins: Cycle 900

The equivalent anion breakthrough curves at cycle 900 are presented in Figure 4.8. In this case, the resin capacity disparity is slightly greater than for the cation case; a function of the resin manufacturing process. The chloride breakthrough curves in Figure 4.8 are far steeper than the sodium curves of Figure 4.7 due to the relative equilibrium properties of the anion and cation resin (cf. section 4.3); the anion resin has an extremely high affinity for the loading ions. The COD curves for the two resins in Figure 4.8 show the same trend as the chloride curves, and the level is indicative of the ability of the anion resins to remove most of the organic material present in the feed water used for the tests. In general, the anion product water COD is less than 20 mg/ℓ provided the feed COD prior to filtration is <90 mg/ℓ. Because the mechanism of COD removal is not well known, an account of the change in the degree of organic removal with input concentration cannot be given. Further, why a certain residual quantity of organic material is not adsorbed by the resin cannot either be explained.

In Figures 4.9 and 4.10 the capacities of the two anion and cation resins are compared over 1 100 load and regeneration cycles. On the basis of an anticipated 24 hour cycle time in an ion exchange plant, the data of Figures 4.9 and 4.10 would be equivalent to three years of plant operation. It is obvious from the curves presented, that no consistent trend in the resin capacities is revealed. The rather erratic change of capacity from one test cycle to another is due to the variability of the composition of the feed water used. For both the anion and cation resins, the ratio of divalent to monovalent ions present in the feed stream has an effect on resin capacity (cf. Figure 3.1). The fact that both resins of each type show the same change trend over the test cycles is indicative of external factors causing the change, and not resin fouling.

4.2232 Bead structure: Although the resin capacity may not have changed over the test period, the structure of the beads themselves may have altered, due either to the relative motion of the beads against one another in the fluidised bed or to the swelling and shrinking which may have occurred during the resin regeneration and wash steps as the external solution concentration was raised and lowered. A rough measure of this structural change can be gained by visual inspection of the beads under a microscope. A comparison of the relative number of whole, cracked or broken beads at various

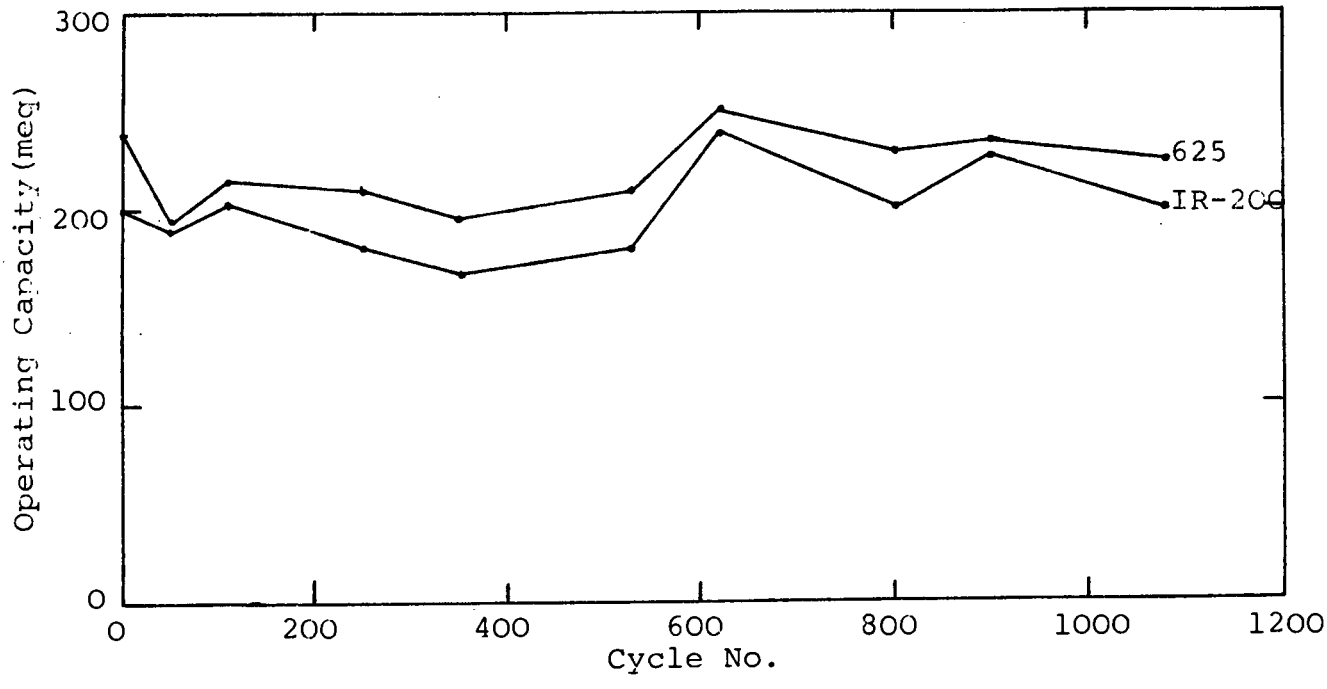

FIGURE 4.9

Resin life tests

Operating capacity versus cycle no: Cation resins

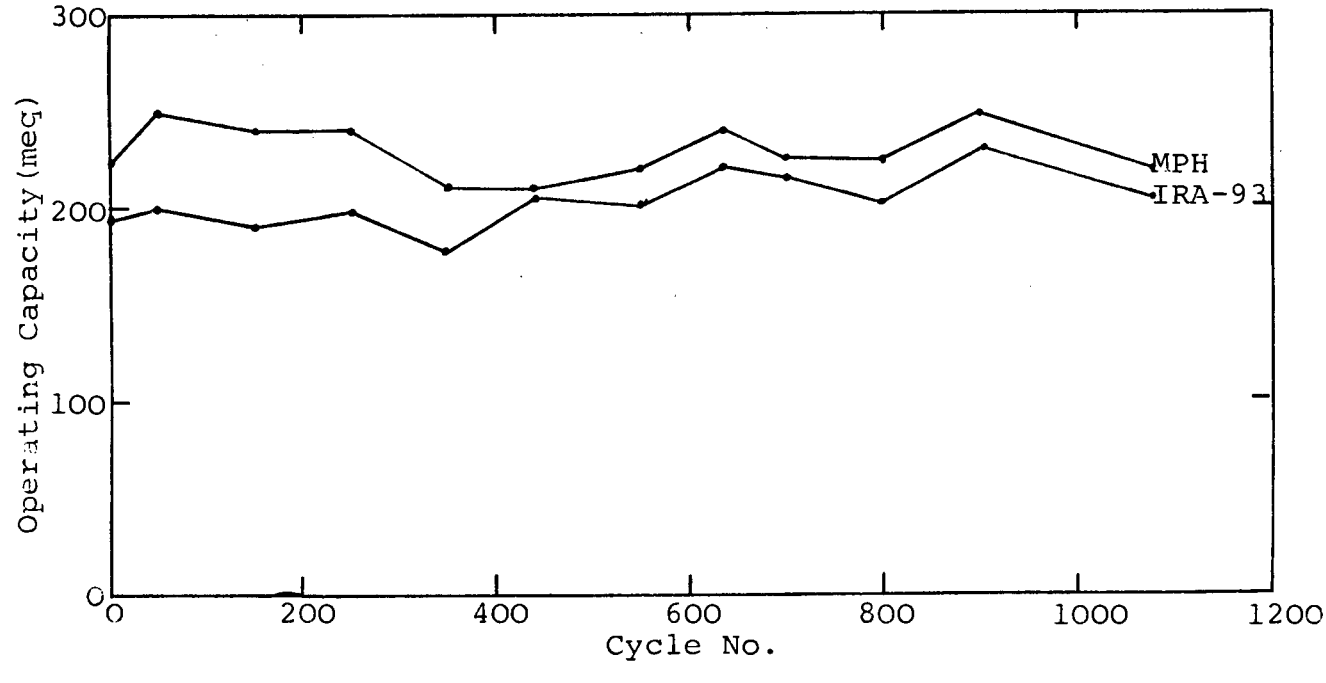

FIGURE 4.10

Resin life tests

Operating capacity versus cycle no: Anion resins

times in the life tests gives an indication of the damage the continuous resin cycling has caused.

Table 4.9 presents the results of the bead count tests (the details are provided in Appendix A) undertaken on the four resins. Each analysis of Table 4.9 is an average of five counts on three samples of resin, one each from the top, middle and bottom of the test columns.

TABLE 4.9

Bead counts on life cycle test resins

Resins	625			200			MPH			IRA-93		
Cycle	%W	%C	%B	%W	%C	%B	%W	%C	%B	%W	%C	%B
0	97,3	0,2	2,5	99,7	0,0	0,3	100,0	0,0	0,0	99,0	0,0	1,0
110	91,1	5,9	3,0	99,0	0,0	1,0	98,9	0,6	0,5	88,6	3,8	7,7
215	93,5	4,6	1,9	99,4	0,3	0,3	98,0	1,0	1,0	91,7	1,0	7,3
457	95,3	4,3	0,4	99,7	0,3	0,0	97,1	0,3	2,7	88,2	0,8	11,0
1040	92,2	7,8	0,0	99,5	0,0	0,5	73,7	3,2	23,1	66,3	2,0	31,7

%W - % of sample which are whole beads

%C - % of sample which display cracks

%B - % of sample consisting of half or piece of bead

Bearing in mind the accuracy of the bead count tests, the following conclusions can nevertheless be drawn from the results: (i) the Zerolit cation (625) and Amberlite anion (IRA-93) resins appear to undergo a certain measure of structural change immediately, (ii) neither cation resin shows, other than the initial Zerolit change, any further alteration in structure, and (iii) after prolonged cycling, both anion resins appear to degrade structurally, the degree of change being approximately the same for both.

Although the anion bead breakage does not have an adverse effect on the resin's exchange properties, it may result in resin loss during the operation of a fluidised bed CCIX column due to the smaller particles being washed out of the column. Fortuitously, however, the anion resins do adsorb a quantity of organic material irreversably causing both a resin colour change and a slight increase in resin density. The density increase compensates, to a certain measure, for the particle size reduction which does occur.

An advantage of the resin bead size change is shown when the loading rate of MPH and IRA-93 are compared as new resins and after the resin life tests. In both cases, faster loading occurs on the 'used' resins, due probably to the size difference of the two samples. A third loading curve on MPH resin, conducted on a sample withdrawn from the ion exchange pilot plant (cf. Chapter 5) after the resin had undergone 18 months of cycling on sewage plant discharge, showed the same loading rate as did new MPH.

4.2233 Conclusions: From the tests conducted, it is concluded that the ion exchange resins investigated can be cycled at least 1 100 times without showing any capacity change. In fact, on the basis of Figures 4.9 and 4.10, a certain measure of extrapolation can be considered. The only change that has been detected during the life tests, has been the alteration of the size distribution of the two anion resins - this has, however, been offset by the concurrent density increase which has occurred. The simultaneous kinetic increase has, as will be demonstrated in Chapter 6, no real advantage in the CCIX system.

4.23 Equilibria

In section 2.2 of Chapter 2 the resin properties affecting the equilibria of electrolyte sorption and ion exchange were outlined and in Chapter 3, equations (3.23) to (3.27), the exchange steps in the desalination scheme with regenerant recovery were presented. In order to predict the degree of mass transfer in CCIX plant, it is necessary to determine the equilibrium properties of the strong cation and weak anion resins for the reactions (3.23) to (3.27) and for the sorption of electrolytes.

The organic loading and life tests of section 4.22 could not distinguish any particular operating difference between the two Amberlite and Zerolit resins. On the basis of availability, therefore, the Zerolit resins were chosen for the pilot plant (cf. Chapter 5), and further detailed kinetics (cf. section 4.24) and equilibrium evaluations were done on these resins.

4.231 Ion exchange reactions: Table 4.4 shows a feed water composition that will be treated by the ion exchange process. Although this water contains a mixture of cations and anions, the major component is NaCl. Further,

both the cation and anion which, after NaCl, constitute the next major portion of the Table 4.4 water are divalent ions. At the concentration level of this water, approximately 0,02N, the resin has an affinity for the divalent ions which is an order of magnitude higher than the monovalent ions [106]. Considering the predominance of the Na and Cl ions and the resin selectivity for the Ca, Mg, SO_4 ions, it was decided to investigate only the load equilibria of Na and Cl, for these latter two ions would determine the treated water quality and CCIX-column design requirements. Similarly, because the loaded resins would contain mainly Cl and Na ions, only the equilibria of the former ion with NH_3 solution in the case of anion resin regeneration, and the latter ion with NH_4 ions in reaction (3.26) as part of the regenerant recovery scheme, were determined. The cation resin regeneration reaction (3.27) involves the ammonium-loaded resin and hydrogen ions and therefore this equilibrium was also determined.

A further objective of the ion exchange equilibrium tests was to determine whether the separation factor (equation 2.10) could be used to represent the equilibrium curve, and further to determine what effect, if any, solution concentration has on the exchange of monovalent ions (cf. the mono-divalent exchange of Figure 2.8).

4.2311 Cation resin: In a series of batch tests (all experimental details on equilibrium determinations are outlined in Appendix B) the relevant equilibria were determined. The test work necessitated the contact of resin and solution, each with different initial compositions, and the determination of the composition of the two phases after equilibrium had been attained.

For the cation load exchange on Zerolit 625, the equilibrium between sodium and hydrogen ions was determined at two solution concentrations - 0,02N and 0,05N - these falling into the anticipated concentration range of a saline water requiring treatment. The results were evaluated in terms of an equivalent ionic fraction (defined in section 2.22) and are plotted as an equilibrium isotherm in Figure 4.11.

In Figure 4.11 the data have been plotted with liquid composition as ordinate and resin composition as abscissa - in contrast to Figure 2.7. This convention has been adopted on consideration of the end-use of the

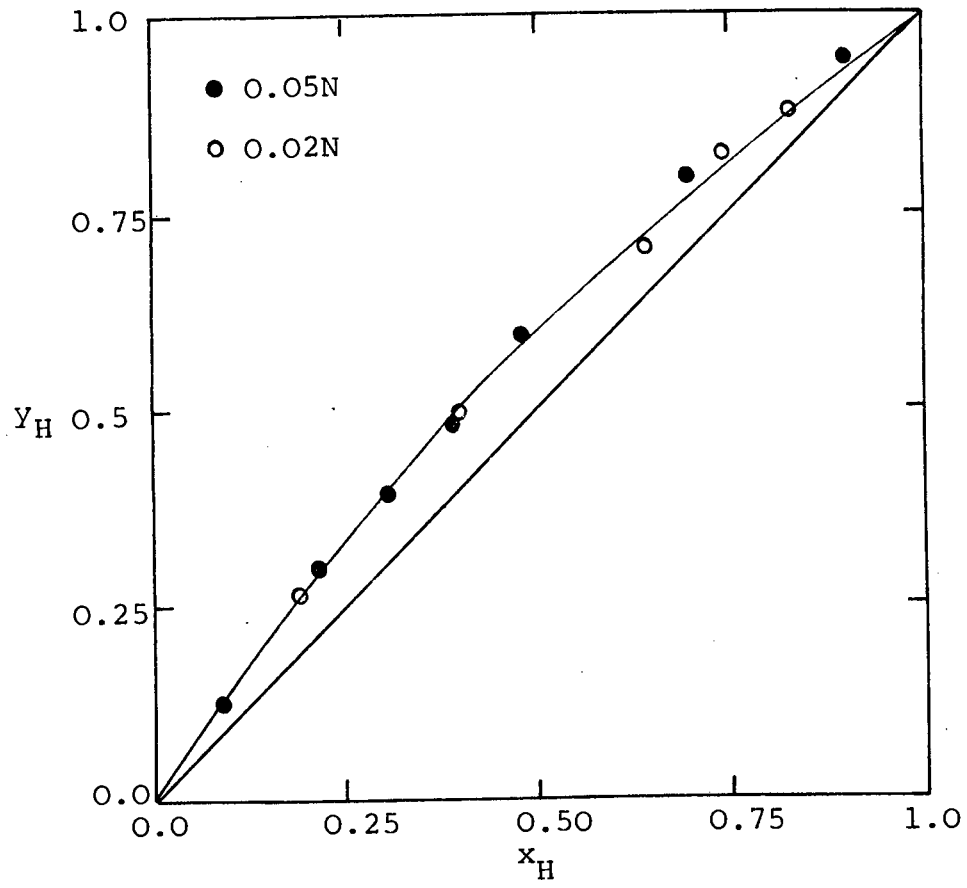

FIGURE 4.11

Sodium-hydrogen equilibrium curves: Zerolit 625

equilibrium curve - the design of a CCIX column. The schematic diagram of a CCIX column (Figure 2.18) shows the direction in which the liquid and resin phases move. The labelling of the equilibrium isotherm axes is thus in accordance with the convention adopted for other column mass transfer devices where the lower density phase is ordinate, and the 'heavier' phase abscissa.

The separation factor equation (2.10) was thus rearranged to the following form

$$y_A = \frac{\alpha x_A}{1 + (\alpha-1)x_A} \qquad (4.3)$$

and fitted to the data of Figure 4.11 by suitable alteration of α. The curve plotted in Figure 4.11 is for α = 1,5. Visual observation shows that equation

(4.3) with a suitable value of α is a good representation of the exchange isotherm and further, at the two concentrations tested, concentration appears to have no effect on the shape of the isotherm or the value of the separation factor.

The equilibrium of the exchange between the sodium-loaded cation resin and ammonium ions was next investigated at three solution concentrations, 0,25N, 0,9N and 1,5N. The results are plotted in Figure 4.12. A curve fit of equation (4.3) was again undertaken and the curve of Figure 4.12 represents an α = 1,2. Although there is some scatter in the 1,5N results, the equilibrium isotherm is nevertheless satisfactorily represented by one separation factor at each of the three concentrations determined. Again, there is no trend with change in solution concentration.

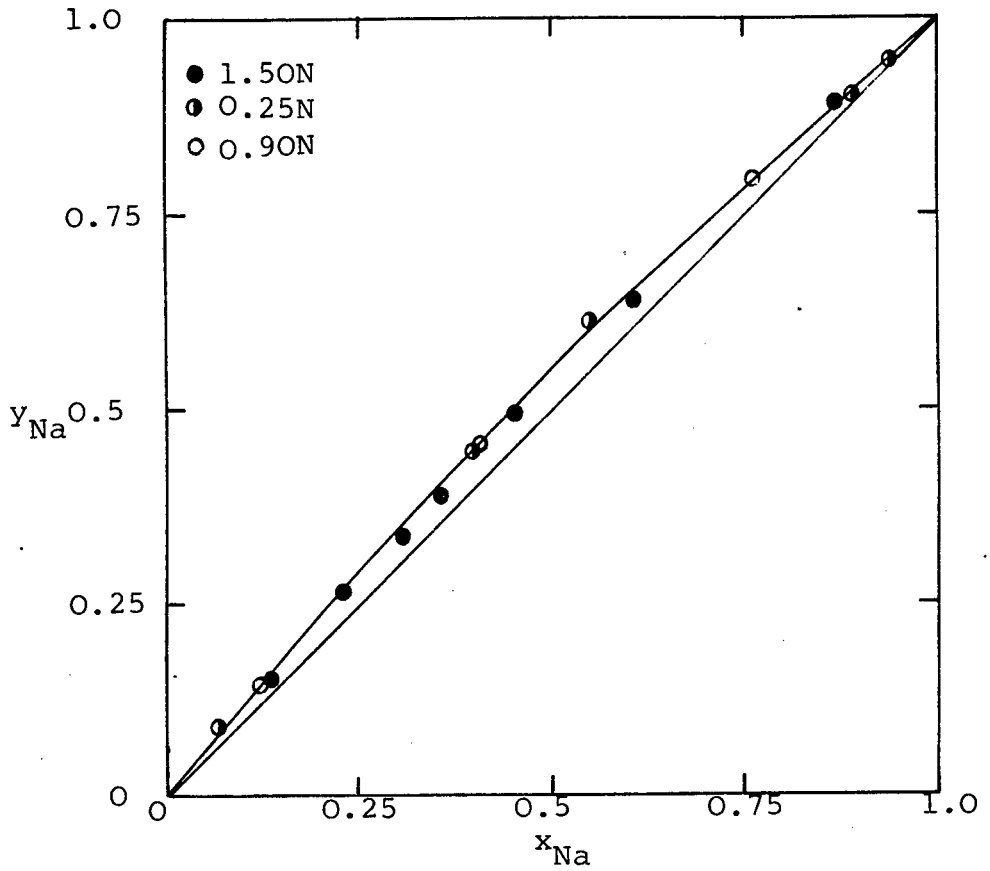

FIGURE 4.12

Ammonium-sodium equilibrium curve: Zerolit 625

Having established the separation factors for the exchange of sodium-hydrogen and ammonium-sodium ions, it becomes possible, by rearrangement of equation (4.3), to determine the α value for the cation regeneration exchange between hydrogen and ammonium ions.

From equation (4.3)

$$\alpha^{H}_{Na} = \frac{y_H \cdot x_{Na}}{x_H \cdot y_{Na}} \quad \text{and} \quad \alpha^{Na}_{NH_4} = \frac{y_{Na} \cdot x_{NH_4}}{x_{Na} \cdot y_{NH_4}}$$

and therefore

$$\alpha^{H}_{Na} \cdot \alpha^{Na}_{NH_4} = \frac{y_H \cdot x_{NH_4}}{x_H \cdot y_{NH_4}} = \alpha^{H}_{NH_4}$$

In Figure 4.13, equilibrium data at 1,ON and 2,ON for the cation regeneration exchange are presented, and the curve represents equation (4.3) with α = 1,8 - the product of the previously determined α values according to the above expression.

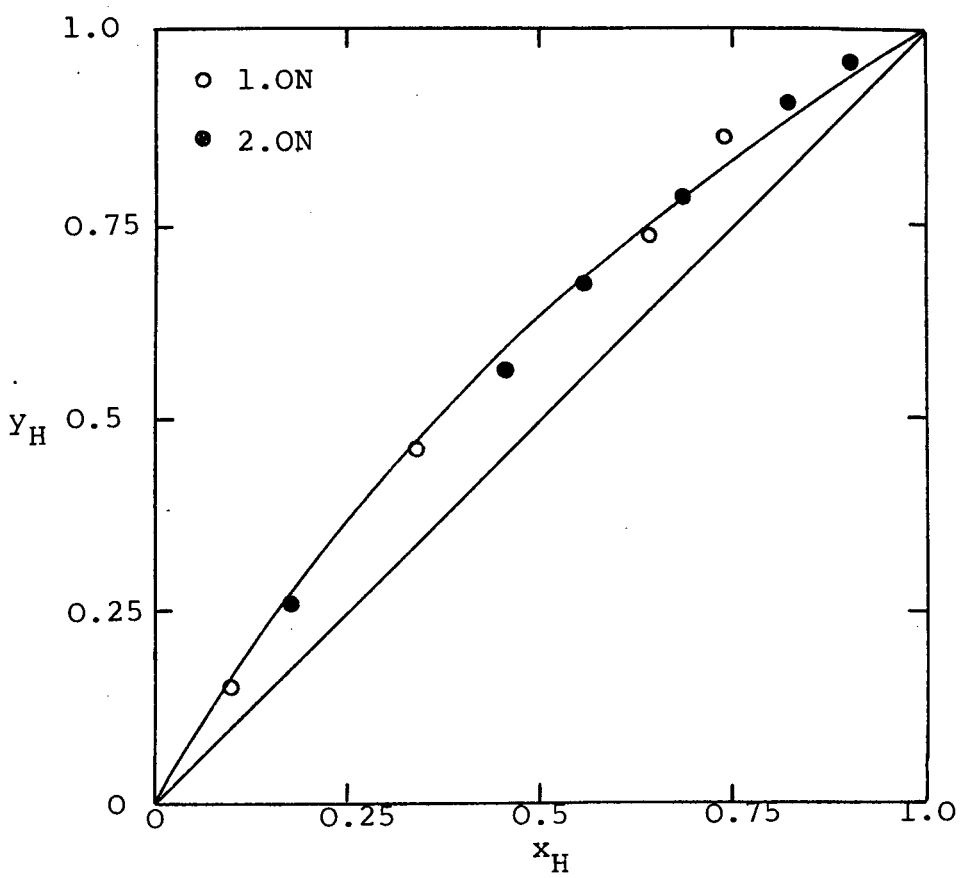

FIGURE 4.13

Ammonium-hydrogen equilibrium curve: Zerolit 625

It is obvious from the data and the curve that the 'fit' is not as 'good' as the two previous cases (Figures 4.11 and 4.12). Although some scatter does exist in the data, it would appear, however, that for this particular exchange (NH_4-H on Zerolit 625), equation (4.3) is not a good representation. A similar but more pronounced 'trend' in the equilibrium isotherm at low hydrogen composition was noted by Weatherley [45] for the exchange of sodium and hydrogen on a Lewatit macroreticular strong acid resin. This deviation is presumably a property of macroporous resins, for the same occurrence is not documented for gel resins. However, the difference between the data points and the curve is not great enough to warrant the use of a new approach for this step, and equation (4.3) with $\alpha = 1{,}8$ will be used here also.

4.2312 Anion resins: The two sets of equilibria determined for the anion resin, Zerolit MPH, are based on the following reactions:

$$R - N + HCl \rightarrow R - NHCl \qquad \text{Anion Load} \qquad (4.4)$$

$$R - NHCl + NH_3 \rightarrow R - N + NH_4Cl \qquad \text{Anion Regeneration} \qquad (4.5)$$

In order to adopt the same isotherm presentation convention used for the cation resins, each of the reactions (4.4) and (4.5) were considered to involve an hydroxyl ion so that the loading and regeneration reactions become

$$R - NOH + HCl \rightarrow R - NHCl + OH \qquad (4.6)$$

$$R - NHCl + OH + NH_3 \rightarrow R - NOH + NH_4Cl \qquad (4.7)$$

In this manner, an equivalent ionic fraction in each phase can be determined from the chloride content of the particular phase and either the resin capacity or the initial solution concentration. This allows the equilibrium isotherms to be presented in the form of x-y plots.

In Chapter 2, the properties of the weak base anion resins were outlined; particularly the effect which pH has on the affinity of the resin for anions. In Figures 4.14 and 4.15 data showing the ability of the anion resin both to 'take-up' and 'release' chloride ions with almost equal 'vigour' in the load and regeneration reactions are presented.

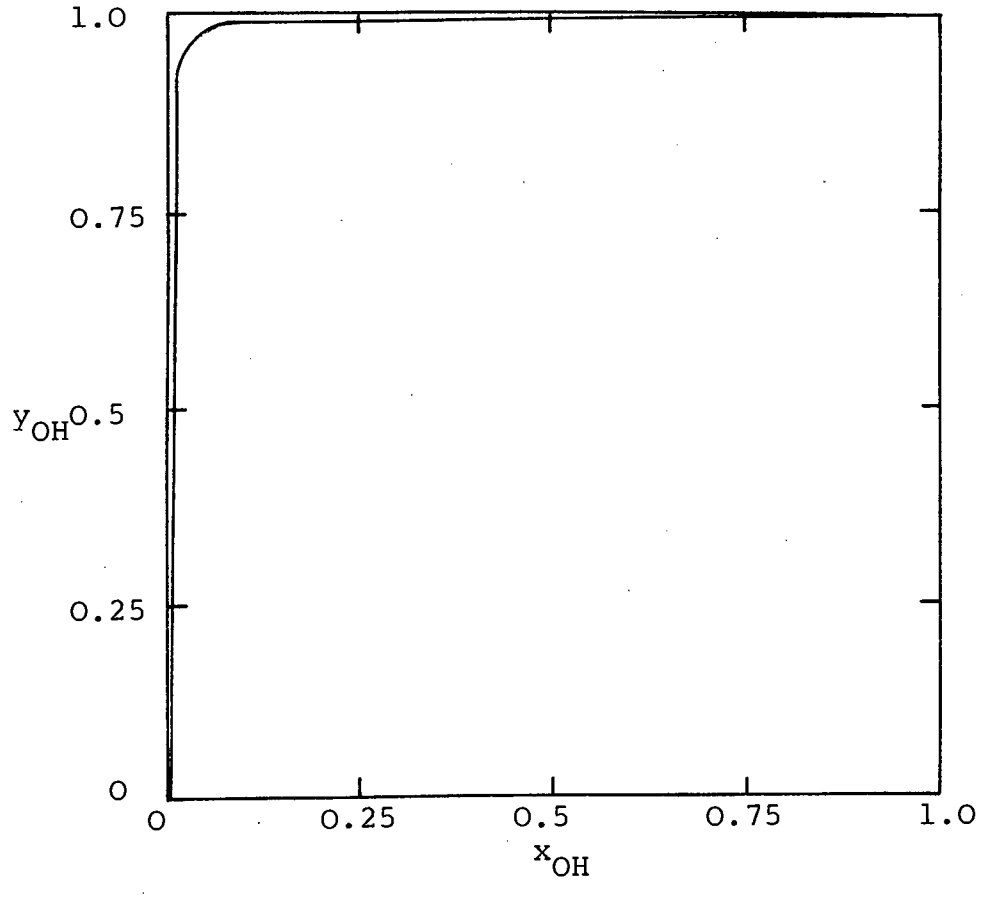

FIGURE 4.14

Anion load equilibrium: Zerolit MPH

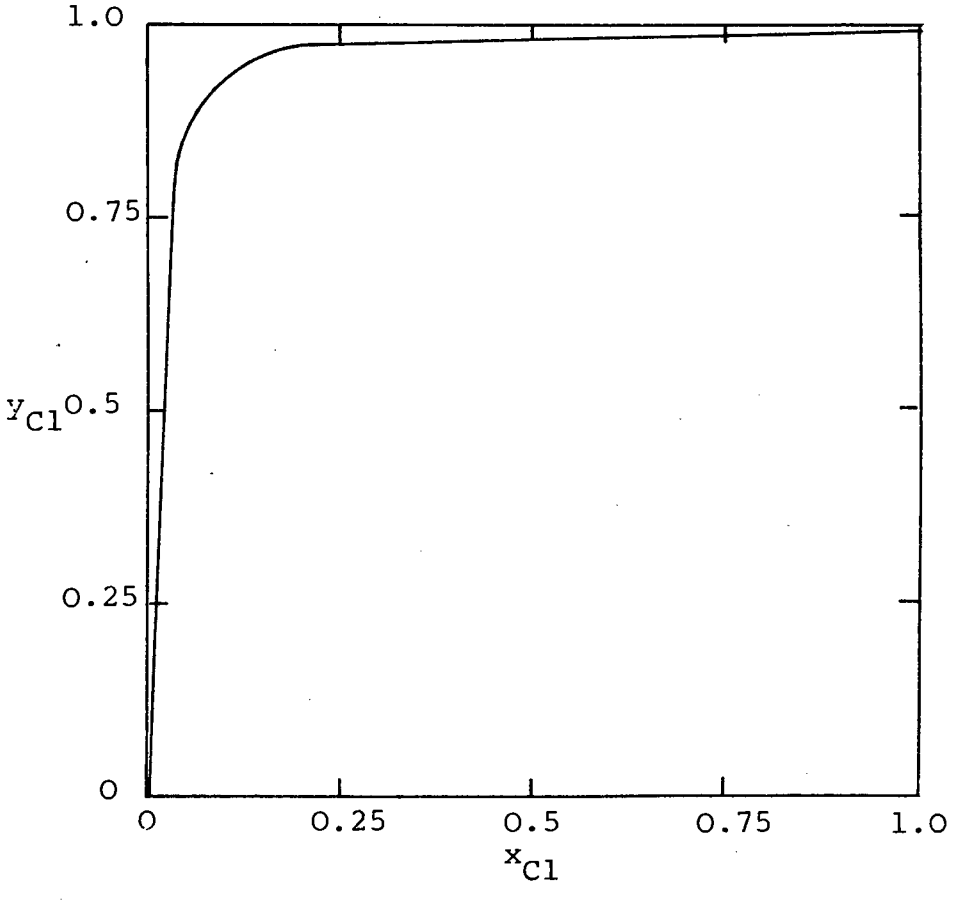

FIGURE 4.15

Anion regeneration equilibrium: Zerolit MPH

In Table 4.10, the α values computed for the two anion exchange curves of Figures 4.14 and 4.15 are given with those previously determined for the cation reactions. The difference in ion affinity of the anion and cation resins is two and three orders of magnitude.

TABLE 4.10

Separation factor values for Zerolit 625 and MPH reactions

Ions A	Ions B	$\alpha_B^A = \frac{y_A \cdot x_B}{x_A \cdot y_B}$
H	Na	1,5
Na	NH_4	1,2
H	NH_4	1,8
Cl	OH	167
OH	Cl	1000

4.232 Electrolyte sorption: One of the major problem areas in an ion exchange desalination process is the wash water requirements of the resins after the regeneration reaction. For fixed bed desalination, the manufacturers of Amberlite resins recommend six bed volumes (1BV = the volume of resin being washed) of rinse water [107]. On a large plant, with water production the aim, the wash water requirements can consume a significant portion of the treated water. In all cases, the degree of resin washing is dependent on the electrolyte sorption properties of the resins concerned.

Like most mass transfer processes, an equilibrium, for electrolyte sorption, exists between the concentration of electrolyte within the pores of a resin and the external solution concentration. A series of experiments (cf. Appendix B) were conducted to determine these equilibrium properties which are, as outlined in Chapter 2, controlled by Donnan exclusion.

In Figure 4.16 the results of the contact of MPH resin with ammonia solution and 625 resin with NH_4Cl and nitric acid are presented, with the ordinate being a measure of the quantity of the particular electrolyte within the pores of a unit volume or resin, and the abscissa the solution concentration.

Two points from the Donnan exclusion principle can be illustrated from the results in Figure 4.16. They are: (i) at low external solution concentrations, electrolyte exclusion is proportionately greater than at high solution concentrations. The two 625 resin tests show this behaviour by the change in the slope of the equilibrium curves with increasing solution concentration; (ii) that a weak resin, in contact with a solution at a pH such that the exchange groups on the resin remain undissociated, will exhibit reduced electrolyte exclusion. The MPH resin of Figure 4.16 in contact with ammonia solution shows the same degree of exclusion throughout the concentration range investigated (deduced from the linearity of the equilibrium curve).

One further interesting point emerging from the results is the parallel curves at high solution concentration for each of the tests. This is obviously indicative of the electrolyte exclusion ultimately being a function of the bead structure, and both MPH and 625 have the same resin matrix, just different functional groups.

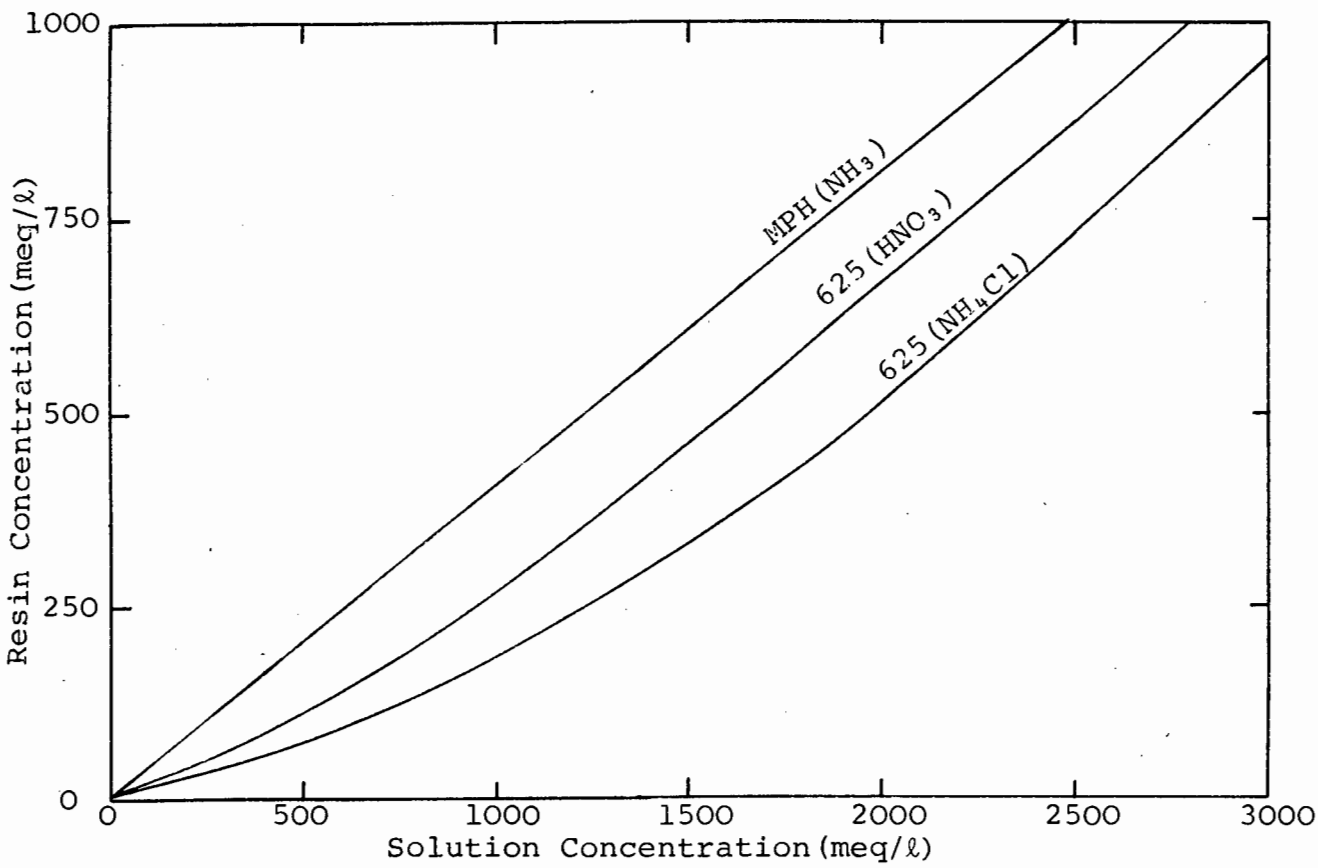

FIGURE 4.16

Zerolit 625 and MPH electrolyte sorption equilibria

4.24 Kinetics

For the design of an ion exchange plant, the rate of the exchange and sorption reactions involved will influence the size of equipment required to achieve desalination, and also the efficiency of the overall IX process. In order to relate the kinetics of the Zerolit resins to the operation of a CCIX column, test work leading to the results to be presented in this section was conducted. The aims of the kinetic investigation were (i) to establish and compare the rates of the various resin reactions when counter-ions and solution properties were varied, and (ii) to compare the measured kinetics with the pore diffusion rate models of section 2.312.

4.241 Ion exchange reactions

The ion exchange reactions on which the equilibria of the previous section and the kinetics of this section are based, are:

$$R - H + NaCl \rightarrow R - Na + HCl \qquad \text{Cation load} \qquad (4.8)$$

$$R - Na + NH_4Cl \rightarrow R - NH_4 + NaCl \qquad \text{Cation exchange} \qquad (4.9)$$

$$R - NH_4 + HNO_3 \rightarrow R - H + NH_4NO_3 \qquad \text{Cation regeneration} \qquad (4.10)$$

$$R' - N + HCl \rightarrow R' - NHCl \qquad \text{Anion load} \qquad (4.11)$$

$$R' - NHCl + NH_3 \rightarrow R' - N + NH_4Cl \qquad \text{Anion regeneration} \qquad (4.12)$$

The solution concentration at which the two load reactions occur is determined by the feed water, but is of the order of 0,02N whilst the concentration of the other exchanges listed above is dependent upon the operating conditions set in the IX plant. However, in order to maximise water recovery, the NH_4/Na and the regeneration reactions would naturally be carried out at the highest possible concentration. Hence, the effect of concentration on the exchange kinetics had to be evaluated.

4.2411 Ammonium-sodium exchange: A comprehensive series of kinetic tests was conducted on the NH_4/Na exchange in order to establish what effect solution concentration and degree of resin conversion has on the rate curves. The trends established for this exchange were then assumed to occur in the case of the other cation exchanges.

All the kinetic (both IX and electrolyte sorption) tests were conducted by measuring the change in the conductivity of the external solution when resin and liquid were vigorously contacted together. On the basis of a solution conductivity-concentration calibration and a mass balance, the resin loading at any point in time could be determined. The method of calculation and details of the experimental procedure are given in Appendix B. The results of the rates of mass transfer are presented in terms of the 'fractional approach to equilibrium' parameter defined by equation (2.15).

The first three rate tests were conducted at three different concentrations; 0,25, 0,5 and 0,75N. The results are presented in Figure 4.17. At the high solution concentrations tested and under the experimental conditions used, the rate is pore diffusion controlled. This being the case, the change in rate for the three concentrations shown by the curves in the figure are due either

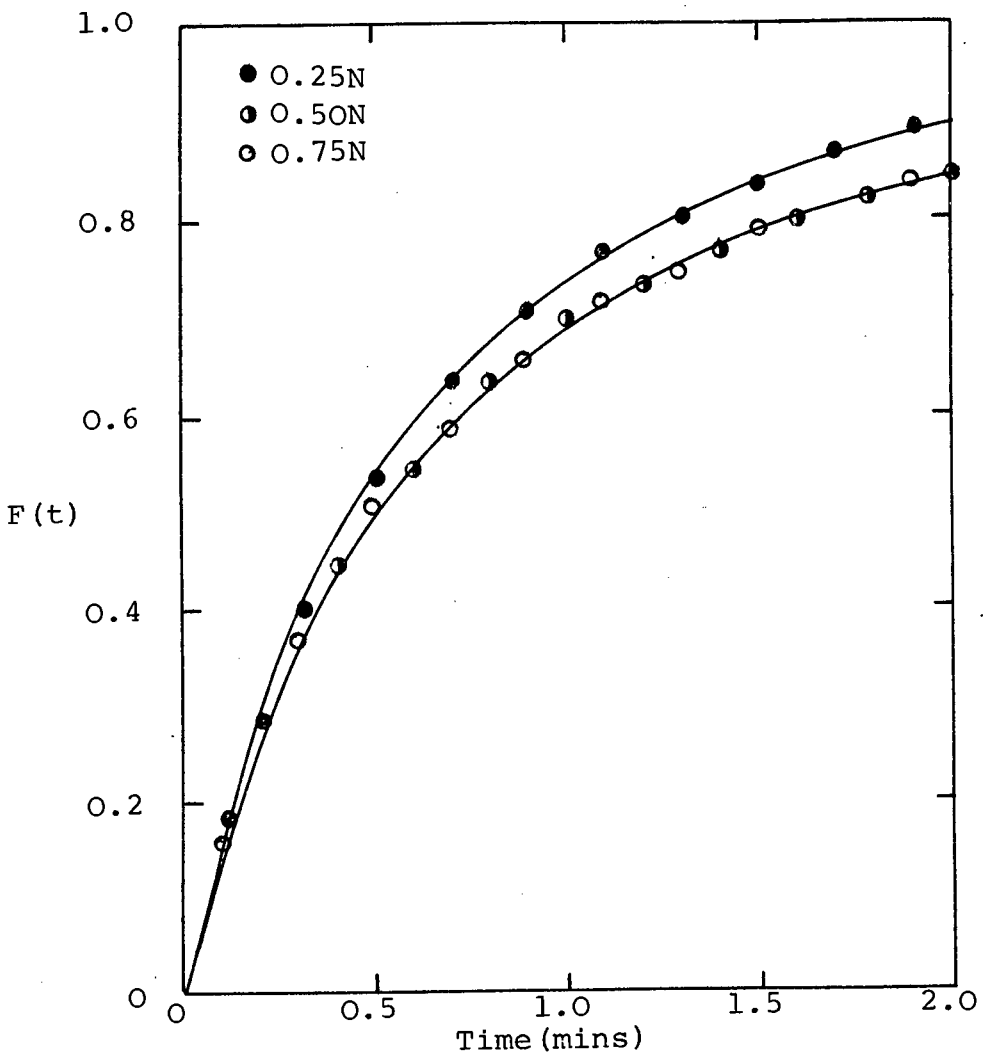

FIGURE 4.17

Ammonium-sodium exchange kinetics, Zerolit 625

Variation of rate with solution concentration

to a variation in the coupled diffusivities (cf. section 2.3121) of the exchanging ions or to a change in the mean diameter of the resin sample used in the tests. The latter effect, a diameter change, occurs in a direction opposite to the one which would be anticipated from the kinetic results, for at high concentrations there is a tendency for the bead radius to decrease (cf. section 2.211) which would lead to a rate increase. The logical explanation for the data of Figure 4.17 is that when resin shrinkage occurs, the mean pore size simultaneously decreases. As a consequence of the increased 'tortuosity' within the bead, the counter-ion diffusivities decrease - hence the rate change. The fact that the drop in rate does not follow with each concentration increase is due probably to resin shrinkage reaching a minimum, at which point the forces within the bead resist any further diameter change, irrespective of external solution concentration. The 0,5 and 0,75N curves thus represent the minimum pore diffusion controlled rate for the exchange of ammonium and sodium ions.

In Figure 4.18, the effect that resin conversion has on the exchange rate is examined using the data of the NH_4/Na reaction at a concentration of 0,5N. The curves represent the exchange rate for four starting and equilibrium values of resin ammonia content expressed in terms of an ion fraction. The purpose of these tests was to assess whether any marked variation of the exchange rate occurred during complete resin conversion from one form to another as shown by Turner [44] for gel resins. The data of Figure 4.18, although showing a slight degree of scatter between one test and the next, do not show that the exchange rate either increases or decreases over the range tested. This conclusion is in keeping with the data of Weatherley [45] on a macroreticular resin.

4.2412 Ammonium-hydrogen and sodium-hydrogen exchanges: Having established that resin conversion is not a major factor in evaluating the rate of Zerolit 625 reactions, the rate of the NH_4/H exchange of equation (4.10) was determined at a solution concentration of 0,5N. The Na/H exchange kinetics were measured at the average IX plant feed water concentration of 0,02N. At this low concentration, care was taken to ensure that the mixing of resin and solution was sufficiently vigorous to ensure that the exchange was pore diffusion controlled. In order to allow for any rate changes which may occur with resin conversion, despite this factor not being evident in

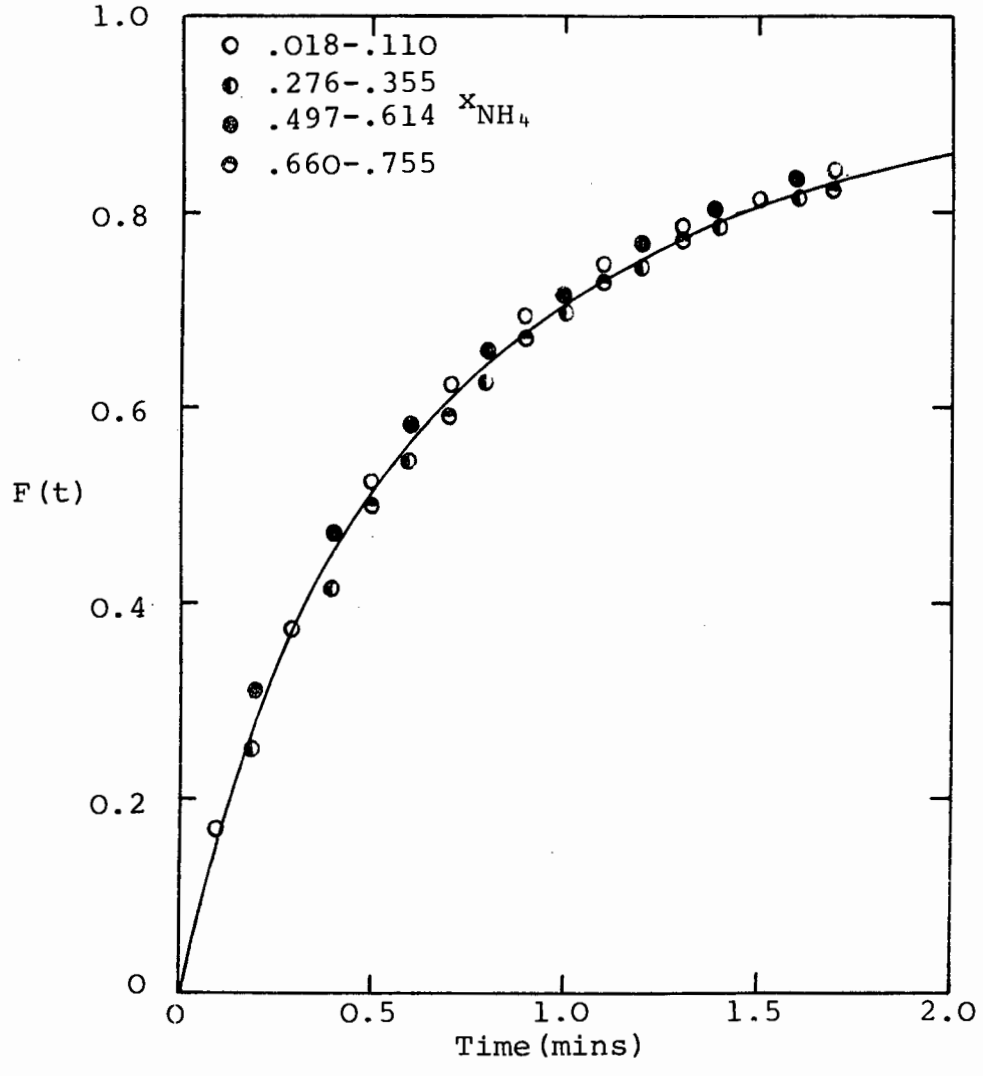

FIGURE 4.18

Ammonium-sodium exchange kinetics Zerolit 625

Variation of rate with resin conversion

the NH_4/Na exchange, the reaction rates were measured for a 20% composition change at the midpoint of the overall reaction, i.e. an ion fraction (I.F.) of approximately 0,5 as a starting point with an I.F. = 0,6 as the equilibrium value. The relevant data are plotted in Figure 4.28 in section 4.331.

4.2413 Anion load and regeneration reactions: The anion load and regeneration reactions of equations (4.11) and (4.12) are slightly different from the cation exchanges in that they do not involve a counter-ion, although the equilibria were calculated on the basis of a counter-ion (cf. equations (4.6) and (4.7). The kinetics of these two exchanges were measured as in the cation case, but account was taken of the simultaneous concentration change

which occurs due to chloride depletion in the load step, and water formation in the regeneration reaction.

The significant feature of the kinetics of the anion load reaction (Figure 4.19) on Zerolit MPH, is the relatively slow rate in comparison with the cation resin. This can be accounted for in terms of the mechanism of the exchange. Because the weak base resin requires an hydrogen ion to protonate the amine exchange site, both the co- and counter-ions (hydrogen and chloride) must diffuse into the resin bead. Now, as the exchange proceeds, so a number of 'loaded sites' are created within the resin. As the loaded sites are now charged, the Donnan exclusion forces hinder the further necessary diffusion of the charged co-ion (hydrogen) into the bead in order that protonation of sites may continue. This accounts for the slowness of the observed rate of the load exchange; in practice, attainment of equilibrium at high resin loading took as long as eight hours.

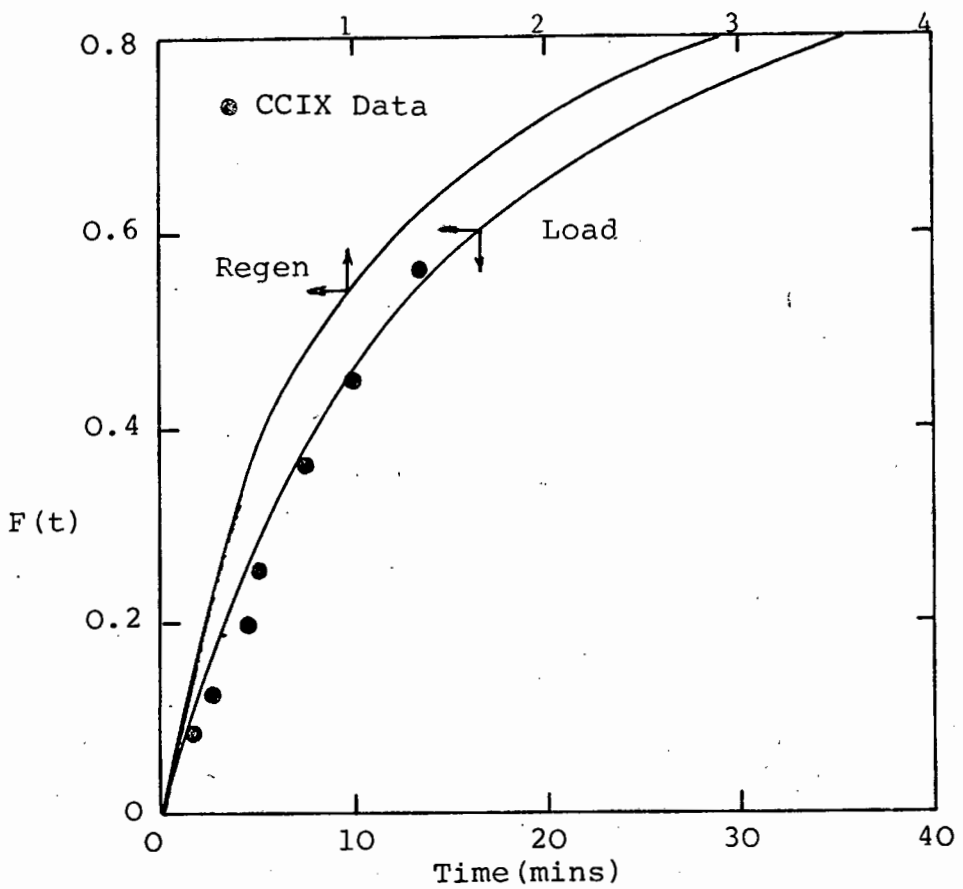

FIGURE 4.19

Zerolit MPH kinetics

The anion regeneration reaction, in contrast, is not controlled by Donnan exclusion to the same extent. This is due to one of the reaction products of the regeneration being the free-base (uncharged) resin and hence no exclusion. Therefore, as the resin stripping proceeds, so the Donnan exclusion disappears allowing co-ion penetration into the bead and further reaction. The exchange rate is thus an order of magnitude faster than the load exchange, as shown in Figure 4.19.

4.242 Comparison of ion exchange kinetic models: In section 2.3122, the development of the bi-disperse kinetic model proposed by Weatherley et al. [45] was outlined. The development of this model resulted from the inability of the homogenous sphere model (cf. section 2.3121) to predict the ion exchange rate of a macroreticular resin. The bi-disperse model considered the resin to contain two pore-sizes, large and small, and consequently a counter-ion diffusivity which was dependent upon the size of the pore.

It was anticipated that the exchange kinetics on the anion and cation Zerolit resins, 625 and MPH, would be similar to those determined by Weatherley, and hence the solution of the bi-disperse pore model equation (2.28) and 2.29) would allow the relevant exchange rates to be predicted. In order to test this supposition, Turner et al's [44] homogenous sphere (HS) model data, Weatherley et al's [45] bi-disperse (BD) pore model data and the measured rates of NH_4/Na, and cation and anion load reactions are plotted in Figure 4.20.

A comparison of the model types is made on the basis of the curve shape in Figure 4.20. The HS model curve shows a higher rate at the start of exchange, but a lower rate as equilibrium is approached. This leads to the HS model curve 'crossing' the BD curve at some point in time. The measured curves on the 625 and MPH resins have the same 'shape' as the BD model curve, indicative of the ability of the BD model to 'fit' the measured curves when a suitable choice of pore radius and counter-ion diffusivity is made.

4.243 Kinetics of electrolyte sorption: On completion of an exchange reaction in a CCIX plant, resin is transferred to a column where the succeeding reaction is to occur. In order to avoid contaminating the product of the succeeding reaction with the electrolyte contained in the resin pores from the first exchange, the resin is washed between reactions with water.

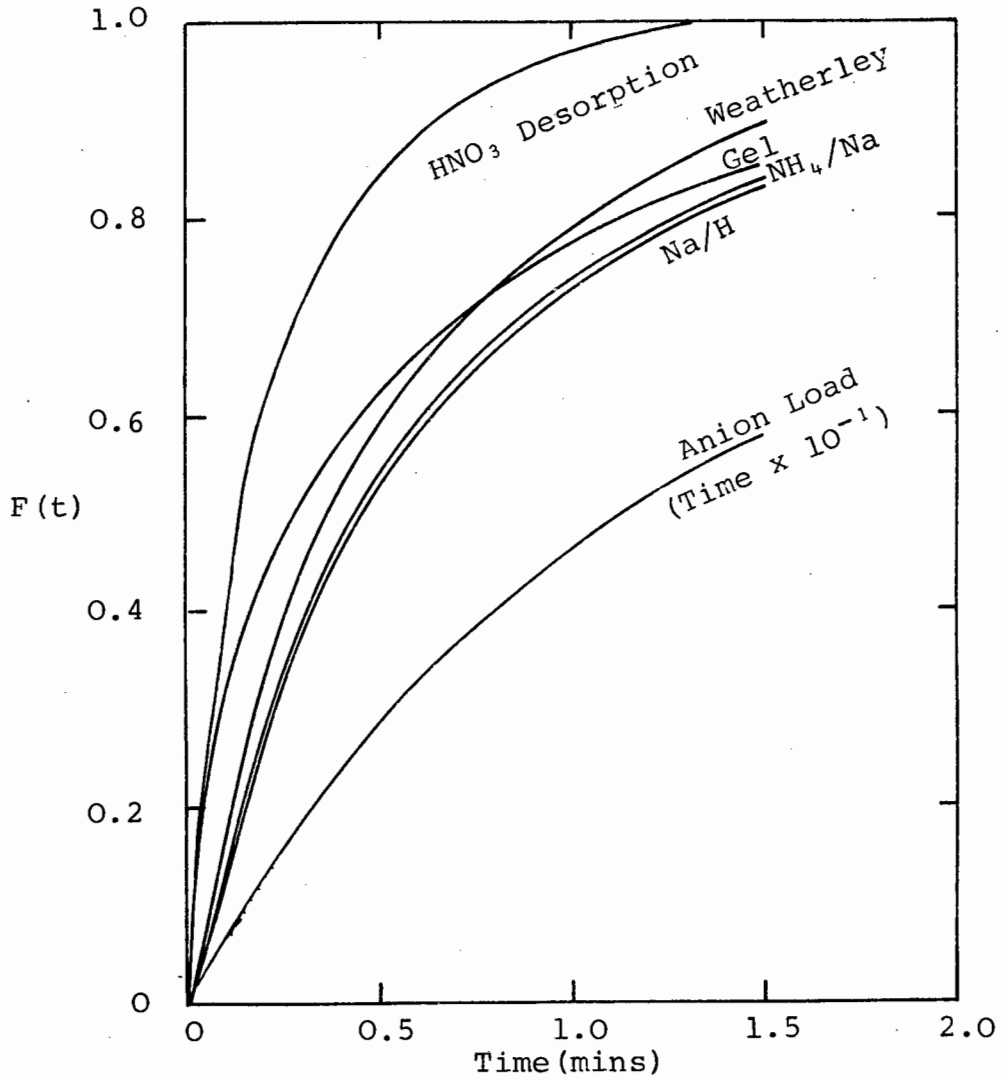

FIGURE 4.20

Comparison of kinetic models for Zerolit 625 and MPH resins

During the resin wash step, the electrolyte within the resin bead diffuses out until an equilibrium condition (cf. section 4.232) is attained. The rate at which electrolyte diffuses is controlled by the diffusivity of the co-ion (cf. section 2.33) and, for a macroreticular resin, the rate curves should follow the bi-disperse pore model solutions of the flux equations.

In Figure 4.21, kinetic curves for NH_4Cl and HNO_3 desorption from 625 and NH_4OH desorption from MPH resins are presented. For the cation resins, the fractional attainment of equilibrium is faster in the electrolyte desorption process than it is for an ion exchange reaction. This is due to the Donnan exclusion principle, which effectively changes the co-ion diffusivity by creating a potential gradient within the resin bead; thereby

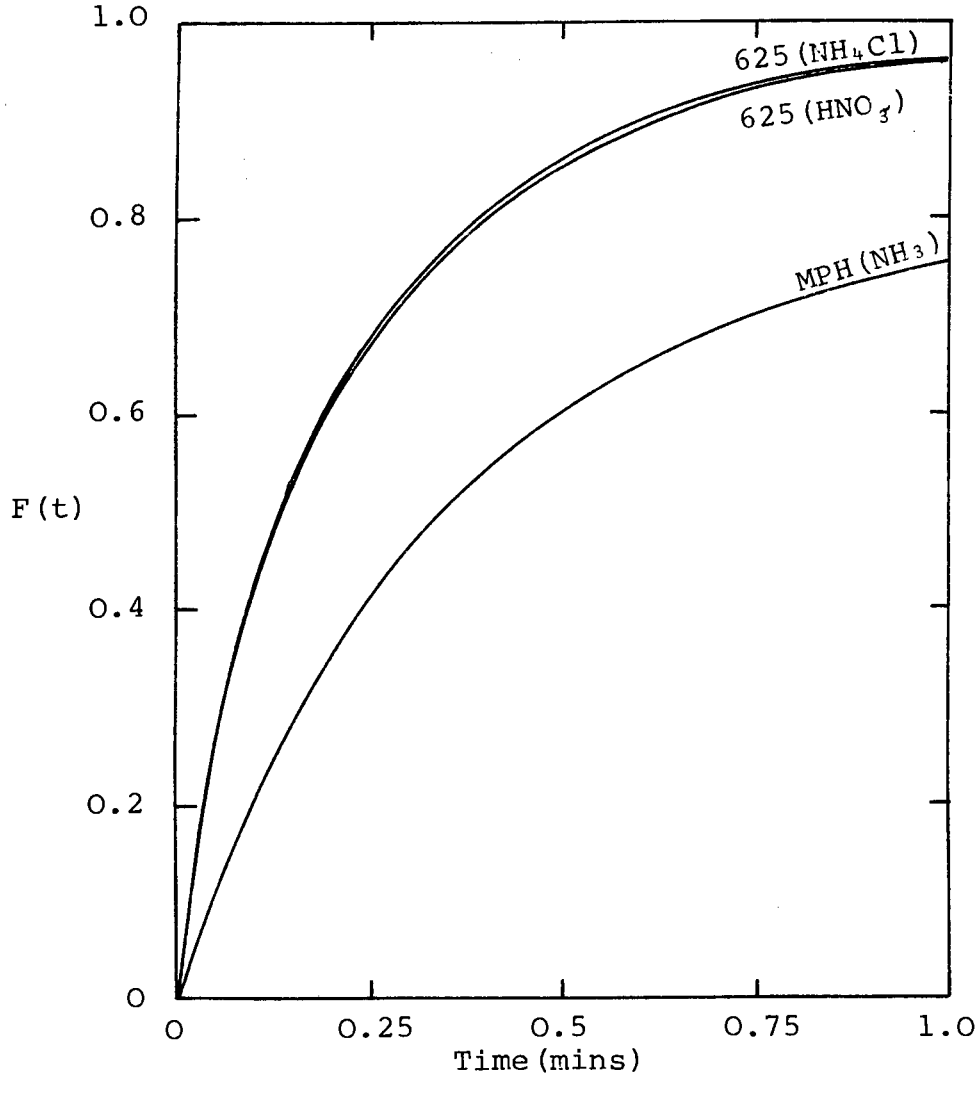

FIGURE 4.21

Electrolyte desorption kinetics Zerolit 625 and MPH

assisting the desorption step. For the anion resin in the FB-form, because there is no charged functional group within the bead matrix, the electrolyte desorption does not have the added Donnan potential driving force, hence the slower electrolyte desorption rate for the anion resin when compared with the cation resin.

In Figure 4.20, the HNO_3 desorption rate-curve is plotted with the HS and BD model comparison curves. The 'shape' of this kinetic curve shows that the BD model is also applicable for electrolyte sorption. Therefore, as in the ion exchange case, solution of the relevant equations (2.28 and

2.29) with the necessary resin parameters will predict the rate of the electrolyte sorption mass transfer steps.

4.3 PROPERTIES OF THE CCIX COLUMN

In this section, the properties of the CCIX column based on the Cloete-Streat principle (cf. section 2.432) chosen for use in the ion exchange desalination process are outlined. For column test purposes, a 9,4 cm diameter column containing either 4, 8 or 12 1,5, 1,0 or 0,5 metre stages respectively was used, and the results are based on the Zerolit 625 cation and MPH anion resins.

Included in this evaluation are (i) the operation of the CCIX column, (ii) a determination of the validity of the proposed steady state model of section 2.4323, (iii) a comparison of the CCIX column 'stage efficiency' and the batch fractional attainment of equilibrium for the exchange reactions involved in the desalination process with regenerant recovery, outlined in equations (3.23) to (3.29).

4.31 Operation and evaluation of a CCIX column

The CCIX column operates as a periodic process with liquid and resin flows occurring sequentially rather than simultaneously, with the flow sequence repeated on a continuous basis. The time lapse between the repeated occurrence of an event is termed a cycle and within each cycle the following operations take place: (i) for the major portion of the cycle, liquid enters the bottom of the column at a set concentration and flow rate. During this period the resin within each stage of the column is fluidised and product solution overflows at the top. (ii) following the liquid flow period is a resin settle period in which the resin in each stage is allowed to form a packed bed. (iii) after the settle period, a downward flow through the column pulls the resin from each stage to the stage below. One stage volume of resin (the pulldown volume, PV) simultaneously leaves the bottom of the column. This is the resin 'pulldown' period.

Together, the above three steps constitute one CCIX column cycle. A detailed outline of the valve sequencing and control of each of these steps is outlined in Appendix C together with the calculation procedure, outlined briefly below, used to preset the column conditions.

4.311 Operating conditions: The column operating conditions are set on the basis of the resin capacity, the feed concentration and flow rate and the required degree of either resin or liquid conversion. For the tests conducted to determine the validity of the steady state model, column conditions were set to achieve a complete conversion of both resin and liquid streams, with the conversion of each stream spread equally over the whole column. In order to attain these or any other conditions, the following factors had to be considered.

4.3111 Stoichiometric ratio: The S-ratio is defined as the ratio of resin and liquid equivalents which move through the column. From equation (2.44),

$$S = \frac{y_{A_t} - y_{A_b}}{x_{A_t} - x_{A_b}} \qquad (4.13)$$

i.e. the ratio of the change in liquid and resin compositions over the column. Because the total solution concentration and resin capacity remain constant, equation (4.13) represents a straight line.

For complete conversion of both resin and liquid, assuming that each stream is pure A or B form when it enters the column, i.e. $y_{A_b} = 1,0$ $x_{A_t} = 0,0$, then

$$y_{A_t} - y_{A_b} = -1,0 \text{ and } x_{A_t} - x_{A_b} = -1,0 \qquad (4.14)$$

and the stoichiometric ratio, equal to the slope of the operating line, has a value of 1,0, and lies on the diagonal of an x-y diagram.

Should either the composition of the entering liquid or resin streams be different from 1,0 or 0,0 or the desired degree of resin or liquid conversion be altered, suitable adjustment of the operating line slope will achieve the required change.

4.3112 Resin pulldown volume: The volume of resin which moves from one stage to the next and leaves the column during the pulldown period of the cycle is determined only by the resin fluidisation. This resin 'stage volume' is the volume which, when expanded by the set feed flow rate, fluidises to fill the particular stage under consideration.

An analysis of column operation shows that the pulldown volume, for greatest column efficiency, should equal the volume of resin present in each stage at the set flow conditions. If the pulldown volume is less than the stage volume, then a degree of backmixing (which is inherently less efficient than plug flow (cf. Levenspiel [74])) is introduced into the column operation. Alternatively, if the pulldown volume is greater than the stage volume, resin bypassing (an inefficient utilisation of resin) occurs. In practice, if the complete stage volume of resin was pulled down in each cycle, a small depletion of the total resin inventory in the column occurred over a number of cycles. For this reason, the actual resin pulldown volume was set at 90% of the stage volume and the stoichiometric ratio adjusted accordingly.

4.3113 Upflow time and settle time: The upflow time is determined by the required stoichiometric ratio when the feed flow rate - and thus the pulldown volume - and feed concentration are set. The pulldown volume and resin capacity together determine the resin equivalent flow per cycle. The stoichiometric ratio and the resin equivalent rate dictate (by definition of S) the number of liquid equivalents required per cycle. Therefore, for any given feed concentration, with the feed rate and S-ratio set, the duration of the feed flow-time (the upflow-time) is altered to achieve the required liquid equivalents per cycle.

The resin settle time is determined by experiment for a particular resin, per cent BE and stage height; for each of these variables will dictate a different setting. In general, this time will vary between 0,5 and 2,0 minutes.

4.312 Evaluation of a CCIX column: The performance of a CCIX column is evaluated by analysing the input and output resin and liquid streams and determining the inter-relationship of these stream compositions through the mass balance equation (4.13) and the flow conditions existing within the column. After a review of the various possible methods of evaluating the CCIX results, the method outlined in the proposed steady state model of section 2.4323 was adopted. Assuming for the present (section 4.32 below verifies the assumption), that the technique is valid, the following method of analysing the column results can be adopted and the various inferences outlined can be drawn from the analysis technique.

4.3121 Stage volume and contact time: On the basis of plug flow of liquid through a fluidised resin bed (shown to be valid by Turner et al. [67] and Kataoka et al. [108]), the time an element of liquid is resident within a CCIX stage of given volume can be calculated from the fluidised bed voidage (equation (4. 2)) and the liquid volumetric rate. This time, the contact or space time of the liquid, is defined by equation (2.48). Because the contact time is dependent upon the fluidised bed voidage which in turn is dependent on the fluidisation properties of the resin (cf. equation (4. 1)), it has to be evaluated for each particular resin and CCIX stage-volume.

Three stage volumes, 1 125, 2 250 and 3 375 mℓ, were used in the model testing experiments. For each of these volumes, the contact time for both Zerolit 625 and MPH (FB-form) has been evaluated using the resin fluidisation curves of Figure 4.3 and equation (4.2). The results of the calculation are presented in Figure 4.22. The degree of resin conversion within each stage of the CCIX column is then related to the contact time.

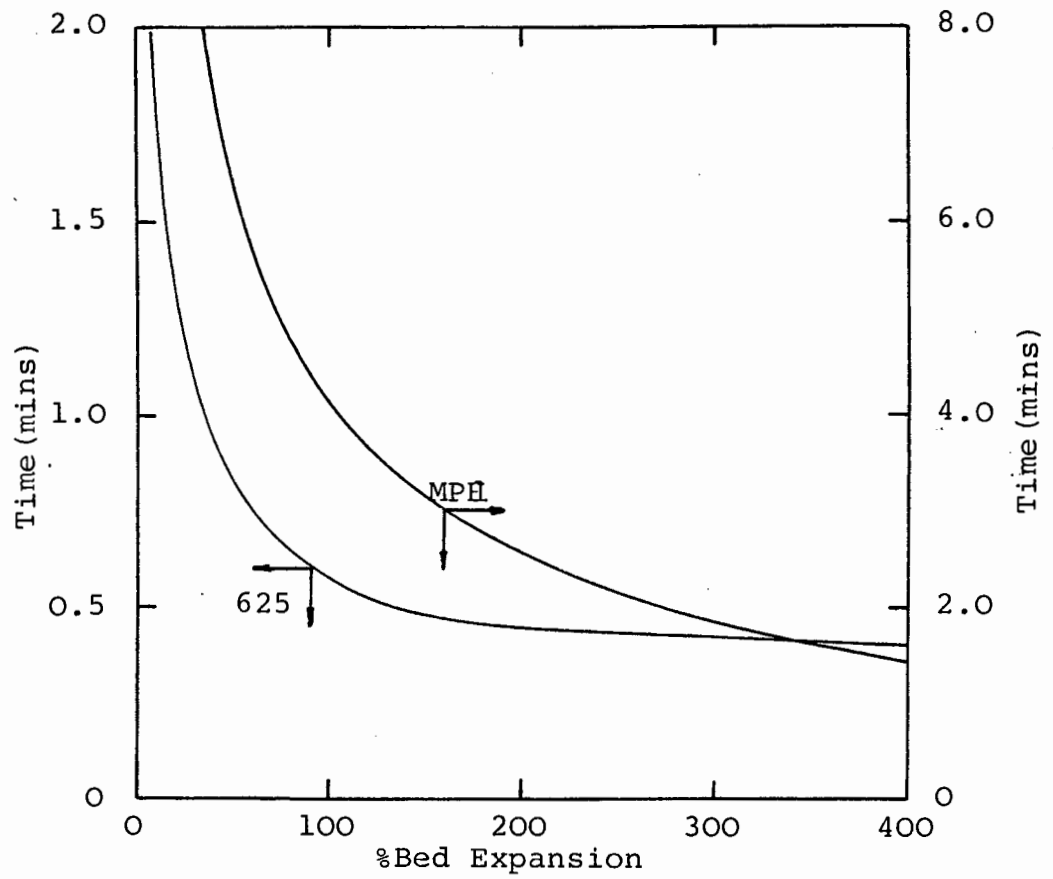

FIGURE 4.22

Contact time versus %BE Zerolit 625 and MPH, 0,5 m stage

4.3122 Operating line slope and number of stages: In Figure 4.23 two operating lines are plotted on an x-y diagram with an equilibrium curve computed from equation (4.3) with $\alpha = 3,0$. The operating line lying on the diagonal is based on a feed resin composition $x_t = 0,99$ and feed liquid composition $y_b = 0,01$. The slope of the operating line (the stoichiometric ratio) was computed so that column operation would result in product resin and liquid composition x_b and y_t of 0,01 and 0,99 respectively - hence the slope of 1,0.

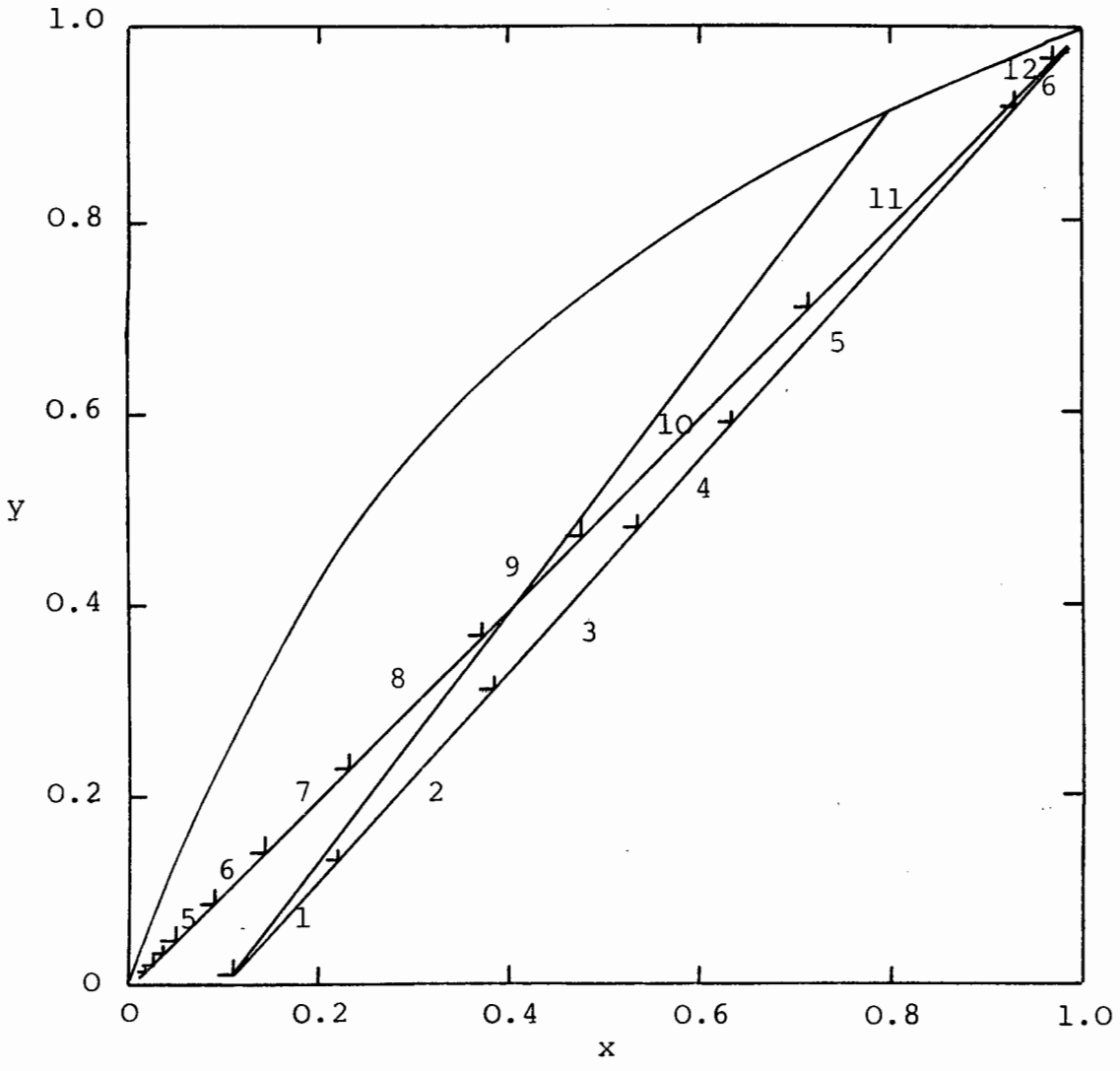

FIGURE 4.23

CCIX column operating lines and equilibrium curve plotted on an x-y diagram

Rearrangement of the 'stage efficiency' equation (2.47) yields

$$x_n = \frac{x_{n-1} - \eta.f(y_{n-1})}{1 - \eta} \qquad (4.15)$$

Now, for $x_{n-1} = x_b = 0,01$, and, for the purposes of illustrating the calculation procedure an assumed average stage efficiency $\eta = 0,5$, the steady state resin composition x_1, at the top of stage 1 of the column (cf. Figure 2.18) can be computed from equation (4.15). Using the computed x_1-value as the new x_{n-1} in the above equation, a series of computations will sequentially calculate the resin compositions in each stage of the column. Performing the calculation shows that after 12 stages, the feed resin composition is attained indicating that, with an assumed 50% 'stage efficiency' and the assumed conditions a 12 stage column is required to perform the desired resin and liquid conversion.

Should, however, only the product liquid composition be important, i.e. $y_t = 0,99$, then, with the same feed resin and feed liquid compositions as before, the operating line slope may be changed to reflect a new product resin composition. The second operating line of Figure 4.23 with $S = 1,11$ demonstrates such a situation. In this case, with $x_b = 0,11$ and η again assumed equal to 0,5, a stage-wise calculation shows that six stages are now required to achieve the conversion. Similarly, by suitable variation of the stoichiometric ratio the resin conversion, $x_b = 0,01$, can be achieved in fewer exchange stages but at the expense of the degree of liquid conversion at the top of the column.

A unique situation arises when one 'end' of the operating line lies on the equilibrium curve; in distillation theory this would refer to a 'pinch' point. A segment of an operating line illustrates a 'pinch' point in Figure 4.23. This phenomenon would occur when, typically, the required product liquid conversion is greater than can be achieved with the given feed resin composition, e.g. referring to the equilibrium curve of Figure 4.23 a pinch point is formed if the required $y_t = 0,95$, while the actual $x_t = 0,80$ or alternatively a 'pinch' at the bottom of the column - if the required $x_b = 0,02$, while the actual $y_b = 0,10$. In both these cases, the maximum conversion of either liquid or resin would be to a composition

in equilibrium with the feed stream with which it is in contact and not to the desired x_b or y_t composition.

To determine the stage efficiencies of a CCIX column, the procedure outlined above is used in conjunction with a series of intermediate liquid samples taken from the top of each CCIX stage when the column is at steady state. Analysis of the input and output liquid and resin streams fixes the terminal points of the operating line and the samples taken at the intermediate points must also lie on this line. The intermediate samples are thus y_i values for each stage. From the y_i compositions and the operating line, x_i values are computed. The x_i compositions plus the relevant $f(y_i)$ values enable η_i to be calculated via equation (2.47).

4.3123 Efficiency of CCIX stages for resin washing: After an ion exchange regeneration reaction, the sorbed electrolyte has to be washed out of the resin. This wash step accounts for the fairly large consumption of the plant product water on fixed bed systems. However, a more efficient resin wash can be achieved in CCIX equipment.

An evaluation of the number of stages required for resin washing can be made on a basis analogous to the evaluation of the number of exchange stages - by using an operating line and an equilibrium curve. By defining the following variables:

C_{L_t}, C_{L_b} - concentration of electrolyte in the liquid

C_{R_t}, C_{R_b} - concentration of electrolyte in the resin

V_L , V_R - volumetric flow rates of liquid and resin

t , b - top and bottom of the wash section

A steady state mass balance on electrolyte over the wash section yields

$$V_R(C_{R_t} - C_{R_b}) = V_L(C_{L_t} - C_{L_b}) \tag{4.16}$$

which is the equation of a straight line under steady state operation. When equation (4.16) is plotted with the relevant equilibrium curve (cf. Figure

4.16), the sequential calculation of the previous section can be used to determine the number of stages required to reduce the electrolyte concentration of the resin from C_{R_t} to C_{R_b}. The efficiency of the resin-liquid contact can then also be measured in terms of a modified form of the ion exchange efficiency equation (2.47).

4.32 Discussion of CCIX results

In this section, the results of the experimentation on a CCIX column are outlined. These results are used to demonstrate (i) the validity of the assumption of steady state in a CCIX column, albeit a pseudo steady state, (ii) the evaluation of stage efficiencies for the various exchange reactions of the proposed desalination scheme, and (iii) the influence the contact time in a CCIX stage has on the efficiency of operation of the column.

4.321 Demonstration of steady state CCIX operation: The pseudo steady state operation of a 12 stage CCIX column is evaluated in terms of the product liquid (y_t) and resin (x_b) compositions in Figure 4.24. The graph shows the variation of the two streams with cycle number over 22 cycles. The compositions of the product streams were evaluated from a sample consisting of, in the case of the liquid, a series of equal volume samples taken at specific time intervals during the duration of the upflow period, and in the case of the resin, a representative sample from the pulldown volume.

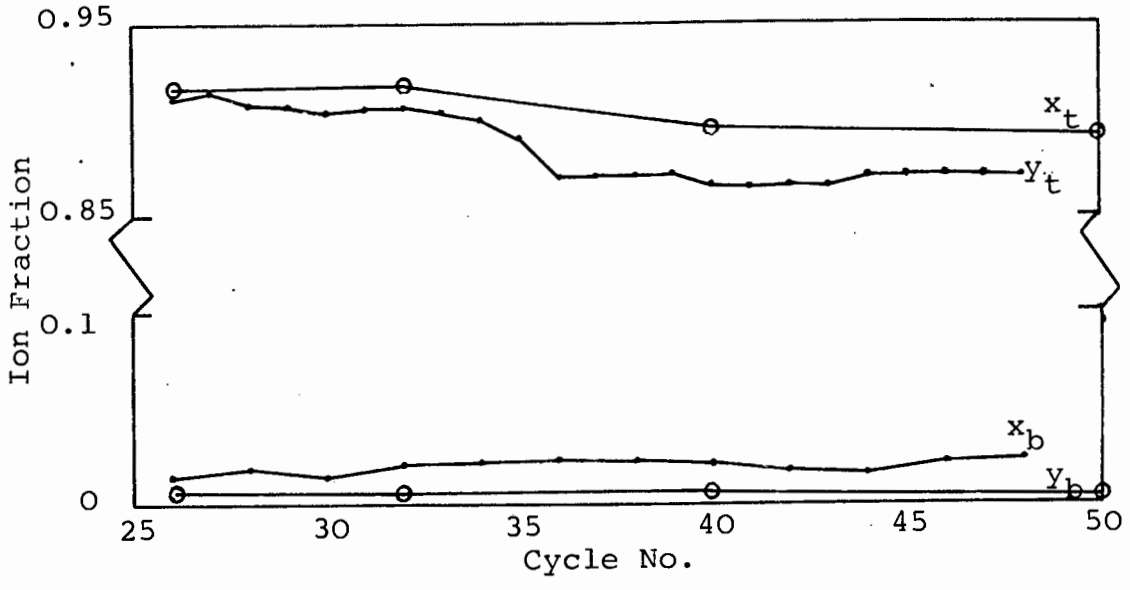

FIGURE 4.24

Variation of product resin and liquid stream compositions during CCIX column operation

The curves show that, provided the feed liquid (y_b) and resin (x_t) stream compositions remain constant, the column will reach a steady state and product compositions (y_t and x_b) will also remain constant. When a change in feed occurs, illustrated in Figure 4.24 by the input resin, x_t, composition change at cycle 32, a new steady state will result.

Because the flow of the two phases in the column is not continuous, the compositions of both liquid and resin do vary during the cycle. This is not illustrated in Figure 4.24 because of the composite sampling technique used. However, in Figure 4.25, an analysis of 5 separate equal volume liquid samples, taken at 3 minute intervals during a 17 minute upflow period, from the top of each stage of a CCIX column is presented. The same sampling pattern was then repeated after a further 8 CCIX cycles as the column approached steady state. From these separate data points, the composition profile change within each stage of the column is clearly indicated. The two interesting points are (i) that the direction of the composition change in each stage is the same and that the change proceeds in the direction anticipated, viz. as the resin is depleted of ions, so too is the liquid;

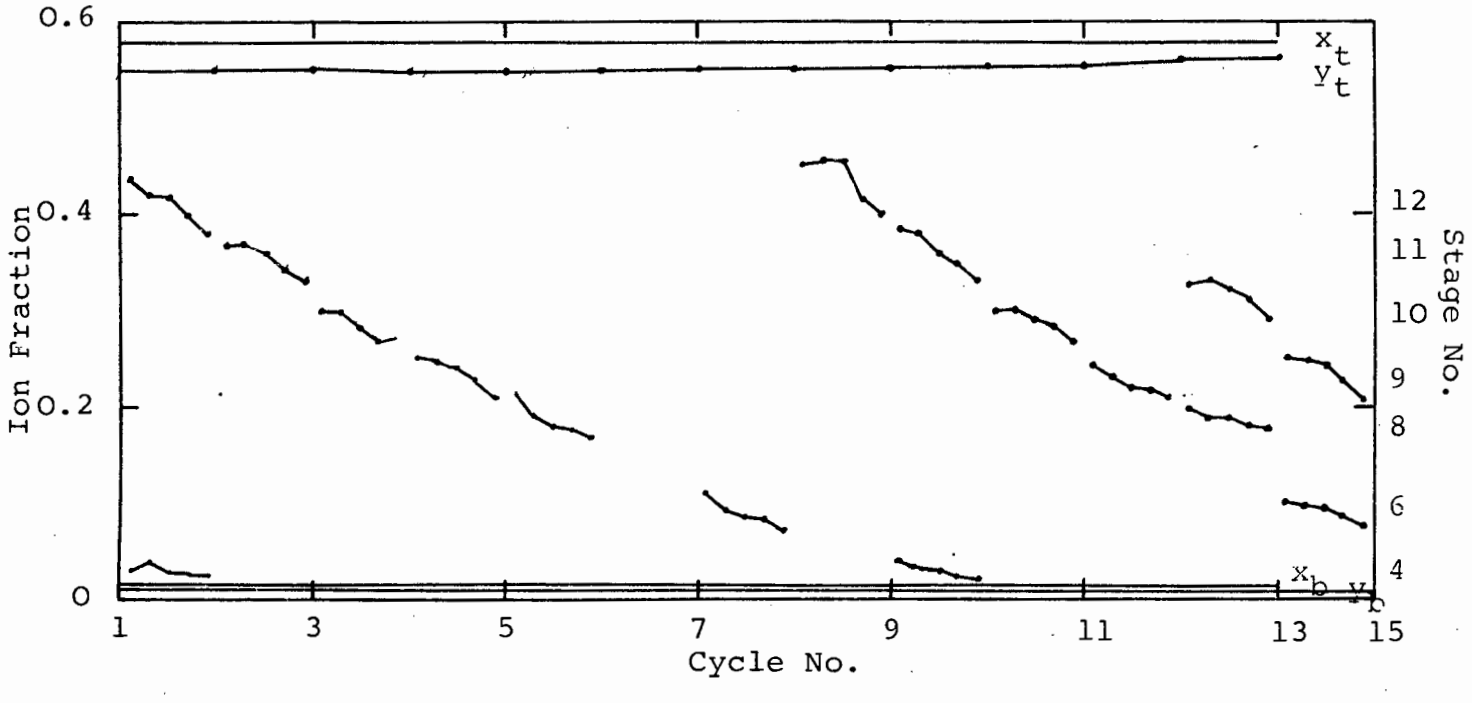

FIGURE 4.25

Change in liquid composition profile in a CCIX column with cycle no.

and (ii) that after eight further cycles, the profile change within a stage maintains the same pattern and the composition variation occurs between the same limits although perhaps at a higher or lower average value as the column approaches steady state.

Together, the results of Figures 4.24 and 4.25 show the validity of the steady state assumption used in the derivation of the stagewise model of section 2.4323. The results of the operation of the CCIX column under various flow conditions is evaluated below on the basis of the proposed model.

4.322 Determination of CCIX stage efficiencies: In Table 4.11 the steady state results of an exchange of ammonium and sodium ions at total solution concentration of 0,5N and 0,23N in a CCIX column are presented. These results will be used to demonstrate the calculation of CCIX stage efficiencies.

Figure 4.26 is a plot of the NH_4/Na equilibrium curve and the CCIX operating line based on the feed and product resin and liquid compositions of the 0,5N exchange of Table 4.11. The operating line has a slope of 1,002 indicating that it is almost parallel to the diagonal of Figure 4.26 and no pinch point condition exists. The overall stream conversions occur, therefore, in almost equal proportions over the whole length of the column. This is shown by the intermediate stage liquid compositions, y_i, which are depicted by the horizontal lines in Figure 4.26. From the mass balance considerations of equation (2.45), the intersections of the y_i liquid compositions and the operating line give the resin composition at the column cross-section at which the liquid sample was taken, viz. the top of each stage. From the x_i resin compositions, the degree of resin conversion $(x_i - x_{i-1})$ can be determined for each column stage. This difference, together with the equilibrium allows the computation of the 'stage efficiency' using equation (2.47) and the technique of section 4.3122.

The efficiencies of each of the twelve stages is indicated in Figure 4.26. Although all the stages in the column should be equivalent in terms of the mass transfer which can occur in each, the random variation in the computed stage efficiencies of both the runs in Table 4.11 indicates that there is in fact some variation between stages. This relatively small change is due to any one of the following:

TABLE 4.11

Steady state results of the NH_4/Na exchange in a CCIX column

Feed Conc.	0,50N		0,23N	
%BE	50		25	
Contact Time	0,82 mins		1,22 mins	
Sample	I.F. Na*	Stage Eff. η	I.F. Na	Stage Eff. η
Feed Liq. y_b	0,0043		0,0045	
Prod.Liq. y_t	0,8851		0,9759	
Feed Resin x_t	0,8990		0,9663	
Prod.Resin x_b	0,0197		0,0061	
Stage Samples				
y_1	0,0365	0,666	0,0224	-
y_2	0,0931	0,727	0,0342	-
y_3	0,1398	0,612	0,0462	-
y_4	0,2084	0,657	0,0824	0,808
y_5	0,2815	0,626	0,1110	0,677
y_6	0,3452	0,558	0,1937	0,827
y_7	0,4469	0,650	0,2780	0,760
y_8	0,5638	0,664	0,4444	0,831
y_9	0,6382	0,555	0,5636	0,742
y_{10}	0,7262	0,605	0,7511	0,821
y_{11}	0,8085	0,613	0,8556	0,783
y_{12}	0,8691	0,580	0,9413	0,843
	Average η	0,63	Average η	0,79

I.F. - Ion fraction, i.e. $y_{Na} + y_{NH_4} = 1,0$

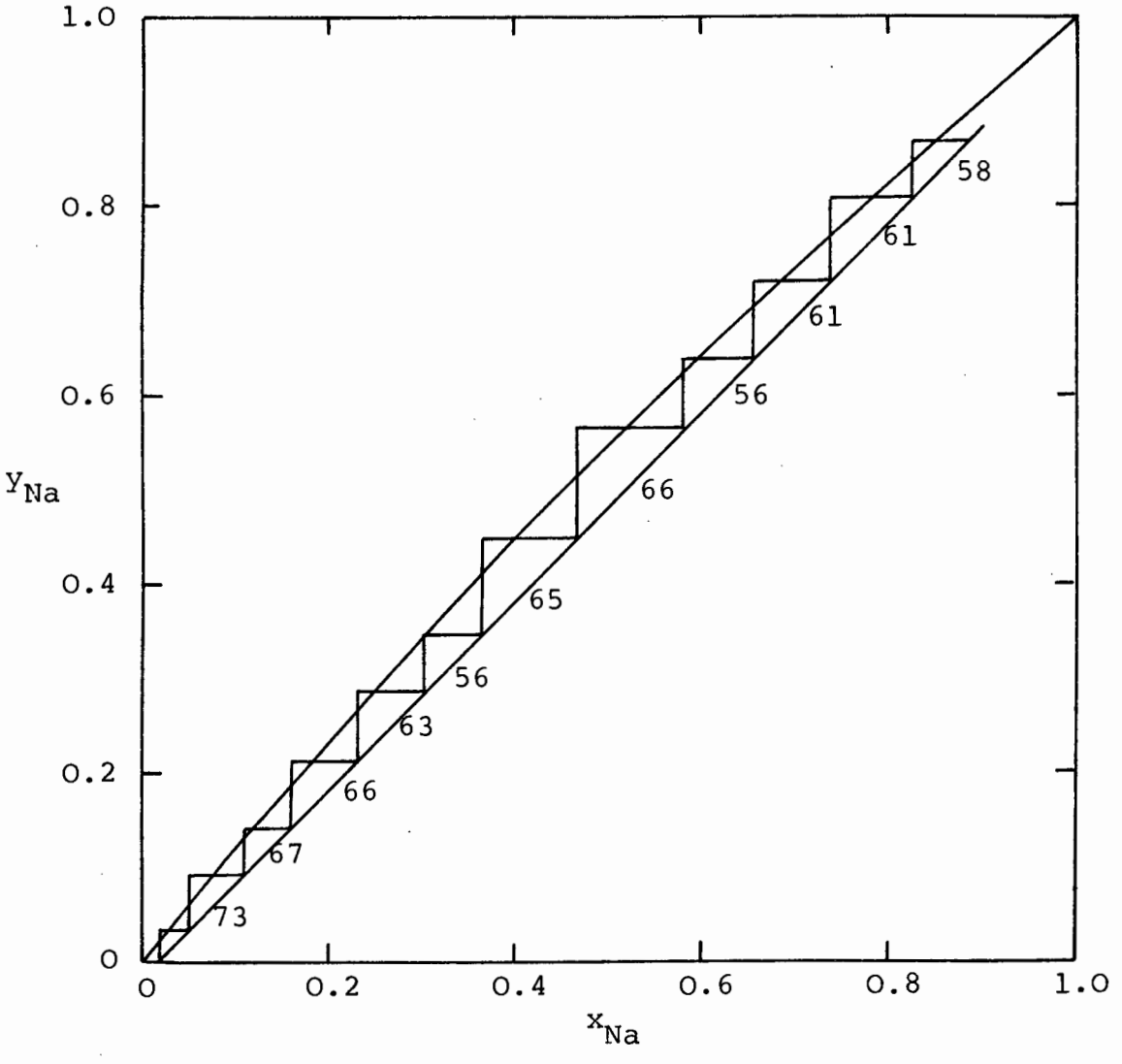

FIGURE 4.26
Calculation of CCIX stage efficiencies

(i) the particle size distribution of the resin in each stage of the column may not be exactly the same, therefore the bed expansion and hence the resin volume within each stage would not be equal;

(ii) the volume of resin which moves from one stage to the next during pull-down may vary through the column, leading either to backmixing or bypassing of resin, both of which would cause an efficiency fluctuation;

(iii) slight flow changes from one stage to the next could result in liquid bypassing in some of the column stages.

For the purposes of evaluating a CCIX column an average value of the stage efficiency for a particular set of conditions would not result in a significant error. For the comparison of kinetic data in the following section, such an averaging procedure is adopted.

The other important point which is obvious from the vertical-horizontal McCabe-Thiele type construction of Figure 4.26, is that each stage appears to achieve a conversion which extends past the resin-liquid equilibrium condition. This level of stream conversion is equivalent to a Murphree stage efficiency (cf. Smith [75]), an efficiency used in distillation theory, of greater than 100%. Stage (tray) efficiencies of this order are achieved in distillation columns when the tray is of the cross-flow type. The seemingly high efficiency is merely indicative of a measure of countercurrent flow within the CCIX stage (as with the cross-flow distillation tray). The physical CCIX stage can be considered to consist of a number of perfectly mixed equilibrium contact volumes, each contributing to the overall conversion achieved in the physical stage and together constituting the volume of the physical stage. An infinite number of these contact volumes would be equivalent to plug flow, the basis upon which the theory of section 2.4323 is proposed.

4.33 Comparison of batch and CCIX kinetics

In section 2.4323 a proposed design method for a CCIX column was outlined based on a stagewise calculation procedure. Further, it was postulated that, under plug-flow conditions in a CCIX column with mass transfer in the ion exchange reaction controlled by pore diffusion, a direct comparison could be made between the 'fractional approach to equilibrium' parameter of the IX kinetic curve and the CCIX 'stage efficiency' - provided the contact time in the CCIX stage and the reaction time in the kinetic experiment were the same. In this section, the average stage efficiencies for a number of CCIX conditions are compared with the batch kinetics of the relevant exchange reaction.

4.331 Cation exchange: The data of Table 4.11 represent two CCIX tests on the exchange of ammonium and sodium ions. A further series of such tests was conducted at various concentrations and bed expansions in order to provide a range of stage efficiencies for comparative purposes. Details of the full range of tests is outlined in Appendix C.

In order to vary the contact time in a CCIX stage, two alternative techniques can be adopted: (i) the %BE can be altered by changing the solution flow rate through the column, (ii) the height of the CCIX stage can be changed so that the contact time in a stage alters. Within the constraints of physical operation, it is not possible to change the stage height without simultaneously reducing the number of exchange stages which can be accommodated in the test area. Too severe a reduction in the number of stages would mean that fewer sample points would be available for intermediate liquid sampling and less reliance could then be placed on the average stage efficiency calculated from the test run.

The degree to which the %BE can be changed is dependent upon the concentration of the feed solution, for together the BE and feed concentration set the frequency with which resin must be moved (cf. section 4.3113). Thus, at high solution concentrations it is only possible to have low bed expansions and hence long contact times (cf. Figure 4.22) if unstable CCIX column operation is to be avoided. Alternatively, at low feed concentrations high flow rates through the column are necessary to both reduce upflow time, with consequent cost savings due to higher resin utilisation (cf. Chapter 6), and ensure that the ion exchange reaction remains in the region of pore diffusion control of the rate. Hence, at low concentrations, the %BE must perforce be high and contact time of liquid in a stage relatively low.

For the reasons outlined, it was not possible to achieve as wide a spread of CCIX contact times as was desired. However, a satisfactory time variation was achieved for the ammonium-sodium exchange and where this was not possible in the 'other' exchange reactions sufficient data to provide proof of the theory in the light of NH_4/Na results are presented.

In Figure 4.27 the batch kinetics curves for the NH_4/Na exchange at three concentrations are presented. Superimposed on the two curves are the data from the calculation (according to the method in section 4.322) of the average CCIX stage efficiencies for the series of tests conducted at various solution flow rates and concentrations and outlined in Appendix C. The results presented in the figure show clearly that the CCIX stage efficiency can be predicted from the batch kinetic curve at the appropriate concentration. Despite the slight scatter in the CCIX data, the same trend

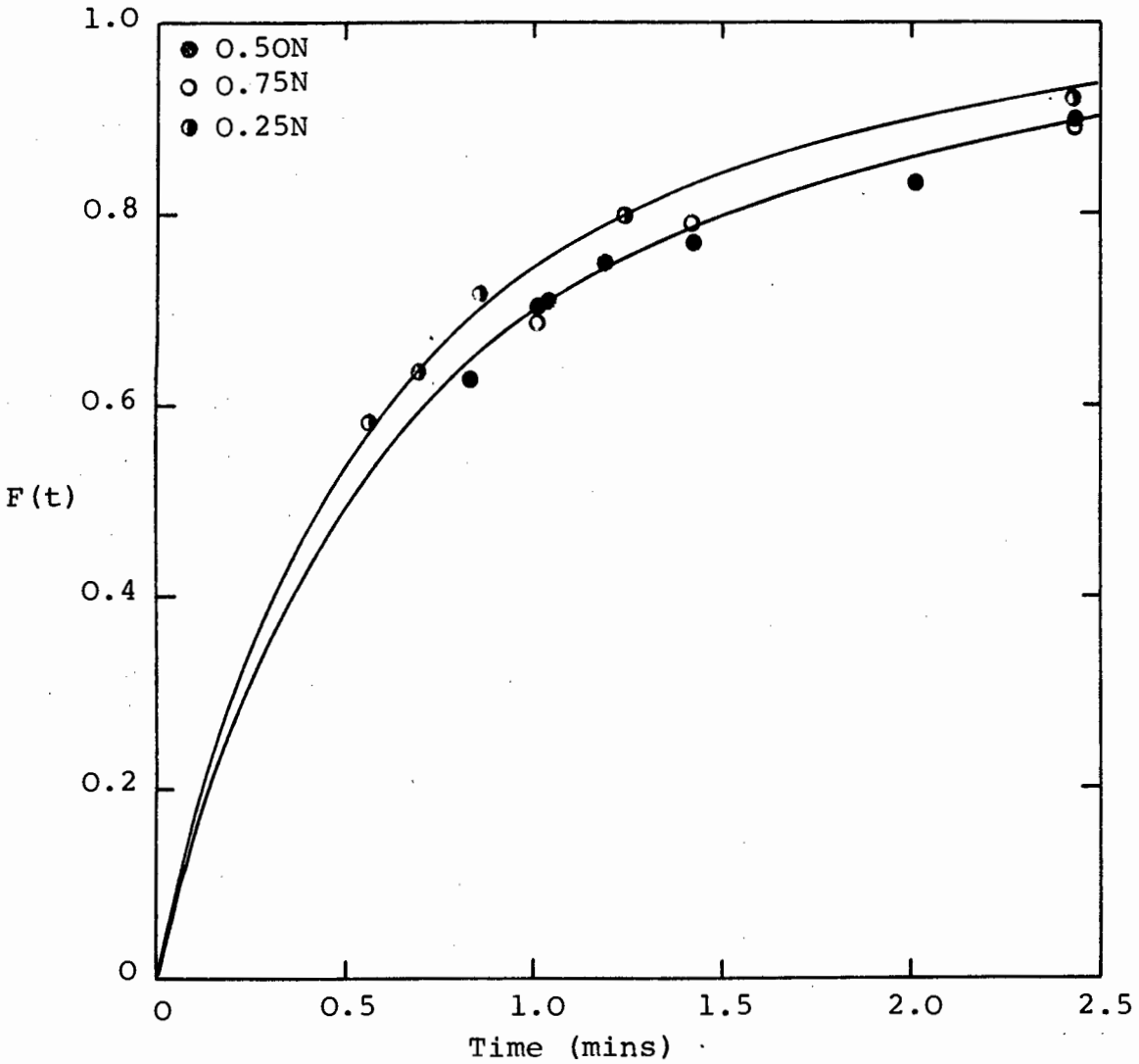

FIGURE 4.27

Comparison of batch and CCIX kinetics:
Ammonium-sodium exchange on Zerolit 625

in results for the conditions investigated is obvious and proves that the kinetics F(t) value and the CCIX η value are directly comparable.

Figure 4.28 shows a comparison of the batch and CCIX results for the exchange of sodium-hydrogen and ammonium-hydrogen on Zerolit 625. In these two cases, because of the concentration constraints, the contact time range of the CCIX data could not be extended beyond that presented in the figure. Nevertheless, the data confirm the result shown by the NH_4/Na exchange and further proves the relationship between pore diffusion controlled batch and CCIX data.

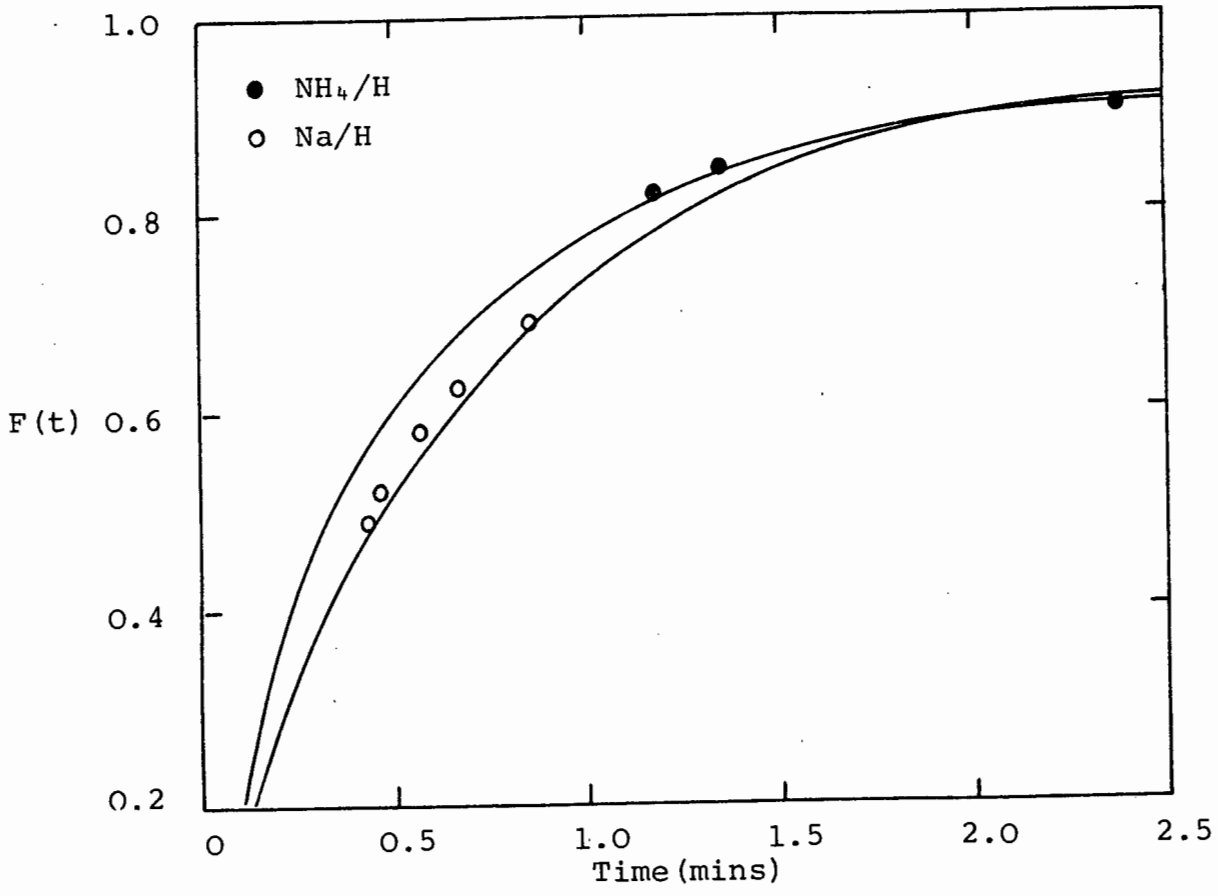

FIGURE 4.28

Comparison of batch and CCIX kinetics:

Ammonium-hydrogen and sodium-hydrogen exchange on Zerolit 625

4.332 Anion exchange: The very favourable anion load and regeneration equilibria (Figures 4.14 and 4.15) meant that complete conversion of both resin and solution occurred in very few CCIX exchange stages. Because of the limit to which the %BE could be raised, and the stage efficiency concurrently reduced, in an effort to force exchange to occur over a greater number of stages, it was only possible to establish data for the anion load reaction. The load reaction data were only established because of the low feed solution concentration (hence the %BE could be increased) and the slow kinetics of this reaction (which meant that at the high %BE the stage efficiency was low). For the anion regeneration reaction (equation (4.12)), at the lowest regenerant solution concentration that was considered, 0,50N, the highest %BE which could be used was 80% giving a contact time (cf. Figure 4.22) of 4,8 minutes. From the kinetic curve of Figure 4.19 it is seen that,

at this lowest possible contact time, maximum conversion is achieved. Maximum conversion with the very favourable equilibrium curve means that total exchange occurs in one 0,5 m CCIX stage, so that a batch kinetic comparison would have no meaning in this case.

In Figure 4.19, CCIX stage efficiency data are superimposed on the kinetic curve for the anion load reaction. The results of the comparison again show that for an anion resin exchange, as for a cation exchange, batch kinetic data can be used to predict the performance of a CCIX column under steady state conditions.

Although not measured, it can be inferred from the comparisons presented for the exchange of ions on both anion and cation resins, that the anion regeneration reaction and also the resin electrolyte sorption processes can be predicted in a CCIX column via their respective batch kinetic curves. Both these mass transfer operations are controlled by the same solution-resin parameters and ionic diffusion fluxes that control the exchange reactions which have been shown to comply with the steady state theory of section 2.4323.

CHAPTER 5

OPERATION OF THE CCIX PILOT PLANT

5.1 INTRODUCTION

In the foregoing chapters, the principles and properties of ion exchange and how these relate to the combined desalination and organic removal process when IX is applied to the treatment of sewage plant wastewaters, have been discussed. In the results so far presented, the ability of the cation and anion resins to perform their required tasks and of a CCIX column to operate with the strong acid-weak base resins has been outlined. However, for the IX tertiary treatment process to function, the ion exchange reactions (4.8 to 4.12) have to be performed simultaneously and continuously in separate interconnected CCIX columns. The major objective of the pilot plant tests was therefore to evaluate the ability of ion exchange in CCIX columns to perform a tertiary treatment and desalination function on a continuous basis.

The principle of CCIX operation, although attempted when ion exchange as a unit operation was first placed in service, has only in the last few years reached the point of commercial exploitation and then only due to completely new design concepts, and equipment technology advances. Today still, large scale use of CCIX is limited to two interlinked columns and then predominantly in the metallurgical industry and uranium recovery. For the operation of CCIX in a tertiary treatment role with regenerant chemical recovery, it is necessary to run, under stable steady state conditions, five interlinked columns. The columns operate at very different solution flow rates and concentrations and contain two resin types (cation and anion) each with their individual hydraulic and ion exchange properties. The pilot plant tests had also therefore to establish that operation of this degree of CCIX plant complexity was possible.

The test work was divided into two major phases, outlined respectively in sections 5.2 and 5.3 below. The first phase involved plant construction, flowsheet checking, hydraulic tests and desalination of synthetic feed solution. The objectives of this phase were (i) to establish whether the complex CCIX flowsheet could be operated, and (ii) to develop the necessary

plant control strategy and check procedures to perform the required operation. During this period, results were largely of a qualitative nature, and decisions made on the basis of visual observation, except for the initial desalination tests. Again, the purpose of these initial desalination tests was to confirm that stable chemical operation could be achieved simultaneously with hydraulic stability.

The second phase of the test work was centred around the treatment of water obtained from the Milnerton and Athlone sewage works. The compositions of the discharge streams from these two works is different, and the aim was to determine the ability of the pilot plant to treat successfully both water types by removing organic and inorganic components on a continuous basis while also achieving the recovery of regenerant chemicals. The results of this phase of the test work are documented in section 5.3.

5.2 PROCESS FLOWSHEET DESCRIPTION AND PRELIMINARY TESTS

The size of the pilot plant, in terms of feed throughput, was based on three factors (i) the maximum total daily volume which could reasonably be provided by water cartage from a sewage treatment works remote to the pilot plant site; (ii) the minimum CCIX column diameters (sized on the basis of plant throughput) which would provide satisfactory phase contact; and (iii) the dissolved solids concentration of the water that the pilot plant would be required to treat. After due consideration, the plant was designed to operate continuously treating 5 kℓ/day in two anion and three cation CCIX columns according to the flow diagram of Figure 5.1.

5.21 Discussion of stream compositions

In Figure 5.1, below each of the five CCIX columns another 'vessel' is indicated. This 'vessel' is termed the 'catchpot' and its purpose is to catch and hold the volume of resin and liquid that leaves the bottom stage of the column during the resin pulldown period. Thus, in the figure, both a liquid and a resin stream is depicted leaving the bottom of the column and entering the catchpot. In practice, the liquid volume associated with the pulldown resin is 120% of the resin volume. This quantity of liquid (the pulldown liquid), with composition equal to that of the feedstream entering the column in question, reduces the nett liquid flow upwards through the

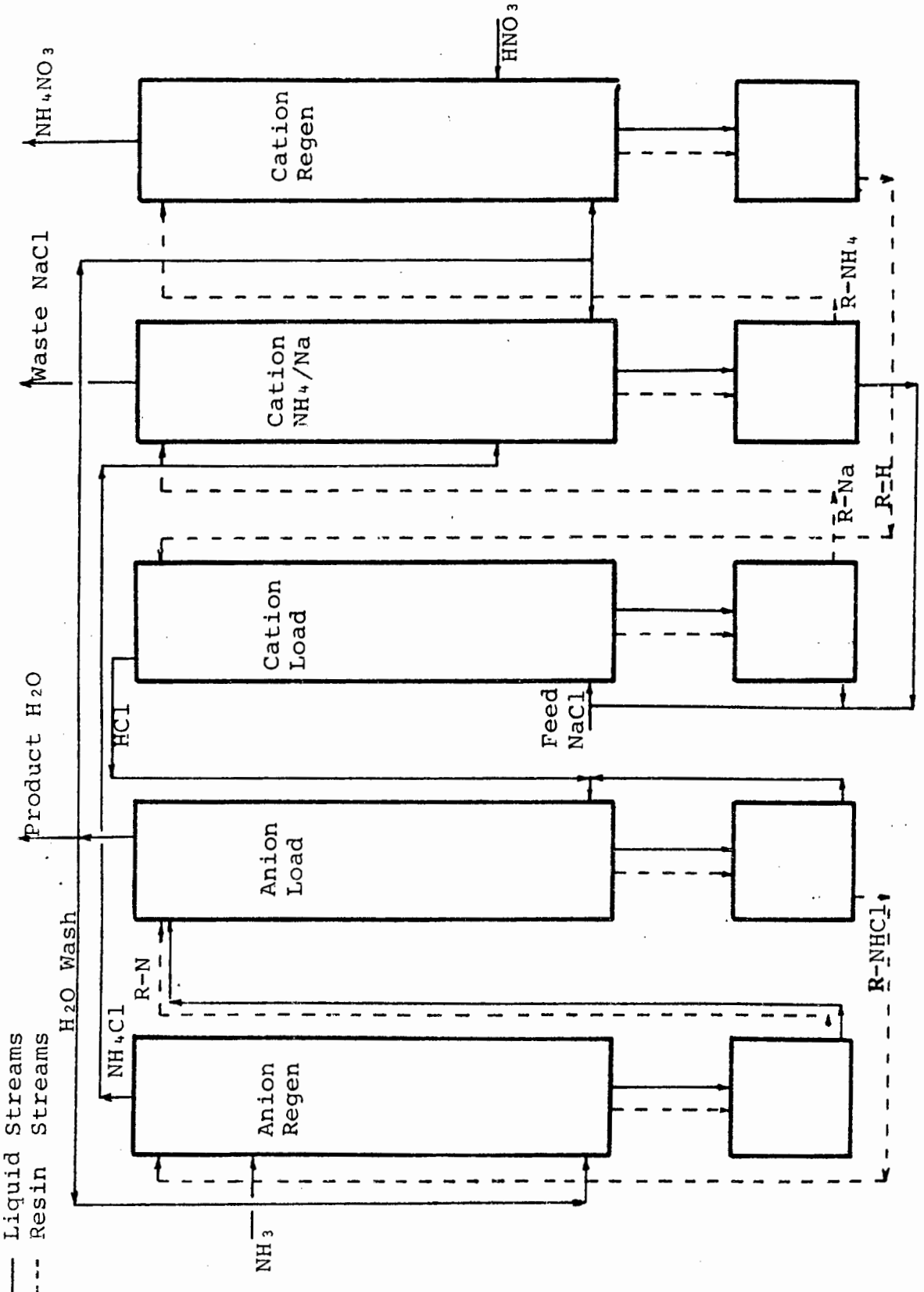

FIGURE 5.1

Flow diagram of CCIX pilot plant

column and has to be accounted for in the mass balance calculations. In the case of three of the columns, the pulldown liquid and resin are separated in a 'dewatering' operation (discussed in section 5.22) and each phase proceeds to a different destination. As will be indicated below, this separation is necessary for optimum plant operation.

5.211 Cation columns: The three cation columns in the plant are linked through the cation resin flow, for a resin balance has to be maintained within each of the columns. Because the stream concentrations entering the cation load, ammonium-sodium and regeneration columns are so different (0,02N to 3,0N) the upflow time and pulldown volumes are very different. This means that transfer of resin from the load to the NH_4/Na column may occur only once an hour while resin return from the regeneration to the load column will occur every 10 minutes. Naturally, the volume of the respective transfers is such that over a long period equal volumes of resin move through the columns. The comparison merely indicates the critical balance which has to be maintained.

5.2111 Load column (C1): Feed water enters the bottom of the cation load column (concentration approximately 0,02N) and flows upwards through the fluidised resin. The counter-current contact between this NaCl containing water and regenerated resin (hydrogen-form) results in resin conversion to the sodium form (reaction 4.8) and formation of hydrochloric acid. The HCl liquid stream goes to the anion load column by way of a tank which provides buffer capacity.

At the end of the upflow period, a stage volume of Na-form resin and liquid enters the catchpot. While the next upflow cycle proceeds, the dewatering step occurs. Because the resin has to be moved to the top of the NH_4-Na column where it will contact a concentrated stream, (approximately 1,0N) it is necessary that as little low concentration feed water (0,02N) as possible be carried with the resin - hence the dewatering step. The water which leaves the resin in the C1 catchpot is recycled to the main feed tank, for it has the feed composition. The dewatered resin is then transferred to the NH_4/Na column using some of the liquid product from the NH_4/Na column to facilitate the transfer.

5.2112 Ammonium-sodium column (C2): This column receives predominantly sodium loaded resin from the load column, and contacts this resin with the anion regeneration column product liquid stream which, at a concentration of approximately 2,0N, contains ammonium cations and feed water anions, organics and hydroxide ions. The result of the reaction (equation 4.9) is NH_4-form resin and a liquid stream containing all the salts originally present in the feed stream.

As indicated in Figure 5.1, another stream besides the anion regeneration product, enters the NH_4-Na column. This second feedstream serves to wash the NH_4-loaded resin in the bottom stages of the C2 column. The wash is required to remove all traces of chloride ion (the major anion in the anion regeneration product stream) from the resin. This is necessary because this resin is next to be contacted with the recovered regenerant NH_4NO_3 (AN) stream, where chloride ions would be a contaminant not suitable for the proposed fertiliser end use of the AN. Because the resin wash stream is simply recycled CCIX plant product, it has the same composition as the product water.

The concentration of the waste brine stream leaving C2 is controlled by two factors (i) by the concentration of the anion regeneration column (A2) product stream, and (ii) by the nett volume of recycled plant product water used for resin washing which flows upwards and dilutes the NH_4-containing feed stream. In general, after allowance has been made for liquid leaving C2 with the pulldown resin, an excess of wash is introduced so that a two-fold dilution within C2 occurs. Naturally, a lesser dilution can be set but then resin washing will be less efficient.

The C2 pulldown resin volume is dewatered in the catchpot in order to prevent dilution of the AN stream with the C2 wash water. As the pulldown liquid from C2 contains only diluted A2 product salts (mainly NH_4Cl), it is recycled to the pilot plant feed for desalination. The volume of this recycle stream relative to the total feed is approximately 1%, so it has a negligible effect on the C1 column conditions.

On completion of the dewatering step, the NH_4-form resin from C2 is transferred to the cation regeneration column using AN solution to assist the 'air driven' (cf. Appendix C) resin flow.

5.2113 Regeneration column (C3): This column, in which reaction (4.10) proceeds between NH_4-form resin and nitric acid, is exactly analogous in operation to the NH_4/Na column. The acid stream is injected three stages from the bottom of the column, at a concentration set to give a desired AN concentration when the acid is diluted with recycled plant product water. Here, the recycled water serves to wash residual HNO_3 from the cation resin in the C3 wash stages.

On completion of an upflow period, the regenerated pulldown resin and liquid are both transferred to the top of the cation load column without a dewater step. Because the pulldown solution will contain only dilute HNO_3, no harm occurs when this stream contacts the C1 overflow stream containing HCl, for the relative volume ratio is again of the order of 1%, and the residual HNO_3 will load onto the anion resin.

5.212 Anion columns: The two anion columns are interlinked by virtue of the resin flow between them, and together they are linked to the cation columns by the feed which the anion load column receives and the product which the anion regeneration column sends to the NH_4/Na column. The 100-fold concentration difference of solution in the two anion columns means, as with the cation columns, that the frequency and volume of resin transfers from one column to the other are very different; six litres every hour for the load column compared with 0,5 litres every 5 minutes for the regeneration column.

5.2121 Load column (A1): The acid containing water from C1 is reacted with free base resin according to reaction (4.11) in the anion load column. The liquid stream leaving the column is the treated product water, and the resin entering the A1 catchpot is loaded with all the feed water anions and organics.

Loaded anion resin is dewatered prior to transfer to the regeneration column to prevent dilution of the A2 product stream. Because the dewatered solution is predominantly A1 feed, it is recycled to the A1 feed tank. The loaded resin is dispatched to the top of the anion regeneration column using the A2 product solution for the transfer.

5.2122 Regeneration of column (A2): Stripping of the loaded anion resin is accomplished with ammonia-solution according to reaction (4.12). Like the cation regeneration column, the NH_3 concentration and wash water flows are metered to achieve a desired product solution composition. The difference, however, between C3 and A2 operation is the point at which the regenerant is introduced. In C3, the reaction is not favourable and needs a large number of contact stages to achieve completion but the resin washing is achieved relatively easily (cf. the equilibria of section 4.3). In contrast, A2 regeneration proceeds extremely easily but resin washing (due to the equilibrium) is much more difficult. Therefore, most of A2 column is taken up with resin washing.

Incomplete removal of ammonia from the regenerated anion resin causes contamination of the plant product water with nitrogen. As the product stream from the CCIX plant would, if intended for potable use, have to be disinfected by chlorination, ammonia contamination of the product stream would result in a high chlorine demand and thus increased costs. The ammonia level is consequently critical, and, from economic considerations, must be kept to <10 mg/ℓ as N.

No dewatering is practised on the A2 pulldown resin, for the solution in contact with this resin is simply product water which is utilised for washing. When A2 resin is transferred, this solution merely returns to the point from which it was originally derived.

5.22 Plant sizing and hydraulic tests

The purpose of the plant hydraulic tests was threefold: (i) to establish the reliability of the plant control equipment, (ii) to ensure that the resin and solution balances in the plant could be maintained for an extended period of operation, and (iii) to train the plant operating staff during a non-critical phase of operation.

5.221 Column sizes: The pilot plant column dimensions were constrained to a certain extent by (i) the floor area and height available for erection; (ii) the need to allow for flexibility in the operation of the system under various conditions, and (iii) the available sizes of material from which it was decided that the plant columns should be constructed.

After due consideration the construction material chosen was polyacrylic (perspex) tubing and sheeting. The choice was based on (i) the chemical resistance of this material to inorganic salts, ammonia, hydrochloric and nitric acids at the concentrations which would occur within the plant; (ii) the ease with which perspex could be machined should modifications be required; (iii) the fact that perspex could be readily 'glued' if repairs had to be effected; (iv) all constructed equipment would be 'clear' and visual observation of phenomena within the columns could be made, and (v) the availability of the material.

5.2211 Load columns: The load column diameters were determined by allowing for a 50% bed expansion of loaded resin when the flow rate was 5 kℓ/day. On this basis, and choosing available perspex tubing sizes which would give approximately the correct bed expansion, the anion load column diameter was set at 200 mm and the cation load column diameter at 100 mm.

For all columns in the plant, the stage height chosen was 0,5 metres. Consideration of the kinetics and equilibria of the load reactions meant that the anion and cation columns had respectively five and seven stages. The number of cation load stages was increased at a later point in the plant operation and this will be discussed in section 5.3.

5.2212 Regeneration and NH_4/Na columns: The diameters of these three columns was abitrarily set at 50 mm, the smallest diameter which would suffice to provide stable column operation without the formation of bridges during resin fluidisation and without flow maldistribution due to possible wall effects.

The number of half metre stages in each column was constrained to twelve due to height considerations. These twelve stages were divided between wash and exchange stages with the division being three, four and ten wash stages respectively for the cation regeneration, ammonium-sodium and anion regeneration columns.

5.222 Column control: Each column in the pilot plant is individually controlled and an overall balance of resin and solution is maintained, in the first instance, by the settings for the control parameters for each column and secondly, by operator intervention to correct instabilities

should they occur. The exact details of the control functions and the valve sequencing required to achieve the necessary control is outlined in Appendix C. The various periods in a column cycle may be summarised as follows:

5.2221 Upflow, settling, pulldown: Each of these periods is regulated on the basis of time, with the calculation of the duration of the upflow based on the conversion requirements of either resin or solution, and calculated as outlined in Appendix C. During the upflow period, the solution flow rate into the column is controlled through an automatic sensing device based on the position of a float within a rotameter tube. Deviation from the set point causes a needle valve to open or close to provide the necessary correction.

On completion of the upflow period the feed flow is switched off through pneumatic actuation of a Saunders valve, and the resin settle period commences. The length of this period is set to allow complete settling of the fluidised resin within each stage of the column, and varies from column to column within the plant.

After resin settling, resin pulldown is actuated. This is the only operation in the control of the column which is not based on a time cycle. Instead, a sensor placed at the top of the column causes switching to occur when the liquid level in the column has dropped by a certain preset volume. In this manner, the volume leaving the bottom of the column can be accurately controlled, and resin pulldown volumes can be set within 10 mℓ of a desired volume. When the liquid level sensor terminates pulldown, the upflow recommences.

5.2222 Dewatering, resin transfer: On commencement of the upflow cycle, resin is immediately transferred from the catchpots of the two resin regeneration columns. For the other three columns, dewatering starts.

At the bottom of each catchpot is a slotted resin screen which allows solution but not resin to pass through the screen openings. Dewatering is achieved by pressurising the catchpot with air and opening the other side of the screen to atmosphere. The compressed air then pushes all pulldown liquid out of the resin void volume. A certain amount of resin 'drying'

also occurs thereby fractionally reducing the volume of solution present in the resin bead pores. The length of the air blow period is controlled to achieve a desired moisture reduction.

Following the dewater step, solution from the top of the column to which the resin is proceeding, is allowed to enter the catchpot. Sufficient time is allowed during this step to ensure that the solution volume is sufficient for the subsequent resin transfer. A volume equal to the pulldown volume, i.e. 120% of the resin volume was found necessary.

Resin transfer is accomplished by again pressurising the catch pot with compressed air and opening the discharge line to the top of the next column. In this manner, the resin-solution mixture is 'pushed' to the top of the next column. The air pressure is set so that head and friction losses in the transfer lines are just overcome, and air flow rate is throttled so that resin transfer proceeds as slowly as possible, to prevent any possibility of the transfer solution being 'blown out' of the resin with consequent clogging of the line with dry resin.

5.223 Continuous operation: The results of the hydraulic test phase were purely qualitative. A total of 96 hours of plant operation in which all control functions were set to perform as if desalination was occurring, was satisfactorily concluded. During this period, resin pulldown volumes were checked, dewatering systems evaluated and plant control strategy modified as required.

The objectives of this phase of the programme were achieved, and the first part of the operation of five interlinked CCIX columns satisfactorily concluded. The major doubt prior to operation, the maintenance of resin and solution inventories throughput the plant, was dispelled and the hydraulic tests proved that the CCIX plant could be controlled.

5.23 Desalination of synthetic feed solutions

Having established the hydraulic feasibility of plant operation, it was necessary to prove that chemical stability could be achieved concurrently with hydraulic stability. In order to test plant desalination capability, two synthetic feed solutions were used. Feed A of Table 5.1 containing

TABLE 5.1

Synthetic feed composition for pilot plant tests

Component	Composition (mg/ℓ)	
	Feed A	Feed B
Na	514	350
Ca	10	33
Mg	5	56
NH_4 as N	0	17
Cl	750	600
SO_4	0	140
NO_3 as N	0	10
TDS	1 280	1 265

predominantly NaCl was followed by feed B. Feed A was made from tap water dosed with NaCl and so contains only small quantities of hardness ions. The normality of feed A was set to equal that which occurs in the sewage plant discharge stream that would subsequently be tested, and the composition of feed B was set equal to that of the same HTE stream. The choice of a 'pure' NaCl feed for initial testing was to facilitate plant monitoring and so enable the detection of continued non-steady operating conditions should these occur. Feed B was specifically designed to simulate the HTE water.

5.231 Plant operating conditions: The purpose of these tests was to determine whether steady state could be achieved within each of the interlinked CCIX columns. A feed flow rate of 5 000 litres/day was set and feed A introduced to the plant with the intention of operating until a steady state in all columns had been attained. All other plant conditions were arranged so that salt removal would approach 100%, and the purities of the waste brine product from the NH_4/Na column and the AN product from the cation regeneration column would also approach 100%. To achieve these purities, the ammonia and nitric acid excesses were 50% and 100% respectively. The ammonia excess was not so much to change the stoichiometric ratio in the anion regeneration column (the reaction has a very favourable equilibrium) but to provide extra ammonia in the NH_4/Na column by way of the NH_4Cl feed (cf. Figure 5.1). This extra ammonia increases the level of resin conversion in C2 and thus raises the AN purity.

On completion of the test work on feed A (Table 5.1) the pilot plant feed was switched to the simulated HTE water under exactly the same stoichiometric conditions. The results of both test phases are discussed together.

5.232 Discussion of results: Three days after startup on feed A steady operation in each column of the plant was achieved. Because feed was introduced to regenerated resins, the plant product water composition always showed a high level of desalination. The switchover from feed A to B could really not be detected, other than a slow rise in hardness and sulphate ions in the AN and waste brine streams respectively. Average stream compositions for two days of steady operation on each feed are presented in Table 5.2.

TABLE 5.2

Average stream compositions during CCIX plant operation on synthetic feed solution

Feed	Stream	Flow (ℓ/day)	Day	Concentration (mg/ℓ) Na	Ca	Mg	NH_4-N	Cl	SO_4	NO_3-N	TDS
A	Product Water	4350	1	15	-	-	10	40	-	1,2	73
			2	10	-	-	7	14	-	0,9	37
	Waste Brine	300	1	7000	32	25	1000	12000	-	-	20000
			2	7400	35	32	1240	13000	-	-	22000
	Amm. Nitrate	300	1	700	140	45	2500	25	-	10000	48400
			2	1780	140	44	5830	0	-	9100	49800
B	Product Water	4350	1	30	0	0	18	74	0	0,1	127
			2	37	0	0	29	79	0	0,3	153
	Waste Brine	250	1	6480	61	127	2480	11750	3210	-	24800
			2	5770	66	147	2657	11950	2850	-	24200
	Amm. Nitrate	350	1	90	600	332	3280	68	0	7869	40400
			2	110	760	571	3124	53	0	9245	47700

5.2321 Product water: The product water compositions show that better than 90% removal of feed water TDS was achieved during the operation of the CCIX plant with a simultaneous water recovery level of 87% (i.e. the ratio of product to feed water). These results prove that the plant is capable of performing the required desalination. However,comparison of the results for feeds A and B show the following:

(i) although the water recovery is the same, the TDS level of the product is increased in the case of feed B;

(ii) the ammonia levels of both streams are relatively high; in feed B product, unacceptably high.

The ammonia level increase (feed B) is due to a reduction in the wash water used in the anion regeneration column. The wash water reduction increases the A2 column product concentration and hence the waste brine concentration (cf. Table 5.2) and is one method by which total water recovery can also be raised. The disadvantage of the wash water decrease is the resultant lower ammonia removal in the anion wash stages (due to the change in the operating line slope). This means higher NH_4 levels in the product water and, in turn, higher chloride and TDS levels, for HCl which should load onto the anion resin now reacts with the ammonium hydroxide present and leaves the column as NH_4Cl.

A further reason for the TDS increase during the treatment of feed B was the feed water composition which now contained higher levels of hardness ions. These ions, for which the resin has an extremely high affinity, will strip loaded sodium ions. The equilibrium conditions within the column are thus changed, and higher sodium levels occur in the solution leaving the cation load column. Because the anion resin is not capable of splitting neutral salts, any sodium ions which enter the anion load column will pass through the column in combination with chloride, thereby increasing the product water TDS.

The other interesting comparison to be drawn from the product water analyses is the respective nitrate levels. The reduction in nitrate level for the second feed case was due to an increase in the wash water on the cation regeneration column. This wash increase removed more free nitric acid from the cation resin prior to the resin's return to the cation load

column. A lower HNO_3 level in the resin means less of this species in the feed to the anion load column and consequently (bearing in mind the relative equilibria and kinetics in A1) less nitrate in the product. Simultaneously with the C3 wash increase comes a reduction in the AN concentration from C3.

The product analyses have proved the viability of the desalination but have simultaneously shown how critical the inter-relationships in stream compositions within the CCIX plant are, and how a seemingly unrelated change can effect the product water composition.

5.2322 Waste brine: The waste brine stream should contain all the salts originally present in the feed water, but at a considerably higher concentration. The analysis figures in Table 5.2 show that this is the case except that the waste brine also contains a certain fraction of ammonium ions. This represents a loss of ammonia from the system and is due to the need to run the C2 column with an excess of NH_4 in order to attempt to convert the resin fully and thus obtain a higher AN purity. To achieve complete resin and liquid conversion in a CCIX column means that the operating line must lie on the diagonal in an x-y diagram and then a large number of contact stages are also required. With the eight exchange stages in C2, ammonia loss is the penalty paid for increased resin conversion.

The concentration of the waste brine, even without the ammonia content, represents an approximate 20-fold feed water concentration. The concentration change which occurs with an A2 wash water flow change indicates how the waste brine strength can be still further increased.

The higher ammonia level in the feed B test can be explained by considering the presence of the divalent hardness ions which are strongly held by the resin. An unfavourable equilibrium for resin conversion to ammonia form now exists. Consequently, more ammonia loss will occur during attempted resin conversion. The equilibrium can, however, be altered if the concentration is increased (cf. Figure 2.8).

5.2323 Ammonium nitrate: The cation resin is converted to hydrogen form in C3 with formation of nitrate salts. The purity of the recovered AN product is dependent upon the level of resin conversion in C2, while the concentration of the stream depends on the input acid concentration

and the wash water flow. The total nitrogen content of the AN stream reflects the level of regenerant recovery that has been achieved in the process. Because a large excess of acid is required for the exchange, the pH of the AN stream is low, and nitrate nitrogen is recovered as free acid rather than AN.

The degree of nitrogen recovery, as a percentage of feed ammonia and nitric acid, is >95% for both feed streams; the only nitrogen loss being the ammonia content of the waste brine stream. The contamination of the AN with calcium or magnesium is not necessarily a problem if the fertiliser end use of the stream is considered. However, chloride ions, present if the C2 wash is not sufficient, can prove damaging when AN is used as a fertiliser.

5.3 TREATMENT OF SEWAGE PLANT DISCHARGE STREAMS

The culmination of the development of the CCIX system was the determination of the plant's ability to perform a combined desalination and tertiary treatment function on a sewage plant discharge stream. In this section, the results of this phase of the test work are discussed.

For the purposes of testing the process, water from two sewage treatment works was investigated. The first of these, Milnerton, treats sewage from mainly domestic origin. The inorganic solids level of this water is, however, high due to sea water infiltration into the sewer system. Consequently, the predominant inorganic contaminant is NaCl. The liquid flow into Milnerton was below the works design capacity during the period that the CCIX tests were conducted, and so the residual organic level of this water, measured in terms of the COD, was <90 mg/ℓ. In Table 5.3 an average analysis of the Milnerton HTE during the test period is reported.

Athlone sewage treatment works, the source of the second water used to evaluate the CCIX plant performance, treats a predominantly industrial waste under overloaded plant conditions. The high loading level meant that during the test period on the HTE water, the COD level fluctuated between 120 and 250 mg/ℓ. The inorganic content of the Athlone water is lower than that of Milnerton and the water has the composition specified in Table 5.3.

TABLE 5.3

Average compositions of sewage plant discharge streams used as pilot plant feed

Component	Milnerton HTE	Athlone HTE	Athlone PC Plant Effl.
Na	326	120	148
Ca	65	45	76
Mg	62	18	6
NH_4-N	8	13	1
Cl	528	205	211
SO_4	188	118	105
NO_3-N	11	21	14
PO_4	31	-	0
COD	89	120-210	27

One further water was also tested in the pilot plant. This particular water was produced as a product stream from a physico-chemical (PC) reclamation plant treatment of Athlone HTE. The PC plant consists of lime flocculation, sedimentation, aeration, ammonia stripping and filtration. The inorganic content of the PC plant water is similar to Athlone HTE, but the organic content is considerably lower. Table 5.3 shows the analysis.

Each of the above waters was used as feed to the CCIX plant at different periods during the test programme. The particular water was collected on a twice weekly basis and placed into storage at the pilot plant site. From storage the water was sand filtered, analysed (from which the data of Table 5.3 are provided) and fed to the CCIX plant and the various results outlined below were obtained.

5.31 Operation on Milnerton HTE

The Milnerton water was the first choice for plant testing for it had already been used in the resin life tests (section 4.22) and its composition, when determined over a long period of time, had shown little variation.

The tests on Milnerton water were conducted in two parts: (i) the pilot plant was operated at a feed flow rate of 3 100 litres/day according to the flow diagram of Figure 5.1, and (ii) the feed flow rate was increased to the design level of 5 000 litres/day. The objectives of the two phases of operation were:

(a) phase one - to operate below design level in order to assess the degree of desalination and COD reduction which could be achieved:

- to determine simultaneously the level and purity of the recovery of the regenerant chemicals;
- to evaluate the degree of salt and organic concentration which could be achieved in the waste brine stream and thus determine the water recovery;
- to assess what problem areas existed in the operation of the plant, and formulate methods of overcoming these problems.

(b) phase two - to compare the performance of the plant with that achieved under the previous flow rate conditions.

5.311 Discussion of operation at 60% of design flow rate: Plant operation at a flow of 3 100 litres/day extended over a two month period, during which time minor equipment malfunctions were corrected and slight adjustments made to resin flows in order to achieve steady state. At the end of this period, two weeks of steady plant operation were achieved, and these results are reported.

5.3111 Product water: All pilot plant solution streams were sampled on an hourly basis during startup and approach to steady state in order to follow and record transient operation. From these hourly samples an average daily stream composition was computed, and for the last seven days of steady operation these average values of the product water composition are recorded in Table 5.4.

Comparing the pilot plant product water composition with the feed water composition of Table 5.3, shows the high level (96%) of desalination which was consistently achieved during plant operation. The product water has a residual TDIS of under 60 mg/ℓ, of which all are univalent ions and approximately 60% is NH_4Cl. The resin affinities for di- and trivalent ions ensures that Ca, Mg, SO_4, PO_4 and any heavy metals present in the feed are completely removed in the IX process.

TABLE 5.4

Pilot plant product water analysis

Feed: Milnerton HTE Flow: 3 100 litres/day

Day	Concentrations (mg/ℓ)								
	Na	Ca	Mg	NH_4-N	Cl	SO_4	NO_3-N	PO_4	COD
8	<5	0	0	24	28	0	1,4	0	13
9	<5	0	0	29	15	0	3,2	0	9
10	<5	0	0	18	11	0	1,2	0	9
11	<5	0	0	17	11	0	1,0	0	22
12	<5	0	0	18	12	0	1,0	0	21
13	<5	0	0	17	15	0	0,6	0	22
14	<5	0	0	17	10	0	1,6	0	26

The relatively high NH_4Cl level in the product is again due to ammonia contamination of the water. As outlined in the previous tests on the synthetic feeds, there are two possible sources of ammonia contamination. The first, inefficient washing of the anion resin, is a bigger problem when organic material is present in the feed water for, as outlined in section 4.22, the organic loaded anion resin 'picks up' ammonium ions which are subsequently released in an hydrolysis step. This effectively changes the electrolyte sorption equilibrium curve and makes the anion wash even less efficient. The other 'source' of ammonia ions is from incomplete regeneration of the ammonium loaded cation resin in C3 column. Considering the NH_4-H equilibrium of Figure 4.13, and the concentration of the Milnerton feed at 0,022N, a calculation shows that >94% of the cation exchange sites must be converted to hydrogen in order for the NH_4-N level in the stream leaving the cation load column C1 (cf. Figure 5.1) to be <10 mg/ℓ. Any NH_4 ions entering A1 column (the anion load) will pass through the column taking with them an equivalent quantity of chloride ions, leading to product water contamination.

The only component of the HTE feed not present in the previous tests, the organic material, is removed from the water by the anion exchange resin simultaneously with the inorganic anion loading. This removal is reflected in the COD level of the product, which on average is <20 mg/ℓ, a 75% COD

reduction. This result was, however, anticipated from the data of the resin life tests previously conducted (section 4.22) but, in this context, the result proves that the CCIX plant is capable of providing a combined desalination and tertiary treatment in one step on a continuous basis.

5.3112 Waste brine composition: The composition of the waste brine discharge stream from the NH_4/Na column during the seven day period of steady state operation is presented in Table 5.5.

TABLE 5.5

Average composition of plant brine discharge

Feed: Milnerton HTE Flow rate: 3 100 litres/day

Day	Concentration (mg/ℓ)								
	Na	Ca	Mg	NH_4-N	Cl	SO_4	NO_3-N	COD	TDIS
8	3590	84	203	2160	7296	2740	323	588	18120
9	4760	85	274	2030	7270	2600	175	518	18270
10	3630	114	235	1160	6550	2320	327	593	15790
11	3847	74	217	1420	6780	2290	414	831	16870
12	3130	53	170	1090	6150	2384	412	584	15110
13	2848	50	160	1120	6760	2320	270	591	14760
14	3220	45	170	900	7347	2675	398	582	16400

The TDIS of the waste brine averages 16,5 gm/ℓ, of which 20% is ammonium and nitrate ions. This means that an effective 11-fold concentration of feed water ions has occurred (1,2 gm/ℓ to 13,2 gm/ℓ) during the operation of the plant. This level of concentration is a function of the plant operating conditions, for, if the NH_4/Na wash is reduced or the anion regeneration product stream concentration increased, the concentration of the waste brine would be higher.

The ammonia present in the brine is the excess used to achieve resin conversion in C2 column, and represents an NH_4 loss. During this period of plant operation, a small fraction (10%) of the anion regenerant did not enter the NH_4/Na column because of flow control problems. This is reflected in the mass balance calculations presented later, but, in terms of the operation of

C2, means that the level of resin conversion to NH_4-form and the concentration of the waste brine are approximately 5% lower than they could be under the set conditions.

The nitrate level of the brine stems from incomplete cation resin washing in the regeneration column after the resin contact with nitric acid. As previously outlined, this nitrate loads on the anion resin, is stripped off by the ammonia in A2 and ultimately ends up in the waste brine as a nitrate loss.

The ratio of Ca/Mg to Na ions presents in the C2 product stream shows a 5-fold decrease when compared with the feed stream. This change is due to the separation of ions which occurs when the strongly held divalent hardness ions are not stripped off the resin in the NH_4/Na column by the anion regeneration product stream. This incomplete resin conversion is reflected in the AN purity discussed below. The resin affinity can be altered by changing the solution concentration (cf. section 2.2). The ratio of chloride to sulphate in the waste brine and feed is identical, indicating that these two species are equally well stripped from the anion resin with the excess of ammonia used.

The other major brine stream constituent, the organics, show, in terms of the COD measurement, only half the level of concentration that typically the chloride ion shows in going from feed to waste brine stream. The reason for this has not been clearly established, but can possibly be accounted for by the precipitate which formed in the NH_4/Na column and was carried out of the column by the waste brine stream. The precipitate was extremely dark in colour, indicative of organics. All other pilot plant streams were free of organics, and the resin life tests had not indicated an organic build-up on either the anion or cation resins, so all the organics must have left the plant via the waste brine.

5.3113 Ammonium nitrate stream: The average analysis of the cation regeneration product stream over the seven day steady state period is outlined in Table 5.6. The nitrate level of the stream is based on the nitric acid concentration and the resin wash level, the average of the values presented indicates a concentration of 2,25N.

TABLE 5.6

Average composition of plant AN discharge

Feed: Milnerton HTE Flow rate: 3 100 ℓ/day

Day	Concentration (mg/ℓ) Na	Ca	Mg	NH_4-N	Cl	NO_3-N
8	7440	3740	3020	14820	50	27560
9	6770	4120	3060	13590	80	27240
10	6230	4550	2790	14080	30	28730
11	7650	5050	3540	16420	10	33730
12	8480	5550	3380	14600	10	36480
13	8860	5620	3520	17410	20	38130
14	8370	4750	2920	16740	40	32200

The AN stream cation balance indicates that, on an equivalent basis, 2,5% of the stream contains free nitric acid, while Na, Mg, Ca together constitute contaminants in the attempt to obtain a high purity AN product. These latter metal ions are present due to incomplete resin conversion in the preceding exchange. However, on a mass basis Table 5.7 shows that together ammonia and nitrate make up 91,4% of the stream with Mg, Ca, Na together a further 8,3%. This shows that the CCIX plant can achieve one of its subsidiary objectives, the recovery of regenerant chemicals. The purity of the AN stream is ultimately dependent upon the economics of the

TABLE 5.7

Average purity of AN discharge

Component	mg/ℓ	% of total
Na	6 820	3,9
Ca	4 610	2,7
Mg	3 040	1,7
NH_4	19 370	11,1
Cl	30	-
NO_3	140 160	80,3
H	500	0,3
Total	174 530	100,0

process, for, with a large number of stages in the NH_4/Na column or a wasteful excess of NH_4 ion, the purity can be raised but at the expense of capital or lost ammonia costs. Chapter 6 discusses the economics of the recovery.

The extremely low level of chloride present in the AN is an indication of the efficiency with which the C2 column both washes and then dewaters the cation resin which has been in contact with NH_4Cl. This level of resin wash is achieved in four stages with the favourable desorption equilibrium curve (cf. Figure 4.16), while the nitrate level in the waste brine reflects the desorption equilibrium of this electrolyte in three stages. In both cases, the liquid to resin wash ratio is the same. The dewater step of column C2 does effectively add a further wash stage which the cation regeneration column does not have. Both washing results are thus equally good when the relative operating conditions are considered.

A further objective of the regenerant chemical recovery system is the production of a concentrated AN stream. The concentration of the stream is, as previously mentioned, a function of the column conditions, and the ability of the resin to withstand high acid concentrations. The resin life tests were conducted with a 3,0N acid without any damage done to the resin. The AN stream concentration, shown in Table 5.7 to be 174 gm/ℓ (17,4%), was achieved with an acid concentration of 2,25N.

5.3114 Mass balance: A mass balance on the four major ionic species present in the pilot plant stream, viz. NH_4, Na, Cl, NO_3 is detailed in Table 5.8. Various inferences regarding the operation of the plant can be drawn from these results, accepting that the low volume NH_4Cl output stream (which should have entered C2) was due to a leak in the system and is not typical of normal operation (compare with Table 5.10):

(i) Product water - the product water recovery during this test phase is calculated at 92%, with an average composition of 55 mg/ℓ (158 gms in a total flow of 2 857 litres).

(ii) Regenerant recovery - based on the operational results presented, the ammonia loss (the NH_3 not present in the AN stream as a percentage of NH_3 feed) was 37%, of which 14% was with the 'special' NH_4Cl discharge. A similar calculation for nitrate yields a total loss of 4%. Overall, this means a total nitrogen recovery in the AN stream of 82,5%.

TABLE 5.8

Mass balance of major components in CCIX plant operation

Feed: Milnerton HTE Flow: 3 100 litres/day

Stream	INPUTS			OUTPUTS			
	Feed	Acid	Ammonia	Product	Waste Brine	NH_4NO_3	NH_4Cl
Volume(ℓ/day)	3100	28	8	2857	201	68	10
Mass (g/day)							
Na	1010	0	0	14	715	463	0
NH_4-N	25	0	1540	56	290	1025	220
Cl	1637	0	0	56	1402	2	221
NO_3-N	34	2310	0	3	66	2152	17
TDIS	3807	10230	1981	158	3337	11832	637

(iii) the waste brine stream constitutes 6% of total discharge from the plant, and the AN stream 2%. Together, these two streams discharge 15 kg of dissolved material daily, with 80% (12 kg) present in the AN flow. On this basis, the CCIX plant requires 4 kg of ammonia plus nitrate for every kg of dissolved NaCl present in the feed water; of the 4 kg, 84% or 3,35 kg is nitrate.

5.3115 Qualitative observations: During the operation of the CCIX pilot plant, a number of qualitative observations were made which, although not measured nor perhaps measurable, would be of assistance to other workers attempting to repeat the operation. For this reason, these observations are recorded below.

(i) The Zerolit MPH anion resin colour slowly changes from light straw to dark brown during the course of the organic loading. The colour does, however, appear to stabilise, confirmed both by the life tests and the CCIX operation.

(ii) The Zerolit 625 cation resin undergoes a slight lightening of colour during the first week of operation. Further, hydrogen-form cation resin is darker in colour than either Na or NH_4-form resin. This is most evident in the cation load column, where successive stages from the top downards have

varying proportions of each resin colour, presumably changing as the resin loading proceeds and indicating plug flow.

(iii) During the passage of HTE through the cation load column, the water colour changes from brown to deep yellow as a portion (<10%) of the COD is removed. In the anion column, complete colour removal occurs, and the deep yellow feed becomes 'tap water white'.

(iv) The anion regeneration product solution contains >90% of the feed water organics concentrated approximately 20 to 30-fold. It consequently is extremely dark in colour and at the higher concentration levels, is virtually black. During the passage of this solution through the cation resin in the NH_4/Na exchange column, the concentration is halved by wash water and the colour lightens to a very dark brown.

An excess of NH_4 ions is used in the anion stripping reaction in order to provide an excess of these ions for cation resin conversion. This excess ensures that the stream pH is high, approximately 9 to 10. Consequently, a certain amount of $Ca(OH)_2$ precipitation also occurs in column C2 (with the sulphate content of the stream, gypsum also forms in C2). The precipitate is of the scaling type, and forms large sheets on the column walls. During formation the precipitate must adsorb organic material, for it is dark brown in colour. In an attempt to suppress some of the precipitate formation, the pH of the anion regenerant product was lowered to a neutral value. Although this reduced the precipitate, it also resulted in some of the organics present in the column being adsorbed by the cation resin. The AN product colour thus changed from a very pale yellow to brown during this test. It would therefore appear that the high pH within C2 must be maintained in order to retain the high level of organics in the solution phase. Under these conditions, the waste brine stream is rather messy, containing as it does a milky dark organic-salt mixture.

(v) The length of the upflow period for stable operation of a low density anion resin CCIX column is critical. Sufficient time must be allowed to enable the resin to attain a steady fluidised bed, and in the case of a 0,5 metre stage, the minimum time, irrespective of bed expansion was found to be 4 minutes. Any attempt at faster operation resulted in inventory depletion.

Further, if the pulldown volume was set at slightly more than the volume of resin present in a stage, inventory depletion also occurred over an extended period of operation. This was more evident for the anion than the cation resin. As a result of this fact, it was necessary to determine the fluidisation characteristics of the particular resin in its lowest density state (free base form for the anion resin) and to base column settings on the highest bed expansion occurring within a column. This was particularly necessary where the %Be changed where a feed stream entered midway up a column.

5.312 Operation at plant design flow rate: The next phase of the CCIX plant test programme was to evaluate plant performance at the design flow rate of 5 000 litres/day using Milnerton HTE as feed. Operating conditions were slightly altered from the first tests (besides the alteration required specifically to cater for the higher plant throughput) in order (i) to raise the waste brine concentration, and thereby increase the water recovery, and (ii) improve the cation regeneration by using a greater excess of acid.

In Table 5.9, the flow and average results obtained from an analysis of the plant discharge streams during a week of steady continuous operation on the Milnerton HTE water of Table 5.3 are presented. The results are discussed below.

TABLE 5.9

Composition of CCIX plant discharge streams

Feed: Milnerton HTE Flow: 5 000 ℓ/day

Stream	Flow (ℓ/day)	Component Concentration (mg/ℓ) Na	Ca	Mg	NH_4-N	Cl	SO_4	NO_3-N	COD	TDIS
Product	4650	26	0	0	33	70	0	4	20	156
Brine	250	5900	377	476	1800	9000	3270	438	1178	23300
AN	120	300	2000	1300	10400	50	0	29000	-	145450

5.3121 Product water: The product water TDIS shows a 250% increase when compared with the figures in Table 5.4, due to higher levels of the univalent ions Na, NH_4, Cl, NO_3. The large increase in anion content can, to a certain measure, be discounted, for these ions have increased as a result of the cation increase and the nonexistent 'salt-splitting' properties of the anion resin.

The TDIS increase is, however, not unexpected for the plant had to work 'harder' with the higher flow rate. This meant that contact times within column stages were reduced and thus stage efficiencies were reduced. Since the actual number of stages in each of the columns was not increased to compensate for the reduced efficiencies, higher TDIS levels had to follow.

The dissolved salt level of the water produced by the plant is well within potable water salinity (cf. Table 1.1) at 156 mg/ℓ (Cape Town domestic water supply is approximately 120 mg/ℓ) but the NH_4-N content at 33 mg/ℓ is unacceptably high. Despite the higher plant throughput the average COD reduction achieved has remained almost constant with the product water containing an average 20 mg/ℓ.

5.3122 Waste brine: The previous NH_4Cl flow malfunction was corrected and meant that the total flow of the anion regeneration product entered the NH_4/Na column. Consequently, column C2 had a greater excess of NH_4 ions which meant: (i) a higher level of NH_4-N in the brine discharge; (ii) a slightly higher stream TDIS due to the higher NH_4Cl volume and thus a proportionately lower dilution by the C2 wash water; (iii) a more efficient stripping of Na, Ca and Mg from the loaded cation resin and higher levels of these components in the discharge; when the results of Tables 5.9 and 5.5 are compared.

5.3123 Ammonium nitrate: The composition of the AN stream reflects the greater conversion achieved in the C2 column exchange, for although the concentration is lower when compared with Table 5.6, the ammonia and nitrate constitute 97,8% of the stream as opposed to the previous 91,4%. This is primarily due to a reduction in the Ca, Mg, Na from a combined 8,3% to 0,9% on a mass basis. Because of the slight excess of acid employed in these tests, the ammonia content of the stream is also marginally down from 11,1% to 9,2%. The AN content of the stream is thus 41% instead of the previous 49% and the free nitric acid rises to 56,8% from 42,1%.

5.3124 Mass balance: A mass balance on the results in Table 5.9 highlights the following points: (i) the water recovery at the higher flow rate was 1% higher at 93% largely due to a slightly reduced waste brine stream flow; (ii) the total recovery of NH_4-N in the plant was 67% and the total NO_3-N recovery was 99,5%. Together, the total recovery of regenerant nitrogen

in the AN stream represents 88% of the nitrogen feed; (iii) the efficiencies of the high concentration anion and cation regeneration and NH_4/Na columns were not affected to the same extent with the higher feed flow, for, these columns operate at bed expansions 50 to 100% lower than the load columns. From the data in Chapter 4, it is seen that at low bed expansions, contact times are long and that the kinetic curves, from which the stage efficiencies can be calculated, have asymtotes at high contact times. Consequently, the change in flow resulted in the cation load contact time being reduced from 1,0 to 0,75 minutes and the cation regeneration contact time from 1,37 to 1,30 minutes. The relative stage efficiency changes were 73% to 65% and 86% to 85%. The stage efficiency comparison shows why the product water composition altered significantly while the 'other' stream compositions varied very little.

5.313 Tests conducted on a modified flowsheet: The operation of the pilot plant on Milnerton HTE at the two tested flow rates has proved that the CCIX system can provide a combined desalination and tertiary treatment. The one area of operation which still needed improvement, other than the concentration of the brine and AN discharge streams, was the nitorgen level in the product water. With the present plant flowsheet (Figure 5.1), the nitrogen level would be lowered by (i) improving the anion resin washing, and (ii) increasing the level of cation resin regeneration, both of which can be achieved by increasing the number of stages in which these two operations are conducted. Improvement could also be effected by (i) changing the equilibria of the exchange and sorption reactions involved, or (ii) by removing the ammonia in a subsidiary exchange reaction.

In order to test whether nitrogen level reduction could be achieved the following flowsheet adjustment were made and tested.

5.3131 Acidic anion resin wash: In Figure 5.2, a flowsheet modification is shown which uses the cation product stream as wash solution instead of the product water stream as originally outlined in Figure 5.1. The purpose of this change is to provide an acidic wash to the anion column in order to aid the organic-ammonia hydrolysis reaction by lowering the pH within the wash section of A2 and thereby effectively altering the ammonia

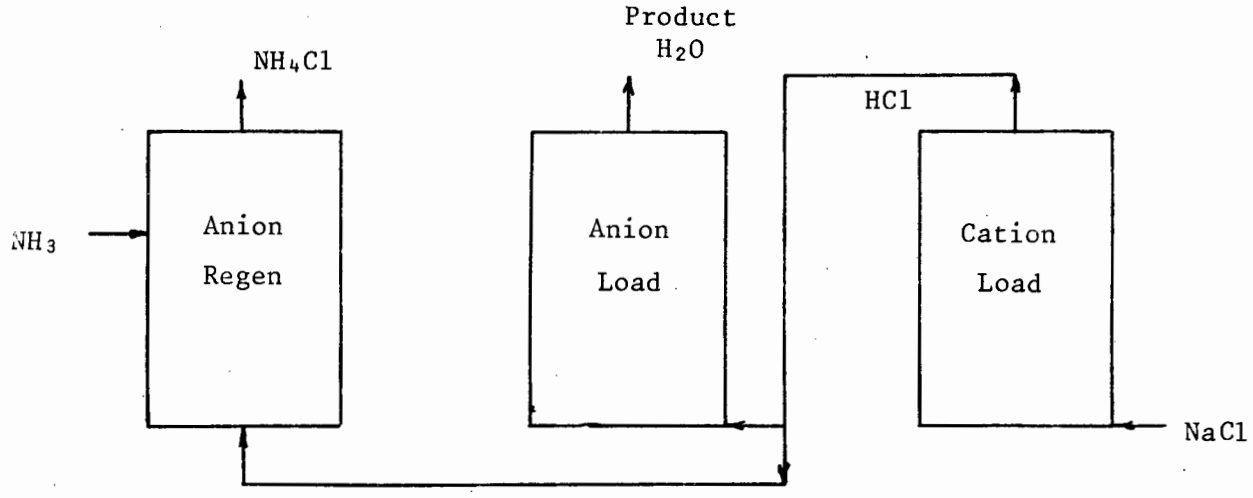

FIGURE 5.2

CCIX plant flowsheet with acidic anion wash

desorption equilibrium. The HCl content of the new wash stream together with the volume required to achieve resin washing would result in a 10% loading of the anion resin, if no NH_4Cl formation occurs. This level of anion loading, coupled with the very favourable equilibrium of the anion load reaction (Figure 4.14) means that, provided the anion resin flow is adjusted to compensate for the percentage of loaded resin, very little change in the chloride level of the product water stream will occur.

Table 5.10 compares the results achieved in the previous tests at the 5 000 litre/day flow and those achieved with the acidic anion wash. With product water as the wash stream, the results show that 61% of the 33 mg/ℓ NH_4-N comes from inefficient anion washing. The results using the acidic wash show that the NH_4-N level has been reduced to 13 mg/ℓ of which 8% now comes from the anion resin. This improvement has been achieved without altering the flow conditions, and shows how, by an effective equilibrium change, the wash has been improved.

The major portion of the remaining NH_4-N in the product stream is now due to leakage from the cation resin because of incomplete resin stripping in the regeneration column.

TABLE 5.10

Results of CCIX plant operation with acidic anion wash

Anion Wash	Stream	Concentration (mg/ℓ) Na	Ca	Mg	NH_4-N	Cl	SO_4	NO_3-N	COD
Product Water	Cation load*	26	0	0	13	528	188	24	82
	Product water	26	0	0	33	70	0	4	20
Cation Load	Cation load*	17	0	0	12	528	188	16	84
	Product water	14	0	0	13	31	0	2	16

* The stream leaving the cation load column.

5.3132 Product water recycle: Because it would necessitate an even larger excess of nitric acid to improve the cation regeneration in the fixed number of stages available in C3, the flowsheet of Figure 5.3 was devised and tested. This adjustment incorporates a product water recycle stream. As the cation resin is 69% loaded with Na ions and as the NH_4/Na exchange is favourable (cf. Figure 4.12) by incorporating the product water recycle ammonium ions present in the product water can now be exchanged for Na ions on the loaded cation resin. In this manner, the ammonia level in the water leaving the plant can be altered by varying the recycle proportion. Further, it may even be economically advantageous to reduce the degree of cation resin regeneration and then 'pick-up' the ammonium ions through the recycle flow exchange.

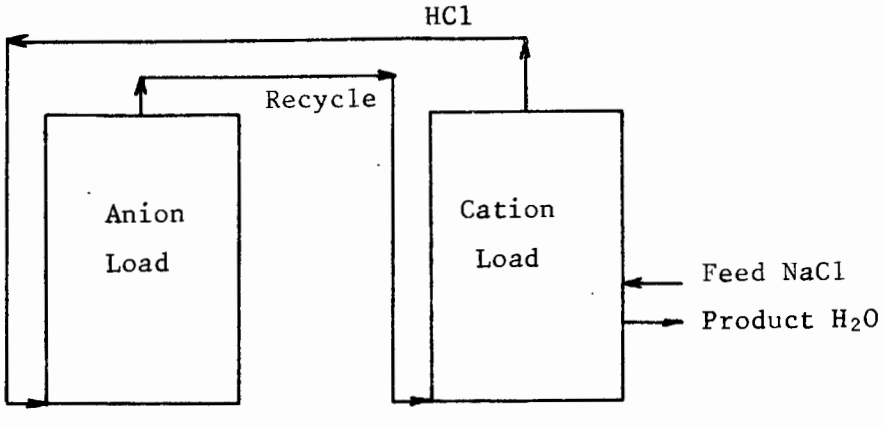

FIGURE 5.3

CCIX flowsheet with product recycle

5.32 Operation on Athlone waters

Two separate test phases were conducted on Athlone sewage plant water. For the first phase, Athlone HTE was treated in a physico-chemical (PC) tertiary treatment plant and the discharge from the PC plant used as feed to the CCIX plant. This pretreatment in a PC plant was conducted as it was felt that the IX process would be unable to treat a water with the very high COD present in Athlone HTE (cf. Table 5.3). Following the treatment of the PC plant water, Athlone HTE was in fact tested in the IX process in order to actually verify whether the IX process was able to perform a tertiary treatment and desalination on a water with a high organic loading. The results of the two test phases are reported below.

5.321 Treatment of Athlone PC plant water: This water, as previously mentioned, has been filtered, flocculated, dosed with lime and stripped of ammonia. The average water composition fed to the IX plant is recorded in Table 5.3. Because the TDIS of this feed was low (610 mg/ℓ) when compared with the Milnerton water (1 280 mg/ℓ), the CCIX plant conditions were set to accept a flow of 6 000 litres/day and the flowsheet altered back to that presented in Figure 5.1 (i.e. without recycle or acid wash). The only other alteration made to the IX plant conditions, was the raising of the concentration in the cation regeneration column in order to facilitate the recovery of a high concentration AN solution.

5.3211 Discussion of results: Table 5.12 presents the average flows and compositions of the feed water and discharge streams during a period of steady state operation in the CCIX plant.

TABLE 5.12

Average results during the treatment of Athlone PC plant water in the CCIX plant

Stream	Flow (ℓ/day)	Concentration (mg/ℓ) Na	Ca	Mg	NH_4-N	Cl	SO_4	NO_3-N	COD	TDIS
Feed	6000	148	76	6	1	211	105	14	27	609
Product	5800	5	0	0	17	23	0	3	13	51
Brine	110	7050	1150	220	1190	10300	4140	-	920	24390
AN	40	2170	11460	760	21500	-	-	44700	-	240000

On Athlone PC plant feed, the CCIX plant was able to effect a 97% recovery of water. This high recovery is due to the lower resin flow rate required to treat this lower concentration water. With a reduction in resin flow comes a simultaneous reduction in wash water and regenerant flows and thus a greater saving of product water, hence the higher recovery.

With the product water recycle removed from the flowsheet, the ammonia level of the treated water is once again high at 17 mg/ℓ. The stream TDIS at 51 mg/ℓ shows an effective 92% desalination which, at the high feed flow rate of 6 000 litres/day shows the flexibility of the CCIX process to adapt to alternative conditions. Although the load column contact times were significantly reduced by the flow increase, the high desalination level was achieved by converting the cation load column recycle and wash stages into feed water exchange stages and adding an extra stage to the anion load column. In this manner, the overall load column efficiencies were retained.

The composition and concentration of the waste brine discharge stream is not very different from that achieved on the Milnerton water. This result was not unexpected, for the composition of this stream reflects the feed composition while the concentration depends upon plant operating conditions. At a TDIS level of 24 gm/ℓ, the brine stream shows a 40-fold concentration of feed water TDIS while the discharge volume constitutes only 2% of plant discharge.

The nitric acid feed concentration was set to 3,0N for this investigation, equal to the concentration used in the resin life tests. The NO_3-N level in Table 5.12 reflects this concentration setting. At high concentrations, the stripping of divalent cations is facilitated and in fact satisfactory regeneration was achieved with a 40% excess of acid. The purity of the AN stream, as before, is dependent upon the NH_4/Na exchange. The total volume of the AN stream discharged in these tests, 40 litres/day, was <1% of the plant throughput. A stream analysis yielded the following composition: 51% NH_4NO_3, a free HNO_3 content of 43%, 5% Ca and 1% Na. At 240 gms/litre the TDIS is probably the highest that can be achieved from the cation regeneration reaction without damaging the resin through osmotic shock. The total nitrogen content of the AN flow represents a 92% recovery of regenerant feed nitrogen. Here again, the major loss is ammonia in the waste brine stream.

5.322 Treatment of Athlone HTE water: Athlone HTE water was used as CCIX feed only to determine whether, on this high COD water, the IX system could simultaneously remove both organic and inorganic water constituents. The feed water and product water compositions during plant operation at a flow of 6 000 litres/day are presented in Table 5.13. No attempt was made to determine what percentage of either chemicals or water were recovered or what waste brine concentration was achieved, during these tests.

TABLE 5.13

Average results of pilot plant treatment of Athlone HTE

Stream	Concentration (mg/ℓ)							
	Na	Ca	Mg	NH_4-N	Cl	SO_4	NO_3-N	COD
Feed	120	45	18	13	205	118	21	120-210
Product	0	0	0	11	7	0	0	50-90

In an attempt to reduce the product water COD levels, large resin and solution excesses (equivalent to changing the stoichiometric ratios and thus the operating line slopes) were used in the respective load and regeneration columns. Consequently, effectively complete desalination was achieved, other than the low levels of NH_4Cl in the product water. Despite the adjustments to the plant conditions, COD levels of <50 mg/ℓ could not be consistently achieved. During this phase of operation up to 40% of actual COD reduction occurred on the cation resin (in contrast to the <10% on Milnerton HTE). This phenomenon duplicates the resin test results of section 4.222.

Further, the anion resin changed from dark brown to black during the Athlone HTE loading, and for an extended period after Athlone HTE feed had been stopped, organic material continued to be stripped from the anion resin.

A comparison of the treatment results of Athlone HTE and Milnerton HTE leads to the conclusion that the CCIX plant is capable of performing a combined desalination and tertiary treatment provided the feed water COD is <90 mg/ℓ, otherwise only desalination can be achieved.

CHAPTER 6

DESIGN AND COSTING OF AN ION EXCHANGE TERTIARY TREATMENT PLANT

6.1 BACKGROUND

One of the objectives of this work has been to develop a process which performs the required desalination at the lowest possible cost. In order to determine, on the basis of the design criteria and experimental work already presented, the cost of such an ion exchange tertiary treatment process, a design and economic evaluation is presented in this chapter.

The objective of this design and cost study is to evaluate the inter-relationship that the costs of equipment and chemicals may have on the operation of the ion exchange plant and in this manner, to determine critical cost areas, and to develop plant operating strategies.

As the next step in the continuation of research work on the ion exchange process will probably be on the scale of a demonstration plant rather than a full-scale plant, the design presented is based on a daily water flow of one megalitre. To a certain extent, this does not allow the full effect that possible economies of scale would normally have for plants of this type. However, this is offset by not accounting for likely operating labour or manpower charges involved in running the plant, for it is assumed that, at the level of one megalitre per day, such a plant would be annexed to an existing water treatment facility.

Details of the costs of chemicals, equipment and services necessary for this economic evaluation were obtained from local suppliers of the required commodities, and are in terms of prices ruling at the present time. The evaluation presented highlights the effect of the change in cost of the major running cost item, chemicals, on the design and operation of the IX plant. Should the information presented be required for projections into the future, care must be exercised in the degree of emphasis placed on the conclusions drawn, for, as is shown in the study, price escalations can radically alter the overall evaluation.

6.2 BASIS OF DESIGN AND COSTING

As mentioned above, all design calculations are based on a total daily feed water flow rate of 1 megalitre. However, other items used in the calculation are detailed below.

6.21 Water salinity levels

The major portion of this study is based on the desalination of the water with the composition outlined in Table 6.1, the water composition upon which most of the CCIX experimentation was conducted. However, for comparison, the costs of reducing the TDIS of a 700 mg/ℓ water to 500 mg/ℓ is also included. This situation would arise in 'other' areas of South Africa, and 200 mg/ℓ represents a typical salinity increase which occurs each time water passes through the user cycle, e.g. the Pretoria domestic water supply has a TDIS of 250 mg/ℓ while the Daspoort sewage plant discharge water has a TDIS of 450 mg/ℓ [109].

For the high salinity Table 6.1 water, a range of product water compositions are evaluated, varying between 50 mg/ℓ and 500 mg/ℓ of TDS.

TABLE 6.1

Composition of water used in cost study

Cations	Na	Ca	Mg	NH_4-N	Total
Conc. (meq/ℓ)	16,10	1,60	2,67	0,07	21,0
(mg/ℓ)	370	32	37	1,0	-
Anions	**Cl**	**SO_4**	**PO_4**	**NO_3-N**	**COD**
Conc. (meq/ℓ)	16,06	3,75	0,22	0,86	-
(mg/ℓ)	570	180	16	12	85

6.22 Capital and operating costs

Costs of the major items required for the evaluation are presented in Table 6.2. Details of each are presented below.

6.221 Capital items

(a) Columns: The capital costs of the CCIX columns were obtained from the Atomic Energy Board [110] who have constructed similar units for uranium

recovery. A scaling factor of 0,8 is used for evaluating column costs where the number of stages or diameter is different from that for the basic column.

(b) Resin: The cost of the cation and anion resins Zerolit 625 and Zerolit MPH were obtained from the local supplier on the basis of a delivery of more than two cubic metres of each. The volume of resin required varies with the CCIX plant duty and is evaluated for the various levels of salinity reduction presented.

(c) Capital: The initial cost of resin and capital was discounted over a 10 year period at an annual charge of 10% in order to place an annual value on the cost of capital.

TABLE 6.2

Cost factors used in the cost study

Item		Cost Cost
Chemicals:	Nitric Acid	R5-00/kg equiv.
	Ammonia	R2-50/kg equiv.
	Sulphuric Acid	R3-25/kg equiv.
	Lime	R1-00/kg equiv.
Columns:	1 m ϕ x 10 m	R110 000
Resin:	Cation	R2000/m^3
	Anion	R4000/m^3
Capital:		10% p.a. over 10 years

6.222 Running costs

(a) Chemicals: The annual and daily value of chemicals required was calculated from (i) the desired salinity reduction, and (ii) cost information supplied by local producers on the basis of bulk chemical delivery.

(b) Resin: In the light of test work conducted, resin life was set at three years. Running costs were consequently charged with the replacement of 34% of resin volume annually.

(c) Utilities: The cost of utility items such as power, compressed air etc. are not included in the overall costing, for they represent a cost item which is less than 0,5% of the chemical costs and consequently have no influence on the overall cost.

6.223 Recovery of regenerant chemicals: Evaluations of the optimum cost of the IX tertiary treatment plant are made on the basis of (i) recovery of as much of the regenerant chemicals as is economically feasible, (ii) no recovery of regenerant chemicals but still using HNO_3 and NH_3 to perform the regeneration, and (iii) no recovery but using lime and sulphuric acid as regenerants.

Where recovery of chemicals is practised, it is assumed that the recovery will offset the purchase price of the chemicals so that the regenerants will now cost 10, 30, 50 and 70% of their original price, depending upon the level of recovery. On the basis of these costs, the cost of desalination has been evaluated.

If no chemical recovery is envisaged, the IX flowsheet may be altered and one IX column eliminated whilst still achieving the same degree of desalination. Further, it is then no longer necessary to restrict the regenerants to being ammonia and nitric acid. Alternative acids (hydrochloric, sulphuric) and bases (caustic soda, lime) can be considered for the resin stripping duty. This alternative is included in the cost evaluation, for it is one that is likely to occur where the 'throw away' cost of an alternative acid and base is less than the nett cost of recovered chemicals.

6.23 Determination of column sizes

The method used to determine the size of a CCIX column required to perform a particular duty was based on the theory outlined in section 2.4323 and tested in Chapter 4. The technique was used in the following way for the purposes of the cost evaluation.

6.231 Number of exchange stages: For any particular column, the number of exchange stages was calculated on the basis of the desired resin and liquid compositions entering and leaving the column, the total flow of both resin and solution in the column and the stage efficiency. The computation can either be performed numerically or graphically, depending upon the equilibrium relationship.

For the purposes of this investigation, the calculation procedure of section 4.31 was computerised and the equilibrium expressions and kinetic

data, for the relevant exchanges evaluated in Chapter 4, were used. The stage efficiencies were evaluated from the particular column contact time via the particular bed expansion (e.g. Figure 4.21 and 4.22)

From the two figures it can be seen that, as bed expansion increases, stage efficiency decreases. There will then be an optimum bed expansion when the cost of increased stages (required to perform the exchange when the stage efficiency decreases with BE) for a given column diameter is counterbalanced by the increased throughput from the column. Experimentation has shown, however, that above a bed expansion of 200% unstable operation of the column occurs. This restricts the upper limit of operation.

Naturally, should a resin with a greater density be used in the CCIX column, the throughput for the same 200% bed expansion will be proportionately higher. Providing the high density resin does not have inferior kinetics, the use of such a heavy resin would result in reduced desalination costs in that smaller diameter columns would suffice for a given volumetric flow rate.

6.232 Resin volume: Together, the flow rate and bed expansion determine the column diameter. Experience on uranium CCIX plants has shown that the optimum stage height is 100 cm. This then allows the calculation of the volume of each stage.

On the basis of stage volume and bed expansion, the quantity of resin in each stage is calculated. This, together with the actual number of stages, gives the total volume of resin per column. (Appendix C gives an example of the calculation.)

When, at the end of each liquid flow cycle, 90% of the volume of the resin in each stage is 'pulled down', this volume sets the resin flow per cycle through the column. Now, for a given operating line slope, the liquid flow time is adjusted so that the required liquid equivalents are introduced between resin flow periods. If the bed expansion is high, then the resin pulldown volume is low and if the liquid concentration is high then the time required, to introduce the liquid equivalents, at the liquid flow rate necessary to achieve the high bed expansion, becomes short. Practical experience dictates that the minimum liquid flow time required to achieve resin fluidisation and prevent unstable operation is 15 minutes. This means that, for the CCIX columns operating with

solution concentrations of greater than 0,5N, the bed expansion, column diameter, liquid flow rate, and stage efficiency are fixed by the minimum flow time.

6.3 EVALUATION OF INDIVIDUAL COLUMN COSTS

A flow diagram of an IX plant with regenerant chemical recovery would be the same as that presented in Figure 5.1. Because columns are interlinked by resin and liquid flows, resin or liquid conversion within one column affects the performance of other columns within the plant. (cf. The pilot plant studies of Chapter 5.) An optimum economic design of the IX process must necessarily therefore be in terms of a global minimum cost. However, in order to assess the effect of changes in operating parameters on the costs of individual columns, and so perhaps eliminate certain variables from the global determination, the following calculations for the individual columns are presented.

6.31 Cation columns

6.311 Regeneration column: The cation resin rate through the plant used in this section of the evaluation is based on removal of all but 50 mg/ℓ of the sodium content of the water composition presented in Table 6.1. Using this resin flow rate, the effect of regenerant acid cost and degree of resin conversion on the cost of operating the cation regeneration column is evaluated.

The reaction occurring in the cation regeneration column when chemical recovery is practised is the following:

$$R - NH_4 + HNO_3 \rightarrow R - H + NH_4NO_3 \qquad (6.1)$$

6.3111 Effect of regeneration level on product water quality and costs: The resin leaving the regeneration column contacts the water at the top of the cation load column (cf. Figure 5.1). Now, the metal cation content of the water leaving the cation load column can only be as low as the level which exists in equilibrium with the resin with which it is in contact. Therefore, the degree of resin stripping in the regeneration column affects the metal cation level in the product water. Figure 6.1 shows the ammonium and sodium contents of the water (Y_{T_i}) leaving the cation load

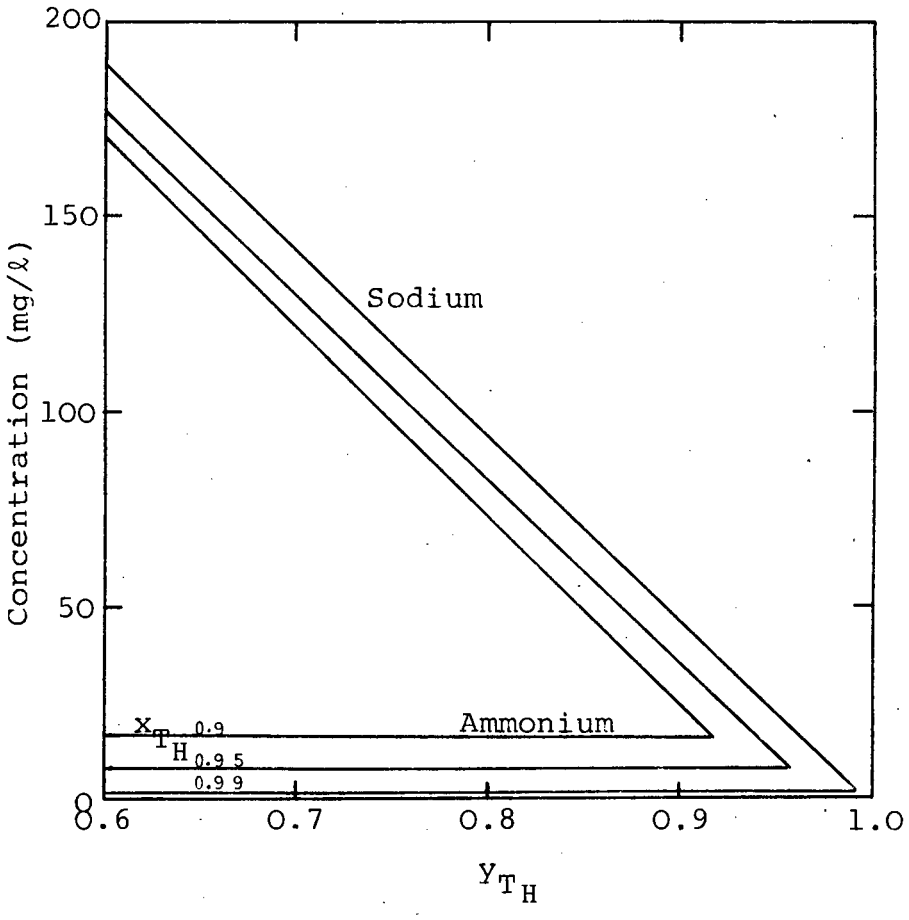

FIGURE 6.1

Composition of water from cation load column

column as a function of the hydrogen ion content of the resin (x_{T_H}) entering the cation load column (x_{T_H} = 1,0 for 100% hydrogen) and the hydrogen ion content (y_{T_H}) of the de-cationised water. The intersection of the ammonium and sodium curves indicates the liquid composition in equilibrium with the regenerated resin.

The information in Figure 6.1 indicates that if the ammonia content of the water leaving the cation load column has to be less than 10 mg/ℓ, then the hydrogen content of the regenerated resin entering the load column must be higher than 96%, i.e. (x_{T_H}>0,96). In this manner, the allowable ammonia content of the product water automatically constrains the level of resin conversion in the regeneration column when chemical recovery is practised.

The required resin conversion can be achieved by one of two modes of column operation:

(a) a large excess of acid can be employed in a limited number of column stages, or

(b) by using less acid, but a greater number of exchange stages. (An increase in contact time will have little effect on the regeneration column because of the already high (>90%) stage efficiency existing in the column due to the enforced low %BE.)

The relative cost of acid and stages determines the optimum conditions. Naturally, the optimum cost for 90% resin conversion would be expected to be lower than the optimum cost for 99% resin conversion.

In Figure 6.2, the daily cost of regenerating, at a fixed stage efficiency, fully loaded NH_4-form resin to different levels of hydrogen content is shown as a function of the excess acid required to achieve the conversion. As the acid excess is reduced, so more column stages are required to achieve a given conversion and thus an optimum for each regeneration level (%H on the resin) is determined from a summation of the acid cost, the resin replacement costs and the discounted column plus resin capital costs.

Looking at the resin plus column cost curves of Figure 6.2 it is seen that it costs progressively more, under the same excess acid conditions, to achieve higher levels of resin conversion. This is reflected in the total cost curves which show a minimum cost which steadily increases with resin conversion and simultaneously moves to higher excess acid levels in an attempt to offset the column costs.

6.3112 Effect of acid cost on regeneration cost: In order to assess the effect of the relative cost of acid and column plus resin, a series of total cost curves for 95% resin conversion were calculated and are presented in Figure 6.3.

Naturally, as acid cost decreases so overall regeneration costs decrease. However, as the cost of acid decreases so it has less influence on the total cost curves in Figure 6.3, and the curves flatten indicating that ever larger acid excesses may be used to achieve resin conversion. The opposite occurs

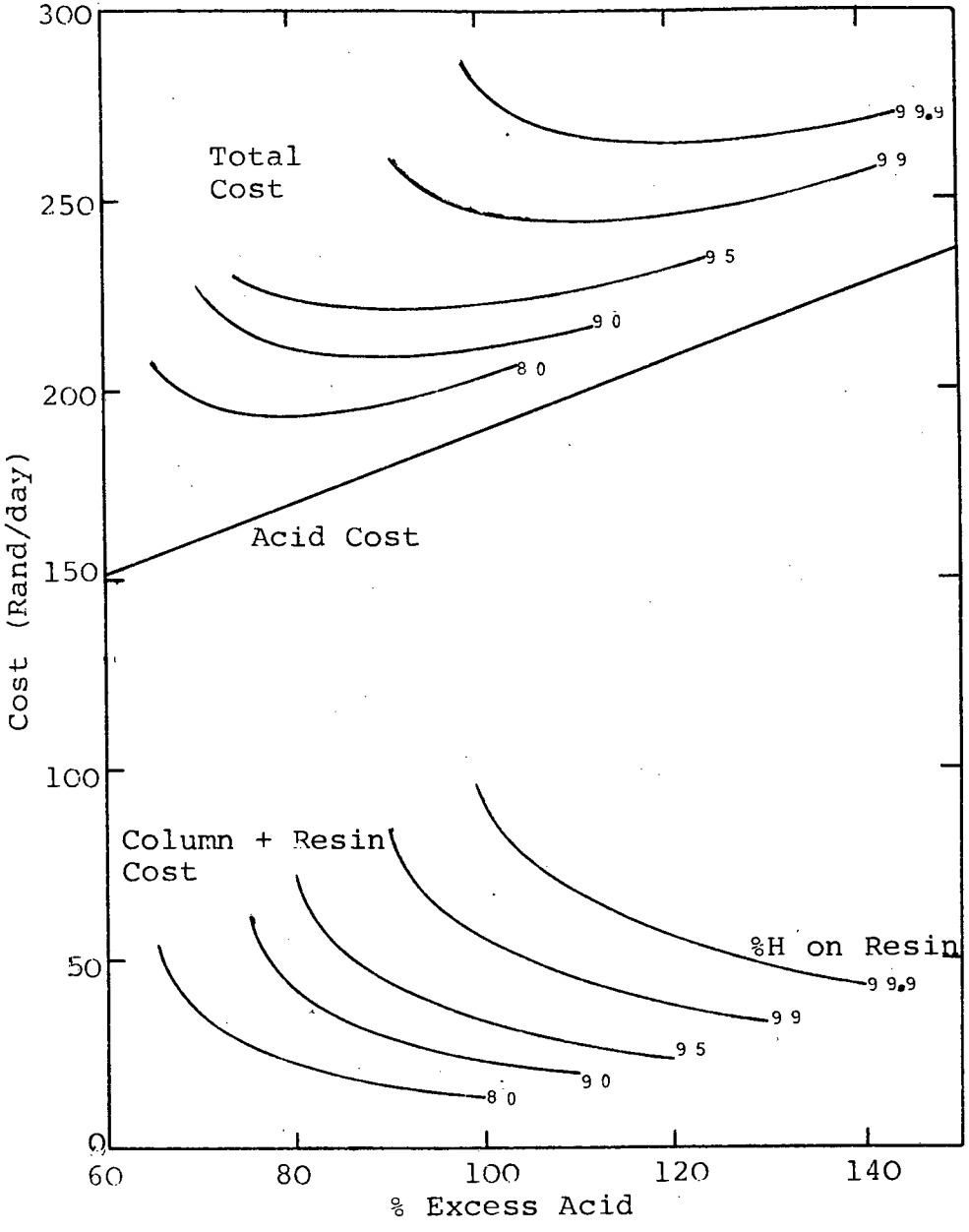

FIGURE 6.2

Change in cation regeneration costs with degree of resin regeneration

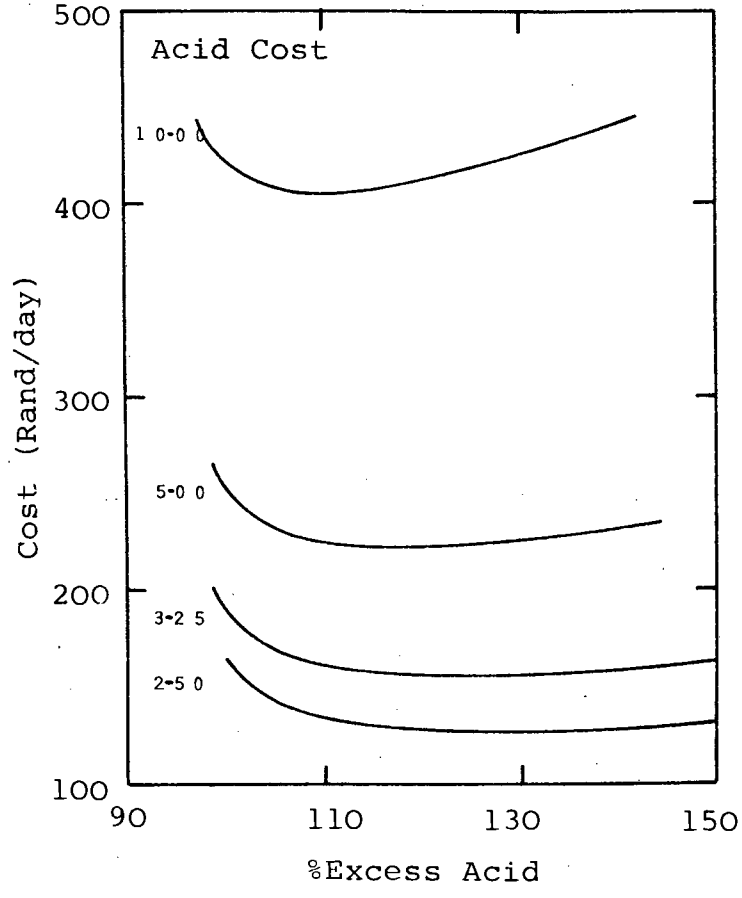

FIGURE 6.3

Effect of acid cost on the cost of the cation regeneration column

at high acid cost, and the total cost curve has a more definite minimum, with the minimum cost moving towards a lower excess acid optimum with increasing acid cost. The acid cost is now becoming the over-riding factor.

6.312 Ammonium-sodium exchange column: The ammonium-sodium (AS) exchange column is used only if regenerant chemical recovery is practised. In the column, spent anion regenerant is contacted with loaded cation resin and the following exchange occurs:

$$R - Na + NH_4^+ \rightarrow R - NH_4 + Na^+ \qquad (6.2)$$

The resin leaving the bottom of this column enters the cation regeneration column.

The purpose of the ammonium-sodium column is to recover the ammonium ions present in the spent anion regenerant and so facilitate the formation of ammonium nitrate in the cation regeneration column. The cost, therefore, of operating the AS column must be counterbalanced with the value of ammonia recovered.

The two factors in operating the AS column which together will lead to lowered operating costs are: (i) to recover all the ammonia entering the column, and (ii) to convert fully the resin leaving the column. Each of these alternatives can be achieved at the expense of the other so that an optimum degree of recovery and resin conversion must be determined. This is calculated by imposing a penalty on the operation of the AS column for ammonia that is not recovered and resin that is not converted equal to the value of ammonia which is 'lost' from either column or resin.

6.3121 Effect of resin conversion: In Figure 6.4, the daily costs of the column plus resin and the 'lost' ammonia are presented for various degrees of resin conversion to ammonia form and varying levels of ammonia in the waste brine leaving the column. From these two costs, a summation produces the total cost of operating the AS column on a daily basis.

The 'loss of ammonia' cost curves (straight lines in Figure 6.4) show the total value of ammonia lost from the system when the ammonia content, on an equivalent basis, of the liquid stream leaving the column is respectively 4, 8, 12 and 20% and the degree of conversion (also on an equivalent basis)

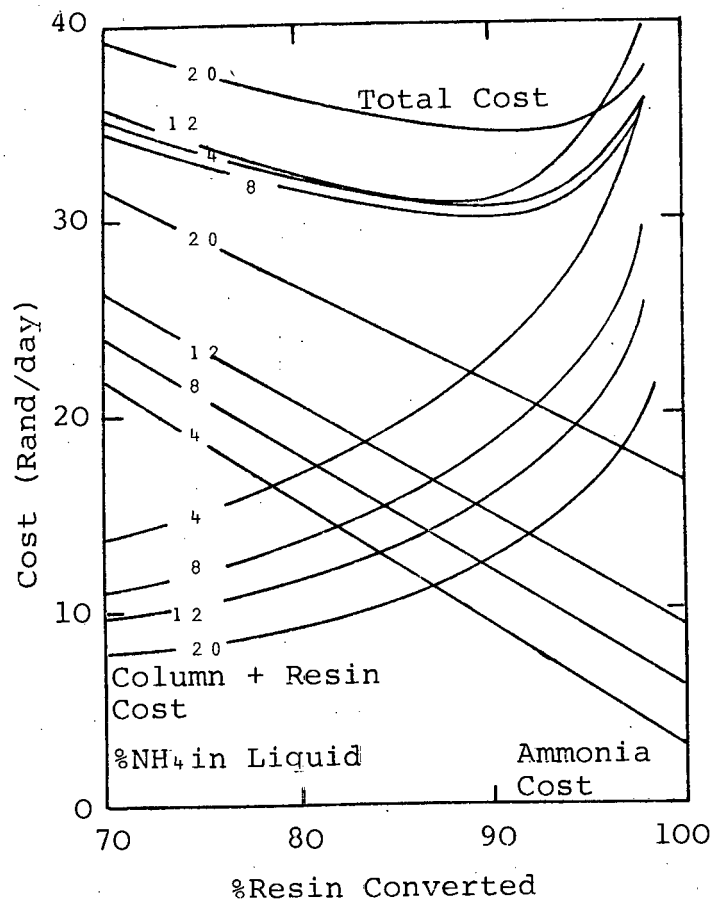

FIGURE 6.4

Costs of ammonium sodium exchange column

of the resin leaving the column is given by the abscissa. For a given 'waste brine' ammonia level, the cost of 'lost' ammonia decreases with increasing resin conversion and conversely, for a given resin conversion, the lost ammonia cost decreases with decreasing ammonia content in the 'waste brine' stream.

The discounted capital cost of column plus resin varies, as anticipated, with the degree of resin conversion. More stages are required for high conversion and consequently the cost increases. However, the cost of column plus resin also increases when resin conversion is held constant but ammonia content of the waste brine is decreased. This is shown by the column plus resin cost curves of Figure 6.4.

Now summing the two AS column costs produces the total cost curves in Figure 6.4. Initially, the minimum cost of operating the AS column decreases with decreasing ammonia levels in the waste brine and the curve minimum occurs at approximately the same resin conversion level of 93%. However, a point is reached at a certain waste brine ammonia level where the total cost minimum moves 'back up' and also to lower resin conversion. This is due to the cost of column plus resin becoming the dominant cost in the summation as opposed to the cost of lost ammonia. There exists, therefore, at all resin plus column and ammonia costs, an optimum set of conditions for operating the AS column in order to achieve an overall minimum operating cost.

6.3122 Effect of change in ammonia cost: Figure 6.4 showed the effect of change in ammonia recovery on the cost of operating the AS column. Using the procedure adopted in Figure 6.4, the total cost of the AS column on a daily basis can be computed for varying levels of total ammonia recovery, i.e. the percentage of ammonia entering the AS column which leaves with the loaded resin. The results of such a calculation are presented in Figure 6.5 for three ammonia cost levels.

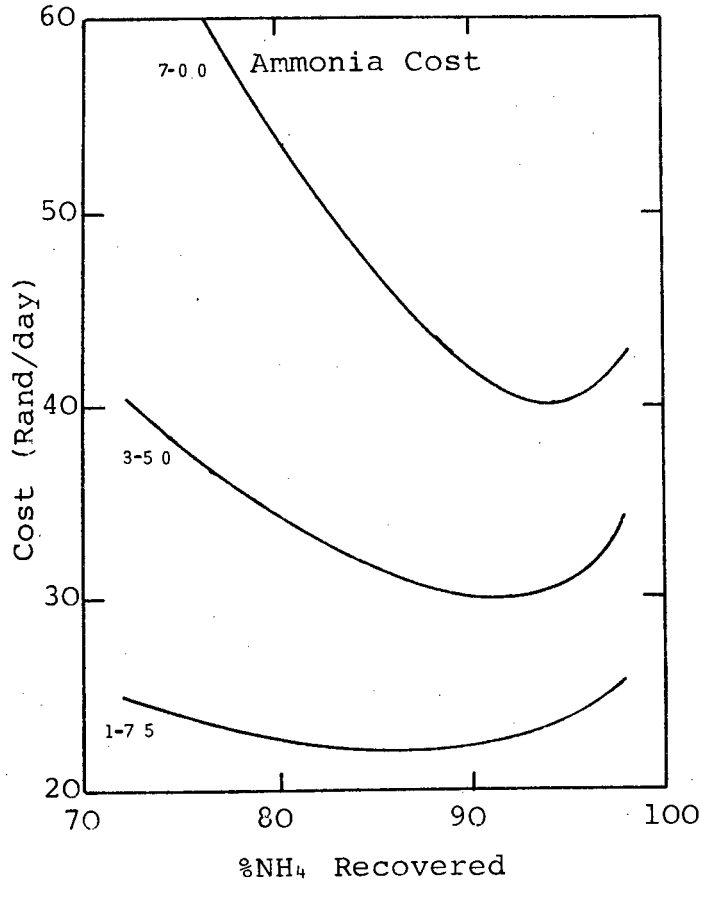

FIGURE 6.5

Variation of ammonium sodium column costs with cost of ammonia

As ammonia cost increases, so the total cost of running the AS column increases, but so also does the optimum ammonia recovery level. For low ammonia cost, a flat total cost curve is computed indicating that the degree of ammonia recovery is not critical because column plus resin costs dominate. At high ammonia cost, a very obvious cost minimum exists at a particular ammonia recovery level. The three curves together in Figure 6.5 indicate that optimum operation of the AS column is entirely dependent upon the relative costs of chemicals and equipment, and that operation has to be accurately controlled at set conditions to achieve minimum cost when the cost of chemicals increases significantly.

6.313 Cation load column: The cation load column receives regenerated resin at the top and saline water at the bottom and contacts these two phases together so that the following reaction occurs:

$$R - H + Na^{+} \rightarrow R - Na + H^{+} \qquad (6.3)$$

Unlike the AS and cation regeneration columns, the solution concentration in the load column is low and there is therefore no need to limit the liquid flow time to fifteen minutes as there is in the other two columns. Instead, the restriction imposed on the operation of the load column is based on the degree of resin fluidisation which may be allowed, and an upper limit (based on practical experience) of a 200% bed expansion is set. Consequently, because the allowable linear velocity through the column (and hence the fluidisation and liquid contact time) can be altered, a further degree of freedom is introduced in the optimisation of the load column - the stage efficiency.

When regenerant chemical recovery is practised, the maximum ammonia content of the water leaving the cation load column dictates the hydrogen content of the resin entering the load column (cf. section 6.311). When this restriction does not apply, then it is the allowable sodium or TDIS level of the water that dictates the degree of resin regeneration. As the allowable sodium level is generally an order of magnitude or more higher than the ammonium ion level, this can have an important bearing on the cost of regenerating cation resin (cf. Figure 6.2). Any analysis of the load column must necessarily therefore include the cost of producing the regenerated resin for load column duty.

6.3131 Effect of resin bed expansion: In section 4.3122 a method for determining the stage efficiency for various column operating conditions was outlined.

In order to determine the optimum cost of desalination for various stage efficiencies, the following points must be considered:

(i) stage efficiency decreases with increasing bed expansion as a consequence of the resin kinetics and the change in contact time within the stage. This means that the number of stages and therefore the cost of the desalination increases with bed expansion;

(ii) in order to achieve a higher bed expansion, the throughput through a given diameter column must increase. The unit cost of water therefore decreases with increasing bed expansion. An optimum cost for the load column depends on the relative change in costs of increased stages and throughput.

Figure 6.6 presents two cost versus bed expansion curves for the cation load column removing 70% and 90% (on an equivalent basis) of feed water cations. The curves in Figure 6.6 show that cost varies inversely with bed

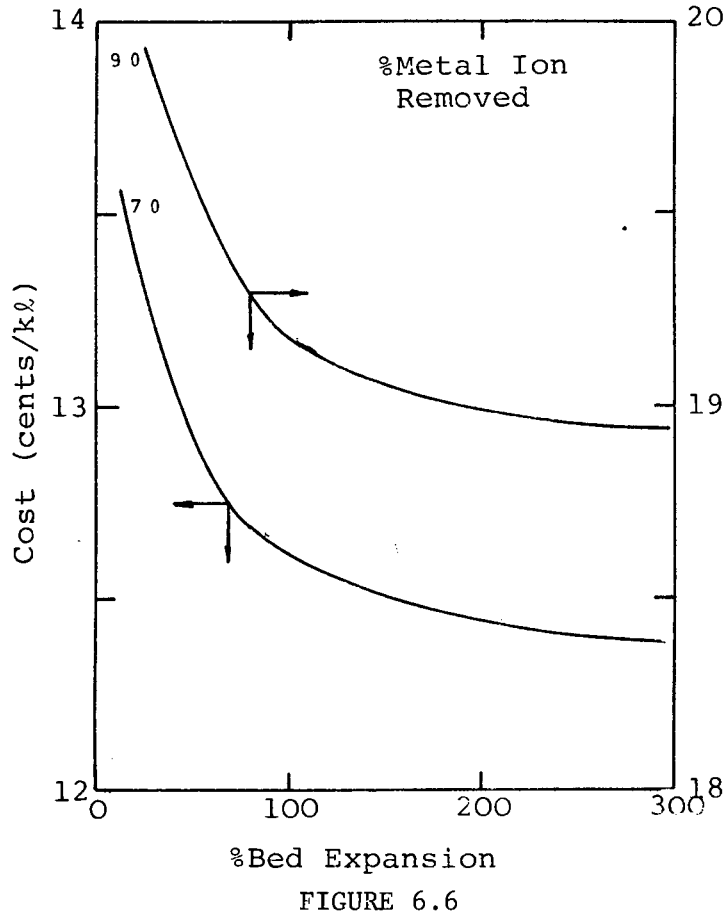

FIGURE 6.6

Effect of bed expansion on cation load column costs

expansion, and up to 300% BE does not pass through a minimum. The reason for this behaviour is the relatively small change in contact time with BE (cf. Figure 4.22) at high bed expansions, and the small rate change of the kinetic curve (cf. Figure 4.21) at high contact times. For the particular cation resin, Zerolit 625, the conclusion to be drawn from the curves in Figure 6.6, is that the column must be operated at the highest possible bed expansion in order to produce lowest costs.

Should the resin kinetics, for some reason, decrease significantly then the curves of Figure 6.6 may well pass through a minimum at a BE of less than 200%. Any increase in resin kinetics will have no effect on the economically best operating conditions - a bed expansion of 200%.

The resin property that can cause a significant change in operating costs, is the density. If the density increases by 10%, with the kinetics and cost of resin remaining the same, then, for a 200% BE the throughput would be 100% higher and the stage efficiency would be 30% lower. The result would be a resin plus column cost increase of 40%, but a throughput increase of 100%, giving a nett 30% decrease in the cost of water from the cation load column.

6.3132 Effect of treated water quality: The cation content of the water leaving a load column operated at maximum stable BE (constant stage efficiency) can be varied by:

(a) changing the number of stages in the column, or
(b) changing the relative ratio of resin to liquid which contact in the column, or
(c) varying the degree of regeneration of the resin which enters the load column.

The third possibility is, however, governed by the maximum permissible cation content of the treated water - Figure 6.1 outlines the effect of changing the resin regeneration.

Figure 6.7 compares the costs of producing various treated water qualities in the cation load column with the degree of resin regeneration as a parameter. The obvious conclusion to be drawn from the curves, is that costs decrease with degree of cation removal irrespective of resin regeneration

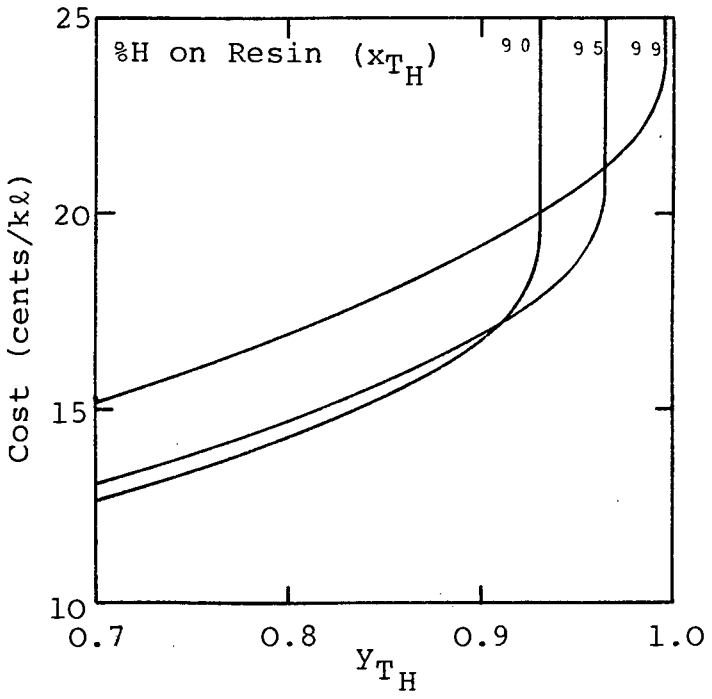

FIGURE 6.7

Effect of treated water quality on cation load column costs

level. However, should a treated water metal cation content of 20% (on an equivalent basis Y_{T_H} = 0,8) be required, it is marginally cheaper to produce this quality with 90% rather than 95% regenerated resin. The same quality could also be produced with 80% regenerated resin at a still lower cost.

If a water quality with 5% metal cations (y_{T_H} = 0,95) is required, the curves show that the 95% regenerated resin is cheapest. This quality cannot be produced with the 90% resin because of equilibrium considerations, just as much as a 2% water cannot be produced with the 95% resin. The conclusion to be drawn from the cost comparison of Figure 6.7 is that there exists, for each particular water quality an optimum set of column operating conditions for both the cation load and regeneration columns which will produce treated water at the lowest cost and further, that these conditions are dependent on both resin properties and the relative cost of chemicals and equipment.

6.32 Anion column costs

6.321 Load column: The anion load column containing a weak base resin is only capable of removing anions that are associated with hydrogen ions. Because of this resin property, treated water quality is controlled by the degree of metal cation removal in the cation load column and the anion load column removes only mineral acidity according to the following reaction:

$$R' - N + HCl \rightarrow R' - NHCl \qquad (6.4)$$

The affinity of the anion resin for the mineral acids is extremely high, cf. Figure 4.14, and consequently, it is possible to achieve the required degree of anion removal in one resin-liquid contact stage - because of the high selectivity, a countercurrent contact is not necessary.

The anion resin kinetics, in contrast, are relatively slow, cf. Figure 4.19, and this fact, together with the low density of the resin means that stage efficiency changes significantly with bed expansion. Extra column stages are required therefore, not for equilibrium contact purposes, but for greater resin-liquid contact time.

6.3211 Effect of stage efficiency: Figure 6.8 compares the unit cost of water from the anion load column at various resin bed expansions. As anticipated, in view of both the resin kinetics and resin density, the cost

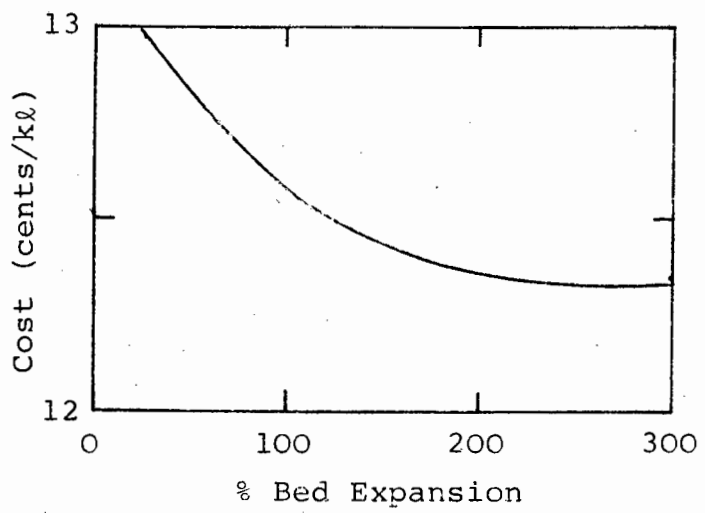

FIGURE 6.8

Effect of bed expansion on costs of the anion load exchange

of removing anions from the water decreases with increasing bed expansion. Although the kinetics are extremely slow, the low resin density means that throughput has to be low (and hence contact time high) for a given bed expansion and this then compensates for the kinetics.

In order to effect a reduction in the cost of operating the anion load column, both throughput and resin kinetics would have to be improved simultaneously. Increasing only the exchange rate would simply enforce the conclusion that bed expansion must be as high as possible for minimum cost, while a change in resin density with the same kinetics would move the optimum bed expansion to a value of less than 200%. A heavier resin with a smaller bead size distribution would achieve a lowering of anion load costs.

6.322 Regeneration column: The anion regeneration column receives loaded resin which is then countercurrently stripped with a base, typically ammonia solution, according to the reaction

$$R' - NHCl + NH_3 \rightarrow R' - N + NH_4Cl \qquad (6.5)$$

Provided a slight excess of ammonium ions remain present throughout the reaction, complete resin stripping is achieved. The equilibrium is very favourable and the curve has a shape similar to the load exchange (cf. Figure 4.15) but the kinetics of equation (6.5) are much faster than the anion load exchange. Because of the low anion resin density, the fifteen minutes liquid flow time limitation which is imposed for stable column operation allows a bed expansion of 80% in the anion regeneration column. This flexibility of bed expansion together with the kinetics means that a possible optimum BE for lowest cost exists.

A determination of the costs of the anion regeneration column at various bed expansions is presented in Figure 6.9. Like all the other columns where this comparison has so far been made, lowest cost occurs at the highest possible BE and throughput.

The flow diagram of Figure 5.1 shows that ammonia is introduced near the top of the anion regeneration column, with the bottom stages of the column being utilised as wash stages. The number of wash stages is, in fact, critical for the stripped anion resin contacts the final product water

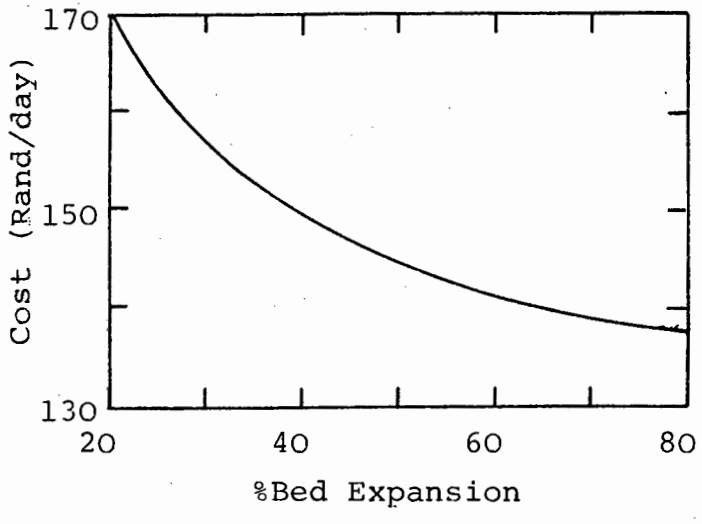

FIGURE 6.9

Effect of bed expansion on cost of anion regeneration

when it enters the anion load column. Any residual ammonia which remains in the anion resin would then contaminate the product water. Therefore, 80% of the countercurrent stages in the anion regeneration column serve to wash resin rather than strip resin, and it is the wash stages which are the major consideration in both the design and cost of this column.

6.4 DETERMINATION OF PLANT SIZE, CAPITAL AND RUNNING COSTS

Using the optimum conditions for each column determined in the previous sections, the size and costs of a plant to treat one million litres a day has been evaluated. The determination has been carried out for the following levels of desalination:

(i) based on a feed water with the composition of Table 6.1
   (a) product water with salinity levels of 50, 100, 200, 300, 400 and 500 mg/ℓ respectively
   (b) each salinity level with and without regenerant chemical recovery;

(ii) removal of 200 mg/ℓ of TDIS from a water containing 700 mg/ℓ of TDIS (equivalent to the mineral load increase which occurs with each water pass in the Pretoria area).

6.41 Overall cost of desalination and tertiary treatment

For each of the conditions mentioned above, the total optimum cost of treating a kilolitre of water has been calculated, and is presented in Figure 6.10. As anticipated, the water treatment costs increase as the treated water TDIS decreases. In each case presented, the cost varies almost linearly with product water TDIS and as the degree of chemical recovery increases, so a family of parallel curves is generated. When chemical recovery is not practised, the slope of the cost curve changes, so that for certain product water qualities, the lowest desalination cost occurs with this mode of plant operation.

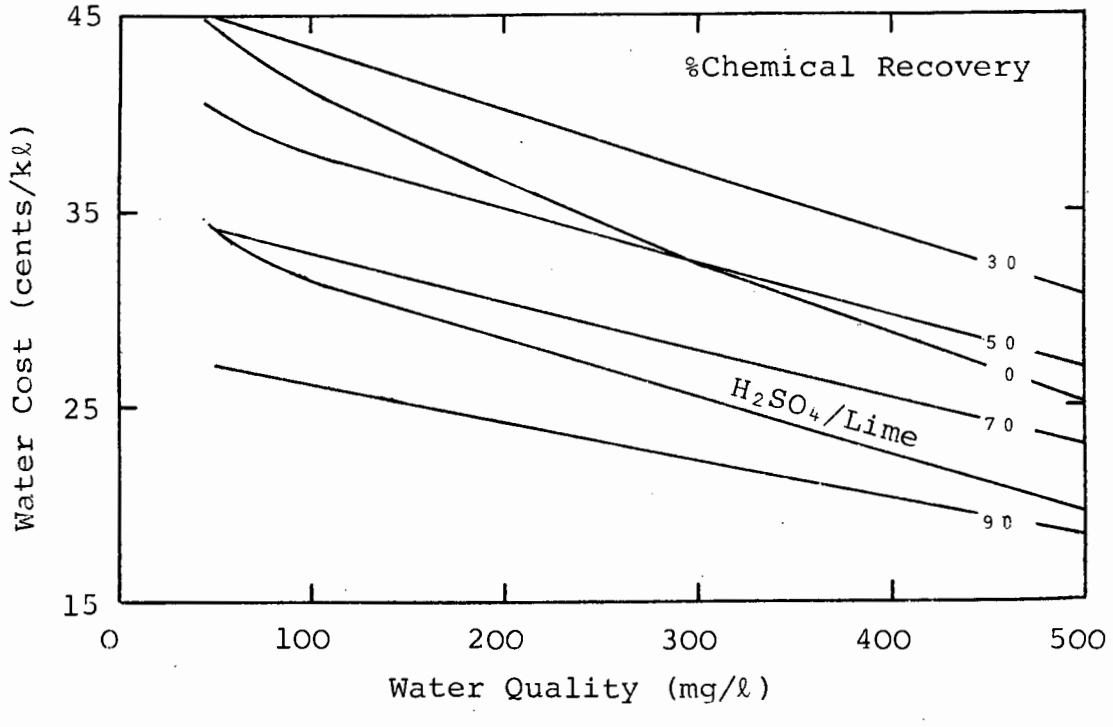

FIGURE 6.10

Total cost curves for an ion exchange tertiary treatment plant

From Figure 6.10, it is seen that, under all the conditions considered, the desalination cost with 90% chemical recovery is the lowest. Interpolating between the 90% and 70% recovery curves leads to the conclusion that the H_2SO_4/lime regeneration system is only more expensive than 80% chemical recovery at a product water TDIS of less than 250 mg/ℓ. Similarly, for a 500 mg/ℓ TDIS water the chemical recovery needs to be greater than 60% to give a lower desalination cost than that achieved with the ammonia/nitric acid system without

recovery. At 300 mg/ℓ TDIS, the chemical recovery can be reduced to 50% and the cost will still be lower than using ammonia and nitric acid without recovery.

The lower cost of the zero chemical recovery systems, using either ammonia/nitric acid or lime/sulphuric as regenerants, is due to the flexibility that zero recovery allows. When recovery is practised, the ammonia content of the treated water dictates the level to which resin must be regenerated. This stringent limit means a large excess of acid must be used for resin stripping (cf. section 6.311). With no recovery, one column is excluded from the flowsheet and the operation of the cation regeneration column is altered to the extent that, under certain conditions, only a slight excess of acid is required in fewer column stages (cf. Table 6.5), while still producing a regenerated resin which, in equilibrium with de-cationised water, produces the required treated water quality. This reduction in excess acid and column stages is, except for 90% recovery, sufficient to offset the cost of chemical recovery.

Although not included in Figure 6.10, the cost of removing 200 mg/ℓ of TDIS from a 700 mg/ℓ sewage plant discharge was evaluated in order to provide some measure of comparison. The calculation, based on lime and sulphuric acid as regenerants, determined that it would cost 13,4 cents/kℓ as opposed to the minimum cost of 18,7 cents/kℓ for the 1 300 mg/ℓ water on which the curves of Figure 6.10 are based.

6.411 Daily running costs: The daily ion exchange plant running costs on which the water costs of Figure 6.10 are based, are presented in Table 6.3 for the three cases of

(i) 90% chemical recovery with 50 and 500 mg/ℓ product water
(ii) Sulphuric acid/lime as regenerant chemicals with 50 and 500 mg/ℓ water
(iii) TDIS reduction from 700 to 500 mg/ℓ using sulphuric acid/lime as regenerants.

In each of the above, the total daily running cost comprises the cost of (a) chemicals
(b) capital - for initial column and resin purchase
(c) resin replacement.

TABLE 6.3

Daily running costs

Regeneration System	HNO_3/NH_3 90% Recovery				H_2SO_4/Lime				H_2SO_4/Lime Daspoort	
Water TDS (mg/ℓ)	50		500		50		500		500	
	Cost	%	Cost	%	Cost	%	Cost	%	Cost	%
Cation Load	26,83	9,8	11,99	6,4	39,58	11,6	17,78	9,0	20,09	15,0
Regen	31,06	11,3	23,46	12,6	38,46	11,2	21,56	10,8	17,12	12,7
AS	31,22	11,4	24,40	13,1	-	-	-	-	-	-
Anion Load	76,06	27,7	45,39	24,3	76,06	22,2	45,39	23,0	37,99	28,3
Regen	57,80	21,1	44,17	23,6	57,80	16,8	44,17	22,4	18,85	14,0
Acid	32,00	11,6	22,11	11,7	109,39	32,0	55,65	28,2	37,75	28,1
Base	19,51	7,1	15,43	8,3	21,04	6,2	12,96	6,6	2,60	1,9
Total (R/day)	274,48		186,95		342,33		197,51		134,40	
(cents/kl)	27,4		18,7		34,2		19,8		13,4	

The capital and resin replacement costs are given as a total for each column in Table 6.3, so that the costs can then be broadly divided into chemical costs and column costs.

In Chapter 3, it was stated that the cost of chemicals is generally the major cost item in an ion exchange desalination system, and that in order to effect cost reductions chemical costs must be reduced. Table 6.3 shows that this has been accomplished, for, in the cases presented, chemical costs are below 40% of total running costs. Where the cost of desalination (cf. Figure 6.10) is higher than the options presented in Table 6.3, it is the chemical costs which have increased to become the single major cost item.

An interesting point to emerge from Table 6.3, is that when chemical recovery is practised, column costs constitute 81,3 and 80,0% respectively of total costs for the 50 and 500 mg/ℓ product waters whilst with sulphuric acid/lime this fraction is lower and the relative figures are 61,8 and 65,2%. For the third case, that of Daspoort water the comparable figure is 70%. This comparison shows that regenerant chemical recovery fulfils its objective of reducing chemical costs, and the capital charges become the major cost consideration.

6.412 Capital costs: The plant capital costs, for the lowest cost modes of operation, are presented in Table 6.4. For a given product water, the chemical recovery system has, due to the extra column and resin required in the flowsheet, the highest capital cost. In each case, the plant capital cost decreases with increasing product water TDIS. This is due to the reduction in the number of stages each column requires to perform the lower level of desalination. Table 6.5 shows this variation.

TABLE 6.4
Capital Costs

Regeneration System		HNO_3/NH_3 90% Recovery		H_2SO_4/Lime No Recovery		H_2SO_4/Lime Daspoort
Water TDS (mg/ℓ)		50	500	50	500	500
Columns:						
Cation	Load	60 146	26 889	88 708	39 846	45 038
	Regen	56 402	44 654	69 667	40 036	33 839
	AS	55 963	47 489	-	-	-
Anion	Load	86 866	54 764	86 866	54 764	68 195
	Regen	92 396	76 122	92 396	76 122	38 186
Resin:	Cation	12 679	6 338	11 478	4 948	4 081
	Anion	39 685	22 947	39 685	22 947	21 639
Total		404 137	279 203	388 800	238 663	210 978

The load and regeneration column diameters are fixed by the resin fluidisation and liquid flow time, and so consequently are the capital costs for a given throughput. However, should a heavier resin be used in the plant, the cost of the load columns would be considerably reduced - a 15% resin density increase would halve the load column capital costs.

6.413 CCIX plant size: Table 6.5 lists the sizes of the columns for the various regeneration options when treating one megalitre per day. The only point of interest, and one which was outlined under the capital costs discussion, is the decrease in the number of column stages in each of the columns when product water quality changes from 50 to 500 mg/ℓ. The other size changes which occur for the 50 to 500 mg/ℓ TDIS variation are the

TABLE 6.5

Size of 1 megalitre/day CIX plant

Regeneration System	Water Quality		Cation Load	Cation Regen	Cation A/S	Anion Load	Anion Regen
HNO_3/NH_3		Diam(cm)	100	50	50	240	60
90% Recov.	50	Stages	7	13	14	5	20
		Res.Vol(ℓ)	1858	2174	2307	6867	3054
		Diam	100	40	40	240	45
	500	Stages	3	12	11	3	20
		Res.Vol	679	1304	1186	3858	1882
H_2SO_4		Diam	100	50	-	240	60
Lime	50	Stages	12	17	-	5	20
No		Res.Vol	3020	2719	-	6867	3054
Recovery		Diam	100	50	-	240	45
	500	Stages	4	9	-	3	20
		Res.Vol	1110	1364	-	3858	1882
H_2SO_4		Diam	100	35	-	240	20
Lime	500	Stages	5	11	-	4	20
Daspoort		Res.Vol	1294	747	-	5074	335

diameters of the regeneration and ammonium-sodium columns. In each case, they are reduced. This change is due to the lower resin flow through the CCIX plant when the product water TDIS is increased because, for a given feed water rate, less resin is required to achieve the lower dissolved solids reduction. The load column diameter cannot decrease for it is constrained by the allowable bed expansion but the regeneration column diameters are constrained by the liquid flow time.

If the resin-liquid ratio in the regeneration columns remains constant, then, for a lower resin flow rate, a proportional decrease in liquid flow rate must occur. A lower liquid flow rate into a constant diameter column results in a lower bed expansion and a longer liquid flow time. If the liquid flow time is held constant, then the diameter can be decreased - the optimum design condition.

For the evaluation of the water treatment costs using lime and sulphuric acid as regenerant chemicals, the same kinetic and equilibrium properties have been assumed to exist between Zerolit MPH and lime and Zerolit 625 and sulphuric acid as have been established for nitric acid and ammonia. This is a reasonable assumption if the kinetics are considered to be pore diffusion controlled, and Donnan exclusion of the co-ions applies. On this basis, the calculated number of stages required to achieve a given regeneration is thus the same for either regeneration system under identical conditions.

6.42 Conclusions

A comparison of the cost figures presented in Chapter 3 with those of Figure 6.10 and Tables 6.3 and 6.4 shows clearly the time disparity of the two evaluations. In section 3.221 the conclusion was reached that in fixed bed columns there was little to choose between the costs of nitric acid/ammonia and sulphuric acid for resin regeneration. With possibe cost savings by recovering chemicals, the ammonia-nitric acid system appeared the more attractive.

Since the initial cost study, the costs of the oil-based ammonia and nitric acid have escalated so rapidly that the situation now arises where a major portion of regenerant chemicals must be recovered if the ammonia/nitric acid scheme is used in order to be competitive with the alternative regenerants. The escalation in the price of sulphuric acid and lime has not been nearly as high during the four year gap between the cost evaluations.

CHAPTER 7

CONCLUSIONS AND RECOMMENDATIONS

7.1 CONCLUSIONS

The work presented has provided certain conclusions to problems which have been posed by ion exchange and water treatment researchers and by policy makers concerned with the future provision of potable water; for, in the investigation and development of an ion exchange process for desalination and tertiary treatment, new techniques in both the ion exchange and water recovery fields have been developed.

Amongst the results in the field of ion exchange resins and reactions which this work has provided are the following:

(i) The operation of a continuous countercurrent ion exchange column has been shown to reach a steady state condition and the resin and liquid stream compositions at this steady state can be predicted from a knowledge of the kinetics and equilibria of the relevant exchange reactions and the operating conditions of the CCIX column.

(ii) The kinetics of the ion exchange reactions investigated conform to the ion exchange theory based on a modification of the Nernst-Plank equations proposed by Helfferich and developed by Turner and Weatherley.

(iii) The equilibria of the ion exchange reactions investigated can be represented by a separation factor equation; and the equilibria of the electrolyte sorption reactions support the principle of Donnan exclusion.

(iv) The ion exchange resins are capable of simultaneously removing organic and inorganic components from a secondary sewage effluent over an extended period of time without any deleterious effects to the ion exchange properties of the resins tested.

(v) The measured exchange rate of the weak anion and strong cation resins investigated are very different, with the latter resin almost an order of magnitude faster than the former.

(iv) The functional group characteristics of the tested anion and cation resins show that the anion affinities of the former resin are one and two orders of magnitude greater than the cation affinities of the latter resin and that on the anion resin both load and regeneration reactions have a favourable equilibrium in contrast to the cation resin on which an affinity reversal occurs during resin regeneration.

During the development of the ion exchange desalination and tertiary treatment process, the following was achieved:

(i) A new method for the recovery of regeneration chemicals when using ammonia and nitric acid was developed.

(ii) A pilot plant consisting of five interlinked CCIX columns was operated on a continuous basis under steady state conditions.

(iii) During the plant operation, regenerant chemicals were recovered, salts and residual organics were removed from a secondary sewage water, and those feed water salts and organics concentrated up to 20-fold before being discharged.

(iv) A cost and feasibility study on the CCIX tertiary treatment process showed the complex interrelationships that exist in the plant and how these must be considered if an optimum plant configuration is to be designed.

7.2 RECOMMENDATIONS

In providing the answers that it has, the work presented has simultaneously posed a number of further questions, some of which, if answered, would shed more light on the theory and process outlined, and their further investigation is recommended.

7.21 Theory of ion exchange

The following points, if clarified, would support the work presented.

(i) a detailed investigation of the flow properties within a CCIX column and the degree of resin mixing in a CCIX column stage;

(ii) solution of the pore diffusion kinetic differential equations and comparison of the predicted and measured kinetics, leading perhaps to the development of a technique which will allow the calculation of reaction rates from a knowledge of the mobility and charge properties of the exchanging species;

(iii) a characterisation of the resin equilibria on the basis of molecular species involved instead of determination by an empirical separation factor equation; a comparison of the measured separation factors with the following exchanging ion properties, charge, ionic radius, degree of hydration, may show some correlation and hence lead to a prediction of the separation factor.

7.22 Process development

During the process development and subsequent cost study, the following questions which were raised warrant further investigation.

(i) A comparison of the cost studies presented shows the effect of cost escalation on the process viability. Whereas initially both sulphuric acid ammonia and nitric acid ammonia regeneration systems without chemical recovery were equally costly, the increase in the cost of the oil based nitrogen chemicals has radically altered this position. Now, 90% chemical recovery is necessary when HNO_3 and NH_3 are used to regain the previous cost equality of the two regenerant systems. On the basis of this cost comparison, it becomes essential to investigate thoroughly the use of lime and sulphuric acid as regenerant chemicals. The investigation must naturally include kinetic and equilibrium studies plus operation in the pilot plant.

(ii) Both the operation of the pilot plant and the feasibility study of Chapter 6 have indicated that, should anion or cation resins with higher densities become available, these resins would assist plant operation and improve plant economics. However, after a certain density increase a simultaneous kinetic increase must also occur in order for the resins to be of benefit. It is therefore recommended that a watching brief be maintained on future resin developments, and that, should any higher density resins become available, these be subjected initially to kinetic and fluidisation tests and then, should these first tests prove favourable, to pilot plant investigation.

(iii) The ion exchange process development has been aimed at treatment of a specific secondary sewage plant discharge stream. The ability of the resins to exchange ions under a range of concentration conditions has simultaneously been shown. This being the case, consideration should be given to the broader potential of the process in treating waters having widely different salt compositions and salinity levels. Using the predictive theory presented, preliminary kinetic and equilibrium tests will readily prove whether these alternative waters are amenable to treatment by the IX process developed in this work.

(iv) Finally, the proof of potable water production would be to set up a demonstration plant at a sewage works site and produce water for recycle to domestic and industrial users. The construction and operation of such a plant is recommended for it will clearly indicate the ability of ion exchange to provide desalination and tertiary treatment on a continuous long term basis and establish the use of ion exchange to produce water of potable or industrial levels as required.

REFERENCES

1. Henzen, M.R., "Die herwinning opberging en onttrekking van gesuiwerde rioolwater in die Kaapse Skiereiland", Report for N.I.W.R., C.S.I.R. August 1973.

2. "Report of the Commission of Inquiry into Water Matters", Republic of South Africa, 1970.

3. Heunis, B., "Regional planning for the optimum use and re-use of water in the Cape Peninsula", Report by N.I.W.R. (C.S.I.R.) for Cape Provincial Administration, 1974.

4. Prentice, S.W., "Mineralisation of Sewage", M.Sc. Thesis, University of Cape Town, 1972.

5. American Water Works Assoc. J., 64, November 1972.

6. Probstein, R.F., "Desalination", American Scientist, 61, 280-293, (1973).

7. Quinn, R.M., Hamilton, R.S., Anderson, J.R., Weiss, C.O., "Some economic factors relating to the use of reverse osmosis and ion exchange for the treatment of water and waste water", A.I.Ch.E. Symp. Ser., 68, 262-269, (1972).

8. Bresler, S.A., Miller, E.F., "Economics of ion exchange techniques for municipal water-quality improvement", J.A.W.W.A., 64, 764-772, (1972).

9. Cillie, G.G., van Vuuren, L.R.J., Stander, G.J., Kolbe, F.F., "The reclamation of sewage effluents for domestic use", Proc. Third Int. Conf. on Water Poll. Res., Munich, Germany, 1966.

10. Van Vuuren, L.R.J., Henzen, M.R., Stander, G.J., "The full-scale reclamation of purified sewage effluent for the augmentation of the dom domestic supply of the City of Windhoek", Proc. Fifth Int. Conf. on Water Poll. Res., 1970.

11. Henzen, M.R., Funke, J.W., "The appraisal of some significant problems in the re-use of waste water", J. Inst. Wat. Poll. Cont. 70 (2), 177-186, (1971).

12. Pollio, F.X., Kunin, R., "Tertiary treatment of municipal sewage effluents Env. Sci. Tech. 2, 54-60, (1968).

13. Kunin, R., "Elements of Ion Exchange", Robert E. Krieger, New York, (1971).

14. Suhr, L.G., Kepple, L., "AWT plant gets tough with ammonia", Water and Wastes Eng., 12 (3), 26-30, (1975).

15. Koon, J.H., Kaufman, W.J., "Ammonia removal from municipal wastewaters by ion exchange", J. W.P.C.F., 47 (3) 448-465, (1975).

16. Grimshaw, R.W. Harland, C.E., "Ion Exchange: Introduction to Theory and Practice", Chemical Society, London (1975).

17. Dorfner, K., "Ion Exchangers. Properties and Applications", Ann Arbor, Michigan (1972).

18. Martinola, F., Meyer, A., "Determination of the inner surface of macroporous ion exchange resins", Ion Exch. & Memb., 3, 111-116, (1975).

19. Kunin, R., "Ion Exchange Resins", Robert E. Krieger, New York (1972)

20. Kaczmer, B.U., Traser, S., "Synthesis of various snake-cage polyelectrolytes consisting of polyacrylamides and an anion exchanger", Markromol. Chem. 177 (7), 1981-1989, (1976).

21. Moyers, E.M., "The Synthesis, Characterisation and Application of Chelating Ion Exchange Resins", Iowa State Univ., Ames, Iowa 1976.

22. Gustafson, R.L., Filius, H.F., Kunin, R., "Basicities of weak base ion exchange resins", Ind. Eng. Chem. Fundam., 9 (2), 221-229, (1970).

23. Helfferich, F., "Ion Exchange", McGraw-Hill, New York, (1962).

24. Lal, B.B., Douglas, W.J.M., "Equilibrium water sorption and volumetric behaviour of ion exchange resin spheres", Ind. Eng. Chem. Fundam., 13 (3), 223-227, (1974).

25. Diamond, R.M., Whitney, D.C., "Resin selectivity in dilute to concentrated aqueous solutions", in Marinsky, J.A., editor "Ion Exchange", Vol.1, Marcel Dekker, New York (1966).

26. Cosgrove, J.D., Strickland, J.D.H., "Cation exchange resins. The Applicability of the mass-action law to the exchange of univalent ions", J. Chem. Soc., 1845-1853, (1950).

27. Bucher, J. Diamond, R.M. Chu, B., "Anion exchange resin selectivity as a function of resin composition, revisited", J. Inorg. Nucl. Chem., 36 (3), 645-647, (1974).

28. Boari, G., Liberti, L., Merli, C., Passino, R., "Echange equilibria on anion resins", Desalination, 15, 144-166, (1974).

29. Philbrick, F.A., Holmyard, E.J., Palmer, W.G., "A Textbook of Theoretical and Inorganic Chemistry", J.M. Dent & Sons, London (1949).

30. Rao, M.G., David, M.M., "Single particle studies of ion exchange in packed beds: Cupric ion - sodium ion system", A.I.Ch.E.J. 10 (2), 213-219, (1964).

31. Reichenberg, D., "Ion exchange selectivity", in Marinsky, J.A., editor, "Ion Exchange", Vol.1, Marcel Dekker, New York (1966).

32. Semmens, M., Gregory, J., "Selectivity of strongly basic anion exchange resins for organic acids", Env. Sci. & Tech., 8 (9), 834-839, (1974).

33. Weiss, D.E., Bolto, B.A., McNeill, R., Macpherson, A.S., Suidak, R., Swinton, E.A., Willis, D., "An ion exchange process with thermal regeneration", Aust. J. Chem., 19, 561-796, (1966).

34. Ackermann, G.R., Barrett, J.H., Bossler, J.F., Dabby, S.S., "Industrial deionization with Amberlite XD-2 - A thermally regenerable ion exchange resin", A.I.Ch.E. Symp. Ser., 73 (106), 107-111, (1977).

35. Boyd, G.E., Adamson, A.W., Myers, S.L., "Kinetics of ion exchange adsorption processes", J. Am. Chem. Soc., 69, 2836-2848, (1947).

36. Vermeulen, T., "Theory for irreversible and constant-pattern diffusion", Ind. Eng. Chem., 45, 1664-1670, (1953).

37. Glueckauf, E., "Theory of chromatography: Part 10. Formulae for diffusion into spheres and their application to chromatography", Trans. Faraday Soc., 51, 1540-1551, (1955).

38. Crank, J., "The Mathematics of Diffusion", Oxford Univ. Press, New York, 1956.

39. Carslaw, H.S., Jaeger, J.C., "Conduction of Head in Solids", 2nd Edition, Oxford Clarendon Press, 1959.

40. Schlogl, R., Helfferich, F., "Comment on the significance of diffusion potentials in ion exchange kinetics", J. Chem. Phys., 26 (1), 5-7, (1957).

41. Helfferich, F., Plesset, M.S., "Ion exchange kinetics: A nonlinear diffusion problem", J. Chem. Phys., 28 (3), 418-424, (1958).

42. Plesset, M.S., Helfferich, F., Franklin, J.N., "Ion exchange kinetics: A nonlinear diffusion problem. II Particle diffusion controlled exchange of univalent and bivalent ions", J. Chem. Phys., 29 (5), 1064-1069, (1958).

43. Kataoka, T., Yoshida, H., "Resin phase mass transfer in ion exchange between different ions accompanied by resin volume change", J. Chem. Eng. Jap., 8 (6), 451-456, (1975).

44. Turner, J.C.R., Church, M.R., Johnson, A.S.W., Snowdon, C.B., "An experimental verification of the Nernst-Planck model for diffusion in an ion exchange resin", Chem. Eng. Sci., 21, 217-325, (1966).

45. Weatherley, L.R., Turner, J.C.R., "Ion exchange kinetics - Comparison between a macroporous and gel resin", Trans. Inst. Chem. Eng., 54, 89-94, (1976).

46. Ruckenstein, E., Vaidyanathan, A.S., Youngquist, G.R., "Sorption of solids with bidisperse pore structures", Chem. Eng. Sci., 26, 1305-1318, (1971).

47. Marchello, J.M., Davis, M.W., "Theoretical investigation of agitated ion exchange beds", Ind. Eng. Chem. Fundam. 2 (1), 27-31, (1963).

48. Kuo, J.C.W., David, M.M., "Single particle studies of cation exchange in packed beds: Barium ion - sodium ion system", A.I.Ch.E.J., 9 (3), 365-370, (1963).

49. Glaski, F.A., Dranoff, J.S., "Ion exchange kinetics: A comparison of models", A.I.Ch.E.J., 9 (3), 426-431, (1963).

50. Smith, T.G., Dranoff, J.S., "Film diffusion controlled kinetics in binary ion exchange", Ind. Eng. Chem. Fundam., 3 (3), 195-200, (1964).

51. Martinola, F., "The Lewatit fluidised bed process", The Chemical Engineer, 281 (1), 25-27,34, (1974).

52. Gilwood, M.E., "Saving capital and chemicals with countercurrent ion exchange", Chem. Eng., 74 (26), 83-88, (1967).

53. Haines, A.K., Tunley, T.H., te Riele, W.A.M., Cleote, F.L.D., Sampson, T.D., "The recovery of zinc from pickle liquors by ion exchange", S.A. Inst. Min. Metall. Colloquium, Sept. 1973.

54. Naden, D., Evans, J.P., "The use of continuous ion exchange (CIX) in copper recovery problems", J. Appl. Chem. Biotechnol., 24, 687-700, (1974).

55. Newman, J., "Moving bed ion exchange as a re-use tool", A.I.Ch.E. Symp. Ser., 70 (136), 472-476, (1973).

56. Higgins, I.R., "Continous ion exchange of process water", Chem. Eng. Prog., 65 (6), 59-62, (1969).

57. Doshi, M.R., Parekh, B.S., Gill, W.N., "Removal of copper from wastewater by continuous countercurrent ion exchange process", A.I.Ch.E. Symp. Ser., 70 (136), 390-399, (1973).

58. Bingham, E.C., Chopra, R.C., "A closed cycle water system for ammonium nitrate producers", Int. Water Conf., 32rd Annual Meeting, Pittsburgh, Penn.,Nov. 1971.

59 Gold, H., Todisco, A., Sonin, A.A., Probstein, R.F., "The AVCO continuous moving bed ion exchange process and Iarge scale desalting", Desalination, 17, 97-109, (1975).

60. Blesing, N.V., "Ion exchange applications in desalination and hydrometallurgy", Amdel. Bull., 12, 23-44, (1971).

61. Cloete, F.L.D., Streat, M., British Pat. 1070251.

62. Rosenbaum, J.B., Ross, J.R., "A countercurrent column for fluidised bed ion exchange for uranium ore slurries", Int. Symp. Hydrometallurgy, AIME, Chicago, Ill., 1973.

63. Horn, F.J.M., "Periodic countercurrent processes", Ind. Eng. Chem. Proc. Des. Dev., 6 (1), 30-35, (1967).

64. Horn, F.J.M., Lin, R.C., "Periodic Processes: A variational approach", Ind. Eng. Chem. Proc. Des. Dev., 6 (1), 21-30, (1967).

65. Rowe, P.N., Claxton, K.T., "Heat and mass transfer from a single sphere to fluid flowing through an array", Trans. Inst. Chem. Eng., 43, T321-T331, (1965).

66. Rowe, P.N., Claxton, K.T., Lewis, J.B., "Heat and mass transfer from a single sphere in an extensive flowing fluid", Trans. Inst. Chem. Eng., 43, T14-T31, (1965).

67. Snowdon, C.B., Turner, J.C.R., "Mass Transfer in liquid fluidized beds of ion exchange resin beads", Proc. Int. Conf. on Fluidisation, Amsterdam, 1967.

68. Turner, J.C.R., Snowdon, C.B., "Liquid side mass transfer coefficients in ion exchange - the H^+/Cu^{++}-Cl^- system", Chem. Eng. Sci., 23, 1099-1103, (1968).

69. Turner, J.C.R., Snowdon, C.B., "Liquid side mass transfer coefficients in ion exchange: an examination of the Nernst-Planck model", Chem. Eng. Sci., 23, 221-230, (1968).

70. Koloini, T., Zumer, M., Sopcic, M., "Mass transfer in the liquid fluidised beds of ion exchange resins composed of different size fractions", Vestnik Solvensbega Kamysbega Drustva, 23, 67-71, (1976).

71. Dodds, R., Hudson, P.I., Kershenbaum, L., Streat, M., "The operation and modelling of a periodic countercurrent solid-liquid reactor", Chem. Eng. Sci., 28 (6), 1233-1248, (1973).

72. Slater, M.J., "Continous ion exchange in fluidised beds", Can. J. Chem. Eng., 52, 43-51, (1974).

73. Streat, M., Gupta, A.K., "The separation of metals by continuous ion exchange", Inst. Chem. Eng. Symp. Ser., 42, 1-13, (1975).

74. Levenspiel, O., "Chemical Reaction Engineering", John Wiley & Son, New York, 1962.

75. Smith, B.D., "Design of Equilibrium Stage Processes", McGraw-Hill, New York, 1963.

76. Van Winkle, M., "Distillation", McGraw Hill, New York, 1967.

77. Zastrozny, E.P., "Practical Cost Estimating for the South African Chemical Process Industry", South African Coal, Oil and Gas Corporation, Nov. 1971.

78. Downing, D.G., "Calculating minimum cost ion exchange Units", Chem. Eng., 72, 170-176, (1965).

79. Downing, D.G., Kunin, R., Pollio, F.X., "Desal process - Economic ion exchange system for treating brackish and acid mine drainage waters and sewage waste effluents", Chem. Eng. Prog. Symp. Ser., 64 (90), 126-133, 1968.

80. Evans, S., "Nitrate removal by ion exchange", J.W.P.C.F., 45 (4), 632-636, (1973) and "The Ducol Process - Laboratory demonstration of feasibility", Israeli Pat. 36445, (1972).

81. Applebaum, S.B., "Demineralization by Ion Exchange", Acadmic Press, New York, (1968).

82. Kunin, R., Fries, W., "Recovery of Waste Brine Regenerant", U.S. Pat. 3791866, Feb. 1974.

83. David, E.J., "Method of Purification of Regenerant Solution", U.S. Pat. 3905903, Sept. 1975.

84. Busch, G.A., Lynn, S. "Deionization of brackish water using thermally regenerated reagents", Univ. California Sea Water Res. Lab. Rep. No.72-2, Nov. 1972.

85. Vermeer, D.J., Lynn, S. Vermeulen, T., "Cation-exchange column behaviour in a desalination process with regenerant recovery", Ind. Eng. Chem. Proc. Des. Dev., 14 (3), 290-297, (1975).

86. Freeth, F.A. Cocksedge, H.E., U.S. Pat. 1301047, April 1919.

87. Rengade, E., "Sur les equilibres de double decomposition entre sels solubes", Chimie Ind., 7 (6), 298-302, (1922).

88. Hunt, H., Boncyk, L., "Liquid ammonia as a solvent. III. The solubility of inorganic salts at 25°C", J. Am. Chem. Soc., 55, 3528-3530, (1933).

89. Moldovan, I., Popovici, N., Chivu, G., "The technology of mineral fertilisers", British Sulphur Corporation, London 1969.

90. Mellor, J.W., "Inorganic and Theoretical Chemistry", Vol.2., Suppl.2., Longmans, London, 1961.

91. Ayres, D.E.R., Westwood, R.J., "The use of the ion exchange process in the extraction of uranium from Rand ores with particular references to practice at the Randfontein uranium plant", in "Uranium in South Africa, 1946-1956", Vol.2, Hortors, Johannesburg, 1957.

92. Hoenigschmid-Grossich, R., "Water demineralisation using the intensive fraction process", paper presented at Int. Conf. on The Theory and Practice of Ion exchange, Cambridge, 1976.

93. Koto, N., "Economic evaluation of Desal process in C.I. system and fixed bed system", CRP Report No.26, Japan Organo, 1972.

94. Takeuchi, T., "An economic comparison of Desal process and the usual process", CRP Report No.44, Japan Organo, 1973.

95. Painter, H.A., "Organic compounds in solution in sewage effluents", Chem. Ind., 818-822, 1 Sept., 1973.

96. Technical Notes on Amberlite XAD resins, Rohm & Haas Co.

97. Kim, B.R., Snoeyink, V.L., Saunders, F.M., "Adsorption of organic compounds by synthetic resins", Presented at WPCF Conf., Denver, Colorado, Oct. 1974.

98. Junk, G.A., Richard, J.J., Grieser, M.D., Witiak, D., Witiak, J.L., Arguello, M.D., Vick, R., Swec, H.J.,Fritz, J.S., Calder, G.V., "Use of macroreticular resins in the analysis of water for trace organic contaminants", J. Chromatography, 99, 745-762, (1974).

99. Oehme, C., Martinola, F., "Removal of organic matter from water by resinous adsorbents", Chem. & Ind., 15, 823-826, Sept. 1973.

100. Hinrichs, R.L., Snoeyink, V.L., "Sorption of benzenesulfonates by weak base anion exchange resins", Water Research, 10, 79-87, (1976).

101. Blesing, N.V., "The fouling of ion exchange resins - from a case study at Nangwarry", Amdel Bulletin, No.17, 38-44, April 1974.

102. Tilsworth, T., "Organic and colour removal from water supplies by synthetic resinous adsorbents", Rep. No. IWR-50, Inst. of Water Res., Univ. Alaska, Jan. 1974.

103. Anderson, C., Maier, W.J., "The removal of organic matter from water supplies by ion exchange", Bull. No.91, Water Resources Res., Univ. Minnesota, Feb. 1977.

104. Brown, J., Ray, N.J., "Anion exchange resin performance in the treatment of River Trent water", Effl. Wat. Treat., 14 (8), 417-422 (1974).

105. "Standard Methods for the Examination of Water and Wastewater", 12th edition, American Public Health Assoc., New York, 1965.

106. Osborn, G.H., "Synthetic Ion Exchangers", 2nd Ed., Chapman Hall, London 1961.

107. Amber-Hi-Lites, No.95, Rohm & Haas Ltd., Sept. 1966.

108. Kataoka, T., Yoshida, H, Ozasa, Y., "Breakthrough curve in ion exchange column - particle diffusion control", J. Chem. Eng. Japan, 10 (5), 385-390 (1977).

109. Henzen, M.R., Water Research Commission, Private Communication, 1978.

110. Boydell, D.W., Atomic Energy Board, Private Communication, 1978.

APPENDIX A

MEASUREMENT OF RESIN PHYSICAL PROPERTIES

A1 VOLUME AND DENSITY

A1.1 Volume Measurement

Resin volume is expressed as either a free settled volume (FSV) or a tapped volume. The measurement technique for each is identical until just prior to the reading being taken when the techniques differ.

Method: In order to measure the volume of a sample of resin, the sample is placed in a beaker and water added. The resin-water mixture is allowed to equilibrate so that resin swelling may reach a maximum. (If the volume measurement is required in the presence of some 'other' electrolyte, this new electrolyte replaces the water in the above step.) If the resin sample has been oven-dried prior to the measurement, a series of water sorption contact steps may be required. Addition of an alcohol-water mixture in the first of the steps, followed by a successive elution of the alcohol from the resin with subsequent water wash steps will facilitate resin swelling. In general, resin should not be allowed to dry out completely, for re-wetting may damage the resin beads through the high swelling pressures which build up.

The fully swollen resin sample is next transferred quantitatively to a measuring cylinder graduated to measure at least five times the resin volume, e.g. to measure 10 mℓ of resin a 50 mℓ measuring cylinder is required. The measuring cylinder is filled completely with the electrolyte solution in which the volume measurement is to take place and a stopper placed in the top; in so doing all air must, if possible, be excluded from the cylinder. The next step is to invert the cylinder and return it to a vertical position at least five times, ensuring that the resin in the cylinder is completely fluidised. After the inversion, the cylinder is placed upright on a horizontal surface, and it is from this point that the two volume measuring techniques deviate.

(a) Free settled volume: The FSV volume measurement is taken by allowing the resin in the cylinder to settle under gravity into a packed bed, and a volume reading at the resin height cross-section taken. The cylinder

inversion is repeated twice more, and two further readings taken. The average of the three is the FSV volume of the sample.

(b) Tapped volume: During the resin settle period the measuring cylinder is continuously tapped until a packed bed of resin has formed. The tapping aids the resin packing and results in the formation of a more compact bed. Again, the volume of the packed bed is measured and the procedure repeated twice more to give an average value. As anticipated, the tapped volume yields a lower average volume reading that the FSV method.

A1.2 Density Measurement

The resin density varies with the counter-ion and degree of conversion, so the first step in a density measurement is to convert a representative sample of resin to the required form. Next, a number (at least five) approximately equal volume (±30 mℓ) resin sample are placed into pre-weighed gooch crucibles. Each sample is then sucked on a buchner flask to constant humidity. This is achieved by placing a damp muslin cloth over the gooch crucible and sucking an airstream through the cloth and resin. When each gooch crucible has been prepared in this manner, it is again weighed. The difference in weights indicates the mass of resin present in the gooch. Each resin sample is now carefully washed out of its respective crucible, and its FSV volume measured. From the sample mass and the volume measurement, the density is calculated. The values for each of the five tests are averaged to yield the bulk density of the resin in the particular counter-ion form.

A2 CAPACITY

The resin capacity is a measure of the exchange sites in a given resin volume. The two capacity measurements in use are the operating capacity (outlined in Appendix B) and the total capacity. Measurement of the total capacity follows the same procedure as the analysis of the resin after a particular test (e.g. equilibrium determinations).

Method: (a) Cation resin: At least three representative volumes of resin which have been converted to the correct form are carefully measured and placed into gooch crucibles. Each of the resin volumes (approximately 20 mℓ) is then sucked dry and washed with 5 successive 15 mℓ distilled water samples

at 15 minutes intervals. The purpose of this wash phase is to remove all traces of electrolyte which may be present in the resin pores.

Following the wash, a volumetric flask is placed beneath each gooch crucible and the ions present on the resin are stripped off and into the volumetric flask using a 2,0N $CaCl_2$ solution. If the resin counter-ions contain Ca, then $Al_2(SO_4)_3$ is used for this duty. By using the divalent Ca ion, for which the resin has a high affinity, complete resin conversion is achieved. The resin stripping procedure found most efficient was to contact the 20 mℓ sample with five successive 10 mℓ $CaCl_2$ samples at 15 minutes intervals. This was followed by 5 successive 15 mℓ water wash steps to elute any residual ions from the resin.

The volumetric flasks are filled to the mark, mixed and the contents analysed. From the analysis, it is possible to determine the quantity of cations present in the volumetric flask and hence present on the resin. This, together with the resin volume measurement, allows the capacity to be determined.

(b) Anion resin: Because the weak base anion resin can lose loaded ions by an hydrolysis reaction during resin washing, the first wash procedure of the cation analysis is replaced by centrifugation. Therefore, for anion resin analysis a sample is centrifuged at 3 000 revs/min for 30 minutes, at the end of which it is accepted that any electrolyte present in the resin pores has been removed.

The remainder of the cation procedure is the adopted except that the stripping solution used in this instance is 2,0N NaOH instead of $CaCl_2$. The analysis and capacity determination are calculated exactly as for the cation case.

A3 FLUIDISATION TESTS

The resin fluidisation is determined from the degree of bed expansion which occurs at a particular solution flow rate. The results are then calculated from equation (4.1). Because the fluidisation is affected by the relative solution and resin densities, which in turn are dependent upon the resin counter-ion and the solution concentration, care must be exercised,

when determining the fluidisation properties, to ensure that the correct resin and solution are used during the test.

Method: A representative sample of resin (approximately 200 mℓ) is placed into a fixed bed perspex (glass or clear PVC) column with accurately known internal diameter of >50 mm. (This diameter choice is necessary to prevent wall effects from interfering with the flow through the column.) The column is constructed with a flow inlet at the bottom and outlet at the top. The resin is supported on a fine mesh stainless steel screen above the inlet point. The mesh also serves as a flow distributor. Solution feed rate is controlled by a needle valve and measured by a calibrated rotameter and enters the column under gravity from a constant head tank.

The mean settled bed height of the particular resin volume is first established by fluidising the resin to an approximate 100% bed expansion and then allowing it to settle under gravity. The settled height is noted, and the procedure repeated twice more. The actual bed expansion is determined by adjusting the flow through the column to some value. The resin then fluidises and the flow rate is maintained until a steady bed height is achieved. The particular bed height and flow rate are noted, the flow rate is raised and a further expansion of the resin occurs. This procedure is repeated until sufficient data points have been measured to establish the bed expansion versus flow curves.

Calculation of results: The % bed expansion is calculated form the fluidised and settled bed heights via equation (4.1). The linear velocity (LV) is determined from the rotameter calibration and the column cross-sectional area.

Results:

Resin Resin Form Solution	Zerolit MPH Chloride Water		Zerolit MPH Free Base Water		Amberlite IRA-93 Chloride Water		Amberlite IRA-93 Free Base Water	
	%BE	LV(cm/min)	%BE	LV(cm/min)	%BE	LV(cm/min)	%BE	LV(cm/min)
	12	3,1	24	2,7	14	2,9	26	2,9
	20	4,7	36	3,5	31	5,9	63	5,9
	35	8,2	62	5,4	51	9,3	95	8,2
	44	10,2	80	6,8	72	12,5	110	93

	53	12,0	93	7,9			
	60	13,4	125	10,2			
	122	25,5	165	13,6			
	180	32,4	210	17,0			
	260	40,0	260	20,0			
			315	24,5			

Resin Resin Form Solution	Zerolit MPH Chloride in NH_4Cl		Zerolit MPH Free Base in NH_4Cl		Amberlite IRA-93 Chloride in NH_4Cl		Amberlite IRA-93 Free Base in NH_4Cl	
	%BE	LV(cm/min)	%BE	LV(cm/min)	%BE	LV(cm/min	%BE	LV(cm/min)
	13	3,1	32	3,0	14	2,9	34	3,0
	21	4,7	48	4,5	23	4,3	52	4,6
	39	8,2	89	8,2	34	6,1	102	8,2
	50	10,1	108	10,2	57	9,3	129	9,9
	62	12,0			82	12,5		

Resin Resin Form Solution	Zerolit 625 H Water		Zerolit 625 Na Water		Zerolit 625 NH_4 Water	
	%BE	LV(cm/min)	%BE	LV(cm/min)	%BE	LV(cm/min)
	11	7,5	11	10,0	9	7,5
	17	11,9	19	16,8	13	12,2
	31	21,2	35	25,0	27	20,9
	41	25,9	50	33,2	36	25,9
	49	31,3	60	39,0	42	31,0
			96	60,0		
			106	64,0		
			157	78,0		
			200	86,0		
			233	91,0		
			395	106,0		

A4 VOIDAGE MEASUREMENTS

The measurement of resin voidage is necessary for two reasons (i) to determine the interstitial solution volume in a packed resin bed, and (ii) to calculate the actual resin density from the bulk density.

Method: The resin voidage measurement is similar to the FSV volume measurement. A measuring cylinder is half filled with water, and a reading of this water volume taken. A representative sample of resin dried to a constant moisture is carefully added to the measuring cylinder. Care must be exercised during the resin addition to ensure that no solution is lost from the cylinder. Once the resin has settled, a second reading of the water volume in the cylinder is taken, and the cylinder is then completely filled with solution. The FSV resin volume in the cylinder is now measured using the procedure of Appendix A1. The test is repeated a further three times on different resin samples so that an average voidage can be determined.

Calculation of results:

Initial solution volume	250 mℓ
Final solution volume	284 mℓ
FSV resin volume	50 mℓ

$$\text{Voidage} = \frac{50 - (284-250)}{50} = \frac{16}{50} = 0,32$$

A5 BEAD COUNTS

The resin bead counts provide an indication of the degree of bead breakage which has occurred during a particular series of tests.

Method: A sample of resin is placed under the microscope at any convenient magnification (X5 was found to be adequate). By examining the beads within the microscope's field of vision the number of whole beads without cracks, the number of whole beads with visible cracks and the number of split or broken beads is counted. The microscope slide is moved so that a second group of beads, still from the original sample, comes into view. The counting procedure is repeated on this and a further two bead groups. This represents the bead count on the first resin sample. A further two resin samples are also counted, and the results summed to produce a representative count on the particular resin.

Calculation of results:

Zerolit MPH ex life tests

Sample 1			Sample 2			Sample 3		
W	C	B	W	C	B	W	C	B
18	1	9	23	0	7	17	0	4
13	2	4	21	1	5	20	1	5
25	1	7	21	1	6	13	1	6
17	1	6	15	1	6	24	0	6
73	5	26	80	3	24	74	2	21

Total whole (73 + 80 + 74) 227 $\quad \%W \frac{227}{308} = 73,7$

Total cracked (5 + 3 + 2) 10 $\quad \%C \frac{10}{308} = 3,2$

Total broken (26 + 24 + 21) 71 $\quad \%B \frac{71}{308} = 23,1$

308

APPENDIX B

MEASUREMENT OF RESIN EXCHANGE PROPERTIES

B1 EQUILIBRIA

The equilibrium conditions of any particular ion exchange reaction are determined by a series of experiments in which resin and solution are contacted together at a fixed solution concentration for a sufficiently long period to ensure that equilibrium is attained. At the end of the contact period, both the resin and the solution phases are analysed and the respective equilibrium ion fractions calculated.

The experimental technique for the anion and cation resins differ only in one respect, that of the resin analysis. Because the anion resin is able to release a loaded ion in an hydrolysis reaction when washed with water, the wash procedure used on this resin type had to be modified. In all other respects, the equilibrium determination procedure for the two resins is identical.

B1.1 Method

(a) Exchange equilibrium: The aim of the equilibrium resin tests was to produce an even spread of data points over the whole of the resin conversion from one form to another. In order to achieve this aim, the following method was adopted.

Using the NH_4/Na exchange as an example, the following steps were involved in the determination:

(i) Two 100 mℓ quantities of cation resin were placed into separate fixed bed columns and each was contacted with a 3N feed solution at a feed rate of 4BV (400 mℓ) per hour. Sample A was converted to Na-form using NaCl feed, and sample B to NH_4-form using NH_4Cl feed. In both cases, a 400% stoichiometric excess of feed was used. Both resin samples were now washed with water until feed and product stream compositions were identical.

(ii) A small exact sample (10 mℓ) of each resin form was removed from its respective column and air dried in a buchner funnel by placing a damp muslin (cotton) cloth over the funnel and sucking air through the cloth and

resin. The resin sample was next weighed and placed in an oven at 105°C and dried to constant weight. The difference in weights was a measure of the resin moisture content.

(iii) For the actual experiment, it was found convenient to contact 10 mℓ of resin with 200 mℓ of solution. If the equilibrium measurement was to be conducted at a particular concentration (e.g. 0,5N) then the necessary feed solution concentration had to be prepared so that when 200 mℓ of the feed was diluted by the moisture content of the 10 mℓ resin sample, the desired concentration was achieved. The required feed concentration was thus evaluated on the basis of the previously determined resin moisture.

(iv) In order to achieve an equal spread of points over the whole equilibrium curve, it was necessary to calculate an approximate resin conversion which would occur when various ratios of both resin forms and feed types (NH_4Cl or NaCl) were mixed together. These various proportions were then contacted together in bottles placed on a shaker table for a 12 hour period. At the end of the contact period, the resin and solution samples were separated and analysed.

(v) The solution analysis involved only the determination of NH_4 (on a colorimetric basis) and Na (using atomic absorbtion spectroscopy). From a summation of the equivalents of each species present, the solution ion fractions could be determined. The resin analysis procedure is more complex. The particular resin sample was placed in a gooch crucible and five successive 20 mℓ aliquots of water placed on top of the resin in order to wash any residual equilibrium solution out of the resin pores and interstices. Between each aliquot, the resin sample was sucked dry on a buchner flask. After resin washing, a divalent cation was used to displace the NH_4 and Na ions from the resin phase. In this instance, five 20 mℓ 2,0N samples of $MgCl_2$ were used to accomplish the resin stripping. The product stream from the stripping was collected in a 200 mℓ volumetric flask. The $MgCl_2$ solution was followed by a further five successive wash steps, all of which were also collected in the volumetric flask. On completion of the resin stripping, the volumetric flask was filled to the mark, mixed, and then samples were withdrawn for NH_4 and Na analysis. From the respective analysis, the quantity of both NH_4 and Na ions in the flask could be determined, and hence the composition of the resin sample.

(vi) In the case of the anion resin, the resin wash prior to resin stripping was substituted by a centrifugation step in order to remove as much pore and interstitial solution as possible. Only through using this modified technique could a mass balance on solution and resin be achieved.

(vii) For the 'other' exchange reactions investigated, the only change in the technique was the form to which the resin was initially converted, and the composition of the feed solutions.

(b) Sorption equilibrium: For these tests the following method was adopted:

(i) An exact sample of resin (usually 50 mℓ) which had been converted to the required form, was successively contacted with five samples of the particular electrolyte concentration at which an equilibrium measurement was required. This contact procedure ensured that the resin pore solution reached an equilibrium with the external electrolyte solution.

(ii) The prepared resin was then sucked 'dry' on a buchner funnel for 1 minute, a quantity of wash water was added to the resin and the whole allowed to equilibrate. After equilibrium had been attained, the wash solution was removed from the resin and replaced by a further volume of water. This procedure was repeated until the resin had been completely stripped of sorbed electrolyte (usually three washes were sufficient).

(iii) The volume of each of the wash samples was measured, the samples were analysed and the quantity of electrolyte in each sample added together to determine the total electrolyte present initially in the resin phase.

(iv) The above test was then repeated for a number of starting solution concentrations, and the points on the electolyte sorption equilibrium curve were thus determined.

B1.2 Calculation of results

(a) Exchange reactions

Conditions: Zerolit 625 resin
NH_4/Na Exchange
Solution Concentration 1,5N

Results:

Sample No.	Liquid Analysis(mg/ℓ)			Resin Analysis(mg/ℓ)		
	Na	NH_4-N	I.F.Na(y_i)	Na	NH_4-N	I.F.Na(x_i)
1	4900	15400	0,162	265	1040	0,134
2	10350	12500	0,335	590	820	0,305
3	12600	12000	0,390	700	760	0,359
4	17000	10200	0,504	900	694	0,441
5	21000	6900	0,649	1250	480	0,613
6	30500	2354	0,888	1850	163	0,874

The liquid and resin ion fractions are calculated as follows:

$$\text{For sample 1, } y_i = \frac{Na/MW_{Na}}{Na/MW_{NA} + MH_4/NW_{NH_4\text{-}N}} = \frac{4900/23}{4900/23 + 15400/14} = 0,162$$

$$x_i = \frac{265/23}{265/23 + 1040/14} = 0,134$$

(b) Electrolyte sorption

Conditions: Resin volume: 50 mℓ of Zerolit 625 NH_4-form with NH_4Cl
Solution concentration: 2,80N

Results:

Wash No.	Wash volume (mℓ)	Wash conc.(meq/ℓ)
1	198	209
2	195	9,8
3	210	0,77
4	200	< 0,4

Calculation: The total electrolyte present in each sample is determined:

Sample 1	0,198 x 209 =	41,4 meq
2	0,195 x 9,8 =	1,9
3	0,210 x 0,77 =	0,16
4	0,200 x 0,4 =	0,08
	Total	43,54

Sorbed electrolyte concentration in resin = $\frac{43,54}{,05}$ = 871 meq/litre

B1.3 Results of equilibrium experiments

(a) Ammonium-sodium exhange. (These results are based on the ion fraction of Na in each phase.)

Concentration	1,5N		0,25N		0,90N	
Sample No.	y_i	x_i	y_i	x_i	y_i	x_i
1	,16	,13	,45	,40	,14	,12
2	,34	,31	,62	,55	,44	,41
3	,39	,36	,92	,89	,79	,77
4	,50	,45	,95	,94		
5	,56	,53				
6	,65	,61				
7	,89	,87				

(b) Sodium-hydrogen results (based on ion fraction hydrogen).

Concentration	,05N		0,02N	
Sample No.	y_i	x_i	y_i	x_i
1	,12	,09	,26	,18
2	,29	,22	,49	,40
3	,38	,31	,71	,64
4	,48	,39	,82	,74
5	,59	,49	,87	,83
6	,79	,70		
7	,94	,90		

(c) Hydrogen-ammonium exchange. (Based on ion fraction hydrogen.)

Concentration	1,ON		2,ON	
Sample No.	y_i	x_i	y_i	x_i
1	,25	,18	,13	,11
2	,56	,46	,35	,24
3	,67	,56	,73	,64
4	,78	,68	,81	,73
5	,90	,82		
6	,95	,90		

(d) Anion load exchange. (Based on ion fraction hydroxide.)

Concentration	0,02N		0,02N	
Sample No.	y_i	x_i	y_i	x_i
1	,994	,72	,993	,73
2	,992	,58	,995	,59
3	,996	,440	,996	,46
4	,994	,300	,997	,32
5	,991	,160	,993	,06
6	,709	,000	,816	,00
7	,636	,001	,734	,00
8	,591	,000		

(e) Anion regeneration exchange. (Based on ion fraction chloride.)

Concentration	0,02N		0,02N	
Sample No.	y_i	x_i	y_i	x_i
1	,60	,01	,93	,08
2	,69	,01	,96	,12
3	,85	,04	,99	,45
4	,89	,05	,99	,73

(f) Electrolyte sorption.

Resin Type	Zerolit 625		Zerolit 625		Zerolit MPH	
Resin Form	NH_4		H		FB	
Electrolyte	NH_4Cl		HNO_3		NH_4OH	
Concentration (N)	Solution	Resin	Solution	Resin	Solution	Resin
	2,80	0,871	2,61	0,905	2,26	0,898
	2,02	0,508	1,54	0,443	1,62	0,673
	1,53	0,332	0,94	0,244	1,52	0,610
	0,48	0,108	0,84	0,225	0,76	0,303
	0,21	0,042	0,47	0,110	0,24	0,097
			0,25	0,045	0,14	0,062
			0,11	0,036		

B2 KINETICS

The kinetics of the individual ion exchange and electrolyte sorption reactions were determined by monitoring the composition change which occurred with time when resin and a solution of given concentration were contacted together. The same method was used for both resin types, and is detailed below.

B2.1 Method

(a) Resin and solution preparation: A sample of resin was converted to the required form using the technique outlined for the equilibrium tests, i.e. by passing a feed solution slowly through the resin in a fixed bed column. For the exchange of NH_4 and Na ions on Zerolit 625, the resin was converted to Na-form. After the conversion, the resin sample was next contacted with successive batches of NaCl solution at a concentration exactly equal to that at which the kinetics was to be measured. The purpose of this contact procedure was to ensure that the pore volume of the resin reached an equilibrium with the particular solution concentration and thus to prevent any dilution from occurring during the actual kinetic test. This procedure constituted the resin preparation phase.

The exchange solution was prepared by accurately making up an NH_4Cl solution to the concentration required for the test.

(b) Measuring procedure: A 100 mℓ sample of Na-form resin in contact with NaCl solution was placed into a 500 mℓ beaker together with a motor driven paddle stirrer and a pair of 'blacked' platinum electrodes. The solution was then vigourously stirred and the conductivity measured by the electrodes recorded as a baseline on a pen recorder.

On addition of 200 mℓ of NH_4Cl solution to the beaker, exchange commenced and the conductivity of the solution changed as the relative proportion of NH_4 and Na ions in solution changed. This conductivity change was plotted as a smooth curve on the paper chart, and monitoring was continued until equilibrium had been reached. At this point, 200 mℓ of the beaker solution was decanted the measuring device control settings adjusted to give a new baseline and a further 200 mℓ of NH_4Cl added to the beaker. A second exchange commenced and was again monitored until equilibrium was achieved. In this manner, a number of successive measurements could be made of the rate of resin conversion for various starting resin compositions.

For each kinetic measurement, a sample of the equilibrium solution was analysed to provide the relative proportions of NH_4 and Na at equilibrium. In order then to calibrate the conductivity cell, successive aliquots of NH_4Cl were added to a fresh NaCl solution in contact with the electrodes. The measured recorder peak height was then correlated with the relative ion proportion of NH_4 and Na after each further NH_4Cl addition. From the calibration curve, the proportion of NH_4 and Na ions present during the actual kinetic test could be determined and thus the resin composition evaluated.

(c) Conductivity measuring device: For the very high concentrations tested (0,5N) the change in conductivity with solution cation change was extremely small. The measuring device had thus to be very sensitive. In practice, the high frequency AC voltage across the electrodes was compared with a reference voltage. The difference between the two voltage sources was next amplified and recorded on a pen recorder. Great care was required in the device construction in order to eliminate 'drift' and spurious signals; for, at the very high 'gain' required to distinquich between the very small composition changes which occurred during particularly the NH_4/Na measurements

a small level of typically electrode polarisation would produce erroneous results, as would a small concentration change if the resin had not been adequately prepared.

B2.2 Calculation of results

The pen recorder trace height was measured at a number of time intervals from the start of the kinetic experiment, and each height was converted to a liquid and then a resin composition through first the calibration curve and then a mass balance calculation. In this manner the resin composition at the start of an exchange was determined and so also was the equilibrium composition. For any time interval, the actual conversion at that time interval could then be related to the equilibrium conversion and a fractional approach to equilibrium, as defined by equation (2.51), computed.

For the electrolyte sorption kinetics, exactly the same procedure was adopted except that instead of measuring the conductivity change which occurred as a result of an ionic change in solution, the conductivity change was a function of the sorbed electrolyte concentration in solution. The system was thus calibrated on the basis of concentration instead of composition.

B2.3 Results of kinetics tests

(a) Ammonium-sodium exchange. (Resin compositions based on NH_4 ion.)

Conc.	0,25N	0,50N	0,50N	0,50N	0,50N	0,75N
x(t=0)	,616	,018	,276	,497	,660	,560
x(t=∞)	,699	,110	,355	,614	,757	,685
Time (mins)	F(t)	F(t)	F(t)	F(t)	F(t)	F(t)
0,2	,307	,282	,251	,313	,285	,272
0,4	,479	,461	,417	,474	,442	,436
0,6	,594	,584	,543	,584	,546	,546
0,8	,678	,664	,628	,661	,635	,628
1,0	,735	,720	,694	,718	,696	,691
1,2	,779	,767	,746	,768	,746	,734
1,4	,819	,803	,786	,805	,777	,775
1,6	,854	,825	,814	,838	,808	,804
1,8	,876	,855	,843	,858	,839	,836

2,0	,903	,875	,871	,884	,858	,860
2,2	,916	,899	,889	,900	,877	,877
2,4	,929	,912	,910	,916	,885	,894
2,6	,947	,928	,920	,926	,900	,910
2,8	,951	,934	,931	,934	,915	,922
3,0	,965	,944	,940	,947	,923	,939

(b) Other exchange reactions

Exchange	Na/H	H/NH_4	HCl/NH_4OH	FB/HCl	
conc.	0,02N	0,50N	0,50N	,02N	
x(t=0)	x_{Na}=,709	x_H=,586	x_{HCl}=1,0	x_{HCl}=0,0	
x(t=∞)	x_{Na}=,750	x_H=,656	x_{HCl}=0,0	x_{HCl}=,758	
Time (mins)	F(t)	F(t)	F(t)	Time(mins)	F(t)
0,2	,296	,374	,195	2	,136
0,4	,468	,549	,309	4	,245
0,6	,586	,655	,390	6	,334
0,8	,672	,720	,455	8	,408
1,0	,736	,773	,511	10	,468
1,2	,785	,811	,558	12	,519
1,4	,822	,843	,598	14	,562
1,6	,852	,859	,634	16	,598
1,8	,877	,877	,665	18	,629
2,0	,900	,900	,692	20	,656
2,2	,915	,907	,718	22	,679
2,4	,926	,921	,745	24	,699
2,6	,936	,931	,770		
2,8	,945	,943	,791		
3,0	,951	,946	,810		

(c) Electrolyte sorption kinetics

Electrolyte	HNO_3	NH_4Cl	NH_4OH
Resin	625	625	MPH
Resin Form	H^+	NH_4^+	FB
Time (mins)	F(t)	F(t)	F(t)
0,1	,428	,416	,207
0,2	,608	,618	,354
0,3	,719	,734	,456
0,4	,798	,809	,536
0,5	,854	,860	,591
0,6	,896	,901	,642
0,7	,923	,927	,692
0,8	,944	,942	,713
0,9	,955	,959	,745
1,0	,966	,968	,750

B3 ORGANIC LOADING OF ANION RESINS

The organic loading tests were conducted on five anion resins, Amberlite IRA-68 and IRA-93, Zerolit MPH, Imacti A27 and Dowex MWA1 using pretreated HTE water. The detailed experimental technique is outlined below.

B3.1 Method

(a) Equipment: Two hundred mℓ samples of each of the resins were placed into separate 25 mm internal diameter 1 000 mm high perspex columns. Each column consisted of a backwash outlet at the top, a feed inlet 400 mm from the top, a backwash inlet at the bottom and a product outlet also at the bottom. Resin was supported just above the bottom ports by a fine mesh stainless steel screen. Flow to the columns was metered through a rotameter and controlled by a needle valve on the outlet line.

The feed, regenerant and wash (tap water) solutions for the tests were kept in separate constant head tanks above the columns and entered the columns under gravity flow. Each tank had a valve on the outlet line, and all three tanks were tied into a common header pipe from which each column was fed.

(b) Operating conditions: All solutions were passed down flow through a packed bed of resin except for the backwash. The operating sequence was as follows:

(i) HTE feed water was prepared by filtration through a gravity sand filter followed by passage through a cation exchange column. Metal removal by the cation resin was monitored to ensure that the feed water contained <25 mg/ℓ Na ions. The prepared HTE feed was pumped into the head tank, and anion column feeding commenced. The feed flow rate for all tests was maintained at 3 200 mℓ/hour (16 BV/hr). The product solution volume was monitored, and a sample of the water taken after every 5BV (1 litre) of product. An analysis of these samples provided the data for the resin capacity determinations. Feeding was continued until column breakthrough had occurred.

(ii) Following resin loading, the feed tank was switched off and the wash water tank connection to the header pipe opened. Each column was backwashed by using the wash water to achieve a 100% bed expansion for a period of five minutes. After the backwash, the re-classified resin was allowed to settle under gravity and the liquid level in the column was lowered to just below the feed point.

(iii) On completion of the backwash the appropriate tank outlet switching started the regeneration. This phase was achieved by injecting a 100% stoichiometric excess of 3,0N ammonia solution at a flow rate of 4BV/hour into each column and then washing the resin with 6 BV of wash water. The regeneration product flow and conductivity were monitored at 100 mℓ volume intervals, and provided the data for evaluating the resin wash water requirements.

(iv) The resin regeneration step was followed by the next controlled loading cycle.

(c) Monitoring: The degree of resin loading was monitored by analysing the product water samples for anions and COD and plotting a breakthrough curve. From this curve, the operating capacity of the resin was determined and compared with previous results. Prior to the commencement of the organic loading tests, four controlled conditioning cycles were conducted on each resin. The purposes of these four cycles was to establish the operating capacities of the new resin samples. For this purpose, a 0,02N synthetic HCl solution was used as the feed stock and the respective breakthrough

capacities and wash water requirements determined. These values were used as a basis for evaluating the degree of resin fouling during the subsequent tests.

B3.2 Calculation of results

The table below presents an analysis of the product water composition during a loading (cycle 14) on the Zerolit MPH resin. Based on the product water composition presented, the breakthrough curve of the figure is plotted. The breakthrough criterion is a product water chloride content equal to 10% of the feed composition, which in the case of the figure is a chloride level of 57,5 mg/ℓ. The column operating capacity is evaluated by determining the total number of equivalents of feed to enter the column up to the breakthrough volume (the volume at which product water Cl = 10% of feed water Cl) and subtracting from this the total quantity of anions which were not loaded onto the anion resin during the load cycle. The difference represents the resin operating capacity under the conditions of the experiment.

Product	Concentration (mg/ℓ)				
Vol (ℓ)	Cl	SO_4	NO_3-N	PO_4	COD
1	26,5	0	<2	0	17
2	18,5	0	<2	0	18
3	16,5	0	<2	0	19
4	10,0	0	<2	0	19
5	16,5	0	<2	0	19
6	14,5	0	<2	0	19
7	12,5	0	<2	0	19
8	13,0	0	<2	0	19
9	16,0	0	<2	0	24
10	20,0	0	<2	0	30
11	46	0	<2	0	37
12	150	0	2,9	0	44
Feed	575	163	10	16	40

The calculation procedure is: (i) a smooth curve is drawn through the data points, (ii) because each data point is based on an analysis of a small sample, the analysis is representative of the product water composition only

at the particular volume at which the sample is taken. The total quantity of anions which pass through the column should be determined from the area under the curve, instead of which an averaging technique is used and the composition midway between two samples is taken to represent the average composition of the product stream between samples; (iii) the average composition and sample volumes are multiplied and summed to give the total anions leaving the column; (iv) the product of the breakthrough volume and feed composition gives the total anions entering the column. By mass balance, the resin operating capacity is determined.

(a) Calculation of anions leaving column.

Sample	Vol (ℓ)	Composition (mg/ℓ)		Leaving (meq)	
		Cl	NO_3- N		
1	1	31	2	(31/35,5 + 2/14) x 1 =	1,02
2	1	24	2		0,82
3	1	19	2		0,68
4	1	16	2		0,59
5	1	14	2		0,54
6	1	13	2		0,51
7	1	12	2		0,48
8	1	12	2		0,48
9	1	13	2		0,51
10	1	17	2		0,62
11	1	29	2		0,96
12	0,15	52	2,1	(52/35,5 + 2,1/14) x ,15 =	0,24
				Total	7,45

(b) Anions entering column

Feed concentration: 20,31 (cf. Table 4.4)

Breakthrough volume 11,15

∴ Anions in = 20,31 x 11,15 = 226,42

(c) Operating capacity 226,42 - 7,45 = 218,97

Results

(a) Anion exchange capacities

Cycle No.	Resin Operating Capacity (meq)				
	MPH	IRA-93	IRA-68	MWA1	A27
0	224	232	309		265
2	205	203	279	236	269
4	204	210	267	237	270
6	201	209	275	235	248
8	205	210	268	236	262
10	211	214	278	231	253
12	210	200	282	231	238
14	219	213	280	231	237
16	202	216	291	228	250
18	206	213	286	229	224
20	212	225	297	227	228

(b) Wash water conductivity values

Resin	Cycle Number	Wash water volume (mℓ)							
		300	400	500	600	700	800	900	1000
MPH	5	1000	430	320	150	120	-	-	-
	10	1000	420	310	170	120	-	-	-
	15	920	420	300	180	130	-	-	-
	20	950	420	300	190	140	-	-	-
IRA-68	5	1100	660	420	300	200	160	120	-
	10	950	460	300	210	120	-	-	-
	15	920	640	360	260	220	170	130	120
	20	1100	840	540	380	250	200	150	110
IRA-93	5	2000	500	300	220	150	100	-	-
	10	1300	800	550	420	330	260	210	150
	15	1900	800	500	420	300	250	180	130
	20	1900	1050	800	560	450	350	300	250

Resin	Cycle Number	Wash water volume (mℓ) 300	400	500	600	700	800	900	1000
MWA1	5	1500	600	400	300	200	150	130	<100
	10	1200	610	420	290	200	150	130	100
	15	1000	600	450	310	205	140	140	130
	20	1100	500	390	310	210	160	150	150
A-27	5	4100	2000	1000	600	310	200	130	100
	10	4000	2100	780	500	250	180	150	140
	15	6000	3000	1500	610	450	300	200	180
	20	4500	1800	1200	590	450	350	300	290

B4 RESIN LIFE TESTS

The resin life tests were conducted on the four macroreticular resins Amberlite IR-200 and IRA-93 and Zerolit 625 and MPH. The test procedure was automated, and controlled resin operating capacity measurements were conducted at specific intervals.

(a) Equipment: The equipment consisted of four perspex columns, 25 mm internal diameter and 1,0 metre high. Each column was filled with 200 mℓ of resin contained between fine mesh stainless steel screens at the top and bottom of the column. The screens prevented both whole and broken resin beads from leaving the column.

The inlet point for each of the columns was just below the bottom mesh and the outlet point just above the top screen. Flow of feed, wash water and regenerant to each column was separately controlled through valves on each feed line and the respective three flow streams were teed together before passing through a rotameter and into the column inlet port.

Because two columns contained cation and two columns anion resin, only two feed, wash and regenerant constant head holding tanks were required. The flow of each solution to a particular column pair was automatically switched on and off by polypropylene lined solenoid valves which were, in turn, controlled by delay timers. The overall control was maintained by three timers, one each to measure the duration of feed, regeneration and wash water flows.

Each complete cycle of feed, regeneration, wash was registered on a counter, and the sequence automatically restarted.

(b) Operation: The operating capacity of each resin column was measured by the breakthrough calculation of Appendix B3 using synthetic NaCl and HCl solutions as the feed. These capacities were used as the control values for subsequent capacity comparisons, and also to set the operating conditions on the life test columns.

The organic containing feed water for the columns was filtered and pumped into the cation feed tank or filtered and passed through a 20 litre bed of cation resin to remove metal ions and then pumped to the anion feed tank. The metal cation level of the anion feed was controlled so that the Na content was always <20 mg/ℓ. An analysis of both the cation and anion feeds was then used in conjunction with the column capacities and feed flow rates to set the duration of the feed flow.

All solutions to the life test resins were passed upflow through a fluidised resin bed. The feed rate was set at 3 200 mℓ/hour which resulted in a 10% bed expansion of the cation resin and a 100% bed expansion of the anion resin. From these flow rates and the resin capacities, the duration of the feed flowtime was calculated at approximately 7 hours. This included time for a 10% stoichiometric excess of feed solution to each column, which ensured that complete resin loading occurred.

Following the feed flow, the regenerant was automatically switched on. For regeneration, 3,0N solutions of HNO_3 and NH_3 were used for the cation and anion resins respectively. A 100% stoichiometric excess of both regenerants was introduced to the columns at a flow rate of 15 mℓ/min. The regenerant excess, concentration and flow rate together set the duration of the regenerant flow period.

Regeneration was followed by resin washing. Here, 1 200 mℓ of wash water was introduced to each column at the regeneration flow rate of 15 mℓ/min. On completion of resin washing, one cycle was counted up and feed flow automatically restarted. The cycle frequency was of the order of 3 cycles/day.

At specific intervals in the life test operation, a manually controlled cycle using the HTE feed was conducted on each of the resins. This controlled cycle sequence consisted of first a measured regeneration, then a wash, and lastly the column loading. The sampling was conducted every liter during the loading and the operating capacity of each column determined on the basis of 10% Cl or a 10% Na breakthrough concentration. After the capacity measurement, each column was opened and samples of resin from the top, middle and bottom of each bed were withdrawn and a bead count (cf. Appendix A5) conducted on each sample. These resin samples were then replaced and further cycling of the resin was continued.

Results:

Cycle	Resin Operating Capcity (meq)				
No.	MPH	IRA-93	Cycle No.	625	200
0	224	194	0	240	200
50	250	200	50	195	191
150	240	191	110	215	204
250	239	197	250	209	180
350	212	178	350	194	168
440	210	205	525	208	179
550	219	200	620	247	239
617	238	219	800	230	201
700	225	216	900	233	228
800	224	202	1080	224	201
900	248	229			
1080	220	204			

B5 CAPACITY TESTS ON THE DESAL ANION RESIN

The Desal anion resin Amberlite IRA-68 operates on the bicarbonate cycle exchanging feed water anions for bicarbonate ions according to the following reaction:

$$R' - NH_2CO_3 + NaCl \rightarrow R' - NHCl + NaHCO_3$$

The loaded resin is next regenerated with NH_3 solution and carbonated with CO_2 dissolved in water. The relevant reactions are

$$R' - NHCl + NH_3 \rightarrow R' - N + HN_4Cl$$

$$R' - N + H_2O + CO_2 \rightarrow R' - NH_2CO_3$$

(a) Equipment: Two hundred mℓ of IRA-68 was placed into a 25 mm diameter, 1,0 metre high glass column. Feed, regenerant and carbonic acid were introduced by means of a positive displacement pump against a backpressure in the column of 1 atmosphere. This high backpressure was found necessary to maintain the required CO_2 solubility.

Feed flow rate was adjusted by the setting on the metering pump used and carbonation of the resin after regeneration was continued until feed and product water CO_2 content were equal.

(b) Operation:

(i) The measurement of the effect of regeneration level on the operating capacity of the resin was achieved by changing the excess of regenerant passed through the resin, flushing the resin with 1 200 mℓ of water, carbonating and then loading with NaCl. The chloride level in the product stream was monitored and the operating capacity was evaluated using the 10% Cl breakthrough technique previously outlined.

(ii) The effect of flow rate was measured similarly to the above, except that in this instance the regenerant excess was maintained constant and the feed flow rate adjusted. The operating capacity was again measured at a 10% Cl breakthrough.

B6 TEST OF AMMONIUM RECOVERY IN FIXED BED COLUMNS

(a) Equipment: Two glass columns containing respectively 300 mℓ of cation and anion resin were set up. Each column had a diameter of 25 mm and height of 1,0 metre. The columns were connected together so that solution leaving the bottom of the cation column entered the top of the anion column. Feed was introduced by a positive displacement metering pump. The settled resin beds in each column occupied approximately half the column volume and the volume above the resin in each column was filled with liquid. Both columns

were operated in downflow mode for both feed and regenerant flows. The column piping was so connected, that feed or regenerant could be passed through either column first before entering the other column and discharging to waste.

(b) Operation: The test was conducted by first regenerating both resins with a 200% excess of regenerants at a flow rate of 4BV/hour. Regeneration was followed by a water wash at the same flow rate. A 0,02N NaCl feed solution was used for resin loading, and the load cycle was continued until the sodium content of the product stream leaving the anion column reached 10% of the feed concentration. The feed flow rate during resin loading was 4 800 mℓ/hour. From the breakthrough curves for both chloride and sodium the operating capacities of both resins were determined.

Anion regeneration and NH_4/Na exchange on the cation column was achieved by passing NH_3 solution sequentially through the anion and cation resins. A 100% excess of NH_3 was used at a flow rate of 1 200 mℓ/hour. The NH_3 was followed by 5,4 litres of wash water which was sufficient to wash both the cation and anion columns. During anion regeneration, the product stream from the cation column was continuously monitored for Na, NH_4 and Cl.

The next step was the regeneration of the now NH_4 loaded cation resin. This was accomplished with 3,0N HNO_3 at a flow rate of 4BV/hour, followed by an 1 800 mℓ water wash.

(c) Results

Step	Concentration (mg/ℓ)			
	Anion Regeneration		Cation Regeneration	
Volume (mℓ)	NH_4	Na	NH_4	Na
250	0	5	150	40
500	0	142	1900	860
750	0	155	4900	80
1000	0	137	95	0
1250	49	6400	18	0
1500	430	16500	0	0
1750	7400	6600		
2000	7000	800		
2250	3300	252		
2500	1520	168		
2750	550	66		
3000	290	23		

APPENDIX C

CCIX COLUMN PROPERTIES

C1 COLUMN DESIGN

A CCIX column consists of a number of interlinked vessels, each of which has to be sized according to the flow conditions and resin properties which will occur during the operation of the column. For the columns used in the pilot plant, the various factors outlined below were considered prior to column construction. These same factors would have to be evaluated in the same manner for larger scale, and to this end the calculations made when the cation load column was designed are listed below.

C1.1 Column diameter

The diameter of the column was based upon the required water volumetric flow rate through the column, the maximum allowable bed expansion, the minimum allowable upflow time and the resin fluidisation properties. For the pilot plant, calculations were made on the basis of the following conditions:

(i) Water flow rate 5 000 litres/day = 3 472 mℓ/min
(ii) Bed expansion 50%
(iii) Minimum upflow time 15 minutes.

From the required 50% bed expansion and the data of Figure 4.3 the linear velocity (LV) through the Zerolit 625 resin which will result in the particular %BE is ascertained.

(iv) Required linear velocity (LV) = 34 cm/min.

$\therefore$ column cross-section = $\frac{3472}{34}$ = 102 cm^2

$\therefore$ column diameter = 11,4 cm

A nominal diameter of 10,0 cm was chosen on the basis of material availability. With this diameter the %BE at the required flow is 57%.

With a 0,5 m stage height and 57% bed expansion, the volume of resin per stage was calculated as follows:

$$\text{Resin volume per stage} = 50 \times 102 \times \frac{100}{157} = 3{,}25 \text{ litres.}$$

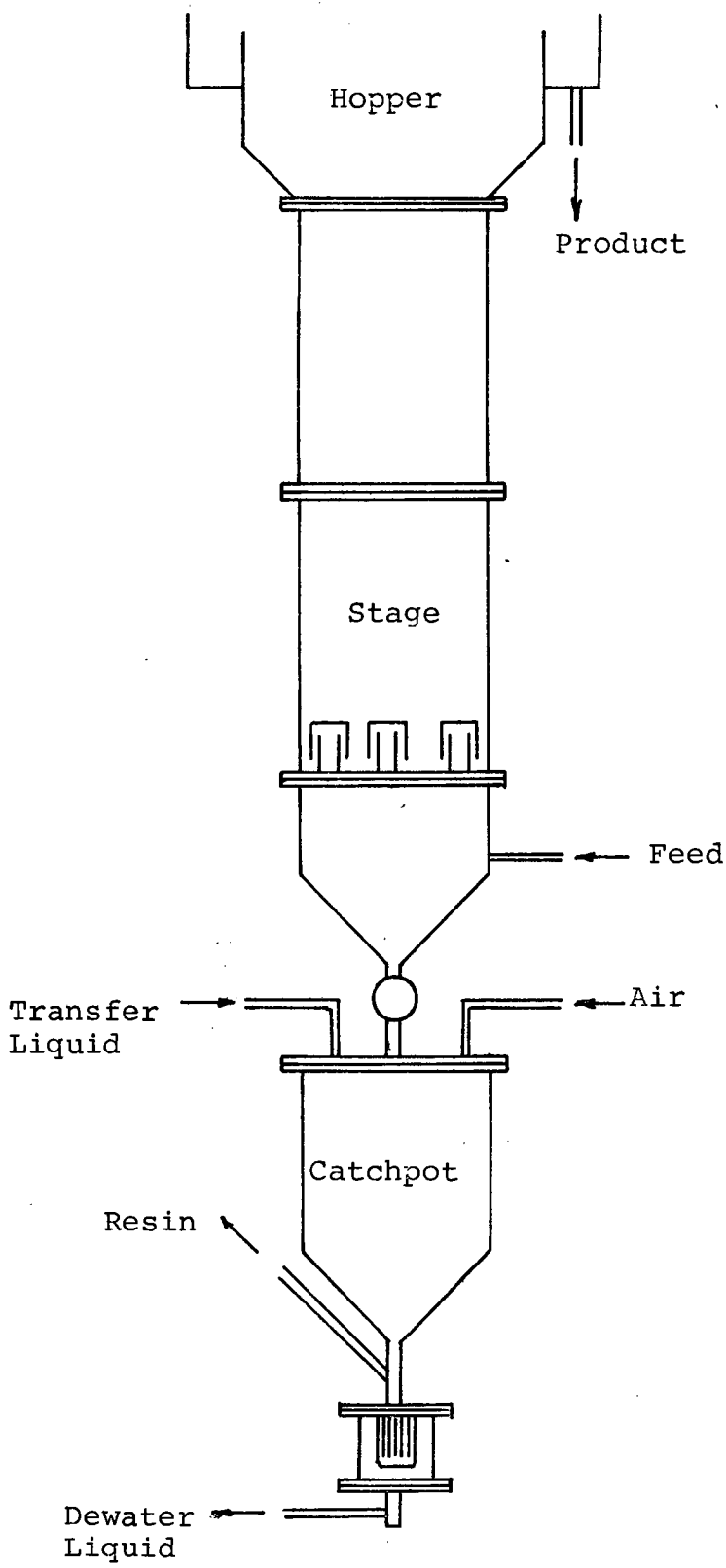

FIGURE C1.1

Schematic diagram of a CCIX column

Assuming an R/L ratio of 1,0, a resin capacity equal to 1,5N and a solution concentration of 0,02N then the approximate upflow time can be calculated:

Resin capacity per stage 1,5 x 3,25 = 4,875 equivalents

$$\text{Upflow time} = \frac{4{,}875}{0{,}02 \times 3{,}472 \times 1{,}0} = 70 \text{ minutes}$$

The calculated column diameter meets with all the plant requirements.

C1.2 Stage separators

The CCIX column has two types of stage separators. The first type, shown in Figure C1.2, resembles a 'bubble cap' from distillation column practice and is used at the bottom of the lowest CCIX column stage. The second type, shown in plan view, fits between and separates each of the other flanged stages in the column.

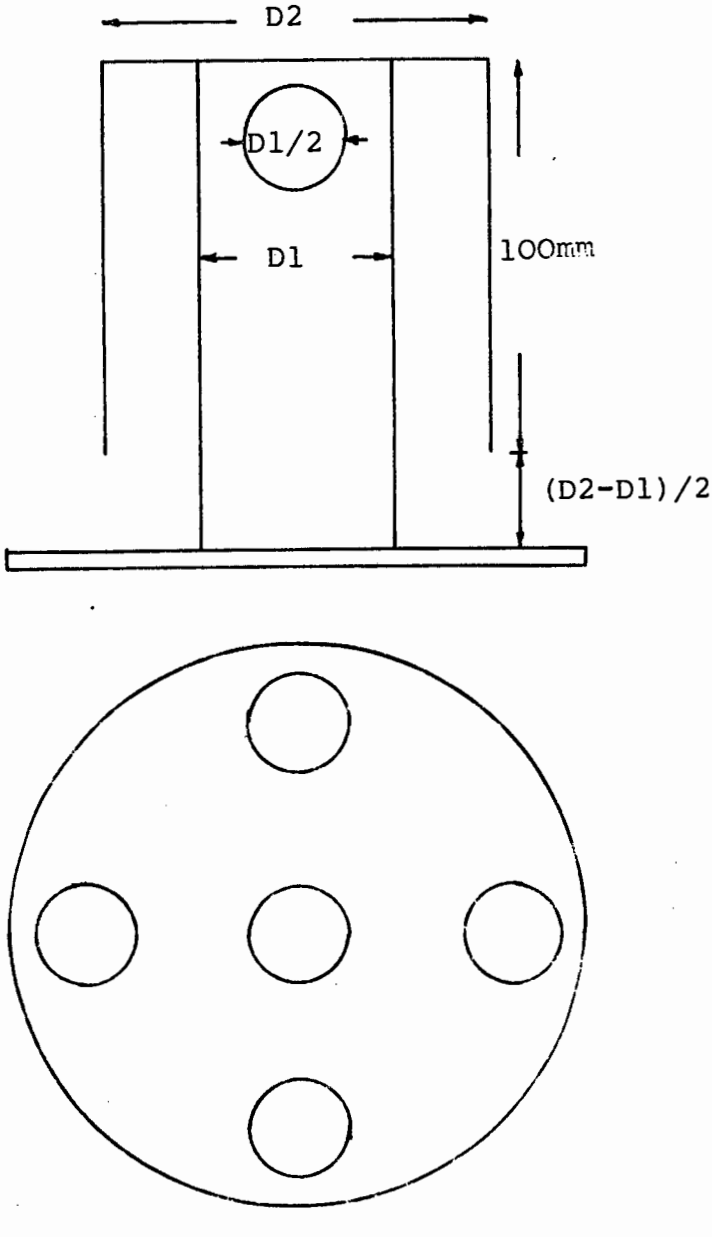

FIGURE C1.2
Diagrams of the CCIX column stage separators

(a) Cap separator: The reason that this design is used at the bottom of the column is to maintain resin inventory in the column. During the start of a resin pulldown, the shaded area of the cap fills with resin before any resin is able to leave the bottom stage. During the cap filling period, all other stages in the column are transferring a volume of resin equal to the volume of the shaded area under the skirt of the cap to the stage below. In this manner, a build-up of resin occurs in the bottom stage of the column. At the start of the next upflow period, the resin in the skirt volume is forced out from under the cap into the bottom stage and thus resin inventory control is maintained in a CCIX column. From the test work conducted on resin inventory control, it was found that the total retained volume under the caps should be approximately 10% of the actual stage volume. In the large diameter anion load column, five caps could be placed within the stage cross-sectional area. For each of the other columns only one cap could fit into the available area.

For the calculation of cap size and placement in large columns the procedure outlined by van Winkle [76] was followed, and the caps placed on a triangular pitch with the distance between cap centres equal to four times the skirt diameter (D_2). In order to maintain the same linear velocity under the skirt and in the riser, the skirt to riser diameter ratio should be $D_2 : D_1 = \sqrt{2}$. With both the cap separator (and the plate separators detailed below) the recommended liquid flow area to column cross-sectional area should be in the ratio of 1:70. This ratio provides a high linear velocity through the cap (or holes in the plate separator) and ensures that no resin passes downwards through a separator during upflow. In the pilot plant, this ratio had to be reduced to 1:20 in order to have the holes sufficiently large to allow resin flow during pulldown. The riser diameter used in the smaller columns was 10mm, but in large scale equipment it would be of the order of 25 mm.

(b) Plate separator: The plate separator serves merely to prevent mixing of resin between stages and as a flow redistributor to prevent flow bypassing along the column walls. As such, the plate separator, as its name suggests, is merely a perforated plate. In large scale equipment the plate hole size would be 10 to 15 mm on a 100 mm triangular pitch giving a hole area to column area of 1:70. For the CCIX pilot plant, the hole size used was 8 mm

on the three small columns, 12 mm on the cation load and 20 mm on the anion load with the hole to total plate area varying from 1 in 10 to 1 in 20.

C1.3 Catchpot

The catchpot at the bottom of each column serves two purposes: (i) it collects the pulldown volume of resin, and (ii) it provides a vessel in which the dewatering can take place. The position of the catchpot can be either below the column, or next to the column. The size of the catchpot is set at twice the volume of a column stage, and has a diameter to height ratio varying from 1:1 to 1:2. In order to facilitate resin transfer out of the catchpot, the bottom is sloped inwards at a 45^{o} angle.

For the pilot plant test work, the dewatering device was mounted directly below the catchpot. This device consisted of a slotted resin filter which allowed liquid but not resin to pass through. The resin was on one side of the filter, and the dewatered liquid pushed through the filter and discharged. The details are indicated in Figure C1.1.

C1.4 Hopper

The hopper constitutes the top of each column and its function is to receive transferred resin and act as a resin feed vessel. The hopper diameter is usually made 10-20% greater than the column diameter in order to reduce the flow velocity through the resin held in the hopper and thus prevent resin carryover out of the hopper. The diameter increase occurs through a 45^{o} conical section connected to the hopper flange.

At the top of the hopper is an overflow weir over which the product solution flows into the launder before being discharged into a buffer tank. The hopper of each CCIX column can in fact be considered as a further column exchange stage. With the low linear velocity and, usually, high resin volume, equilibrium between resin and solution was attained in the hopper of the pilot plant columns.

C1.5 Valves and piping

All the valves used throughout the pilot plant were pneumatically actuated saunders valves with butyl rubber diaphragms and HSB bodies. Actuation occurred through electrical switching of 3-way solenoid valves which

released air pressure on the saunders valve when valve opening was required. The choice of pressure closing valves was made after tests had shown that spring closing valves used to 'leak' if resin particles were trapped between the valve diaphragm and seat.

The piping used in the pilot plant was all high density polythene with resin flow lines 15 mm in diameter and liquid lines 10 mm. Connection between piping and columns or tanks was made through quick coupling screw fittings, which allowed complete flexibility in terms of layout and possible flow path alterations. The saunders valve sizes matched the piping sizes, viz. 10 and 15 mm.

C1.6 Control panel and valve sequencing

The CCIX column control panel consists of three timers controlling the primary column functions, upflow, settle and pulldown and three timers controlling the secondary dewatering function. In the columns without dewatering, the secondary sequence is absent. Each of the three timer sets is interlocked, so that the second (or third) timers of a sequence do not switch on until the first (or second) timers have 'timed' out. In the primary sequence, the end of the third timing period automatically increments a counter and starts the first timer. For the secondary sequence, the sequence switches off completely when the third time period has been completed. The secondary sequence only occurs during the first time period of the primary sequence, and is started each time the primary sequence restarts. Each timer in both sequences was equipped with a manual override function to enable column operation to be manually controlled. The actual function of each of the timers is to switch a relay which provides power to a three way solenoid valve. When the solenoid valve is either powered up or down, pressure is either applied to or released from a saunders valve. In this manner, during each time sequence certain valves are either open or closed.

Figure C1.3 provides a diagram of all the controlled valves in the plant, and Table C1.1 indicates during which time periods each valve is either open or closed. The air stream used for resin dewatering and transfer is filtered and supplied at a controlled pressure of 1,4 atmospheres.

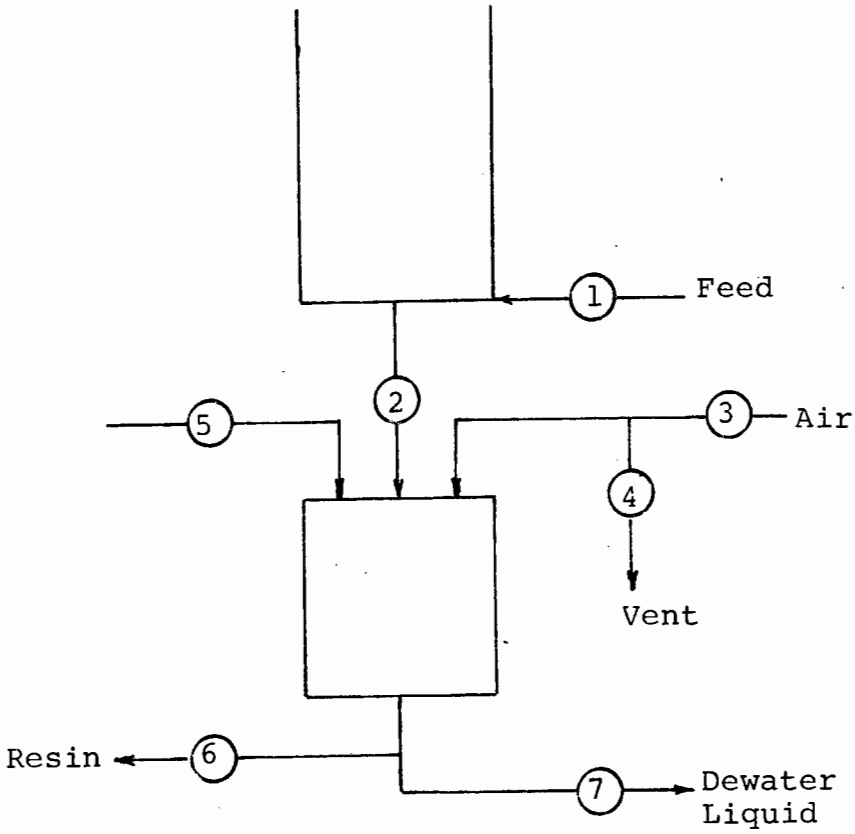

FIGURE C1.3

CCIX column control valves

TABLE C1.1

CCIX column valve sequencing

	Column	Value Number (cf.Fig.C1.3)						
	Operation	1	2	3	4	5	6	7
Primary	Upflow	1	0	-	-	-	-	-
	Settle	0	0	-	-	-	-	-
	Pulldown	0	1	1	0	0	0	0
Secondary	Dewater	1	0	0	1	0	0	1
	Transfer liquor in	1	0	1	0	1	0	0
	Transfer	1	0	0	1	0	1	0

Note: 0 - valve closed

1 - valve open

- - immaterial whether open or closed

The switching of valve no.2, although linked to the third timer sequence, is actually controlled by the liquid level measuring device at the top of each column. Timer 3 of the primary sequence serves merely as an override should the resin sensor malfunction.

In columns which do not have dewatering, valves 5, 6 and 7 are absent and resin transfer occurs automatically on resumption of each upflow period with the same sequence indicated in Table C1.1.

Where two or more feed streams are introduced to the CCIX column, the other streams are switched within the same valve sequence pattern. All the feed saunders valves are 'tied in parallel' to the solenoid valve actuated as valve 1 of Table C1.1 and they are then switched together.

C1.7 Resin and flow control

The feed flow to the columns was controlled by opening or closing a needle valve. The stem of the valve was coupled to a dual direction slow speed (1 revolution every three minutes) high torque motor. A signal, produced from the sensing device in Figure C1.4, switched the motor on in either the forward or reverse direction or switched the motor off. The flow sensor consisted of four light beams at right angles to the flow path of a rotameter tube. The rotameter bob provided the necessary signal by breaking the light beam. Valve control was then effected according to the pattern outlined in the table below Figure C1.4. In this manner, the flow rate into a CCIX column was controlled within the limits set by the 'closeness' of the four light sources, and the size of the rotameter float.

The resin pulldown volume was controlled by a liquid level sensor placed at the top of the column. One connection of the sensor was a stainless steel probe which dipped into the liquid and the other connection (to close the circuit) was permanently immersed in the column solution. A control box determined the resistance between the two circuit connections and the desired switching occurred when the resistance rose to infinity (open circuit) as the liquid level in the column dropped below the probe. By simply raising or lowering the probe level, the resin pulldown volume could be adjusted.

FIGURE C1.4

Flow control device on CCIX columns

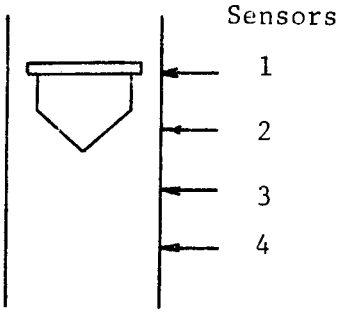

Sensor Number				Valve Action
1	2	3	4	
1	1	0	0	Close
0	1	1	0	Stationery
0	0	1	1	Open

1 - Light beam broken

C2 CALCULATION OF COLUMN OPERATING CONDITIONS AND RESULTS

An example of the calculation procedure used to set the CCIX column operating conditions is outlined below. Once steady state had been achieved, the intermediate liquid samples taken were used to determine stage efficiencies. An example of these calcualtions is also presented.

C2.1 Column operating conditions

Calculation based on following conditions:

Feed concentration:	0,508N
Bed expansion	50%
Stoichiometric ratio	1,0
Resin capacity	1,5N

(i) Pulldown volume (PV)

$$PV = \frac{100}{100 + \%BE} \cdot \text{Stage volume}$$

$$= \frac{100}{150} \cdot 1120 = 746 \text{ m}\ell$$

(ii) Feed volume flow rate (FVF)

At 50% BE feed rate (from fluidisation curves) = 34,0 cm/min
Column cross-section = 22,06

$\therefore$ Flow rate = 22,06 x 34,0 = 750 mℓ/min

(iii) Feed equivalent flow rate (FEF)

FEF = FVF · Feed concentration
= 750 x 0,508 = 375 meq/min

(iv) Resin equivalent rate (RER)

RER = PV · Resin capacity
= 746 x 1,5 = 1119 meq/cycle

(v) Upflow time (UT)

UT = RER/(FEF · Stoichiometric ratio)

$$= \frac{1119}{375 \times 1,0} = 2,98 \text{ minutes/cycle}$$

(vi) Pulldown liquid (the liquid which leaves the column with the resin at pulldown) (PL)

PL = 1,2 PV
= 895 mℓ/cycle

(vii) Extra upflow time (this time is required to replace the pulldown liquid) (EUT)

EUT = PL/FVF

$$= \frac{895}{750} = 1,19 \text{ mins/cycle}$$

(viii) Total flow time (TFT)

TFT = UT + EUT
= 2,98 + 1,19 = 4,17 minutes/cycle

The resin settle time is dependent upon bed expansion and resin density. For the above conditions, the settle time was 30 seconds, and the pulldown occurred in 1 minute. The total cycle time, the sum of TFT, settle and pulldown periods is thus 5,67 minutes.

When two columns are interlinked, then the settle and pulldown times together represent a 'dead time'. In order, therefore to balance liquid and resin flows, this dead time must be considered. Consequently, for the above conditions the average flow rates of liquid and resin entering the column during a cycle would have to be:

Resin Flow: $746/5,67 = 131,6$ mℓ/min

Liquid Flow: $\frac{750 \times 4,17}{5,67} = 551,6$ mℓ/min

However, the period of time during which flow can actually occur is the TFT. Therefore, during the flow time the actual flow rate has to be proportionally higher. Including the 'dead times' with the stoichiometric requirements in a series of interlinked columns makes the solution of the flow balance equations a trial and error calculation. For the pilot plant, the calculation procedure was computerised in order to facilitate the flow balance computation.

C2.2 Calculation of steady state stage efficiencies

The results of the operation of a twelve stage column under the conditions outlined above are listed below. The particular exchange was that of NH_4 for Na ions, therefore the feed liquid (y_b) is mainly NH_4 and the feed resin (x_T) predominantly Na. The product resin (x_b) and liquid (y_T) are thus converted to the NH_4 and Na forms respectively. The Na content of the intermediate liquid samples show a composition profile up the column.

The equilibrium relationship is based on an $\alpha = 1,2$ and the equilibrium expression

$$y = \frac{\alpha x}{1+(\alpha-1)x} \quad \text{or} \quad x = \frac{y}{\alpha-(\alpha-1)y}$$

where y, x refer to Na ion fraction.

The resin and liquid compositions leaving the column locate the terminal points of the operating line. From these compositions the slope and intercept are calculated as follows:

Component	Ion Fraction Na
Feed Liquid (y_b)	0,0043
Product Liquid (y_t)	0,8851
Feed Resin (x_t)	0,8990
Product Resin (x_b)	0,0197

$$\text{Slope of operating line (m)} = \frac{y_t - y_b}{x_t - x_b} = \frac{0,8851 - 0,0043}{0,8990 - 0,0197}$$

$$= 1,002$$

$$\text{Intercept (c)} = 0,8851 - 1,002 \times 0,899$$
$$= -0,0154$$

The analysis of the intermediate liquid sample taken gave the following results (all expressed as ion fraction Na):

Stage No.	y_i	x_i	$x_i - x_{i-1}$	$f(y_{i-1})$	$x_i - f(y_{i-1})$	η
1	,0365	,0518	,0321	,0036	,0482	0,666
2	,0931	,1083	,0565	,0306	,0777	0,727
3	,1398	,1550	,0466	,0788	,0762	0,612
4	,2084	,2235	,0685	,1193	,1042	0,657
5	,2815	,2964	,0730	,1799	,1165	0,626
6	,3452	,3600	,0636	,2461	,1139	0,558
7	,4469	,4615	,1015	,3052	,1563	0,650
8	,5638	,5782	,1167	,4024	,1759	0,664
9	,6382	,6525	,0743	,5186	,1340	0,554
10	,7262	,7404	,0879	,5951	,1452	0,605
11	,8085	,8225	,0822	,6885	,1340	0,613
12	,8691	,8830	,0605	,7787	,1044	0,580

The x_i values are calculated from the y_i values using the operating lines:

$$x_i = \frac{y_i - C}{m}$$

$$x_1 = \frac{,0365 - (-,0154)}{1,002} = ,0518$$

$$x_{12} = \frac{,8961 - (-,0154)}{1,002} = ,8827$$

The $x_i - x_{i-1}$ value for stage 1 of the column is computed from x_1 and x_b, i.e.

for stage 1, $x_i - x_{i-1} = x_1 - x_b = 0{,}0518 - {,}0197$

$= {,}0321$

for stage 12, $x_i - x_{i-1} = x_{12} - x_{11} = {,}8830 - {,}8225$

$= {,}0605$

The equilibrium conditions, $f(y_{i-1})$, is calculated from the equilibrium expression and the intermediate liquid analysis

$$\text{for stage 1} \quad f(y_{i-1}) = x_{i-1}^* = \frac{{,}0043}{1{,}2 - 0{,}2 \times {,}0043} = {,}0036$$

$$\text{for stage 12} = f(y_{i-1}) = x_{i-1}^* = \frac{{,}8085}{1{,}2 - 0{,}2 \times {,}8085} = {,}7787$$

The stage efficiency for any stage is calculated from the definition of η

$$\text{i.e. } \eta_{12} = \frac{x_{12} - x_{11}}{x_{12} - f(y_{11})} = \frac{{,}8830 - {,}8225}{{,}8830 - {,}7787} = \frac{{,}0605}{{,}1044} = 0{,}580$$

C3 RESULTS OF SINGLE COLUMN, STAGE EFFICIENCY TESTS

The analysis figure during the single column tests conducted to determine column stage efficiencies are presented below.

Resin Type	Exchange	Feed Conc. (N)	Flow (mℓ/min)	%BE	Contact Time (mins)	Average η
625	NH_4/Na	0,496	552	35	1,012	0,707
		0,763	552	35	1,012	0,686
		0,516	448	27	1,177	0,743
		0,496	345	20	1,413	0,768
		0,500	545	34	1,017	0,708
		0,508	750	50	0,820	0,626
		0,628	419	25	2,44	0,894
		0,461	419	25	2,44	0,897
		0,730	345	20	1,413	0,790

Resin Type	Exchange	Feed Conc.(N)	Flow (mℓ/min)	%BE	Contact Time(mins)	Average η
625	NH_4/Na	0,237	419	25	2,44	0,913
		0,264	1341	100	0,554	0,580
		0,261	708	46	0,846	0,717
		0,241	960	67	0,695	0,633
		0,230	419	25	1,22	0,788
625	Na/H	0,02	1341	100	0,554	0,580
		0,02	1040	73	0,657	0,626
		0,02	1899	200	0,458	0,523
		0,02	2110	270	0,435	0,487
		0,02	2173	300	0,860	0,689
625	H/NH_4	0,470	460	28	1,18	0,814
		0,470	460	28	2,36	0,899
			356	20	1,34	0,841
MPH	HCl/FB	0,02	160	85	4,5	0,195
		0,02	160	85	13,5	0,559
		0,02	595	350	1,6	0,080
		0,02	348	200	2,5	0,125
		0,02	348	200	5,0	0,253
		0,02	348	200	7,5	0,358
		0,02	348	200	10,0	0,442